SCIENCE CHINA
Physics, Mechanics & Astronomy

• Invited Review •

January 2022 Vol. ? No. ?: 000000
https://doi.org/??

The 2.5-meter Wide-field Survey Telescope (WFST)

A. Author[1*]

[1] CAS Key Laboratory for Research in Galaxies and Cosmology, Department of Astronomy, University of Science and Technology of China, Hefei 230026, China;
[2] School of Astronomy and Space Sciences, University of Science and Technology of China, Hefei 230026, China;
[3] Purple Mountain Observatory, Chinese Academy of Sciences, Nanjing 210023, China

Received ?? ??, 2021; accepted ?? ??, 2021

......hihi....

keyword 1, keyword 2, keyword 3
PACS number(s):

Citation: ??, ??, ??, et al,
, Sci. China-Phys. Mech. Astron. **?**, 000000 (2022), https://doi.org/??

Contents

1 Introduction

Large surveys have played major roles in the development of all fields of the astronomy since later 1950s. The first large sky surveys in optical bands were carried out from 1950s through 1980s with 1.2m Schmidt telescope of Palomar observatory in the northern hemisphere (Palomar Observatory Sky Surveys (POSS) I and II[1] and UK Schmidt telescope at AAO and the ESO Schmidt telescope in Chile in the southern sky. Two micron all sky survey (2MASS) covering three near-infrared bands was completed in 2001 with a pair of matched 1.3m diameter telescopes (Arizona and Chile)[2]. These large sky surveys served as important sources of discovery from solar systems to galaxies and quasars for dozens.

Sloan Digital Sky Survey (SDSS)[3] is one of most ambitious and influential sky surveys in the history of astronomy. With a dedicated 2.5m aperture telescope, it mapped one quarter sky and obtained spectra for millions of galaxies, quasars and stars. SDSS has greatly advanced our understanding of physics of galaxies and accreting supermassive black holes (quasars), and the structure of universe and our own Galaxy in 4 phases of surveys. Apart from their initial designed science goals, the uniform and well-calibrated photometric and spectroscopic data have attracted astronomers in nearly every field to explore the data, leading to thousand scientific publications each year. Followed by the success of SDSS, image surveys in the south sky was carried out by Dark Energy Survey Camera mounted on the 4 meter BLANCO telescope in Chile, reaching a depth 1.5 mag deeper than SDSS over a sky of 5000 square degree, and 2.5 mag deeper than SDSS over 1000 square deg sky with ESO 4m survey telescope. Deeper spectroscopic survey of galaxies and the quasars in northern sky is now carrying out by dark energy spectroscopic instrument (DESI) on the Mayall 4m telescope[4].

Time domain surveys explore temporal changes of the celestial objects, either intrinsically or extrinsically, by observing the sky repeatedly. These variations contain crucial information for deciphering the structure and the nature of these variable sources. Over past ten years, we have seen the booming of the field, which was driven partly by the technology development of wide field survey instruments, and partly by the new discoveries with these facilities. Catalina Real-Time Survey (CRTS)[5] searched rare bright transients over 33000 square degree sky using 3 wide field telescopes. Palomar Transient Factory (PTF/iPTF)[6] and its successor Zwicky transient facility (ZTF)[7] have monitored 3π of the sky with a cadence of 3 days to a week, augmented by spectroscopic follow-up telescopes. Panoramic Survey Telescope and Rapid Response System (Pan-STARRS or PS)[8], All-Sky Automated Survey for SuperNovae (ASAS-SN)[9], and the Asteroid Terrestrial-impact Last Alert System (ATLAS)[10] perform time domain surveys and deliver transient sources. Most of these surveys employ dedicated telescopes with apertures from a few ten cm to 1.3m, with large pixel sizes except for Pan-STARRS, which use the two 1.8m Telescopes and Giga-pixel camera. Pan-STARRS is largely dedicated to the search of near-earth asteroids (NEA) now owing to its funding source. The limiting magnitudes in a single exposure for these surveys are in the range of 17.0 in V for ASAS-SN to 21.8 mag in r for Pan-STARRS.

The demand for time domain surveys at fainter magnitude limits has been growing with the discovery of the kilonova, the electromagnetic emission associated with the merger of two neutron stars, and with the interest in the high-redshift supernova and other transients for the cosmology application and multi-messenger astronomy [**?**, **?**, **?**]. The electromagnetic counterparts of gravitational wave sources detected by advanced LIGO, Virgo network in next five years will be typically 1-2 magnitudes fainter than the magnitude limit of major current time domain surveys. In addition, these transient sources located in bright galaxies, and can be overwhelmed easily by starlight in low spatial resolution images delivered by many current surveys. In the southern sky, Vera C. Rubin Observatory (VRO) with a flagship time domain survey telescope of 8.4 meter aperture will be into operation in the coming year. It will reach single-epoch magnitude limit of 24.5 mag in r-band in a 30-second exposure. However, there is no planned time domain facility in the northern hemisphere or in a similar longitude to reach a required depth.

The Wide Field Survey Telescope (WFST) is designed to explore the dynamic 2π northern sky with five filters (*ugriz*) in a weekly cadence. Additional W band allows to explore asteroids in the solar system sensitively. It has an aperture of 2.5m diameter and a field of view about 3 deg in diameter, and is equipped with a mosaic of 9 9k×9k CCDs on its primary focus. The telescope is being built jointly by University of Science and Technology of China and Purple Mount Observatory, CAS, and is expected to be installed in this autumn at the mountain of Saishiteng, Lenghu. The high throughput of the optical system and good site conditions allow it to reach a depth more than 2 mags deeper than ZTF in a single 30s exposure with a superior image quality. The high altitude and low vapor can attain a relatively good efficiency in *u*-band, making it a unique time domain survey telescope in the northern sky. In addition to their opposite hemisphere location, WFST and VRO are also complementary in longitude with about 158 degree difference.

In this paper, we will describe the main characteristics of WFST systems and the science objectives that motivated the project. We present in order: the design of telescope and camera (Section 2); time domain sciences, including supernovae (Section 3.1), tidal disruption events (TDE, Section 3.2), multi-messenger astrophysics (Section 3.3), active galactic nuclei (AGN,Section 3.4); Milky Way and its neighbors (Section 4); Solar systems (Section 5).

2 System Design and Performance

2.1 Telescope

The Wide Field Survey Telescope (WFST) is a 2.5m optical telescope designed with primary-focus optics to achieve a wide field of view of 3° in diameter. A 3D sketch of the telescope structure is shown in Figure 1. The outlook of the telescope is dictated by its primary-focus optical layout. The focal-plane instrument together with the corrector lenses and filters are mounted as an integrated unit located near the focus of the primary mirror, which is called primary-focus assembly (PFA). The PFA sits on the top end of the telescope tube via a hexapod, which provide both support and fine alignment to the PFA. The primary mirror and mirror cell are located on the other end of the tube. The telescope tube itself is assembled on an altazimuth mount. The top-level telescope specifications are listed in Table 1.

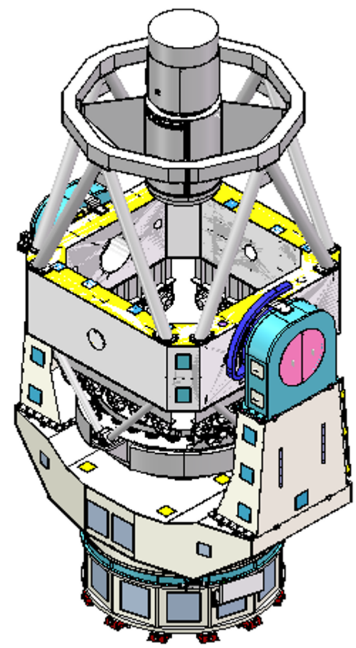

Figure 1 3D model of the telescope structure.

The optical layout of the WFST is shown in Figure 2. The optical system consists of the primary mirror, five corrector lenses, an atmospheric dispersion compensator (ADC), and filters of six observation bands. The 2.5m primary mirror (M1) is an $F/2$ hyperbolic concave surface with high-order aspheric terms. After the corrector lenses, the final system focal ratio is increased to $F/2.48$. The first corrector lens is the largest lens with a diameter of 970 mm. The lens is made of fused silica and has a meniscus shape with a central thickness of 90 mm. The second corrector lens is a negative lens whose concave surface is an aspheric surface. The third and fourth lenses are all spherical lenses. To control chromatic aberrations, the third lens is made of Schott's N-BK7 glass. The fifth lens is a field corrector, which corrects field curvature and reduces distortions. It also serves as the barrier window for the detector dewar. The concave surface of this lens is another aspheric surface. The final focal plane is a flat surface with a plate scale of 30 mm/arcsec. To balance the image quality and system transmission (especially at the U band), a lensm ADC design is finally selected. The ADC consists of a pair of lenses with wedges that rotate in opposite directions to compensate atmospheric dispersion. Such a design avoids the use of flint glasses and hence increase the UV transmission. Raytracing simulations show that 80% of the spot energy is encircled within a diameter of 0.4″ across the full 3° FOV by such a primary-focus optical design.

Item	Specification
Aperture	2.5 m
FOV	3°
Etendue	29.3 m^2deg^2
Wavelength	320~960 nm (u/g/r/i/z/w)
Image Quality	diameter≤0.4″ (80% energy encircled)
Blind Pointing	5″
Tracking	0.1″ (open loop, 1 minute)

Table 1 Top-level specifications for WFST.

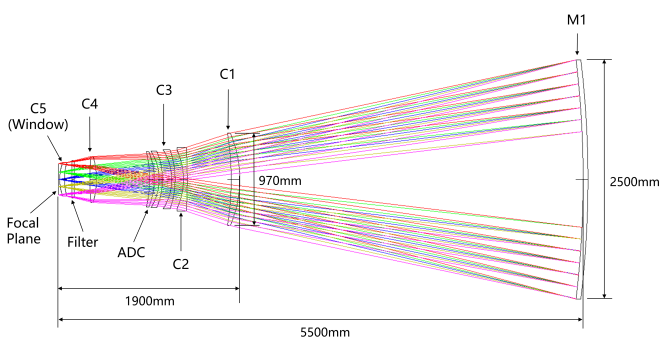

Figure 2 Optical layout of WFST.

The primary mirror for WFST is a 2.5m meniscus thin mirror made of Zerodur and with a thickness of 120 mm. The mirror is uniformly supported by 54 axial supports and 12 lateral supports, which work together to deliver an RMS surface error of 3.7 nm for zenith pointing and 4.2 nm for horizontal pointing under gravitational load. Both axial and lateral supports are actuated by pneumatic actuators based on diaphragm cylinders. The output force generated by each actuator is measured by a load cell as the feedback of a precise control loop. Three out of the 54 axial supports are used as hard points to constrain the axial position of the mirror. Similarly, four additional lateral positioners fix the mirror motions in the lateral directions.

As the core of the primary-focus optics, the PFA is an integrated unit that accommodates five corrector lenses, a pair of ADC lenses, six filters, a shutter and a mosaic CCD camera. The corrector lenses are supported by invar lens cells, which are connected to the invar pads glued to the outer rim of the lenses via flexures. The lens cell is then mounted to the inner shell of the PFA through spacers and adjusting pins, which are used to adjust the tilt and decenter of each lens respectively. A total of 24 lateral supports are used for C1, while the rest of lenses uses 12 supports. The resulting gravitational deformation is less than 6 nm rms for all lens surfaces under various zenith angles. A shutter is located between ADC and C4, which is a two-curtain double-acting shutter with a clear aperture of 500 mm in diameter. A filter switching mechanism is located in the narrow space between C4 and C5. It moves the selected filter into on-line position while keep int other five filters in stow positions around the cryostat of the camera. The PFA also hosts a derotator and a fine focus tuning mechanics integrated with the camera and rotational mechanics for ADC. All the optical and mechanical components are encapsulated in a shell structure made of low-expansion CFRP material. The overall PFA structure spans a total length exceeding 2.5 meters and the total weights is approximately 1.8 tons.

The telescope tube consists of an upper truss and a lower truss, connected by a central hub. A spider structure at the top of the upper truss provide support for the PFA. The PFA is attached to the spider structure via a hexapod, which provides fine alignment of the PFA relative to the primary mirror. The telescope tube is mounted on an altazimuth mount. Both the elevation and azimuth axis utilizes ball bearings driven by direct drive torque motors for high stiffness and rotary precision. An auto-guiding system based on focal-plane guide sensors is employed by WFST to realize closed-loop tracking during operation.

To maintain the real-time image quality of the WFST, an active optics system (AOS) is employed. The flowchart of the AOS is shown in Figure 3. A look-up table based on finite element analysis is first established to correct both rigid-body misalignment errors of the PFA and surface figure errors on M1 due to gravitational deformations at various elevation angles as well as large-scale thermal deformations due to ambient temperature variations. Further, closed-loop active wavefront corrections based on focal-plane wavefront sensors are used to correct the residual errors in the PFA alignment and the low-order bending errors on M1.

The goal of the active wavefront correction is to keep the telescope within seeing limited from PFA misalignment and primary mirror deformations. It utilizes four focal-plane wavefront sensors at the edge of the 3° field to measure the overall wavefront aberrations in real time. These wavefront sensors are curvature sensors with two split CCD detectors, delivering intra- and extra-focal images respectively. The measured defocused images are then interpolated into Zernike polynomials and their differences to the designed values are used as merit functions. An iterative damped least square (DLS) method is applied to minimize the merit function to an acceptable level. The output wavefront corrections, interpreted as the 5-DOF rigid-body motions for PFA and lower-order Zernike correction coefficients for M1, are then sent to the telescope control system, which then drive the PFA hexapod and M1 active supporting system accordingly in each exposure period.

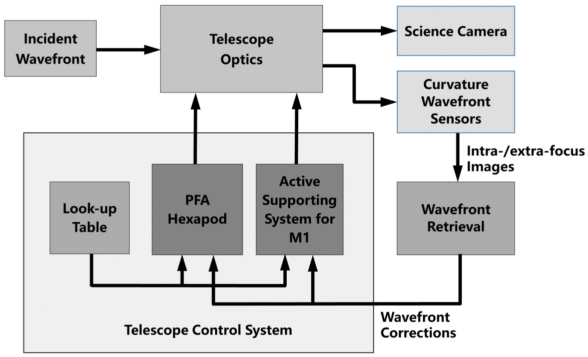

Figure 3 Flowchart of the active optics system for WFST.

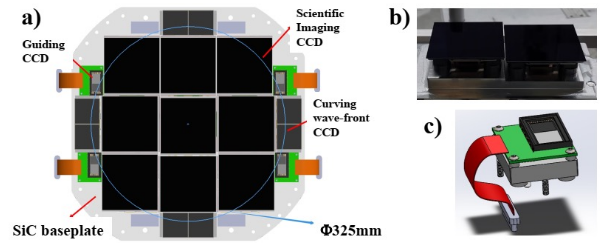

Figure 4 a) The layout of the focal plane of WFST; b) The curving wave-front sensor with 2 CCD detectors; c) The re-packaged mechanics of a guiding CCD.

2.2 Camera

The layout of the focal plane of WFST is shown in Figure 4a. The imaging area is a circle with 325mm diameter which is divided to 3 parts: scientific imaging part, curving wave-front sensors for AOS and guiding sensors for guiding system. The scientific imaging part consists of 9 9K×9K CCDs with pixel size of 10μm which is CCD290-99 from E2V company. It is a mosaicking CCD detector with flatness of 20μm. There are 4 curving wave-front sensors located at each side of scientific imaging detectors as shown in Fig. 4a. Each curving wave-front sensor consists of two CCD detectors de-focusing at ±1mm from focal plane which is CCD250-82 from E2V company with 4K×4K pixels and pixel size of 10μm as shown in Fig. 4b. It is a full frame CCD. 1/4 part of the curving wave-front sensor is inside the FOV and imaging for AOS. So for the CCD controller, half part of CCD250-82 is operated for driving and readout. The guiding sensor is CCD47-20 from E2V with 1K×1K pixels and pixel size of 13μm. It is a frame transfer CCD and can work without a shutter. It is located at two side of scientific detector as shown in Fig. 4a. Each CCD has been repackaged for mosaidlecking installation as shown in Fig. 4c. The surface of the guiding CCD detectors should be in the focal plane with 20μm range. It can be imaging of light star for telescope guiding. the guiding imaging area is very small and only small part of CCD47-20 can image guiding star.

The camera of WFST is at prime focus of the telescope with limited space. The design of camera is very compact. It consists of a vacuum house for CCD detectors, a focal plane component with CCD detectors and its mosaicking parts and cooling parts, electronics, vacuum devices, a cryo-cooling system for CCD detectors, a hydrocooling system for heat dissipation of electronics and a data acquisition system, a imaging control system and a data center for image storage. The camera is shown in Figure 5. The C5 lens is the window of the camera. The CCD detectors are installed on the focal plane base made of SiC which has a small expansion coefficient with temperature variation. The CCD detectors will be cooled to −100°C for reducing the dark current. The focal plane component with CCD detectors is housing in a vacuum vessel. There are two cryo-coolers with two cryo-cooling head for cooling CCDs. The signals of the CCD are connected to the electronics through feed-through at the back flange of the vacuum vessel. The electronics include CCD controllers of CCD290-99, CCD250-82, CCD47-20, the temperature control system of CCD and the data acquisition system. the electronics are sealed in a shell with thermal isolation. A hydrocooling system is installed at the back of the electronics shell and the heat will be dissipated through the hydrocooling system which will reduce the seeing influence tremendously from the heat producing from electronics.

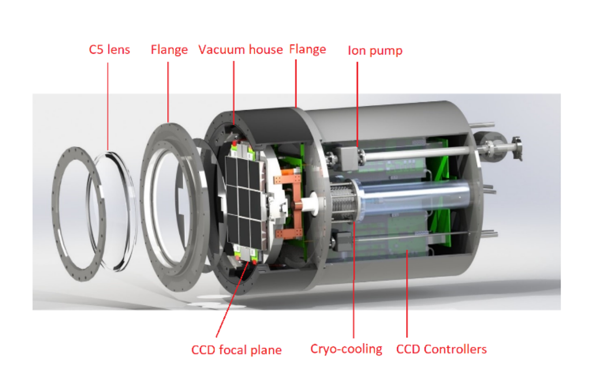

Figure 5 The mechanics of the WFST prime camera.

An imaging control system named camera control system (CCS) is designed for device control, imaging control and interaction with other systems as filter switching, shutter controlling, camera rotation, cryo-cooling, hydrocooling, and vacuum pumps. The CCS is a management system of the camera for CCD imaging control, data formatting and data transmission which will collect all of the imaging data and status date of the camera and transmit the data to a data center for data storage and analysis.

2.3 Lenghu Observing Conditions

The telescope will be located at the mountain top of Saishiteng, Lenghu (93°53' E, 38°36' N), at an altitude of 4200 m. The observing conditions of the site have been tested for three years since 2018 [11]. The monitoring results show that the site is comparable to other outstanding sites in the world, such as Mouna Kea, in terms of atmospheric seeing, sky background brightness, and perceptible water vapor (PWV), etc. Particularly, the median value of the seeing of the site is 0.75 arcsec. The average night sky background brightness is around 22.0 mag arcsec^{-2} when the moon is below the horizon. The brightness is measured using a commercial sky quality meter which has a passband from 400 nm to 600 nm similar to that of a standard Johnson V filter. The sky level can reach 22.3 mag arcsec^{-2} during new moon conditions. The PWV is below 2 mm for 55% of the time. The nightly observing time ranges from 5 hours during June to over 11 hours during January every year. The monitoring data also suggest that the clear time fraction is about 70% and the conditions of a significant number (337) of nights reach photometric in 2021[1)].

2.4 Overall Performance of the System

The goal of the WFST optical design is to achieve a balanced imaging performance for different observation bands and different zenith distances across the full field of view of the telescope. To quantify and assess the overall image quality, the diameter that encircles 80% of the spot energy (EE80) is calculated for different bands and zenith distances. The EE80 maps for the u, z and w bands at zenith distance of 0° and 60° are shown in Figure 6. The EE80 data averaged among all scientific pixels for the three bands are summarized in Table 2. The EE80 is confined to a diameter of 0.41, 0.43, and 0.35 arcsec for the u, z, and w bands respectively. For the other three bands, the image quality is slightly better. It is also clear from Table 2 that the image quality changes very little for zenith angles from 0° to 60°, indicating the effectiveness of atmospheric dispersion compensation in all bands.

1) http://lenghu.china-vo.org/sitecondition

Zenith Angle	**u**	**z**	**w**
0°	0.39	0.33	0.41
30°	0.39	0.33	0.41
60°	0.41	0.35	0.43

Table 2 EE80 diameter in arcsecond averaged over all scientific pixels.

To evaluate the real image quality during operation time, error factors such as manufacture errors, assembly misalignment, gravitational and thermal deformations as well as atmospheric turbulence need to be considered in addition to the designed imaging performance of the optical system. The spreadsheet for the WFST runtime image quality is show in Table 3. The low-order components of the misalignment and deformation errors are expected to be compensated by the active optics system, and the residual errors are estimated to contribute 0.3″ to the final image quality. The overall image quality is largely dictated by the atmospheric seeing. Assuming a median seeing of 0.75″ at the Lenghu site, the overall image quality is expected to be approximately 1″.

Item	**Image Quality (″)**
Design	0.4
Residual of Active Optics	0.3
Atmospheric Seeing	0.75
Dome Seeing	0.4
Tracking	0.1
Overall	1.0

Table 3 The spreadsheet for the WFST runtime image quality.

In addition to the well-tuned image quality, the optical system also manifests low distortion across the full field. The largest distortions appear in the U and W bands, where the maximum distortions are 0.075% and 0.065%, respectively.

The estimated throughput of the telescope optical system is shown in Figure 7, taking into account the reflectivity of the primary mirror and transmissivity of each individual lens material and coating. The sharp dip at the blue end of the u band is due to the cut-off of the N-BK7 glass beyond 350 nm. The overall throughput, including effects of telescope optics, detector and filters, is also plotted in Figure 7 for different observation bands. The averaged throughput is estimated to be 0.39, 0.72, 0.60, 0.56 and 0.33 for u, g, r, i and z bands, respectively.

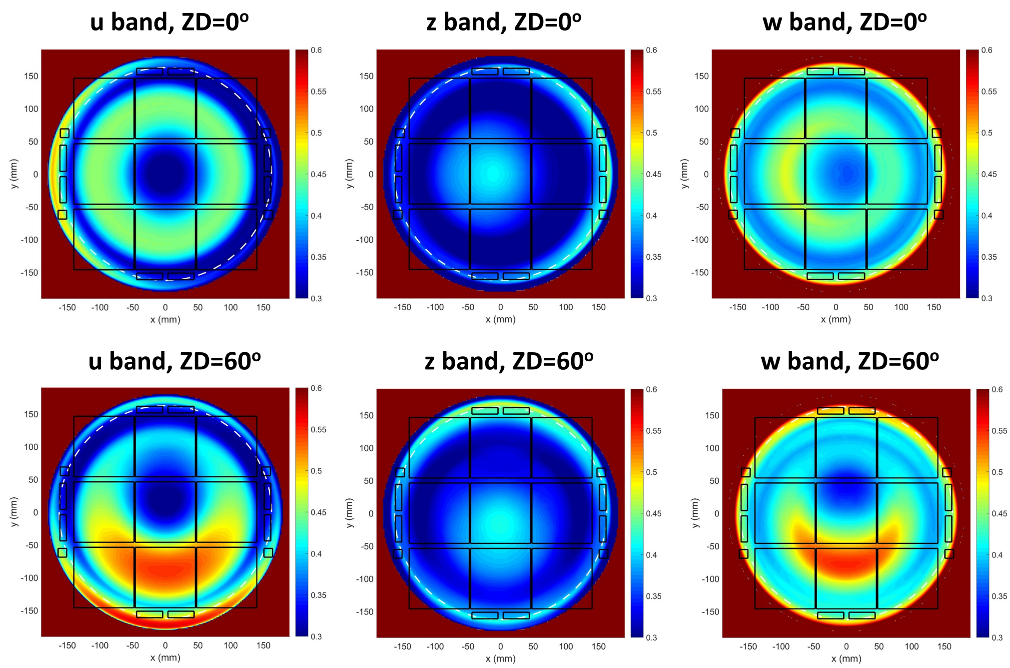

Figure 6 EE80 map for the u, z, and w bands at zenith distances of 0° (upper row) and 60° (lower row). The layout of the focal-plane mosaic CCD chips is also superimposed.

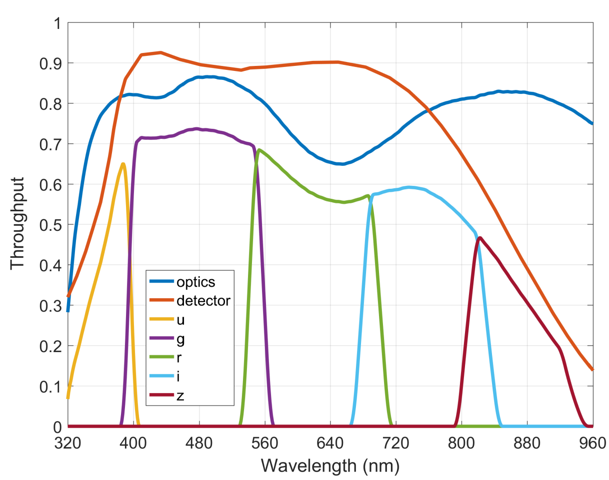

Figure 7 Estimated throughput of the telescope system. ***need more details ***

We estimate the limiting magnitudes that the WFST system can reach based on the system design specifications and relevant data available. We take 22.0 mag arcsec^{-2} as the V band sky background level. There is no sky spectrum observations available for the Lenghu site yet. We adapt a model spectrum obtained from the Gemini telescope web page. Although the atmospheric conditions would be expected significantly different between the mountain area and the oceanic area, this is the only way that we can make this baseline estimate. We check the V band magnitude of the spectrum using a standard Johnson V filter and obtain a value of 20.50 mag arcsec^{-2}. We scale the spectral flux level to a V magnitude of 22.0 mag and take this as the typical sky background emission at the mountain top of Saishiteng. We integrate the spectral flux within each WFST filter passband and obtain the sky contribution to the signal on the detector. An airmass of 1.2 is assumed to scale the atmospheric transmission and the sky emission. An aperture photometry is applied to estimate the limiting magnitudes of the system. The diameter of the aperture is taken as 1.14 times of the FWHM of a point source in each band. The FWHM of each band is computed based on the image quality parameters listed in Table 3. By assuming 64% energy of a point source is contained within the aperture, we compute the point source magnitudes ($\mathrm{Mag_{lim1}}$) that required to make the signal-to-noise ratios (SNR) within the apertures equal to 5 for an exposure of 30 seconds. We also compute the limiting magnitudes ($\mathrm{Mag_{lim2}}$) of stacking images of one hundred 30-seconds exposures with a total integration time of 50 minutes. The results are shown in the Table 4.

Filter	**u**	**g**	**r**	**i**	**z**
$\mathbf{Mag_{sky}}$	22.29	22.12	21.58	21.29	20.29
$\mathbf{Mag_{lim1}}$	22.40	23.35	22.95	22.59	21.64
$\mathbf{Mag_{lim2}}$	24.96	25.89	25.49	25.13	24.19

Table 4 Limiting Magnitudes of WFST.

2.5 Survey Strategy

In this subsection we introduce two major programs of the WFST 6-year survey, the wide-field survey and the deep high-cadence u-band survey, which are designed to meet the constraints imposed by major science objectives of WFST by coordinating the survey depth, area, and cadence. Each survey will use about 45% observing time of the WFST six-year survey. In addition to the major survey programs, we are also considering smaller survey projects, which would use the remaining $\sim$ 10% of the time (about 1,300 hours over six years), for specific purposes such as intensive observations of sky which may not be well covered by the two major surveys (e.g., Galactic plane) and searches for time-critical objects.

The WFST wide-field survey will cover $\sim$ 8,000 deg^2 of sky in the northern hemisphere in five broad bands with a single exposure of 30s, which gives about 108 visits per pointing per band over six years. To achieve a long-term monitoring purpose for specific objects such as active galactic nuclei and variables, the 108 single-band visits will be evenly distributed, i.e., 90 multi-band visits (18 visits $\times$ 5 bands) per pointing per year, corresponding to yearly raw data of $\sim$ 160 TB. Specifically, about 300 different pointings ($\sim$ 2,000 deg^2) with 90 visits per pointing will be observed via the WFST wide-field survey every three months. All u-band observations will be carried out in dark and grey time, as the u band is the band where the most sky background-sensitive measurements are planned. In order to balance the survey efficiency and science goals and to optimize the homogeneity of visits taken from the WFST wide-field survey, we will conduct observations in two bands every night and avoid consecutive observations in the same band except for the u band, which gives a reasonable cadence and time span of multiband light curves for general purposes of transient-related studies, e.g., transient classifications, variability statistics, and time-domain cosmology. On the other hand, the total integration time in each band will reach $\gtrsim$ 45 min over six years, deeper than any single-telescope surveys which have comparable survey area in the northern hemisphere.

To make the best use of the superior u-band imaging performance of WFST for the time-domain astronomy, in addition to the wide-field survey, we plan to carry out the deep high-cadence u-band survey that will routinely monitor $\sim$ 300 deg^2 of sky covered by the WFST wide-field survey in consecutive $\pm$7 days from the new moon every month. Such an innovative survey strategy will provide a unique opportunity of studying transients soon after their occurrences and discovering rare energetic explosive phenomena in the universe (e.g., early-phase supernovae, tidal disruption events, kilonovae; refer §3.1–§3.3 for details). Given the importance of u-band and color information in understanding the nature of various fast transients, our deep high-cadence survey will ensure at least two-band photometries (one must be u band) in hourly cadence. Moreover, together with the next-generation Chinese space missions (e.g., the Einstein Probe (EP) [12]; the Chinese Space Station Telescope (CSST) [13]) that will be launched in the coming years, synchronized multi-wavelength surveys thus can be expected by using both ground-based and space wide-field survey facilities for the first time. By coordinating with EP and CSST observations, we are able to not only promptly identify optical counterparts of various high-energy astronomical phenomena but also get real-time spectral energy distributions of various fast transients via the synchronized multi-wavelength surveys.

Wide-field imaging has become a mainstream tool in various fields of astronomy as can be witnessed by the success of previous/ongoing wide-field survey projects. The excellent survey capability and high u-band sensitivity of WFST opens new opportunities to explore the transient sky, which will add to the legacy by exploring sky in the northern hemisphere with a greater depth and width especially in blue optical wavelengths. A large amount of multi-color light curves with cadences from hours to years enable us to systematically investigate photometric behaviors of transients with different timescales from local to high-z universe. With the six-year u-band data, the final stacked images will reach $\sim$ 26 mag (5σ) for 1,200 deg^2 of sky in the northern hemisphere, which is comparable to the final Rubin/LSST u-band products after 10 years. Together with the WFST wide-field survey, in addition to tens of thousands of multiband light curves, data products such as weak-lensing shape catalogs with photometric redshift and shape information of over 200 million galaxies, $\sim$ 40 thousand photometric selected galaxy clusters, and reference catalogs of astrometry, parallax, proper motion for stars as faint as 23 mag will bring a great legacy value to the entire astronomical community in the era of 20–40m class optical and near-infrared telescopes, wide-field spectroscopic survey facilities (e.g., the MUltiplexed Survey Telescope, the Subaru Prime Focus Spectrograph), and space survey missions (e.g., CSST, Euclid, the Nancy Grace Roman Space Telescope).

3 Time-domain Science

3.1 Supernovae

3.1.1 Supernova Observations, Diversities, and Open Questions

The observation of supernova (SN) has a long history. The first reliable record of an SN can be dated back to AD185, the SN 185, which is recorded in the "Book of the Later Han" by Chinese astronomers. For the next hundreds of years, a few SNe were discovered by chance. The first systematical search of extragalactic transients started from the late 1930s [14] and over 100 SNe were discovered by the Palomar Supernova Search in the following decades [15]. From the 1980s, systematical searches of SNe also started in the southern hemisphere and a significant improvement of the SN detection efficiency starts in the 1990s thanks to the development of Combining charge-coupled devices (CCDs) and the automatic searches with robotic telescopes. As the broad adoption of large-array CCD cameras in various wide-field transient survey projects which focus on SN searches at a wide redshift range [16-23], the discovery rate of SNe has been increasing at an exponential rate in the last two decades. The wealth of SN data has led to significant advancement in our understanding of stellar evolution, SN explosion mechanisms, the chemical enrichment of galaxies, and the fundamental physics of the universe [24-29]. In the coming decade, the rates of transient detections in both northern and southern hemispheres will have growth spurts with wide-field survey projects led by WFST and the Vera C. Rubin Observatory [19, 30], respectively.

Type Ia supernovae (SNe Ia) are widely believed to be the thermonuclear explosion of a carbon-oxygen white dwarf (WD) in a binary system. Even though great success was achieved by using them as a cosmic distance indicator in the 1990s [31-33], the progenitor and the physics leading to the explosion are still under debate [34, 35]. Given that SNe Ia also play a key role in the chemical enrichment of galaxies and the universe [27, 36, 37], the understanding of SNe Ia will further enlighten us on the origin of major chemical species. Currently several progenitor scenarios have been proposed for SNe Ia, which can be generally categorized as the single-degenerate (SD), double-degenerate (DD), and core-degenerate (CD) scenarios. In the SD scenario, a carbon-oxygen white dwarf (WD) accretes materials from a non-degenerate companion star (e.g., a main-sequence or a red giant star) and reaches to the Chandrasekhar's limiting mass [38, 39]. The DD and the CD scenarios involve mergers of two WDs [40, 41] and a WD and an asymptotic giant branch (AGB) star [42, 43], respectively.

The debate between the prevalent progenitor scenarios of SNe Ia has been lasted for a long time. Recently, a growing number of studies suggest that SNe Ia are likely a mixture of the end products of different evolutionary paths. A main issue then is to clarify a relation between different progenitor paths and different SN Ia subclasses. Typical SNe Ia, or "normal" SNe Ia, show a strong correlation between the light curve declining rate and the peak luminosity (the so-called Phillips relation [44]) and their peak luminosities show good uniformity after correcting for this correlation. However, as a tremendous amount of SNe Ia have been discovered in recent years, a considerable number of "abnormal" SNe Ia were reported. The major SN Ia subclasses are SN 1991T-like SNe Ia (91T-like) on the bright end [45, 46] and SN 1991bg-like SNe Ia (91bg-like) in the faint end [47]. Other subclasses including the carbon-rich over-luminous SNe Ia (or "Super-Chandrasekhar" SNe Ia) are even brighter than 91T-like SNe Ia at the peak, which leads to the estimated total mass of ^{56}Ni synthesized in these events exceeds $\sim$1 $M_{\odot}$, and thus a reasonable estimate of the total mass is likely beyond the Chandrasekhar's limiting mass [48-55]. Another subclass of SNe Ia, which has been intensively investigated in the last decade, is SN 2002cx-like SNe Ia (or "SNe Iax" [56-59]). SNe Iax are typically faint, with the luminosities spanning in a wide range between $\sim$-14 and -18 mag. A very rare SN Ia subclass, so-called "SNe Ia-CSM" are spectroscopically similar to Type IIn SNe (SNe IIn) that show blue continuum and strong emission lines of Balmer series, which are clear signatures of SN ejecta expanding into dense circumstellar materials (CSM) [60-62]. Unlike SNe IIn from massive star explosions, the SNe Ia-CSM are explained as SNe Ia exploding within dense CSM and likely relevant to 91T-like SNe Ia [63].

The core collapse of massive stars ($M > 8$ $M_{\odot}$) with retained hydrogen envelopes produces the hydrogen-rich Type II SNe (SNe II), whereas if the hydrogen and sometimes even helium envelopes are stripped we observe stripped-envelope core-collapse supernovae (SESNe). SESNe are classified into Type IIb, Ib, and Ic SNe based on the existences of H and He lines in their spectra [64, 65]. It is not yet clear if SESNe arise from single evolved massive stars or interacting binary systems or both. We are also puzzled by if there is a continuum of properties between SESN subclasses, or if different subclasses represent distinct explosion mechanisms and/or progenitor systems.

Four main subclasses of SNe II, known as SNe IIP, SNe IIL, SNe IIn, and SNe IIb have been identified. SNe IIP ("P" stands for "plateau") display constant luminosity for approximately three months in their light curves and SNe IIL ("L" stands for "linear") show a linear magnitude decline in their light curves [66]. SNe IIn are identified by narrow (few hundred km s^{-1}) hydrogen emission lines with broad bases seen in their spectra [67]. The narrow component of the lines is attributed to slowly-moving CSM ejected by the SN progenitor before explosion. SNe IIn show diverse light curve behavior mainly due to the interaction between SN ejecta and uncertain CSM structures. SNe IIb have been observed to display prominent broad hydrogen lines early in their evolution while later these lines weaken and the spectra become helium-dominated. At later times SNe IIb are similar to SNe Ib, suggesting the progenitors of these "intermediate" events may have experienced a stripping level between those of SNe II and SNe Ib. The observed diversity of SNe II makes us wonder how different are all of these subclasses and how to quantify them. Given that the diversity is most likely relevant to the progenitor systems of SNe II, a further question is what are the different progenitor systems that lead to the different explosions. Despite substantial advancement in our understanding of core-collapse supernovae (CCSNe) in the last few decades, we still do not have a complete picture of their diversity and its mapping to progenitor channels. In addition to the above questions, we also do not yet have an adequate understanding of which CCSNe yield typical pulsars and which yield magnetars, black holes, and gamma-ray bursts.

Through the WFST high-cadence deep imaging survey, tens of thousands of SNe can be expected during the 6-year survey project, and over one hundred SNe within a few days of their explosions ("early-phase supernovae") can be discovered every year (§3.1.6). The great number of well-observed SNe collected by WFST could help us to construct a more complete connection between the evolution of stars and their deaths as SNe.

3.1.2 Early-phase Supernovae

In the last decades, dozens of early-phase SNe Ia discovered by various wide-field survey projects provide unique information about the progenitor system and the explosion mechanism of SNe Ia [28, 55, 68-70]. Theoretically, a prominent brightening in the first few days of the SN Ia explosion can be observed under specific viewing directions due to an interaction between the expanding ejecta and a nondegenerate companion star [71], which makes SNe Ia with additional luminosity enhancement in the early time ("early-excess SNe Ia;" EExSNe Ia) a powerful indicator for the SD progenitor system [71-73]. Since then, surveys for EExSNe Ia have become particularly popular in time-domain astronomy and several EExSNe Ia were successfully discovered since 2012 [28, 55, 70, 74-78].

Theoretically, in addition to the companion-ejecta interaction scenario, an interaction between confined dense CSM and SN ejecta ("CSM-ejecta interaction" [55,79,80]) and vigorous mixing of radioactive ^{56}Ni in the outermost region of SN ejecta ("surface-^{56}Ni-decay" [81, 82]) may produce similar early light-curve excess to that predicted by the companion interaction. Moreover, radiation from short-lived radioactive elements generated by a precursory detonation at a helium shell of the primary WD ("He-shell detonation" or "He-det" [28, 83]) can cause a prominent but relatively red early excess. Previous observations have indicated the multiple origins of EExSNe Ia and the limitation of constraining the origin of the early-excess feature via shallow low-cadence wide-field surveys [28, 55, 78, 84]. Thanks to the deep and wide imaging capability of WFST, we can figure out the progenitor issue of SNe Ia from a unique way—by systematically investigating the light curve from a real early time (i.e., within one day of the explosion).

A major open question for SNe Ia is which progenitor system plays a leading role for yielding SNe Ia. From the early-excess perspective, none of previously discovered EExSNe Ia can be exclusively explained by the companion-ejecta interaction scenario, thus implying a low possibility of the leading position of the SD scenario. Given that only a modest percentage of early-phase SNe Ia can show early-excess emissions under the companion-ejecta interaction scenario due to the viewing angle effect, a large number early-phase SNe Ia discovered by WFST can be used to further test and improve the current companion-interaction models. Moreover, robust evidence of the SD progenitor system can be expected by catching reliable companion-ejecta interaction EExSNe Ia in the near future.

The rise time (i.e., the time from first light to *B*-band maximum brightness) of SNe Ia can be estimated with well-observed early-phase SNe Ia. Statistically, stretch-corrected mean rise time was found to be 17–18 days based on large samples of SNe Ia [85-88], which is in line with studies of individual normal SNe Ia discovered at very early time [68, 69, 89]. With an even larger sample of early-phase SNe Ia, a large scatter of rise times with a mean value of 18.5 days (without stretch correction) was reported by the Zwicky Transient Factory (ZTF) recently [90]. In contrast, EExSNe Ia usually show longer rise times than the mean values obtained from statistics [28, 70, 75], suggesting the existence of a long dark phase of some SNe Ia [91, 92]. With dozens of SNe Ia discovered within about one day of their explosions every year, the WFST early-phase SNe Ia will provide the tightest rise-time constraint of SNe Ia, which may put in the last piece of the earliest radiation puzzle of the SN Ia explosion.

The earliest electromagnetic emission of SNe, known as the SN shock breakout (SBO), only can be observed in the first minutes to hours after the emergence of the shock from the stellar surface for CCSNe. The strength of the CCSN SBO can be used to derive the radius of the exploding star and thus conveys important information about the final evolution and structure of the progenitor [93-95]. Due to the short duration of the SBO, only one event was certainty discovered by ground-based wide-field imager so far [96]. With WFST high-cadence transient survey, we expect to understand the physics of the emergence of CCSN SBO and reproduce the structure of dying massive stars by catching multiple CCSN SBOs every year.

3.1.3 Fast Transients and Interrelationships with Core-collapse Supernovae

Transients with very fast brightness variance in UV and optical wavelengths are of great interest in time-domain astronomy as their extreme photometric behavior not only can be used to investigate the physical properties of their progenitors but also suggests the existence of theoretically-predicted/unknown astronomical objects in the universe. They mainly include (1) specific kinds of CCSNe (e.g., some Type Ib/IIb/Ibn supernovae [97]) which shows much faster light-curve evolution than most of SNe, (2) a newly confirmed transient type, so-called fast blue optical transients (FBOTs) or fast-evolving luminous transients (FELTs) [98], and (3) optical counterparts of binary neutron star mergers, i.e., kilonovae (refer to §3.3).

Recent studies confirm that there are at least two distinct subclasses of FBOTs. One with comparable peak luminosities to typical SNe (hereafter "normal FBOTs," the vast majority of FBOTs discovered in the past) and the other with peak bolometric luminosities $\sim 10^{44}$ erg s^{-1} (hereafter "ultra-luminous FBOT," e.g., AT 2018cow [99]). The normal FBOT likely originates from the CCSN SBO within dense circumstellar materials surrounding a progenitor [98, 100]. If so, the fast-evolving light curve of normal FELTs implies a dramatic mass-loss process in the last few years before the core collapse of the progenitor. By using photometric and spectral information of a considerable number of normal FELTs discovered by WFST in the coming years, the explosion mechanism of normal FELTs and the mass-loss history of massive stars can be systematically investigated.

The origin of ultra-luminous FBOTs is under active debate as the extremely high luminosity and fast-evolving light curve cannot be explained as an extension of the properties of SNe [101-103]. Thus, several alternate mechanisms have been proposed to explain the properties of ultra-luminous FBOTs, which include emission from the interaction of the SN shock wave with a dense CSM [104-106], the injection of energy from spin-down of a young magnetar formed either in a CCSN or a binary neutron star merger [107, 108], accretion onto a newly formed compact object in a failed supernova [104], mergers of binary white dwarfs [109], and tidal disruption of stars by intermediate-mass black holes ("IMBH TDE," see §3.2.3 for details). Recent studies found that ultra-luminous FBOTs usually show prominent accompanying emissions in both X-ray and radio wavelengths, suggesting a compact object in the center of FBOT [102, 104, 110]. Given a very low event rate in the local universe and a much higher luminosity in UV wavelengths of FBOTs, the WFST high-cadence deep u-band survey will be the most promising project to systematically search ultra-luminous FBOTs in the 2020s.

3.1.4 Extreme Supernovae

Superluminous supernovae (SLSNe) show peak luminosity of $\lesssim$ -21 mag in optical [111]. Most of SLSNe are over 100 times more luminous than typical SNe Ia and CCSNe. Due to the low event rate of SLSNe, the first discovery of this extreme SN class was in 1999 [112]. Then, several SLSNe have been occasionally discovered in the 2000s. In the last decade, over 100 SLSNe were confirmed thanks to the unbiased transient surveys with large-array CCD cameras [113, 114]. Observationally, SLSNe show a natural division between hydrogen-poor (SLSNe-I) and hydrogen-rich events (SLSNe-II). Most SLSNe-II show narrow lines (SLSN-IIn), which are similar to those of less luminous SNe IIn [25, 115, 116]. Therefore, they are believed to be extreme cases of SNe IIn whose luminosities are mainly powered by the interaction between ejecta and dense CSM. SLSNe-I are less well-understood, and the physical processes that dominate these explosions are still under debate [113, 117].

A major open question of SLSNe is the energy source powering these extremely luminous and long-lived events. Is a central engine necessarily required to explain SLSNe? If so, what kind of central engine(s) (e.g., magnetar, an accreting black hole, or both) are at work? To figure out these questions, keep enlarging the sample size via high-cadence deep imaging surveys and well-organized follow-up observations is definitely needed. With the 6-year WFST wide-field survey project that will regularly monitoring the northern hemispheres with a cadence of a few days or less, SLSNe at $z \lesssim 1$ should be detected with high completeness thanks to their long-lasting and luminous light curves. Moreover, given the high UV luminosity of SLSNe and a higher event rate as the redshift gets higher (at $z \lesssim 2$), The superior u-band sensitivity and the moderate telescope aperture ensure that WFST the most powerful facility of searching SLSNe at $z \lesssim 1.5$ in the northern hemisphere. SLSNe at high redshift could be a focus of attention in the 2020s not only for the time-domain astronomy but for investigating the star formation history in the high-z universe. Moreover, they may become useful distance estimators for the cosmological measurement in the future [118-120].

An extremely luminous SN type predicted by theory, known as the pair-instability SNe (PISNe) still remains elusive. PISNe are the predicted explosions of massive stars with zero age main sequence (ZAMS) masses of about 130–260 $M_\odot$. They are caused by the high core temperatures in massive stars where electron–positron pairs are copiously produced that in turn result in contraction of the core, followed by explosive oxygen burning that unbinds these ultramassive stars eventually [121-123]. For stars with slightly lower ZAMS masses of 90–130 $M_\odot$, the progenitor can experience multiple non-destructive pair instability episodes that expel material prior to the final core collapse. These pulses can lead to shell collisions that power a SN-like transient. The succession of shell ejections may also be followed by a PISN, the ejecta of which collides with the previously ejected shells. This repetitive shell-collision process, with or without a final PISN, is called a pulsational pair-instability SN (PPISN [124]). Although PISNe and PPISNe belong to the most luminous SN types, only a few candidates were reported due to the difficulty of generating the massive progenitors of PISNe and PPISNe in the low-z universe [125, 126]. Thanks to the large field of view and deep imaging capability of WFST, the sample size of PISNe/PPISNe and candidates can be greatly increased during the 6-year WFST survey project.

3.1.5 Cosmology and Gravitational Lensing

After two decades since its discovery, the nature of dark energy remains as a mystery. There are three ongoing/upcoming large projects for measuring cosmological parameters with SNe Ia: the Hyper Suprime-Cam Subaru Strategic Program (HSC SSP [127, 128]), the Rubin Observatory Legacy Survey of Space and Time (LSST [30]), and the Roman Space Telescope. However, none of them will provide an optimal SNe Ia sample at redshift below 0.5 for cosmological parameter measurements. Roman will find very limited low-z SNe while the nominal-cadence survey strategies of HSC SSP and Rubin LSST will create large multiple/single-filter gaps in their low-z SN light curves that would make SN Ia standardization less accurate. Therefore, a large, unbiased WFST SN Ia sample observed with relatively high-cadence (e.g., 3 days or shorter) will further reduce the uncertainty in the dark energy density measurement in the $0.1 < z < 0.5$ redshift bin, allowing a significant comparison with the well-constrained $z < 0.1$ bin. The WFST SN Ia sample could also be used to refine and extend new models for SN Ia standardization [129-131] and to better constrain relationships between SN Ia distance measurements and host galaxy properties [132, 133].

Among the wide range of independent cosmological probes found in the literature, SNe II are becoming a promising independent method for deriving accurate distances and measuring cosmological parameters. Even though SNe II display a large range of peak luminosities, several methods have been developed to standardize SNe II, such as the expanding photosphere method [134], the standard candle method (SCM [135]), the photospheric magnitude method [136], and the photometric color method (PCM [137]). As the most common and currently the most accurate method used to derive SN II distances, SCM enables us to construct a Hubble diagram with a dispersion of ∼10 percent in distance, suggesting that SNe II are a potentially useful complementary and independent method to constrain the nature of dark energy. Given that previous SN II Hubble diagrams based on the SCM mainly focus on relatively low-z universe ($z < 0.2$) where the differences between the expansion histories are very small, measurements extending far back in time, i.e., SNe II at higher redshift, are required to distinguish among the different cosmological models. With hundreds of WFST SNe II discovered at $z > 0.2$ in the coming years, we are able to directly compare with SN Ia measurement results in the $0.2 < z < 0.4$ redshift bin.

Recent discoveries of strongly-lensed SNe opened up a new frontier in studies of cosmology and early-phase SNe. Strongly-lensed SNe are events where multiple light rays from an SN get converged by the gravity of an intervening object such as a galaxy or a galaxy group/cluster and form multiple lensed SN images. A notable feature of such systems is that there are relative time delays among lensed SN images due to different light paths. It has been well recognised that the time delay of strongly-lensed SNe can be utilized as an independent probe for the Hubble constant H_0 [138]. Nevertheless, before the discovery of the first strongly-lensed SN in 2014 [139], this "time-delay cosmography" technique has only been applied to strongly-lensed quasars, for which time delays can also be measured (§**??**). The most recent work has achieved a 2.4% precision measurement of H_0 from the combination of six strongly-lensed quasars [140], demonstrating that time-delay cosmography is a competitive and complementary approach for measuring H_0. Compared to quasars, time delays can be more easily measured from lensed SNe thanks to their characteristic light curves. Additionally, given that SNe will eventually disappear, more precise lens models can therefore be obtained by analysing systems without contamination from transients themselves. As a result, strongly-lensed SNe are expected to provide tighter constraints on H_0 [141, 142]. In addition, strong-lensing time delays offer a unique approach of studying SNe soon after their explosions. Once a lensed SN is discovered, follow-up observations can be scheduled well in advance to track the entire explosion process of trailing SN images.

To date, only four strongly-lensed SNe have been discovered [139, 143-145], and two of them were successfully used for inferring time delays. A deep wide-field imaging survey with WFST will substantially increase the sample size of strongly-lensed SNe. According to Oguri et al. (2010) [146], over 20 strongly-lensed SNe are expected to be discovered during the 6-year WFST wide-field survey project. With dozens of WFST strongly-lensed SNe in the 2020s, we are embracing new opportunities in studies of cosmology and

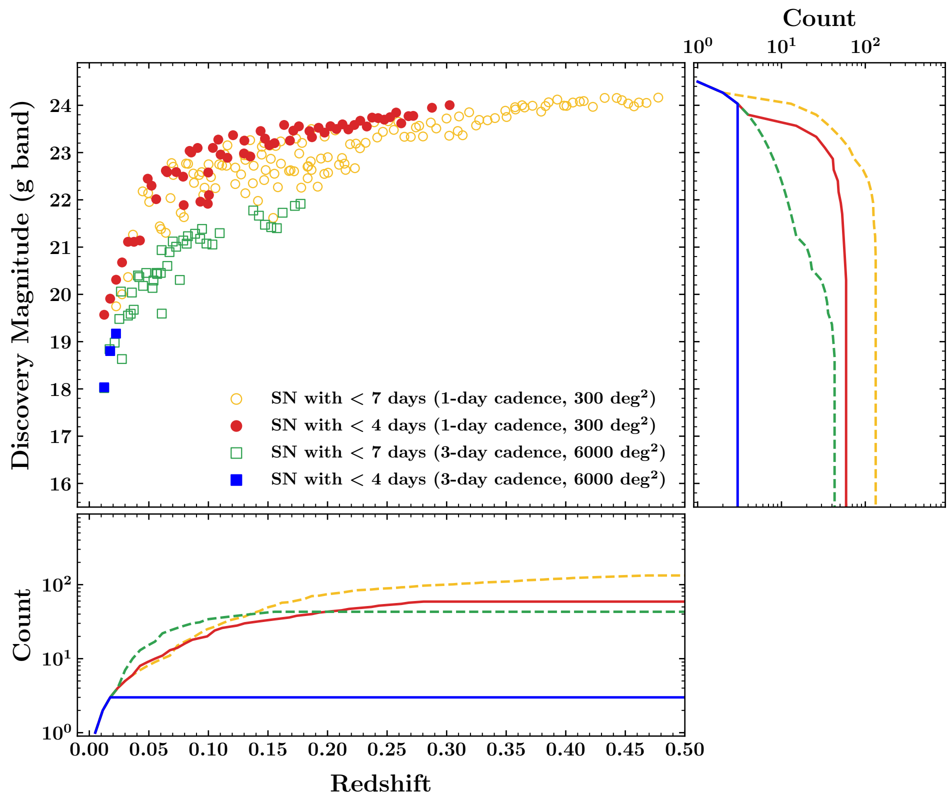

Figure 8 Expected distributions of SNe Ia in the space of redshift and discovery magnitude with WFST 1-day (circles) and 3-day (squares) cadence surveys. The SNe are divided into two groups regarding the time of the second detection t: open and solid symbols correspond to SNe discovered with $t < 7$ days and $t < 4$ days, respectively. Right and bottom panels show corresponding cumulative numbers to the discovery magnitude and SN redshift, respectively.

early-phase SNe.

3.1.6 Supernova Search with WFST

There are three key factors of transient surveys: depth, area, and cadence. By coordinating the three factors, we can maximize the time-domain-related scientific outputs from the WFST survey project. For most of previous/ongoing transient surveys, the biggest shortages are the limited survey depth with small-aperture (< 1.5m) telescopes or the low survey cadence with large-aperture telescopes, which indeed prevent us from systematically investigating photometric behavior of early-phase SNe and fast transients which show faint brightness and fast-evolving light curves in minutes to a few days. Thanks to the large field of view and the moderate aperture of WFST, such interesting objects can be efficiently discovered via the WFST high-cadence deep-imaging survey.

Here we present one-year WFST survey simulations with 3-day and 1-day cadences, corresponding to the wide-field and deep high-cadence surveys, respectively (Figure 8). In order to obtain color information in each observable night, our simulations simply assumed that the telescope monitors the same sky area in at least two bands (e.g., u and g) at the same night. The clear night rate, moon-phase influence, and target visibility were considered in the simulation. To roughly show the SN detection efficiency with WFST, our estimate only focus on normal SNe Ia which have well-established light curve and spectral templates. The SNe were stochastically generated at different redshifts following the event rate derived from local SN Ia samples [147]. The SN Ia light curves were constructed through synthetic photometry by using Hsiao's spectral template [148]. Regarding the dispersion of intrinsic luminosities among SNe Ia, we assumed a uniform distribution of absolute magnitude at maximum light from -18.5 to -19.5 mag. Finally, a random foreground extinction from Milky Way and host galaxy was configured for each SN.

In the simulation, we define a real SN detection when an SN candidate is detected at least twice in different nights. Figure 8 shows distributions of SNe Ia in the space of redshift and discovery magnitude based on two survey modes. Note that the time t shown in the figure is defined as the time of the second detection of an SN. As our major targets, SNe with $t < 4$ days (early-phase SNe; solid symbols) will be intensively observed by other observing facilities in the following few months to get detailed multiband light curve and spectral information. The other group of SNe Ia with $t < 7$ days (open symbols) mainly consists of SNe Ia expected to have good coverage of multi-color light curves from ∼10–14 days before the peak, which will be used for statistically investigating the light-curve behavior of SNe and the SN cosmology in a wide redshift range. In the simulated one-year WFST survey, we expect to discover ∼xxx SNe Ia at z $\lesssim 0.25$ in $t < 7$ days, and particularly ∼xxx early-phase SNe Ia at z $\lesssim 0.1$x via a 1-day cadence survey. The number of early-phase SNe Ia is about xx times larger than that discovered from a 3-day cadence survey, indicating the significance of the deep high-cadence survey for searching early-phase SNe (and other fast transients).

3.2 Tidal Disruption Events

3.2.1 Observational Status and Open Questions

One breakthrough in transient study of the past decade is the detection of a fast-growing number of tidal disruption events (TDEs). A TDE occurs when a star occasionally wanders into the tidal sphere of the supermassive black hole (SMBH) in a galaxy center. The star will be tidally disrupted and partially accreted, producing a flash of electromagnetic radiation on timescales of months to years [149-151]. The event rate is lower than supernova by a factor of hundreds, i.e., $10^{-4} - 10^{-5}$ gal^{-1} yr^{-1}, making TDEs a class of rare transients.

Although being theoretically predicted in 1970s, TDEs were not discovered until late 1990s from the archival ROSAT data [152] as well as a few more subsequent events from XMM-Newton and Chandra (see a recent review [153]), guided by the anticipated radiation peak in soft X-ray or extreme UV bands. However, those TDEs were all found serendipitously from archival data and have scarce synergetic information in other wavelength regimes (see recent progress from SRG/eROSITA survey [154]). Thanks to a variety of wide-field optical surveys dedicated to time-domain surveys, the past decade has seen an explosive growth of TDEs (see recent review of [155, 156]). Particularly, the ZTF survey has raised the discovery rate of TDEs from $\lesssim$2/yr to >10/yr, opening up a new era of statistical studies [157]. Moreover, optical TDEs are discovered in real time now, enabling timely multiwavelength follow-ups.

The study of TDEs has aroused great interest because of its unique scientific values. First of all, TDE provides direct evidence for a SMBH in a quiescent galaxy beyond the current probing regime based on stellar or gas dynamics, particularly in a dwarf and distant one. It is capable of probing even dormant intermediate-mass BHs (IMBHs) and SMBH binaries[158-160]. Moreover, TDE can also serve as an ideal laboratory to explore the accretion physics of SMBHs, i.e., unsettled issue in AGNs, by observing the whole life cycle of BH activities, even witnessing the formation of jets [161, 162]. Monitoring evolution of gas, infrared and radio echoes of TDEs provides a novel approach to study the sub-parsec environments of these distant quiescent SMBHs [55, 163, 164], which is inaccessible with other techniques. Last but not least, in the multi-messenger era, TDE has been considered as an important astrophysical process for the origin of high-energy neutrinos[165] (see more in §3.3.4).

In spite of remarkable progresses and rich scientific values, there are still lots of open questions to be settled. First, the TDEs found so far have show an unexpected preference for post-starburst (or so-called "E+A") galaxies [166], which can not be addressed by known selection effects. Second, the total observed energy is one to two orders of magnitude lower than theoretical prediction, leading to the "missing energy" puzzle [167]. Actually, the origin of the bright UV-optical emission is still a highly debated topic, awaiting for more observational constraints. The associated issue is the connection between optically-selected and X-ray-selected TDEs, i.e., whether there is a simple model to unify them [168,169]. From the observational point of view, the mounting number of nuclear transients, both in normal and active galaxies, has also raised a general question, that is, how to classify these transients into different types of SMBH transient accretion events, such as TDEs, turn-on AGNs and sporadic gas accretion [170]. WFST, in synergy with other multi-wavelength and multi-messenger time domain facility in the upcoming decade, offers us a unique opportunity to answer these and many other challenging questions.

3.2.2 Demography of Dormant SMBHs Revealed by Large TDE Samples

As a direct probe of SMBHs, TDEs can shed light on the distribution(s) of mass (and even spin) of dormant SMBHs [171, 172], which constitute the bulk of SMBHs in the low-redshift universe. However, the sample size of known TDEs is yet too small ($\lesssim$ 100 up to now [156]) to achieve meaningful demography, a larger and more complete sample is desired.

The success of ZTF has proven that high-cadence and multi-band observations on the same night will greatly benefit the TDE search, by providing critical information on both the color and its evolution. In comparison with potential contamination, TDEs show obviously bluer and more steady color than supernova and usual AGN variability [157]. WFST has the potentiality to go further than ZTF on this way with its deeper depth, the availability of u-band, higher photometric accuracy and a better imaging resolution. Particularly, its

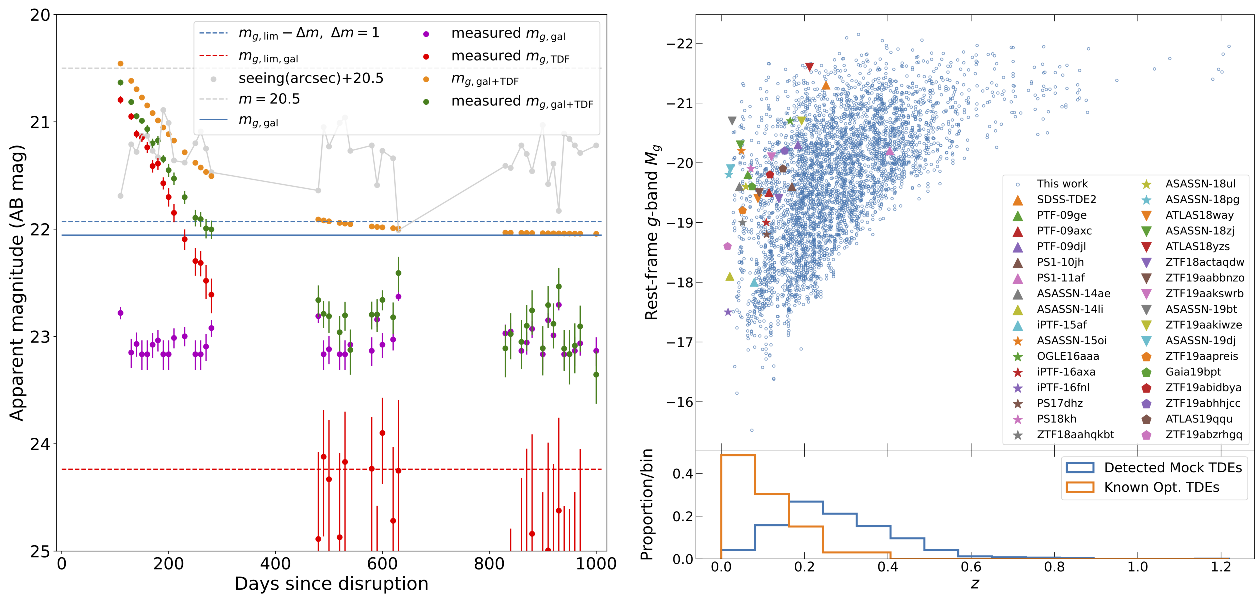

(a) (b)

Figure 9 (a): The g-band light curves of a TDE at $z = 0.253$ as an example of our mock observations. (b) top: The peak absolute g-band magnitude (M_g) as function of redshift for TDEs detected in our mock observations. The 33 optical TDEs summarized in Table 1 of [155] have been also overplotted for comparison. (b) bottom: the histograms of TDE redshift in the mock and known sample.

high sensitivity in u-band, which is the closest band to the SED peak of TDEs, is unique among surveys in the Northern Hemisphere and could play a crucial role in the discovery and characterization of TDEs.

In order to assess the prospect of TDE discovery ability quantitatively, we have performed mock observations by taking into consideration of site conditions, telescope parameters and survey strategy. We start from the billions of galaxies in the 440 deg^2 CosmoDC2 field [173], with assigned TDE event rate for a given galaxy by BH mass[174]. The TDE light curves are generated by the empirical model `MOSFiT` [175]. We assume a uniform survey strategy for the experimental 440 deg^2 field, which will be scanned with 30-second exposures every 10 days at u, g, r, i, z band, respectively. The "observation windows" ($\sim$ 180 days in one year) and the clear night proportion, assuming 70% defined as more than 4 hour of contiguous fully clear time [11], have been also taken into account. In addition to a seeing distribution consistent with on-site monitoring, we have simply applied a sky background of 22.0 mag/arcsec^2 and readout noise of 10 e^-/pixel.

We define that the discovery of a TDE (see the g-band light curve of an example in Figure 9) requires at least: 1) the host galaxy is detectable in the reference image in one band; 2) the excess in the galactic nucleus should be significant in 10 epochs and 2 bands. We have performed 100 mock observations and found that the band combination of g, r is most effective. If we choose the combination of u, g, r, i bands conservatively, aiming to obtain more comprehensive SED information (particularly the u band), it will yield 40 ± 6 TDEs in the CosmoDC2 field, equivalent to a detection rate of 529 ± 81 per year for the whole main survey.

WFST will not only contribute to the growing number of TDE, but also substantially extend the redshift range to $z \sim 1$, as suggested by our mock sample. After a planned five-or-ten-year survey, we expect to obtain a uniformly-selected sample of thousands of TDEs. Combining with the host galaxy properties learned from WFST stacking and CSST high-resolution images, the sample will allow us to probe the occupations of SMBHs among different types of galaxies, and constrain their mass functions in the local universe, which is vital for deciphering the formation and growth history of SMBHs.

3.2.3 Hunting for IMBHs by TDEs

SMBHs are believed to have grown from much smaller seeds. It is generally accepted that IMBHs, with mass in the range of $\sim 10^2 - 10^5\ M_\odot$, are formed shortly after the formation of first generation galaxies. Moreover, exploration and confirmation of IMBHs will certainly advance our understanding of the BH family in the universe as a whole by bridging the gap between SMBHs in galactic nuclei and stellar black holes in binaries. However, the unambiguous IMBHs found so far are still very rare and their formation mechanism is poorly understood[176].

The reported IMBH candidates have been exclusively noticed by their AGN features yet their inactive counterparts have been almost overlooked. The stellar TDEs by IMBHs may provide a unique opportunity for uncovering the dormant IMBHs, which has been tentatively employed to explain the X-ray outburst in an off-centered massive globular cluster or or an ultra-compact galaxy resulted from a minor merger[158]. In addition to normal (main-sequence) stars, white dwarfs (WDs) can be also tidally disrupted by IMBHs and may produce distinctive features. It has been proposed that thermonuclear explosions of WD induced by the strong tidal- compression of IMBH will manifest them as optical transients similar to SNe Ia[177, 178]. As a result, it is possible that some WD TDEs have been misclassified as normal Ia supernovae in the past. Making a distinction between them seems difficult solely through optical emission while they probably show different signatures in other bands, i.e., the X-rays from latter accretion in the WD TDE scheme.

As introduced in §3.1.3, the physical mechanism behind ultra-luminous (peak bolometric luminosity $\gtrsim 10^{44}$ erg s^{-1}) FBOTs, represented by AT 2018cow, is fairly controversial. The IMBH TDE has been suggested as a possible scenario although it would require unusually long-lasting emission of highly super-Eddington accretion[179, 180]. The final solution to the nature of FBOTs might be in two folds: one is to find them early and trigger prompt observations in other wavelength regime (e.g., X-ray, radio), the other is to perform statistical analysis based on a large sample. However, the number of AT 2018cow-like FBOTs to date remains a single digit[181-185] and thus discovering more is highly demanding for a comprehensive understanding. If the IMBH-TDE scenario turns out to be true, the ultra-luminous FBOTs will become a direct, and likely the most efficient, probe of off-centered IMBHs. The defining blue ($g - r < -0.2$ at peak) and fast-evolving characteristics of FBOTs make them ideal targets of deep u-band high-cadence surveys (see details in §2.5). In a 300 deg^2 deep survey field, the expected FBOT number will be tens to hundreds per year in spite of large uncertainties from event rate[186], making WFST one of the most competitive surveys for observing FBOTs and for investigating their origin.

3.2.4 Other Opportunities

Light curves on the rising phase can provide valuable clues on the BH mass, disrupted star mass and even the BH spin[187] but they are poorly explored. ASASSN-18pg, which falls luckily in the TESS field, remains the only TDE with a continuous daily sampled light curve before the peak[188]. On the other hand, the challenge of TDE study in the WFST and LSST era becomes how to distinguish TDEs from other transients and coordinate limited follow-up resources for events with greater scientific values as early as possible. However, regular surveys with cadence of days to weeks is not optimal to discover TDEs at the early rising stage. The planned deep high-cadence field of WFST will be an ideal choice to make progress in this topic.

The timeline of WFST meets ideally with the Einstein Probe[189], that is particularly encouraging for TDE study as the optical and X-ray are absolutely dominant discovery bands in the past decades. It is still not clear whether the optical and X-ray bright TDEs belong to distinctive populations or they can be interpreted in a unified picture, e.g., by the orientation effect[168] or dynamic evolution[190]. Previous studies of TDEs are relatively separate in wavelength regime because of lacking dedicated time-domain surveys carried out simultaneously in both bands. Optical TDEs unveiled in real time have been only monitored in X-ray for a short period after their discoveries. The joint analysis of WFST and EP will hopefully offer us an unprecedented large sample of TDEs with both high-cadence light curves (or upper limits) and their luminosity functions in the optical and X-ray bands.

Besides classical TDEs concerned when a star plunges into tidal radius, it can be also partially tidal disrupted near outside the radius, with only its envelope stripped and ripped apart, leaving behind a compact core. The event rate of partial TDEs should be certainly higher than normal TDEs while it is challenging in observations due to its low luminosity. Recent study shows that there might be dozens of partial TDEs detectable in ZTF survey every year[191], which has been however overlooked if they indeed exist. Given the WFST sensitivity power of detecting weak optical emission, we expect to discover an even larger number of partial TDEs. The issue becomes how to identify them out of massive nuclear transients and to confirm them eventually. Partial TDE scenario has been also proposed as a possible explanation for intriguing periodic optical flares found in the galactic nucleus[192].

The IR echoes of TDEs have proven to be effective for tracing the (sub)parsec environments of SMBHs in normal galaxies which are otherwise extremely difficult to probe[163, 164]. The statistics of environmental differences between quiescent and active galaxies is an essential pathway to explore the triggering and fueling mechanism of AGNs[55]. However, the serious preference to post-starburst galaxies of known TDEs has prevented from a comprehensive characterization because of the absence of star-forming and passive galaxies. WFST will help construct a more complete TDE sample, by containing much more optically-weaker TDEs. The dust and gas echoes basing on a more unbiased sample can shed light on a panoramic picture of the pc-scale environment of SMBHs in various types of galaxies, which will ultimately facilitate our understanding of the activity of SMBHs.

3.3 Multimessenger Events

Stellar transients involve the transients produced during various processes of the stellar evolution, including those during the explosive death, such as SNe, and Gamma Ray Bursts (GRBs), those produced by the compact objects after the explosion, such as pulsars, possibly Fast Radio Bursts (FRBs), as well as those related to the merger of binaries, such as Gravitational Wave Events (GWE). Among them, SNe and GRBs are possibly related to the neutrino events. We report the possible observation of them in this section.

3.3.1 Gravitational Wave Events

The observations of GW170817 [193], GRB 170817A [194, 195] and AT2017gfo [196-215] opened a new era of GW multi-messenger astronomy. Electromagnetic (EM) counterparts to GWE are of great importance in the study of extreme relativistic physics, standard sirens' redshift measurements, etc. In this subsection, we present the prospects of WFST in the search for optical counterparts of GWE.

Kilonovae During the coalescence of binary neutron star (BNS) and part of neutron star-black hole (NSBH) binaries, neutron rich ejecta are released through shocks at the contact interface [216-218], tidal interactions [219, 220] and disk outflows [221-223]. Through the rapid neutron capture (r-process) nucleosynthesis, heavy elements form and decay in these ejecta [224], which power a rapidly evolving, roughly isotropic thermal transient 'kilonova' [225].

The observations of AT2017gfo [196-215], together with GW170817/GRB 170817A [193-195], confirmed the origin of BNS mergers as kilonovae. Beyond AT2017gfo, many kilonova signals have been identified from the GRB afterglows [226-231].

The search for more kilonovae will help us to measure the redshift of GW event, explain the origin of heavy elements in universe, study the nature of ejecta and merger remnants, and constrain the NS equation of state (EOS). We simulate 10000 BNS merger samples in the redshift range $z \in (0, 0.2)$ to analyze the detection capability of WFST for kilonova.

A binary neutron star merger, if the merger remnant object is a strongly magnetized millisecond pulsar (or millisecond magnetar), would lead to a kilonova and an afterglow that are brighter than those from the decay of radioactive heavy elements and the interaction of a relativistic jet and its ambient medium [232-234]. This would provide new constraints on the equation of state for dense neutron star matter, showing that the equation of state could be very stiff. In recent years, the Hubble constant constrained from the type-Ia supernova observations is very inconsistent with that from the CMB observations. This is the well-known Hubble constant tension. These electromagnetic signals together with the gravitational waves from a binary neutron star merger would further provide an independent and unique probe of the Hubble constant [235]. This would undoubtedly help solve the Hubble constant tension.

During the dynamical time, BNS mergers eject neutron-rich matter through shocks at the contact interface [216-218] and tidal interactions in the equatorial planes [219, 220]. Generally, the tidal ejecta will have a sufficiently low electron fraction $Y_e \lesssim 0.25$, with the production of heavy nuclei [217, 236-238]. These ejecta are lanthanide-rich, with a high opacity [239] and named as 'red' components. The polar ejecta will have a larger electron fraction ($Y_e \gtrsim 0.25$) because of the effects of $e^{\pm}$ captures and neutrino irradiation [220, 240, 241]. These ejecta are denoted as 'blue' components due to the lack of heavy nuclei synthesis and bluer colors. After a BNS merger, an accretion disk is formed around the central NS or BH remnant [241]. A fraction of the disk mass will be ejected by the neutrino-heated winds [221, 222] and spiral density waves [223]. The electron fraction and opacity of these ejecta lie between the 'red' and 'blue' components [242], and therefore noted as the 'purple' components.

In NS merger (DNS or BHNS), the binary chirp mass is one of the best measured parameters by GW signal, while the type and mass ratio of two companions is poorly constrained. The properties of kilonova ejecta, which are sensitive to the types of merger and the mass ratio, can be used to diagnose the properties of progenitor. With more samples, the gap between NS and BH can be filled [243]. In DNS merger, the remnant can be a stable NS, a supramassive NS supported by solid body rotation, a hypermassive NS supported by differential rotation or undergo prompt collapse into a BH, depending on the EOS and total masses of the DNS[244]. The mass boundaries of stable, supramassive, hypermassive NS and BH play important roles in probing the realistic EOS.

Using the mass distributions of Galactic double neutron stars fitted by [245] and EOS from GW170817/AT2017gfo constraints [246], we calculate three components' mass and velocity following the estimations in [242, 247, 248]. Using the Modular Open Source Fitter for Transients (`MOSFiT` [175, 249]), we obtain these samples' kilonova light curves. We also calculated their GW signals and the signal-to-noise ratio (SNR) when observed by the second generation (2G) GW detector network. We denote the network of advanced LIGO-Livingston/Handford and advanced Virgo as LHV, and the network of LHV, LIGO-India and KAGRA as LHVIK.

In Fig. 10, we show the distributions of kilonova maximum magnitudes and the corresponding times for BNS mergers with LHV's SNR > 10. Two dashed lines in each panel represent the single-visit depth of a 30s exposure time for WFST and LSST [250]. The redshift limit of LHV is ~ 0.12. WFST can observe kilonovae at a maximum redshift of ~ 0.06 in r band. From the i-band and z-band panels, we can see the maximum magnitude time are concentrated around 1 and 3 days. This is because the fraction of 'red'/'blue' components is strongly influenced by the mass ratio. For BNS with unequal mass ratio, the less massive NS is tidally disrupted before contact, which suppresses the production of shocks and 'blue' components. The 'red' component has a greater opacity and the photons take more time to diffuse, so the kilonova dominated by it takes more time to reach maximum luminosity. Therefore, the i band and z band observations will help us to understand the color evolution of kilonova and the nature of ejecta. Fig. 10 also shows that the u band will reach its maximum magnitude within a few hours. A quick search in the u band will help us to study the evolution of the kilonova in the first few hours, which was missed in the AT2017gfo observations.

Assuming a $80-810$ Gpc^{-3} yr^{-1} local BNS merger rate [251], an observable area of $\sim$ 50% of the whole sky per night, and $\sim$ 70% observable nights, we show the number of BNS mergers per year with observable GW signals and kilonova in Table 5. For WFST and LHV, the multi-messenger observation rates are $\sim 1-13$ per year in g and r bands. The results of u band and i band are slightly worse than r band. The sensitivity of WFST in z band is relatively poor, so this band appears to be unusable in the search for kilonova. The search for kilonovae should concentrate on the u and g bands in the first few hours, in particular u band, and then move to r and i band, especially for those red kilonovae.

Gamma-ray bursts and afterglows For the high-z events, the expected EM counterparts are the short-GRBs (sGRBs) and their afterglows. However, GRBs are believed to be beamed: the gamma radiation is emitted in a narrow cone more or less perpendicular to the plane of the inspiral. Therefore, only a small fraction of BNS mergers are expected to have observed GRBs and afterglows. In [252], we studied the detection rate of distributions of BNS mergers which can be observed by both GW detectors, γ-ray detectors (EP [189]; GECAM [253]; Swift-BAT [254]; SVOM-ECLAIRS [255]; Fermi-GBM [256]), and the optical telescopes for their afterglows (WFST, LSST). We simulated 10^7 BNS mergers in $z \in (0, 0.3]$ and assumed that they all have a Gaussian-shaped jet profile [257], which is supported by the observations of GW170817/GRB 170817A [258-262].

Table 6 lists the the multi-messenger observation rates per year. For LHV, the rate is 0.042-0.425 per year with Swift-BAT and 0.072-0.731per year with SVOM-ECLAIRS. For GECAM and Fermi-GBM, the rates are a few times larger due to their much larger observation areas. The result of EP is slightly worse than Swift-BAT due to its smaller observation area, although it has better sensitivity. After adding Kagra and LIGO-India, the rates of LHVIK are about twice as large as LHV. We select the BNS samples that can be triggered by both GW interferometers and γ-ray detectors and choose the GECAM result as a representative one, show its redshift and inclination angle (ι) distribution in Fig. 11.

After that, we use the standard afterglow models [263] to estimate afterglows on the r band. A phenomenon named jet break is expected when Lorentz factor γ drops below jet's half-opening angle θ_j and materials in jet begin to spread sideways [263, 264]. For an on-axis observer, the light curve is divided into two power-law segments by the jet-break time. For an off-axis observer, the light curve reaches a peak after jet break time and decreases in a power-law thereafter. For off-axis samples, we calculate the afterglows' maximum r-band magnitude M_r. However, for on-axis GRB samples, their afterglows' power law decays with time and we cannot get their maximum M_r from their light curve, so we denote the r-band flux in the jet-break time as M_r in this case, as a comparison with the off-axis samples. Colorbars in Fig. 11 represent the value of M_r. We find these afterglows all reach the design depth of WFST. After multiplying the fractions of observable area and time, the joint observation rates of sGRB and afterglows are less than ~2 per year, which are much smaller than those of kilonova. Therefore, WFST's searching for GW EM counterparts needs to be focused on the kilonova.

Optical counterparts of other GW events Kilonovae and optical afterglow from BH-NS mergers are another type of multi-messenger sources that WFST expects to discover. The two events are named GW200105 and GW200115, as well as several candidates named GW190426, GW190917, GW191219, GW190814, GW200210, were discovered during the third observing time (O3) of the LIGO Scientific Collaboration and Virgo Collaboration (LVC) [265]. Unfortunately, none electromagnetic counterpart was identified. A number of works have attempted to explain the reason for the lack of EM identification in theory (see for instance [266]). It was found that, different parameter distribution including the EOS of NSs, the spin of BH and the mass ratio of the binaries can significantly influence the kilonova luminosity function and EM detection. In the case of primary BH having a high-spin distribution and NS component being less massive with a stiff EOS, the NS can be disrupted by BH form almost all cases to power s bright kilonova and afterglow. In the optimal estimation, WFST is expected to detect this kind of optical counterparts at round $O(1)$ per year [266].

BBH mergers could also emit the EM radiation in some specific cases. For instance, if the BH has the electric charge

		u	g	r	i	z
WFST	LHV	0.6-5.8	1.1-11.6	1.3-12.9	0.8-8.5	0.2-2.4
	LHVIK	0.8-7.9	1.8-18.2	2.0-25.2	1.1-11.8	0.3-2.9
LSST	LHV	1.5-15.3	1.8-17.9	1.8-18.0	1.8-18.0	1.6-16.8
	LHVIK	2.9-29.0	3.8-37.9	3.8-39.0	3.8-39.0	3.2-32.7

Table 5 Number of BNS mergers per year with observable GW signals and kilonova.

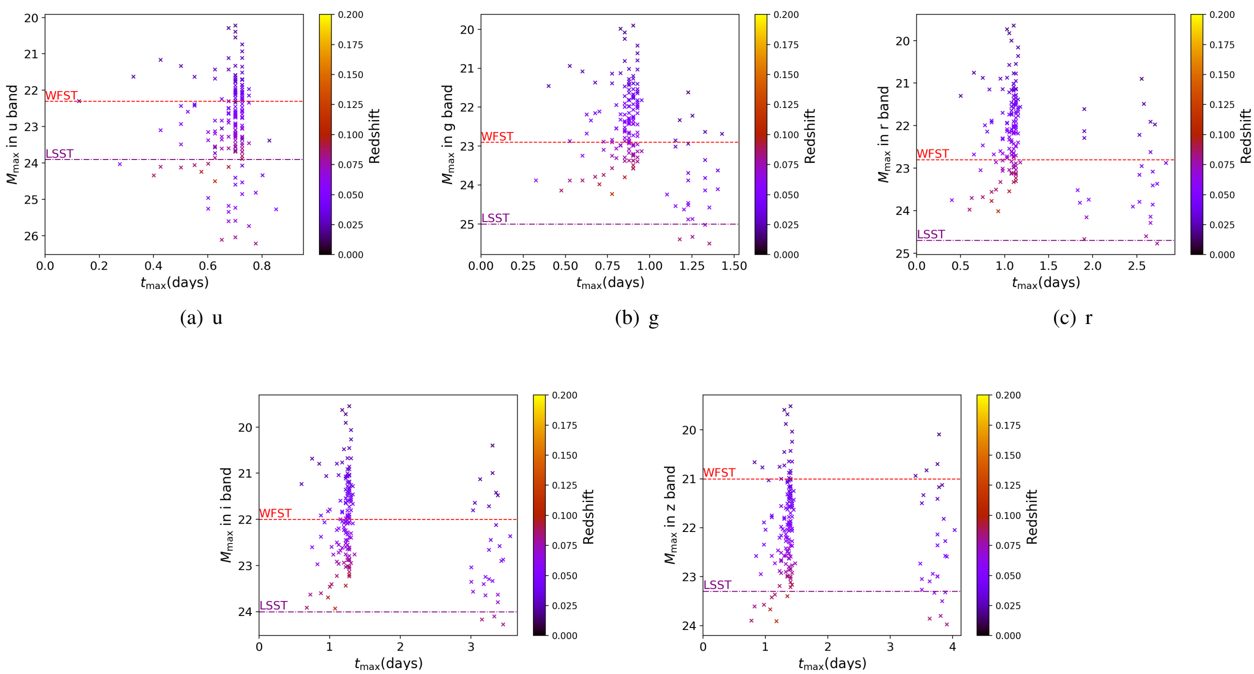

(a) u (b) g (c) r (d) i (e) z

Figure 10 For BNS mergers with GW SNR> 10, the distributions of their kilonova maximum magnitudes and the corresponding times, each color corresponds to the redshift. Five panels represent the results of u, g, r, i, z bands, respectively.

	Swift-BAT	SVOM-ECLAIRS	GECAM	Fermi-GBM	EP
LHV	0.042-0.425	0.072-0.731	0.278-2.820	0.198-2.001	0.029-0.297
LHVIK	0.084-0.856	0.146-1.474	0.553-5.598	0.394-3.985	0.058-0.593

Table 6 The multi-messenger observation rates (with the unit of year^{-1}) for BNS mergers with different γ-ray detectors and GW detectors.

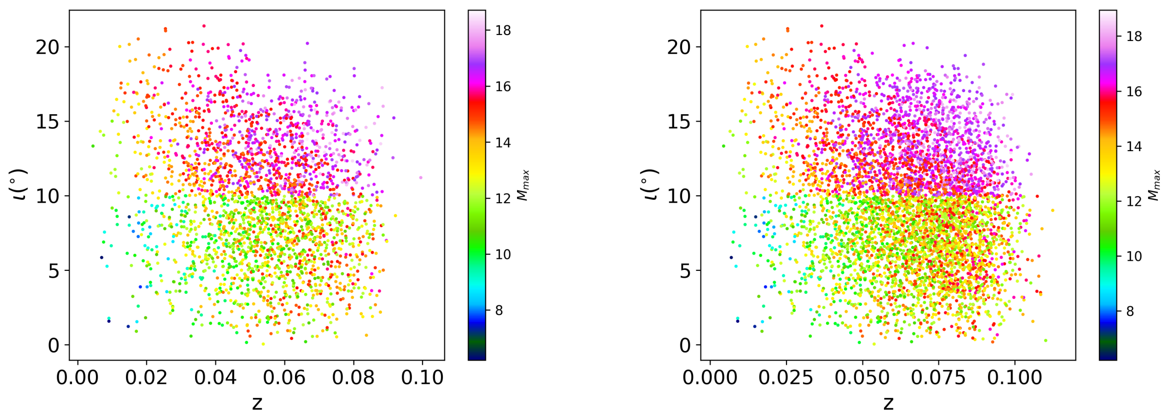

(a) LHV

(b) LHVIK

Figure 11 The distributions of inclination angle, redshift of BNS samples and their afterglows flux, which can be triggered by GW detectors and GECAM. The colorbars show their r-band magnitude of afterglows with $\theta_j = 10°$ [252].

or the BBH locates at the accration disk of galaxy. The event named GW190521 might be the first multi-messenger observation of a BBH event. Graham et al. [267], reported the observation of an electromagnetic signal, ZTF19abanrhr by the Zwicky Transient Facility (ZTF) in a region of the sky consistent with that initially reported by the LVK in an early warning, proposing it as a counterpart to GW190521. The EM flare is consistent with expectations for a kicked BBH merger in the accretion disk of an active galactic nucleus. If true, this would have paramount implications in interpreting GWs from compact mergers, forecasts for future counterparts and measurements of the Hubble constant. EM campaigns that trigger follow-up on GW alerts should monitor AGN on multiple cadences, from days to weeks, in order to search for EM counterparts in the AGN channel.

It is difficult to quantify the detection rate of optical counterparts for these GW events, due to the complex parameter dependence. For WFST, it is necessary to carry on the GW-triggered targetof-opportunity observations, which is important to reveal formation and evolution of these events.

3.3.2 Gamma-ray Bursts

Gamma-ray bursts (GRBs), the most energetic stellar explosions in the Universe, are relativistic jets beaming toward us. The jet is launched by a compact central engine, either a black hole or a rapidly rotating, highly magnetized neutron star. No general consensus on GRB jet properties (e.g., jet composition, emission radius) has been reached in the community. The temporal/spectral evolutions of the prompt/afterglow emissions carry the main information to probe the GRB jet. A large sample of GRB prompt/afterglow lightcurves is crucial to fix the jet properties. Hence, there is high demand for wide-field survey of GRB optical counterparts.

*** what are the most significant science questions to be addressed with WFST **

The Early Optical Afterglow Multiwavelength observations of GRB afterglows in the past years have identified the standard external shock scenario[268, 269], in which the interaction between the blastwave and the surrounding medium heat up the ambient electrons to emit broadband afterglows via synchrotron radiation. Among these samples, the optical afterglow typically starts its data from the time of 10^3 s after the GRB trigger, mainly due to the difficulty of timely optical follow-up after a GRB trigger in the gamma-ray band. Hence the early stage (within 10^3 s) of a GRB afterglow, namely the early optical afterglow, is often missed. A wide-field survey of the GRB optical afterglow could help to expand the early optical afterglow sample and improve our understanding of the GRB jet. While the late-stage optical afterglow is crucial in constraining the structure of the relativistic jet launched from the central engine and the density of the ambient environment[270, 271], the early optical afterglow is unique in learning the composition of the jet, i.e., dominated by baryons or magnetic fields[272-274].

During the interaction between the jet and the surrounding medium, two shocks develop, one propagating outwards into the external medium (called forward shock, FS) and the other one traveling backward into the jet (reverse shock, RS). Consequent bright optical flashes from the RS in the early episode were predicted on theoretical grounds[275-279]. The detection of the early optical afterglow of a few GRBs shows evidence of such an additional emission component arising from a strong RS[280, 281]. Using numerical methods proposed to solve the dynamics of the FS–RS system in literature[282-286], we could relate the contribution of the RS emission in the early afterglow with the magnetization parameter of the GRB jet, i.e., $\sigma = B_0^2/(4\pi\rho_0 c^2)$, where both the magnetic field B_0 and the fluid density ρ_0 are the quantities in the comoving frame of the fluid. Figure 12 shows a set of numerical multiwavelength lightcurves from the FS-RS system. The emerging RS emission makes the lightcurves in the early stage deviate from those in the simple external shock scenario. On the other hand, our results manifest that the contribution of the RS emission becomes significant for the ejecta with σ ranging from 0.1 to 1, otherwise, it is dimmer than the FS emission in the early stage since the weak magnetic field inhibits the synchrotron radiation for $\sigma \ll 1$ while the strong magnetic field as a relaxant weakens the RS itself for $\sigma > 1$. Therefore, observations of a large sample of early afterglows could constrain σ of GRB jets statistically.

The sensitivity line of WFST is well below the early RS flux of a typical GRB, enabling it to catch the early afterglow. Since the duration of the early afterglow is very short, a collaborative survey together with another space wide-field gamma-ray detector (e.g., GECAM[287], SVOM[288]) is highly invoked to increase the chance to obtain complete data of an early afterglow. Considering that 1/5 nights of WFST could be used to perform such a collaborative survey, 1-5 early optical afterglows could be obtained per year. Other timely follow-ups to the trigger of worldwide gamma-ray detectors could also be promising for GRBs having a long gap (longer than the response time of WFTS) precursor, but can not improve the detection rate significantly.

High-redshift Gamma-Ray Bursts Thanks to their extreme brightness and the spectroscopy of the optical afterglows, GRBs can be detected up to very high redshift, as already demonstrated by the detection of GRB 090423 at $z \sim 8.2$ [289, 290] and GRB 090429 at $z \sim 9.4$ [291]. As bright beacons in the deep Universe, GRBs have been viewed as a complementary, and to some extent unique, probe to study the properties of the early Universe. A statistical sample of high-z GRBs can offer important information about: the cosmic expansion and dark energy, the cosmic star formation rate, Population III stars, the reionization epoch, the metal enrichment history, and so on (see [292, 293] for reviews).

In 15-years of operations *Swift* has only detected 9 GRBs with redshift larger than 6, in which a handful of bursts have spectroscopic redshifts and other four are photometric redshifts. Although the confirmed high-z GRBs are rare in the *Swift* era, the theoretical model predicts that bursts $z > 6$ represent more than 10% of the whole population, implying that GRBs are quite efficient in selecting high-z objects [294, 295]. In order to fully exploit the potential of GRBs as cosmological probes, a larger sample of high-z GRBs should be collected. It has been suggested that the best strategy for detecting the largest number of high-z GRBs is to design a facility operating in the soft X-ray band but with a very high sensitivity [292, 295]. For instance, Einstein Probe (EP) operating in the 0.5–4 keV energy band reaching an unprecedentedly high sensitivity, corresponding to a flux, of 10^{-10} erg s^{-1} cm^{-2} for an exposure of 10 s is expected to detect ~ 20 GRBs yr^{-1} sr^{-1} at $z \geq 6$ (~ 6 GRBs yr^{-1} sr^{-1} at $z \geq 8$) [296]. Once high-z GRBs are detected the major issue is to measure their redshifts. The optical afterglows of GRBs fade quickly, and after a few hours they are usually too faint to permit accessing redshift. Fast distribution of the EP alerts to the world community will enable to coordinate follow-up optical observations. In order to rapidly identify high-z candidates that deserve deep spectroscopy in the NIR, we expect that the fast follow-up observations with WFST could help to provide GRB photometric redshift estimates. In the EP era, the identification of candidate high-z bursts would benefit from fast visible/NIR photometry of WFST and subsequently the spectroscopic measurements of large ground-based telescopes.

3.3.3 *Fast Radio Bursts*

Fast Radio Bursts(FRBs) are cosmological millisecond duration radio transients[297]. While some of them repeat, other apparently not[**?**, 298]. Up to 2021, there are hundreds of FRBs reported[298], and 18 of them have arcseconds localization with host galaxies identified[299, 300]. By comparing the host galaxies and sub-galactic environment, it turns out that the environment of FRBs are similar to those of core collapse SNe (CCSNe), type Ia SNe and short-duration GRB (SGRB), and are odd with those of long-duration GRBs (LGRBs) and superluminous SN (SLSNe)[301, 302]. It indicates that the progenitors of FRBs might be associated with those of CCSNe or SGRBs. It was (at least partially) confirmed by the discovery of FRB 200428, an FRB from a Galactic magnetar SGR1935+2154[303-305] which was associated with a SNR. Thus, the current most attractive questions are whether all FRBs are from CCSNe-associated magnetars, or specifically, whether repeating FRBs and apparently non-repeating FRB have the same origin. In optical band, WFST may help to answer these questions from host galaxy and optical counterparts points of view.

Host Galaxy The similarity of host galaxy and sub-galactic environments reveal the possible association of FRBs with other transients. The current sample size is only 18, with 7 repeating FRBs and 11 apparently non-repeating FRBs,

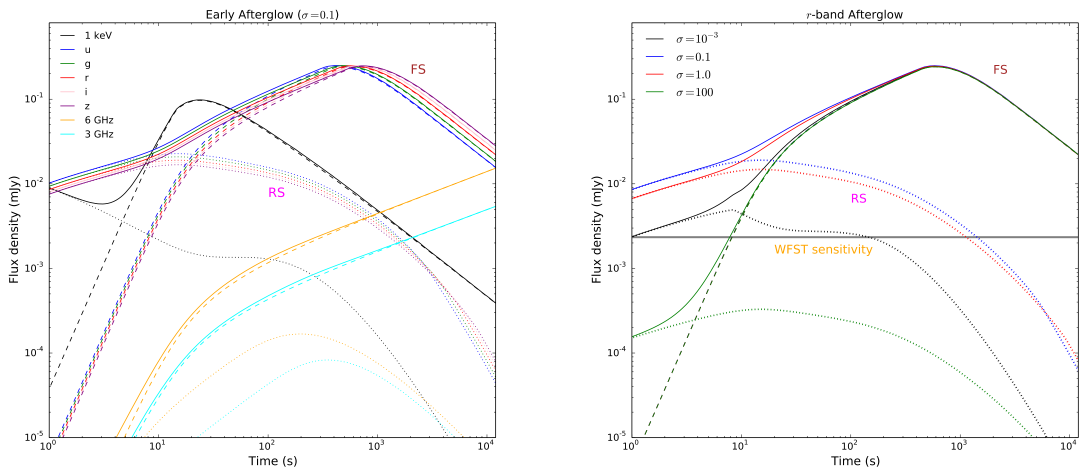

Figure 12 Left: The multiwavelength afterglows of an FS-RS system with $\sigma = 0.1$ as an example of predicted observations of a GRB jet at a redshift of $z = 1$. The initial jet parameter values are $E_{\rm K,iso}$ = erg (isotropic-equivalent kinetic energy), $n = 1$ cm^{-3} (circumburst density), $\Gamma_2 = 200$ (bulk Lorentz factor of the FS), and $\Gamma_4 = 10^4$ (bulk Lorentz factor of magnetized ejecta), the FS microphysical parameters are $\varepsilon_{\rm e} = 0.1$ and $\varepsilon_{\rm B} = 0.01$. The dashed and dotted lines present emissions from the FS and the RS, respectively. The solid lines are the total flux. Right: The r-band lightcurves of FS-RS systems with different values of σ. Other parameters used are the same as those for the left panel. The grey horizontal line exhibits the sensitivity of WFST with an exposure of 30 s.

not large enough to identify the most preferred model, let alone distinguish the most preferred model of repeating FRBs and non-repeating FRBs. The localization of FRBs into arcseconds precision requires wide-field radio arrays similar to Australian Square Kilometre Array Pathfinder (ASKAP). The construction of Square Kilometre Array (SKA) and promotion of Five-hundred-meter Aperture Spherical radio Telescope (FAST) and Canadian Hydrogen Intensity Mapping Experiment (CHIME) enables a detection rate 100 yr^{-1} with annual observational time similar to ASKAP. The deep galaxy sample of WFST in North hemisphere will provide a basic host galaxy information for the FRB host galaxy. In order to exam the possibility to distinguish repeating and non-repeating FRB host galaxies, we enlarge the FRB host galaxy sample size into 72 by resampling the known FRBs[2)] and then examine the difference of each host galaxy properties between repeaters and non-repeaters with K-S test. The host galaxies properties includehost galaxy stellar mass, star formation rate (SFR), specific star formation rate(sSFR), the offset of the FRBs from the center of the host galaxies. It turns out that the null probability between repeaters and non-repeaters are smaller than 0.05, indicating a statistical difference between them. Thus, with the deep galaxy sample pf WFST and a larger arcsecond-localized FRB sample from future radio telescope arrays, we may distinguish the repeating FRBs and non-repeating FRB if they are from different origin and show host galaxy properties similar to current sample.

Optical Counterparts Although the engine and the emission mechanism of FRBs are still unknown, some models predict multi-wavelength counterparts[**?**, 306, 307] which may be detected in the future WFST observations. During the prompt FRB process, the machanisms producing FRBs, the curvature radiation or maser, may also produce emissions extending to higher energy such as optical. These prompt optical radiation would have durations similar to FRBs, millisecond. During the propagation of the FRBs to the earth, it may be inverse Compton scattered to optical band by high energy electrons. If the electrons are from the magnetar magnetosphere, the optical signal would have durations similar to the FRBs, i.e., milli-second timescale. If the FRBs are produced by maser, the electrons producing maser would have a similar effect. If the FRBs are surrounded by supernova remnants with high energy electrons, the optical counterparts may have durations thousand of seconds[307]. If there is outflow ejected with FRB radiation, which was supported by the pair of X-ray counterparts detected in the Galactic FRB 200428[308], the interaction between the outflow with the interstellar medium (ISM) will produce optical afterglows. Based on the energy of FRBs, the duration of optical afterglows is hour timescale[306].

According to the theoretical prediction, the flux radio between optical and radio $\eta_\nu = f_{\rm opt}/f_{\rm radio}$ range from $< 10^{-11}$ to 0.1 [307, 309, 310]. The cases most likely be detected by WFST are inverse Compton scattering of FRBs with neutron star magnetosphere and SNR, which have typical η_ν = 5×10^{-5} and 10^{-4}. Based on the FRB fluence function from

2) https://frbhosts.org/

CHIME observation and assuming FRB durations to be 1 ms, we have the flux function $N(>f_{\rm radio}) = 818^{+229}_{-210}(\frac{f_{\rm radio}}{5\ {\rm Jy}})^{-1.4}$ sky^{-1} day^{-1}. The FRB optical counterpart detection rates in WFST are estimated with $N = N_{\rm FRB}(> f_{\rm opt}/\eta_\nu) * {\rm FOV}$, where $f_{\rm opt} = t_{\rm FRB,o} f_{\rm opt,30}/t_{\rm obs}$ for counterparts with durations $t_{\rm FRB,o} < 30s$ and $f_{\rm opt,30}$ is the 30s exposure r-band limitation of WFST. Field of view FOV = 7 deg^2 is applied here. It turns out that, the event rate of the ms optical counterpart produced by magnetospheric IC is 0.02 yr^{-1} and the hours duration optical counterpart produced FRB-SNR IC is 200 day^{-1} in an ideal case. However, the $\eta_{\rm nu} = 10^{-4}$ used here is mainly an upper limit and possesses significant uncertainty, and the ratio of FRB surrounded by SNR is unknown. Moreover, the duration of this kind of optical counterpart is about one hour. Normal surveys only reveal one observational point and hard to confirm. Thus, it requires radio collaborative observation to confirm. A positive detection of the optical counterpart will definitely open a new window of FRB study, while the negative detections may give limitations to models[310,311].

Moreover, FRBs may be associated with other transients, such as CCSNe if they are from young magnetars produced by CCSNe, gravitational wave signals and SGRBs/kilonovae if they are from magnetars produced by compact star mergers. In this case, WFST will provide a large legacy transients sample for FRB-transient association search.

3.3.4 *Optical Counterparts of High-energy Neutrinos*

If one astrophysical object is able to accelerate particles, for instance, via the terminal shocks, interactions between the accelerated cosmic rays and the surrounding matters or target photons will produce high energy neutrinos and photons. The detection on the electromagnetic counterparts of high energy neutrinos will help us to identify the possible neutrino sources, constrain the distance and properties of those sources, and help us to learn more on the acceleration mechanism and the radiation mechanism. Therefore, searching for the electromagnetic counterparts/transient in coincidence with neutrinos temporally and spatially can play an importance role in searching for the astrophysical neutrino sources.

Currently, high energy neutrinos have been detected by large neutrino telescopes in water (ANTARES[312], Baikal-GVD[313]) and ice (IceCube[314]), from the surface with Auger and from high altitude with ANITA[312]. The IceCube neutrino observatory, the largest neutrino detector to date, discovered TeV-PeV astrophysical neutrinos in 2013 [315], but the origin of those neutrinos are still under debate. Since 2016, the IceCube neutrino observatory start to send public real-time alerts on single muon neutrino-induced track events with a high probability of being of astrophysical origin, via the Astrophysical Multi-messenger Observatory Network (AMON) and Global Cycling Network (GCN). The current IceCube neutrino alerts include gold type notices and bronze type notices, corresponding to rates of about 12/yr and 16/yr, with chances being from astrophysical origin larger than 50% and larger than 30%, respectively. The errors of the direction of neutrinos range from 0.2° to 0.75°.

In the optical real-time follow-up (OFU) program, the IceCube send real-time alerts to the Robotic Optical Transient Search Experiment (ROTSE) and the Palomar Transient Factory (PTF)[6,316] to search for optical counterparts, the triggered observations would be supplemented with a retrospective search through the Pan-STARRS1's wide field survey data [8, 317]. The electromagnetic instruments around the world will also do the follow-up observations in different energy band and messenger, from radio and optical to X-ray, GeV and TeV photons, and gravitational wave, to the direction of the neutrino events, and then report their results on GCN. To the directions of the alert neutrinos, some astrophysical sources, including BL Lacs, flat spectrum radio quasars (FSRQs), TDE and other objects, are found via GeV, X-ray and optical follow-up observations[165,318,319].

Since events from the southern hemisphere are highly contaminated by the muon backgrounds, the IceCube is more sensitive to neutrinos from the northern hemisphere or near the equator, therefore most of these neutrino alerts locates in the northern hemisphere or near the equator. WFST is sensitive to the northern hemisphere, and its wide field of view can cover the angular error of most IceCube observed neutrinos with a single exposure. These facts make WFST a suitable detector to do the follow-up optical observations the IceCube neutrino alerts. In addition, the optical time-domain survey by the WFST would discover more SNe, FBOTs, TDEs, GRBs and AGNs. We can search for associations between the observed neutrinos (including the neutrino alerts and the archival neutrino data) and WFST's archival data. The observations by WFST might help us to identify neutrino sources, further constrain the acceleration mechanism of cosmic rays, the radiation mechanism, the redshift and other properties of the sources.

Blazars Blazars are relativistic jets driven by supermassive black holes with directions aligned with the observer's line of sight, which are important targets of WFST, as will be introduced in Section 3.4. The jets are able to accelerate cosmic rays to high energy, and the interactions between high energy cosmic rays and target photons or matters in or near the acceleration sites will produce high energy neutrinos and photons. Thus, they have been proposed as high-energy neutrino sources for decades[320].

On Sep. 22nd, 2017, the IceCube observatory reported a track-like neutrino events IceCube-170922A with energy of about 300 TeV. The follow-up observations find out that this neutrino event is associated with the optical-TeV active blazar TXS 0506+056 spatially and temporally[321], with a significance of 3σ. The optical follow-up observations were performed by quite a few observatories around the world, including ASASSN, the Liverpool Telescope, the Kanata Telescope, the Kiso Schmidt Telescope, the Southern African Large Telescope(SALT), the Subaru telescope, and the VLT/X-shooter. The spectra, light curve and polarization are measured. The limits of the redshift is derived by using optical spectra from the Liverpool, Subaru, and VLT telescopes, and the redshift was later determined by using the Gran Telescopio Canarias. It is the first time to find the association between neutrinos and point sources with such a high significance. The potential association between the activity of TXS 0506+056 and the neutrino event makes the object a promising candidate source of high energy neutrinos. An excess of high-energy neutrino events from the direction of TXS 0506+056 with respect to atmospheric backgrounds prior to the IceCube-170922A alert was found later, with a significance of 3.5σ[318]. The association between the blazar and neutrinos provides evidence of the idea that AGNs can accelerate very high energy cosmic rays and produce neutrinos via the photohadronic interactions or hadronuclear interactions[318, 321].

Besides the follow-up observations of the real-time neutrino triggers, 11 significant neutrino flares are found associated with 10 AGN counterparts, including FSRQs, BL lacs and radio galaxies, using a sample of muon track neutrino events from 2012 April to 2017 May[322]. In addition, 9 blazars are found possibly associated with the single high-energy neutrino events, including both archival neutrino events and neutrino alert events[319].

GRBs and SNe At the end of its life, a massive star would collapse into a neutron star, a quark star, or a black hole, and produce energetic jets. For massive stars with strong winds, which blow out most of the materials of their stellar envelope, i.e., Wolf-Rayet stars, jets with large injected energy can easily break through the star and produce gamma-ray emission, usually observed as a GRB, which is suggested to be associated with a Type Ib/c SN. These GRB/SNe jets are believed to accelerate cosmic rays and produce high-energy neutrinos via interactions of cosmic rays with target photons or the surrounding matters[323]. Neutrinos can also be produced via interactions between shock accelerated cosmic rays with matters and photons during the shock breakout phase of SNe. The capability of WFST detecting early phase SNe would help us to get the exploding time of SNe, searching for the association between SN SBOs and neutrinos.

In the other case, if jets are not able to break out through the stellar envelope, for example, red/blue supergiant stars, neutrinos and gamma-rays are produced via interactions between accelerated protons and thermal photons in jets choked in the thick stellar envelope or the extended material. The duration of the central engine could be longer than that for long GRBs[324, 325]. Since neutrinos and gamma rays are produced inside the stellar envelope, the source is opaque to gamma-ray photons but transparent for neutrinos. This can explain the lack of association between the observed GRBs and IceCube neutrinos, as well as the tension between the diffuse gamma-ray observations and neutrino observations. A Type II SN is predicted to explode a few hours after the neutrino emission. Once we observe an SN spatially associated with neutrinos, we can trace back to the explosion time according to the observed light curve, and then measure the time difference between the neutrino burst and the explosion.

What's more, as discussed in Section 3.1, some subclasses of SNe are powered via interactions between the ejecta and CSM or the companion, for instance, SNe Ia-CSM, SNe IIn, FBOTs, and SLSNe. The interactions between the ejecta and CSM would produce terminal shocks, which are able to accelerate cosmic rays to high energy. The interaction between cosmic rays and CSM would produce high energy neutrinos, which makes the above subclasses of SNe possible optical couterparts of high energy neutrinos.

IceCube has a real-time program to search for muon-neutrino doublets or multiplets. In order to suppress atmospheric background, two or more muon neutrinos detected within a time interval of 100 s and with an angular distance smaller than 3.5 ° are required to trigger a doublet or multiplet alert. In March 2012, a neutrino doublet alert is triggered. A Type IIn SN PTF12csy at a distance of about 300 Mpc was found 0.2° away from the neutrino alert direction, with an error radius of 0.54°, with a posteriori significance of the chance detection of the neutrino doublet and the SN is 2.2σ. However, the SN is at least 169 days old, and no long-term signal of neutrinos is found over the year, suggesting that the doublet is most likely uncorrelated to the SN. On February 17 2016, the IceCube real-time neutrino search identified a triplet with three muon neutrino candidates arriving within 100 s of one another, with a probability of detecting at least one triplet from atmospheric background as 32%. However, no likely electromagnetic counterpart was detected.

The above multiplet alert is selected by assuming that the duration of neutrino bursts from transients such as GRBs or CCSNe is shorter than 100 s, which is typical for long GRBs. However, as mentioned above, for the chocked jet models or the interaction powered SNe, the duration of neutrino bursts might be longer. The detection on early-phase SNe by WFST will help us to obtain the exploding time of SNe easier, and then we can search for SNe associated with neutrinos in the

WFST's archival data, by assuming a certain time lag between the SNe explosion and neutrinos. Searching for possible associations between GRBs/SNe and neutrinos will provide us with more information on progenitor stars and the radiation mechanisms.

TDEs TDEs, with a star torn apart and accreted to a massive or supermassive black hole at a high accretion rate, should generate a relativistic jet or outflow, which can accelerate cosmic rays to high energies, and further produce neutrinos via interactions between cosmic rays and target photons or matters.

In a systematic search for optical counterparts to high-energy neutrinos with ZTF [165], TDE AT2019dsg was found to be associated with a ~ 0.2 PeV neutrino IC191001A, with a chance probability of about 0.2% − 0.5%. AT2019dsg was discovered by ZTF six months before the detection of IC191001A, and later was classified as a TDE by ePESSTO+ on the basis of its optical spectrum. As mentioned in Section 3.2.4, WFST has a much higher sensitivity than ZTF and can capture weaker TDE emission at earlier stage, and will help construct a more complete TDE sample, therefore, more possible associations between TDEs and neutrinos might be found by WFST.

3.4 Active Galactic Nuclei

Residing at the centres of active galaxies, the luminous quasars or more generally active galactic nuclei (AGNs) are the manifestation of the gas accretion onto massive black holes (BHs) and are believed to play a key role in the evolution of massive galaxies. Although the accretion-BH scenario for the central engine of AGNs has been established since the discovery of quasars over sixty years ago [326, 327], there remain many unresolved fundamental questions [328-331]. For example, how do SMBHs acquire gas? What mechanism is responsible for their variability across multi-wavelengths? Are their activities triggered in persistent or episodic mode and by what conditions?

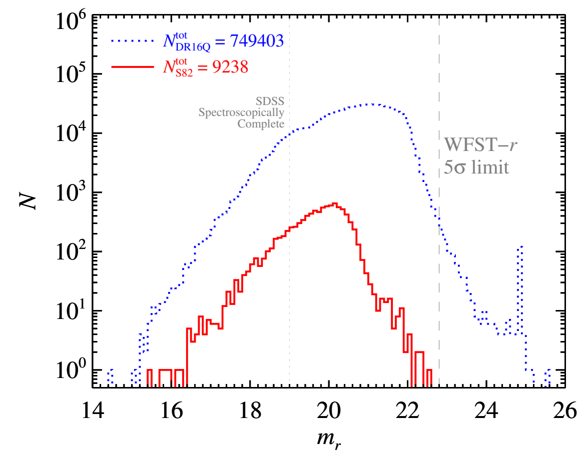

Figure 13 Distributions of the apparent r-band magnitudes for spectroscopically confirmed quasars in the Stripe 82 (S82; red solid histogram; [332]) and in the SDSS sixteenth data release quasar catalog (DR16Q; blue dotted histogram; [333]). Note that only quasars with physical r-band magnitudes are used here. Shown for comparison are the spectroscopically complete limit of ~ 19 mag for SDSS quasars (light-gray dotted vertical line) and the WFST r-band 5σ detection limit of ~ 22.8 mag in a single 30-sec exposure (gray dashed vertical line).

The ongoing and upcoming intensive time-domain surveys are of great benefit to decipher these fundamental mysteries of AGNs, which are otherwise spatially unresolvable. Illustrated in Figure 13, the up-to-date SDSS survey has spectroscopically confirmed nearly ~ 0.75 million AGNs over ~ 10,000 deg^2 primarily on the northern sky (SDSS DR16Q; [333]), while only ~ 1% of them in the well-known Stripe 82 (S82) region of ~ 290 deg^2 along the celestial equator in the southern Galactic hemisphere have decade-long light curves in five passbands ($ugriz$), observed 8 times on average in a 2-to-3-month duration per year between 2000 and 2008 [332, 334]. Later on, there are several completed or ongoing time-domain surveys over the SDSS footprints, however, most of them are too shallow to detect the majority of faint SDSS quasars and have fewer passbands than SDSS. For instance, the CRTS survey covers ~ 26,000 deg^2 but only has a single broad V-band with typical detection limits of ~ 19 − 20 mag from 2005 to 2013 (CRTS DR2; [5]). Meanwhile, from 2009 to 2013, there are deeper PTF/iPTF surveys in g- and R-bands to a depth of R ~ 21.0 mag (PTF DR3; [335]). The ongoing ZTF survey releases gri images observed to a depth of r ~ 20.5 mag since 2018 March (ZTF DR8; [336]). Indeed, the 3π Steradian Survey conducted by Pan-STARRS1 (PS1) between 2009 June and 2014 March in $grizy_{\rm P1}$ five passbands reaches a 5σ depth of $r_{\rm P1}$ ~ 21.8 mag (PS1 DR2; [337]). Therefore, considering the same five passbands as SDSS and a 5σ detection limit of r ~ 22.8 mag in a 30-sec single-epoch exposure (Figure 13), the WFST survey would provide decade-long light curves in five passbands for nearly all SDSS quasars, many of which cannot be observed by LSST in the southern hemisphere. Moreover, the WFST survey would extend the existing light curves to several decades for quasars in S82 and the ten medium deep fields of PS1. Consequently, the WFST legacy survey is expected to be highly valuable for the AGN community.

With these new decades-long light curves, the physical origin of AGN variability can be explored at both longer timescales and toward fainter AGNs with smaller BH masses than currently available. The increasing time baseline would also increase the possibility of identifying new types of rare AGN associated events. Thanks to the deep and high-resolution WFST images, selecting a sample of considerably close AGN pairs is possible using the unique colors of AGNs such that the triggering mechanism of AGN activity can be inspected. Moreover, the long-term variability properties as well as the very deep WFST stacked images to a depth of $r \sim 25.1$ mag would be of service to select quasar candidates fainter than the SDSS spectroscopically complete limit. These quasar candidates would then be natural targets for subsequent master spectroscopic projects, such as LAMOST-II and MUST, exploring even fainter AGNs at high-z with smaller BH masses either to exhaustively understand the BH growth and the co-evolution with galaxy or to globally trace the cosmological evolution of both the intergalactic medium and the large-scale structure of the universe. Several particular AGN science cases are further elaborated in the following.

3.4.1 Physical Origin of AGN Optical Variability

The physical origin of AGN variability in optical is hitherto unclear, though thought to be driven by X-ray reprocessing [338], corona heating [339, 340], or accretion disk turbulence [341, 342]. However, no self-consistent physical model is available for all observed AGN properties. This is not only due to the complex accretion physics involved but also to the large observational uncertainties. The decades-long light curves from the WFST legacy survey will help reduce the observational uncertainties on measuring both the single-band and inter-band variation properties.

Correlations Generally, the AGN variability in each individual band is aperiodic or even stochastic [343], but can be statistically described by a characteristic timescale and a long-term variation amplitude [344]. Then, correlations between these two parameters and the other observational/physical properties of AGNs, e.g., wavelength, redshift, BH mass, bolometric luminosity (Eddington ratio) [332], metallicity [345], X-ray loudness [346], radio loudness [347], and strength of emission lines [348], are scrutinized to shed light on the unresolvable AGN structure and accretion physics. Furthermore, a correlation between the slope of variation amplitude to wavelength and the BH mass is being investigated as a new alternative method for estimating BH mass (M. Y. Sun et al. 2022, in preparation). An important application of measuring the density of outflowing gas using variable properties of broad absorption lines also depends to some extent on accurately measuring the AGN light curve [349, 350]. Hence, obtaining accurate measurements on both timescale and variation amplitude is the primary goal for AGN science in the time-domain era. The WFST legacy survey would extend the existing quasar light curves to several decades such that variation timescales as long as several years could be accurately measured as simulated by Kozlowski ([351]; see also Suberlak et al. [352]).

Coordination and timelags Although the quasar light curve in individual band appears stochastic, the inter-band variation of quasars sometimes shows interesting nice coordination, i.e., brightening or dimming in phase across optical to UV wavelengths. In addition, variation at longer wavelength lags that at shorter one, which is called the inter-band timelag. More complicatedly, uncorrelated variations are also reported [353] and the failure of recovering lags for the vast majority of AGNs seen in Dark Energy Survey fields is unveiled [354]. Regardless of these uncertainties, the inter-band timelags among optical continuum variations of AGNs are simply used to estimate sizes of accretion disk in different wavelengths [354-356]. This is based on an assumption that the inter-band timelags are closely related to the light travel time difference among disk regions irradiated by the central X-ray corona. However, this assumption is doubtful since the role of X-ray reprocessing has been gradually questioned by many observations [357-361]. Instead, a novel origin for the inter-band timelag has been proposed within the thermal disk turbulence scenario [339, 341, 342]. The left panel of Figure 14 shows that for AGNs akin to NGC 5548 observed in the five WFST passbands, the disk turbulence model predicts an intrinsic dispersion of the inter-band timelag as a function of wavelength, which seems to be consistent with current preliminary observations. While shown in the right panel of Figure 14, $\sim 30\%$ accuracy of the measured timelag can be easily achieved by averaging hundreds of AGNs with comparable BH mass and luminosity, despite undesirable observational conditions such as relatively long cadence and/or large photometric error. The only requirement is that quasars should be observed in different bands, e.g., at least in g and r/i, in the same night, i.e., quasi-simultaneous multi-color observations. Several deep drilling fields such as those in the Medium Deep Survey of PS1 frequently monitored by WFST would make this very attractively achievable. Besides being helpful in assessing the timelags among different wavelengths, the

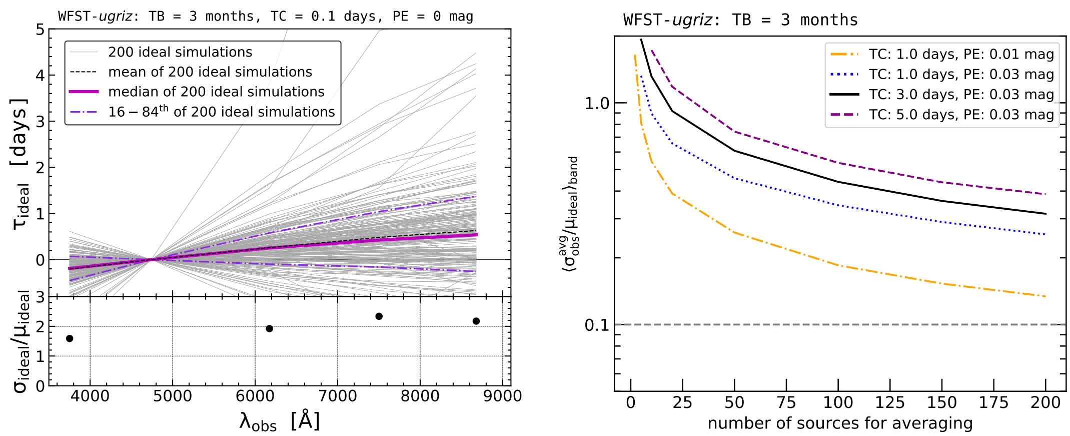

Figure 14 Left panel: relative to WFST-*g* band, the intrinsic inter-band timelag as a function of wavelength implied by the disk turbulence model [341, 342] for AGNs akin to NGC 5548 observed yearly in WFST-*ugriz* passbands, assuming a temporal baseline of 3 months per year, a temporal cadence of 0.1 day, and without photometric error (Z. B. Su et al. 2022, in preparation). In the top subpanel, gray thin solid lines show results of individual simulations, while the median/mean and 16%-84% percentile ranges are shown accordingly. In the bottom subpanel, the intrinsic uncertainty of individual timelag in each band is quantified as the ratio of the corresponding dispersion $\sigma_{\rm ideal}$ to the mean timelag $\mu_{\rm ideal}$. Right panel: considering longer temporal cadences of 1-5 days and photometric errors of 0.01-0.03 mag, the observed uncertainties of the mean timelag decreases significantly with increasing the number of sources used in averaging.

deep drilling fields would further offer a unique opportunity to investigate the true variable SEDs as well as the timescale-dependent color variation of AGNs. The latter has been proposed as a new window to probe and test the accretion disk physics in the era of time-domain astronomy [362, 363]. In sum, the WFST legacy survey would indubitably improve our understanding on the origin of AGN variability.

3.4.2 Particular AGN Variability

Most AGNs show stochastic variations, but as a result of persistently monitoring AGNs in the time-domain era there are emerging new types of AGN variability with unknown physical origin.

Some extremely variable (EV) AGNs are selected according to variations by > 1 mag on timescale of decades [364], larger than normal AGNs varying with typical ~ 0.2 mag on similar timescales [365, 366]. The physical origin of such extreme variability is under debate, but the same mechanism for both extreme and normal variations has been suggested [367]. Interestingly, $> 20\%$ of EV AGNs are spectroscopically confirmed as the rarer changing-look (CL) AGNs [368]. The CL AGNs show dramatic emergence or disappearance of the broad emission lines on timescale of decades, the shortness of which challenges the standard thin disk theory. Although most CL AGNs are intrinsically related to changes in the accretion rate [369, 370], the physics causing such a change is not yet understood [371-376]. Furthermore, the timescale and frequency of the CL AGNs may be used to restrict the episodic and net lifetimes of AGNs [377], which is important to study the AGN triggering mechanism, as well as the physics of the accretion process. Being complemented by archival data, the WFST survey would make several decades-long light curves possible, aiding in the selection of EV and CL AGNs and the understanding of their physical origin.

From nearly a million quasars in the CRTS survey, Graham et al. [378] identified 51 events with strange major flares atop of the normal stochastic quasar light curves. The physical origin is yet unclear, but may be due to microlensing by stars in the foreground galaxies [379] or more appealingly as suggested by Graham et al. [378] associated to explosive stellar-related activity in the accretion disk, such as SN, TDE, or mergers of stellar-mass BHs. Remarkably, the ZTF survey has potentially caught an event of binary BH merger in the accretion disk of an AGN in accordance with a reported gravitational-wave event [380]. With nearly two magnitudes deeper than ZTF, the WFST survey would significantly increase the number of such extraordinary events, probably allowing to ping down their nature.

Periodically varying quasars have been suggested as supermassive BH binary (SMBHB) candidates [381, 382] and several candidates have been reported [332, 383-386]. Recently, from $\sim$ 9000 color-selected quasars in an ~ 50 deg^2 sky area of the PS1 Medium Deep Survey, Liu et al. [387] identified 26 SMBHB candidates with more than 1.5 cycles of variation, which could be verified with new observations from the WFST survey. And more SMBHB candidates are expected in the WFST survey if commissioning deep fields larger than PS1.

Last but not least, the decades-long light curves provided by the WFST survey would also benefit the search for peculiar AGNs with either almost monotonically increasing/decreasing variations or very small variations over long timescales as well as the true turn-on/turn-off AGNs, which would likely reveal the triggering mechanism for AGNs.

3.4.3 Low-luminosity AGNs and IMBHs

The search for low-luminosity AGNs in dwarf galaxies is of particular interest because it turns out to be one of the most practical way to identify candidates of IMBHs [388-391], bridging the mass gap between SMBHs and stellar-mass BHs. Furthermore, the local IMBHs, as relics/analogs of SMBH seeds in the early universe, are essential for our understanding of the seed formation mechanisms and the co-evolution of BHs and galaxies (e.g., [392]). However, the IMBHs with firm observational evidence have been still scarce to date, thus uncovering more is a pressing need (see [176] for a review).

One challenge of finding low-luminosity AGNs in dwarf galaxies is that the weak AGN signal is easily overwhelmed by the star-forming (SF) activity with conventional methods, such as optical spectra, X-ray, and radio detection. Variability has proven to be a useful tool to distinguish real AGNs from SF galaxies and has yielded a considerable number of IMBH candidates in dwarf galaxies, including SF ones, which have been largely overlooked previously (e.g., [393-396]). Recently, the characteristic optical variability timescale has been found to be correlated with BH mass[397], paving a promising way of selecting IMBH candidates with mass estimation purely based on photometric variability. The sharp and high-resolution images obtained from WFST would significantly reduce the dilution of the stellar light from host galaxies in comparison with current time-domain optical surveys. As a result, we can obtain reliable photometry of these weak AGNs. This would allow to detect active IMBH candidates not only in the isolated dwarf galaxies but also in close dwarf companions of large galaxies or even stripped cores of dwarf galaxies in a massive galaxy. In combination with a daily based cadence in high cadence fields, we expect to obtain a large sample of IMBHs with black hole mass estimates.

3.4.4 Off-nuclear AGNs

Observationally, off-nuclear AGNs are spatially offset from and have physical connection to nearby companion galaxies. According to the standard hierarchical structure formation, galaxy merger is naturally expected as well as the subsequent coalescence of SMBH binaries in the gas-rich environment [398-400]. The latter could result in the recoiling SMBH as predicted by many numerical general-relativity (GR) simulations [401-403]. Then, the off-nuclear AGNs could be AGNs with their own host galaxies in the early phase of galaxy merger or ejected AGNs while the recoiling SMBH is still active after merger. Therefore, systematically searching for off-nuclear AGNs in galaxy mergers at different offsets and redshifts would provide important constraints on the role of galaxy merger and the associated AGN fueling and feedback [404-406], while those for recoiling SMBHs contain information of the distribution of mass ratios and spins in SMBH binaries prior to merger, being able to test the numerical GR simulations [400, 407, 408].

However, using multiple approaches, only several hundreds of offset AGN candidates [409-412] and a few recoiling SMBH candidates [413-416] have been reported so far. Recently, by developing a novel variability-based search strategy, Ward et al. [416] presented 52 AGNs in merging galaxies and 9 recoiling SMBH candidates selected from a sample of 5493 optically EV AGNs with flux variations more than 2.5 mag in both ZTF $g-$ and $r-$bands over a 2.5-year period. Their offset AGNs with available redshifts have physical separations typically larger than 2 kpc as a result of the low resolution of ZTF images. The high-resolution multi-band WFST images would thus enable us to select AGN candidates with smaller offsets, manifesting the crucial phase closer to the merger event, and then construct a more complete statistical sample to test relevant physics before and after mergers. A new method for searching off-nuclear AGNs or close AGN pairs based on their color variation properties, e.g., the bluer-when-brighter trend, is being demonstrated. The nature of these off-nuclear AGN candidates found by WFST would be further clarified once combing the extremely high-resolution images provided by CSST.

3.4.5 Strongly-lensed AGNs

Occasionally, AGNs can be strongly lensed by intervening objects, galaxies in particular, and form multiple images. Such strongly-lensed AGN systems have played a vital role in a broad range of topics in astrophysics. They can be used to quantify the total-mass profile and dark-matter substructures in the lens galaxies [417-419] and probe the co-evolution of black holes and their hosts at cosmological distances [142, 420]. When light curves of lensed AGNs are available, strongly-lensed AGN systems can be further used to constrain the stellar initial mass function in the lens galaxies [421-423] and offer a unique opportunity to measure the size and temperature profile of the accretion disk surrounding black holes in the background AGNs [424, 425]. Additionally, strongly-lensed AGNs with measured time delays can deliver independent and precise measurements of H_0, which are of particular importance considering the growing tension in H_0 values obtained via distance ladders and cosmic microwave background observations [426-428].

Discovering strongly-lensed AGN systems has traditionally relied on imaging- and spectroscopy-based methods [429-436]. Recently, several variability-based methods have been developed [437-439], which can fully exploit ongoing and upcoming time-domain surveys such as ZTF, WFST, and LSST. To date, ≈ 200 strongly-lensed AGN systems have been discovered, of which only ≈ 30 have light-curve measurements for individual lensed images [440, 441]. A simulation by [146] suggests that, on average, there are ≈0.06 galaxy-scale strongly-lensed AGN system per $\deg^2$ that have two (for two-image systems) or three (for four-image systems) lensed images brighter than $i = 22$ mag. It is therefore expected that WFST can detect ≈ 1200 strongly-lensed AGN systems. More importantly, WFST will provide multi-band high-cadence light curves for the detected strongly-lensed AGN systems. Such an extensive dataset will undoubtedly lead to a huge leap forward in various scientific applications enabled by strongly-lensed AGN systems.

4 Asteroids and the Solar System

4.1 Overview of NEO Science

A near-Earth Object (NEO) is by definition any object with perihelion q≤1.3 AU and aphelion Q≥0.983 AU. They are often asteroids and comets. Scientifically, observing a sample of the NEOs can tell us more about the primordial materials of Solar System. However, we are also realistic motivated to gather a more complete catalog of these objects, since the chance of an asteroid impact, that's small but definite. Since its formation, the Earth has been subject to NEO impacts, ***and shaped these impacts ?? ***. There is a wide-ranging geologic consensus that the Cretaceous-Tertiary extinction was caused by the impact of a large asteroid or comet 65 million years ago[442]. The widely observed impacts into Jupiter in July 1994 of the fragments of Comet Shoemaker-Levy 9 released energy measuring in the millions of megatons of TNT, and generated fireballs and dark clouds on Jupiter about as large as the Earth. These events provide an object lesson on the effects of large impacts. Based on the realistic threat of impacts, most NEO surveys started in the late 1990s (for example: LINEAR, NEAT, Spacewartch, CSS, Pan-STARRs[443, 444], ATLAS, CNEOST el al.), after three decades of efforts, our knowledge of the near-Earth object (NEO) population has vastly improved: more than 95% of kilometer-class NEOs have been cataloged. Next-generation sky surveys, such as the Large Synoptic Survey Telescope and NEOCam, will catalog smaller NEOs.

Surveys with ground-based optical telescopes are the most efficient way for comprehensive NEO detections. In the next decade, LSST is poised to make powerful contributions to the study of NEOs in the southern hemisphere, WFST will also play an important role in the survey of NEOs. WFST can contribute significantly in two aspects: *** The first is a comprehensive survey and catalogs of NEOs. WFST large mirror size , larger field of view, and high resolution will be uniquely suited to providing such a survey. It's large mirror will be able to detect the faint (r=22.5 mag with 30 second exptime), small objects, it's large field of view (about 6.5 square degrees), will enable frequent repeated observations of a significant fraction of the sky for finding NEOs, and it's high resolution(0.33"/pix), will improve orbital accuracy of faint NEOs. *** On the other hand, a part of NEOs that orbit the Sun on or within Earth's orbit are tricky to detect for ground-based observers due to their proximity to the Sun in the sky. Because of selection effects, they remain poorly characterized, and cataloged. Most objects that fall into this class are known as Atiras or interior-Earth objects. For Ground-based optical telescope, Atiras a are generally only observable in the brief windows during evening and morning twilight. Even though multiple projects have surveyed Atiras, but now we've only found more than 50, and many of them were discovered by ZTF[7, 445]. Observation of the Atiras region have other benefits as well. Twilight observations at near-Sun region will significantly increase the solar phase angle coverage of NEOs and MBAs, improving photometric models and promoting detection, facilitate the discovery of Earth Trojan asteroids[446], if they exist, that would be librating at the Earth-Sun L4 and L5 Lagrange points, where overlapping near-Sun region. Dynamical simulation shows that these objects can survive over timescales comparable to the age of the solar system, implying that a small, ancient population of asteroids may exist in these regions. There is only one known Earth Trojans. Large aperture WFST and excellent night sky conditions of Lenghu, the combination have the advantage of twilight observations (we start observations at a sum altitude of -12 degree until -18 degree end observation). A twilight survey is one way to achieve the science use cases described without impacting WFST survey operations.

4.2 Cometary Activity

Comets are thought to be the least modified solar system objects remaining from planetary formation. Observation and research of comets can help us to understand the origin and evolution of the solar system. Comets can be classified into short-period comets(orbital periods of less than 200 years) and long-period comets(orbital periods of larger than 200 years) according to their periods. Before 2006, comets were thought to have originated in two places. Short-period comets were originated in the Kuiper Belt or scattered disc, and long-period comets were originated in the Oort Cloud. In 2006, a third source of comets was discovered: the main asteroid belt [447]. Main belt comets are in the main asteroid belt, they have similar orbital characteristics with main belt asteroids, but have a tail or coma. As a new class of comet, the main belt comet has become a research hotspot since its discovery. The discovery of a comet in the asteroid belt means that water ice still exists in the belt, providing an opportunity to further in-depth study the source of the earth's water [448] and the solar system's thermal history.

WFST can be used to study the activity of main belt comets and distant comets. There are only 9 main belt comets have been discovered [449, 450] up to now. As the short time and small number of discoveries, the study of the main belt comets are not comprehensive. Therefore, it is very important to search for new main belt comets and study their activity. Within 3 AU, activity of comet can be explained by the standard model of water ice volatilization drive [451], while beyond 3 AU, the activity of comets are mainly caused by the volatilization of volatile gases [452]. As the mode of dust released from the surface of comet nucleus due to the sublimation of gas ice and water ice is different, therefore, the study of distant comets is helpful to study the mechanism of comet activity.

4.3 Trans-Neptunian Objects and Planet Nine

Trans-Neptunian Objects (TNOs), also called Kuiper Belt Objects (KBOs), are asteroids or dwarf planets located beyond the orbit of Neptune, from about 30 AU from the Sun extending to nearly 1,000 AU or even farther. Though more than 2,000 objects have been cataloged so far, they only represent a tiny fraction of the actual populations in this region. It is believed that the Kuiper Belt is populated with millions of objects, including hundreds of thousands larger than 100 kilometers[453, 454].

Diverse structures and characteristics of TNOs can sculpt formation and evolution history of our Solar System in more details, and offer unique conditions to limit unknown parameters appearing in planetary formation/migration simulations. TNOs are classified into several dynamical populations–resonant populations, classical belt, scattering disk, and detached objects. Comparisons between different populations could reveal useful information to infer their respective evolution history. The cold classicals, dynamically defined as having non-resonant orbits and no close encounters with Neptune, with orbital inclinations less than 5°, is a special population with many unusual physical properties, such as distinctly red color, large fraction of wide binaries, generally higher albedos, a steep slope of size distribution at large sizes[455]. All these properties implies that this group may form or dynamically evolve by different processes than other TNOs. Furthermore, various potential correlations among orbital and physical characteristics, such as inclinations and colors, need to be confirmed or denied with larger observe sample[456]. Besides, even one single binary asteroid system, or several high-inclination objects, may impose strong restrictions on planetary formation and evolution[457].

The Planet 9 hypothesis is deduced from several dynamical anomalies of currently known distant TNOs [458]. Distant TNOs, also called detached objects, far beyond the eight-planet dynamical region, can unfold the far reaches of the solar system in an indirect way. However, there are only 14 detached objects detected, with five chaotic ones being thought not ideal to represent dynamical statistics due to their instability[459]. Therefore, larger sample are necessary to further limit or exclude the existence of Planet 9.

5 The Milky Way and Its Satellite Dwarf Galaxies

5.1 Star Formation

5.1.1 Young Stars

The mass accretion rate ($\dot{M}_{\rm acc}$) is a crucial parameter for understanding the evolution and dissipation of circumstellar disks, and therefore also for understanding the process of planet formation. Young stars commonly show accretion variability at various timescales caused by different physical mechanisms, e.g. non-steady accretion on timescales of hours, the global instabilities of the magnetospheric structure on timescales of months [460, 461]. In addition, the interaction between circumstellar disks and the young massive planets could induce pulsed accretion activities [462]. A search for pulsed accretion activities from young stars also provide us a new tool to search for young massive planets. Measurement of accretion rates for the young stars in such environments provide us a way to understand the evolution of circumstellar disks in low-metallicity environments.

Gas from the disk is lifted out of the disk midplane by magnetic pressure and is funneled onto the star along the magnetic field lines. The infalling flow hits the stellar surface at approximately the free-fall velocity, causing a strong "accretion shock" on the stellar surface [463]. Ultraviolet/optical excess emissions arise as the gravitational energy of the infalling material in accretion processes is radiated away in the accretion shock and thus have been used as a very direct measure of the accretion rate [464]. The WFST survey will include the u band which cover the Balmer excess emission and provide the $\dot{M}_{\rm acc}$ measurement among the best methods. Figure 15 (left) shows a relation between the WFST u-band

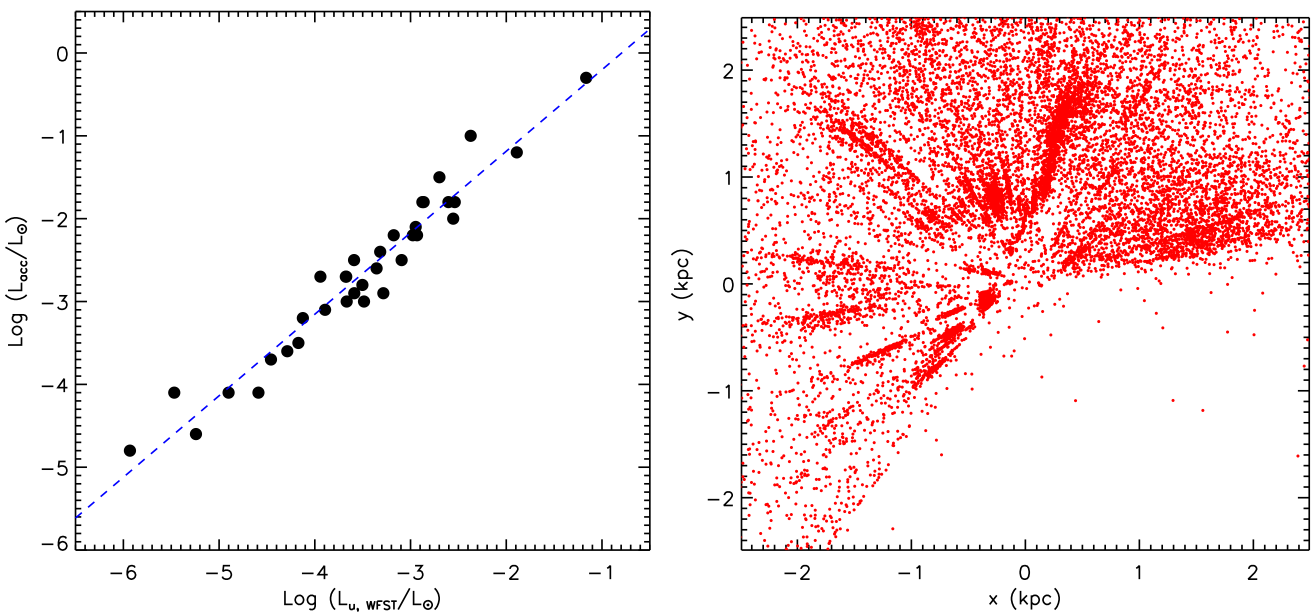

Figure 15 Left: Relation between the WFST u-band brightness and the accretion luminosity. Right: A bird's-eye view of the distribution of young stars with circumstellar disks which can be observed with WFST, looking down on the Galactic disk with the sun at the center.

brightness and the accretion luminosity for a sample of young stars in the literature [465]. The WFST synthetic observation are performed on their VLT/X-shooter spectra and the accretion luminosity are taken from [465]. The tight correlation shown in the figure promises that WFST u-band photometry can provide accurate measurements of accretion rates for young stars. Using the data from the Gaia EDR3 and allWise, we collect more than $\sim 1.8\times10^4$ young stars with circumstellar disks which can be observed by WFST, see the right panel in Figure 15. Thus, with WFST we will measure the accretion rates and their variability for a large sample of young stars for the first time.

5.1.2 *Accretion Burst Events*

How young stars gain mass from surrounding environment through disk accretion is still a open question. Traditional models usually assume a steady accretion with a constant accretion rate [466]. However, these steady accretion models predict significantly higher luminosity than observed for the young stars [467]. To solve this "luminosity problem", Kenyon & Hartmann (1995) [468] proposed a episodic accretion scenario, which assumes that a large fraction of total disk accretion occurs in some short-lived bursts. Accretion bursts were first observed for the low-mass young stars [469], and recently have been observed for a few high-mass young stars [470]. However, it is unclear how often young stars remain accretion outburst phase and which mechanisms drive the their accretion outbursts.

EXors and FUors are two types of young stars which are believed to undergo accretion outbursts. Fuors phenomenon are most prominent during the star formation stages. FUors increase in brightness by 5 magnitudes or more within one year and remain bright for decades [469], while EXor outbursts have relative shorter timescales (~yrs) and lower amplitude [471]. It is still unclear there are any physical distinctions between them because there are too few known FUors and lack of observational data for these FUors before their outbursts. Among $\sim 1.8\times10^4$ young stars with circumstellar disks which will be monitered by WFST, it is expected to detect the 0.5-7 FUor outburst events per year according to the PTF survey [472]. While a combination of data from all-sky infrared surveys can fully characterize the evolutionary stages of these young stars, the WFST time-domain survey will significantly contribute in understanding the accretion history of the young stars during different evolutionary stages.

5.2 Mapping the Milky way

5.2.1 *3D Dust Distribution*

Dust distribution is a necessary piece of the Galactic structure studies. Dust extinction is a commonly-used dust mapping technique. By measuring the reddening and extinction towards a large number of stellar objects, a continuous dust density distribution can be recovered. Based on the modern wide-field optical photometric and spectroscopic survey data such as SDSS, Pan-STARRS1, and Gaia, the three-dimensional (3D) Galactic dust distribution can be mapped in the arcmin-scale spatial resolution, with which the structures of dust Galactic disk such as warp and spiral arms have been revealed [473-476]. The WFST survey is over 2−3 magnitude deeper than Pan-STARRS1 (in r band). Therefore we expect to obtain 3D dust maps using WFST data with higher resolution and dynamical range than previous 3D maps, which will be helpful to trace the Galactic dense regions associated with star formation and constrain the Galactic models. Especially, the high sensitivity and photometric accuracy of the WFST survey will allows us to investigate the diffuse interstellar medium at high Galactic latitude such as the intermediate-velocity clouds (IVCs) that are considered as an inflow of gas consisting of recycled disk material and thus believed to be connected to a Galactic fountain process [477].

5.2.2 *Stellar Clusters*

Stellar clusters in the Milky Way are ideal test beds for the stellar evolution from the pre-main sequence to the post-main sequence, given by the large age spread over several magnitudes from a few to tens of Myr (open clusters) to a few to tens of Gyr (globular clusters) [478, 479]. The co-eval, co-spatial, and iso-metallic stellar members provide abundant information of the stellar astrophysics. Despite their importance to stellar astrophysics, most star clusters have been relatively poorly studied due to their large distances or their large angular sizes.

The detecting limit of the finally stacked images from WFST survey in the r band goes to r = 25 mag, 2−3 magnitude deeper than the Pan-STARRS1 survey. For the open clusters confined in the galactic plane, Figure 17 estimates the minimum stellar mass detected by WFST varying with distance from near to far. For clusters with distances within the 5 kpc from the sun, WFST can resolve stellar mass down to $\lesssim 1\ M_{\odot}$, and ensure rather complete mass estimate for these open clusters. The relative young open clusters and the even younger embedded clusters (better studied in the IR wavelengths) represent the current star formation rate of the Milky Way [480]. The 3D distributions of these two types of young clusters map the 3D star formation rates of the Milky Way, which, together with the 3D molecular gas map [481], provide the largest view of baryon cycle of the Milky Way. For the nearby ($\lesssim$1 kpc) young clusters, WFST's accuracy, sensitivity, and multi-epoch observations allow for the detection of their members down to the brown dwarf mass range, a much better characterization of low-mass star formation in stellar clusters, and an deep investigation of initial mass functions.

Gaia mission has provided a list of reliable members for more than 200 known clusters within 2 kpc from the Sun [482]. These clusters range in age from 10 Myr to several Gyr [483] and thus are excellent calibrators for the mass–dependent relationship between stellar rotation and age. While ones obtain the ages of these clusters from color-magnitude fitting using the Gaia data [483], the rotation periods of individual members in each cluster can be derived from the WFST time-domain survey. A calibrated mass–dependent relationship between stellar rotation and age will be the key to investigating the star formation history of the milky way.

5.2.3 *Structure of the Milky Way*

The stellar structure of the Milky Way is composed of four components: a bulge, a thin disk, a thick disk, and a diffuse stellar halo. The knowledge of the structure of the Milky Way has been significantly improved with the data from various surveys, e.g. SDSS, Pan-STARRS, LAMOST, and Gaia, and the development of new technologies. However, there are still many unknown issues about the fine structures of the Milky Way, and there are still many unresolved problems in its formation mechanism.

As a space facility, the GAIA satellite can observe the entire sky, while its magnitude limit is ∼ 20 mag and it is not suitable for studying dense stellar fields. In order to investigate the precise structures of the Milky Way and their formation mechanism, it is necessary to perform a deep survey which covers a large field of view and can detect a larger number of low-mass stars to large distances, see the bottom panel in Figure 16. An accurate three-dimensional distribution of stars in the Milky Way and a decomposition of the Milky Way into different components are crucial for constraining the formation mechanism of different components of the Milky Way. To distinguish the different components, one need to measure the metallicities of individual stars which requires deep and high precision photometric data in *ugr* bands [484]. Current surveys with large field of views are either lack of the u-band filter (e.g. Pan-STARRS) or too shallow in u-band (e.g. SDSS or SkyMapper). The upcoming LSST will reach a depth of r = 27 mag from the co-added images, but its observational area is limited in the southern sky.

The six-year WFST co-added images will reach depths of u = 24.6, g = 25.2, and r = 25.1 , which is ∼ 2 magnitude deeper than the existing SDSS data, and will obtain high-precision multi-color measurement of nearly 5 billion stars in the Milky Way and detect main sequence stars at large distances (see Figure 16). The multi-band photometric data (including u band) of the deep sky survey can measure the photometric metalicities of stars, which will be critical to distinguish the halo stars from the disk stars, and also more accurately determine photometric distances of stars. The large

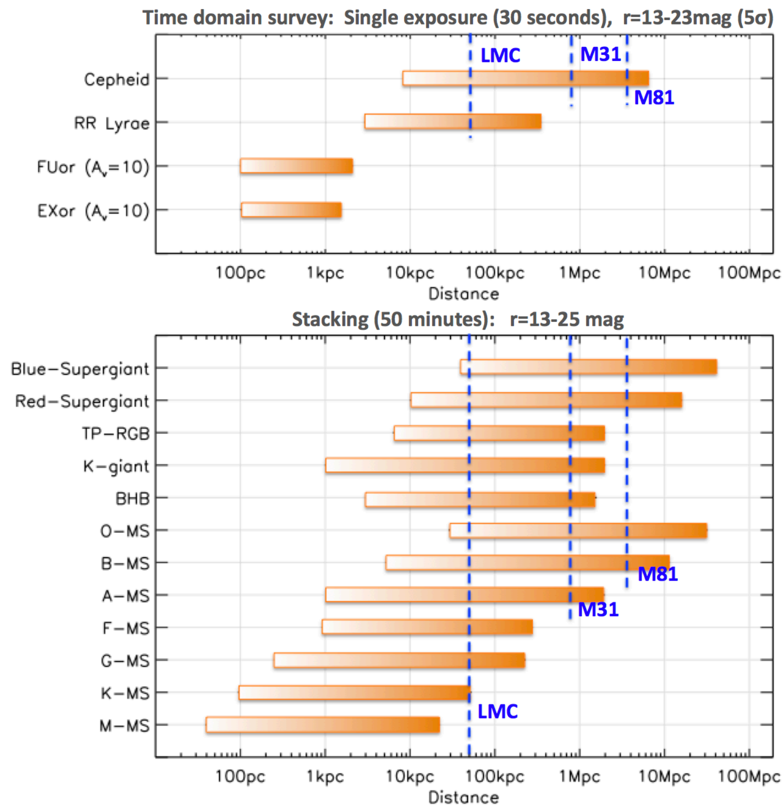

Figure 16 Detectability of different types of stars vs. the distances in the WFST images with single exposure (top) and stacked images (bottom)

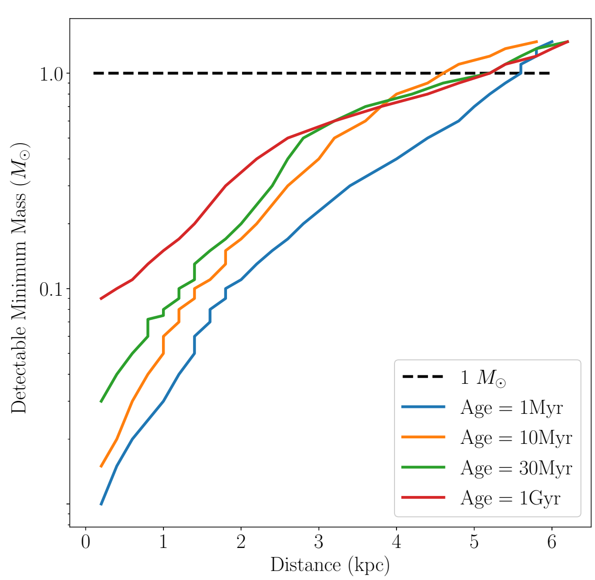

Figure 17 The minimum stellar mass of the open cluster member varies with distance from near to far. The isochrones of low-mass stars at 4 ages are shown in different colors [485]. For open clusters, an empirical relation $A_V = 1.5\,\mathrm{mag\,kpc^{-1}}$ is used in the distance module.

samples of metal-poor stars can be used to investigate the metallicity distribution function (MDF) of the Galactic halo and then to constrain the Galactic chemical evolution models. With the metalicities and distances of stars, we can study the structure of the Milky Way at a more precise and farther distance. In particular, the WFST survey will expect to detect many more (several tens) debris streams at large distances ($R > 50$ kpc) from either dwarf galaxies or globular clusters.

5.2.4 *Astrometry and Variable Stars*

The WFST survey can survey more than 6000 square degrees per night, and cover the whole northern sky in one band every three nights. The six-year survey will obtain the high-quality imaging data of the the whole northern sky in *ugriz* bands at more than one hundred epochs. With these multi-epoch data, it is expected to measure the proper motions (σseveral mas yr^{-1}) of one billion stars in the northern sky and obtain the multi-dimensional information (such as proper motions, parallaxes, positions, and metalicities) of ~100,000 nearby stars. With such information, one can construct the local gravitational potential field and constrain the mass distribution and structure model of the Milky Way. The WFST's sensitivity and accuracy will allow for the detection of the hypervelocity stars in the galactic halo at distances up to more than 10 kpc. The multi-band photometric data can be used to measure the metalicities of these hypervelocity stars which are important to distinguish their origination [486].

The WFST time-domain survey will detect millions of variables. Among them, RR Lyrae Stars and Classical Cepheids are two of most important ones which can be served as standard candles to measure distances, eclipsing binary stars (EBs) are key in the study of stellar physics, and X-ray binary systems, including high-mass X-ray binaries and ow mass X-ray binaries, are ideal astrophysical laboratories to understand the formation and evolution of the normal star, compact objects, and the mass transfer in the binary system [487]

RR Lyrae Stars are old (>10 Gyr) low-metallicity, horizontal-branch pulsating stars which are periodic variable and have been used as standard candles to measure distances. Currently the completeness on RR Lyrae Stars from the existent surveys like Gaia and PanSTARRS drop to $\lesssim$50% for the distance $\gtrsim$ 80 kpc [488]. Given that the WFST survey is over one to two magnitude deeper than the Pan-STARRS1 survey, the survey will significantly increase the samples of RR Lyrae Stars at large distance in the Milky way as well the ones in nearby dwarf spheroidal galaxies, see the top panel in Figure 16. These RR Lyrae Stars at large distance are extremely important to study the Galactic halo and investigate the structure of the Milky way near the viral radius (~200–300 kpc [489]) of the Milky Way's dark matter halo. For the Galactic thick disk, it is still not well established if it is a distinct component, if it is flare or warp, and how it is relate to other Galactic components (thin disk, halo, and bulge) in the chemistry, spatial extent, and kinematics [490]. The deep WFST time-domain survey at low latitude, where the extinction is relatively higher than the halo, to search for RR Lyrae will play a key role in solving these puzzles.

Classical Cepheids are among the most important standard candles to estimate accurate distances within the local group. Different from the RR Lyrae Stars, Classical Cepheids are young ($\lesssim$400 Myr) and have been used to study the thin disk structure of the Milky Way and trace the detailed morphology of the thin disk till the Galactocentric distances of ~15 kpc [491-493]. The WFST survey expect to detect the Classical Cepheids at the distance more than 5 Mpc, see the top panel in Figure 16. When completing the sample of Classical Cepheids in the Milky Way and depicting the Galactic structure in more detail, the sample of Classical Cepheids in different galaxies can be used to address the intrinsic variation of Cepheid properties.

Eclipsing binary stars (EBs) are very important for the study of stellar physics. The accurate physical properties (i.e., masses, radii, temperatures, luminosities) of two component stars can be obtained through the analysis of EBs. These properties can strictly tests of stellar evolution models, especially for the models at the low mass ranges where the evolution models are very uncertain. Meanwhile, there are many open issues in eclipsing contact binaries (ECBs), such as the merging of binary stars, the evolution of the common envelope, and the short-period limit [494]. The detection limit of the WFST survey in the r band down to r≈23 mag with 30-second exposures. This means that more faint EBs can be discovered by WFST. According to the well-known period-color relationship of ECBs [495, 496], the ECBs with the shortest period has the lowest temperature. Search for faint main-sequence ECBs can further study the reason of the ECBs period cut-off. For example, an ECBs system with M2V+M2V components can be observed within 4 kpc with a magnitude of r≈22 mag.

X-ray Binaries are composed of a normal star and a compact object, either a neutron star or a black hole[497]. According to the mass of the optical companion, X-ray binaries, conventionally divided into high-mass X-ray binaries (usually $\geq 10\ M_\odot$, [498]) and low mass X-ray binaries (usually $\leq 1\ M_\odot$, [499]). High Mass X-ray Binaries have two main sub-groups, the supergiant X-ray binaries and the Be/X-ray binaries. Till now, there are only 114 high mass X-ray binaries which have been catalogued in the Galaxy and about 60% of them are known as Be/X-ray binaries[498]. In a Be/X-ray binary, the compact companion is usually a neutron star [500], but Be-black hole binary systems have also been discovered [501]. Most of Be/X-ray binaries are hard X-ray transients and they usually show two types of X-ray outbursts: Type I X-ray outbursts, of which the X-ray luminosity $L_X \sim 10^{36-37}$ erg s^{-1} and the interval is the orbital period, and Type II X-ray outbursts, which are much brighter ($L_X > 10^{37} ergs^{-1}$) and have no obvious connection with the orbital period [502]. Long-term optical observations indicate that significant optical changes precede the X-ray outbursts[503]. Therefore, it is very important to monitor a sample of Be/X-ray binaries to study the relationship between the optical variability and the X-ray outbursts. Low Mass X-ray Binaries are systems in which a neutron star or black hole is accreting materials from a low mass companion donor star via Roche lobe overflow. About 200 low mass X-ray binary systems have been catalogued in our Galaxy [499] and most of them are X-ray transients, which have been seen in outburst. Population synthesis indicates that there are about 2.1×10^3 LMXB system with neutron star accretors in our Galaxy [504] and the majority remains uncharacterised. The time-domain survey of WFST can be used to find the periodic variability in the lightcurves and discover more new LMXB candidates.

5.3 Satellite Dwarf Galaxies in the Local Group

The dwarf galaxies around the Milky Way and M31 are the most low-mass galaxies that can be observed in the Universe. These objects are of great interest due to their unique position in astrophysics. Bright stars can be resolved in these systems even with ground-based telescopes, making them excellent targets to study the star formation histories, chemical enrichment as well as the initial mass function in the low-mass halos [505, 506]. In addition, their abundance and spatial distribution can put stringent constraints on structure formation theory on length scales smaller than $\sim$ 1 Mpc[507]. Like their massive counterparts, dwarf galaxies are also dark-matter dominated. Although dark matter cannot be detected directly, it is possible to detect it through the products of its decay. Considering their physical scales and distances, dwarf galaxies in the Local Volume are ideal laboratories for detecting such dark matter decay signals[508].

The search for faint dwarf galaxies in the Local Volume has been continued since the serendipitous discovery of the first such system in 1930's. Only 11 Milky Way satellite galaxies were discovered prior to the Sloan Digital Sky Survey (SDSS). During the past two decades, more than 50 new Milky Way satellite galaxies were discovered, thanks to the advent of large imaging surveys such as SDSS. Most of the known Milky Way satellite galaxies have comparable luminosities with globular clusters but with much lower surface brightness, making them difficult to identify directly in the images. In practice, these galaxies are found as statistically significant fluctuations in the number densities of cataloged stellar objects.

The 6-year WFST co-added images will reach a depth of $r = 25.1$ and cover 20000 deg^2 of the northern sky, which are well suited for the searching of faint dwarf galaxies in the Local Volume. This is ~ 2 magnitude deeper than the SDSS and comparable to that of the Dark Energy Survey (DES)[509]. The DES covers $\sim$ 5000 deg^2 of the southern sky, and $\sim$ 20 Milky Way satellites are found in the DES footprints. Under the simple assumption that the Milky Way satellites are distributed isotropically, then one will detect ~160 Milky Way satellites in the full sky down to $r \sim 25$. For the SDSS footprints observed in the northern sky, $\sim$ 40 satellites are expected to be detected down to this magnitude limit. Subtracting the classical and newly found satellite galaxies in the SDSS footprints, $\sim$ 20 new Milky Way satellite galaxies are expected to be found in the era of WFST. However, this number should be treated as an up limit since the observed satellite galaxies are not distributed randomly but seem to cluster near the Large Magellanic Cloud.

We have simulated the capability of WFST in detecting dwarf galaxies. The detection efficiency is quantified by simulating model dwarf galaxies embedded in star fields typical to those observed by WFST. A Milky Way star fields background is constructed with galaxies[510]. The stars of simulated galaxies follow the Kroupa et al initial mass function[511]. Our simulated galaxies are assumed to have old and metal-poor stellar population as observed, spanning a stellar age range of $7 - 12$ Gyr and a metallically range of $[\mathrm{Fe/H}] = [-2.2, -1.5]$. We search dwarf galaxies with the algorithm developed by reference[512]. We show the detection efficiency as a function of distance and galaxy absolute $V-$band magnitude in Figure 18. Within the viral radius of the Milky Way (~ 300 kpc), galaxies with $M_V < -4$ are guaranteed to be detected by the WFST stacked images. Within 1 Mpc, the detection limit is $M_V < -6$.

6 Galaxy Formation and Cosmology

Modern optical imaging surveys significantly deepen our understanding of the universe. Especially recent years, with the help of high quality imaging data from SDSS [513], CFHTLenS [514], Dark Energy Survey (DES) [515], HSC-SSP [516] and KiDS [517], we can explore our universe with unprecedented accuracy, a.k.a an era of precision cosmology. Nonetheless, tensions emerged between CMB observations [518] and optical survey measurements, e.g. σ_8 tension between weak lensing and CMB, as well as H_0 tension between

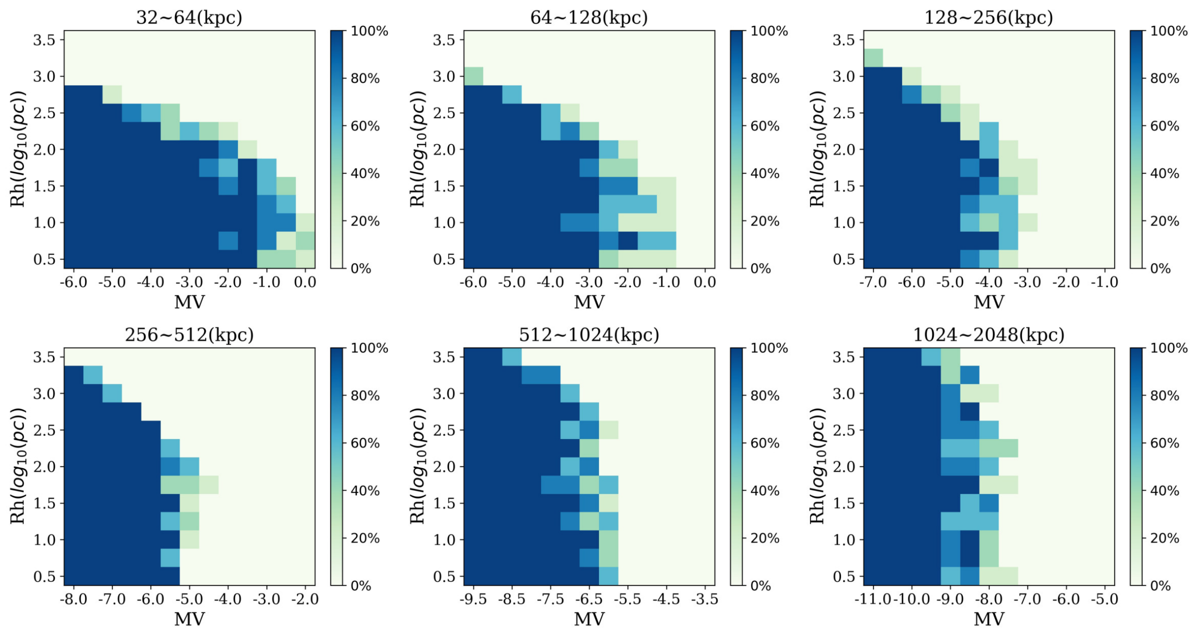

Figure 18 Detection efficiency of searches for dwarf galaxies. Detection efficiency is shown as a function of azimuthally averaged physical half-light radius and absolute V-band magnitude in different bins of heliocentric distance. The detection efficiency ranges from 0% to 100%, as shown in the color bar.

CMB constraints [519] and time-delay, SNIa measurements. This leads people to probe weather it is due to some hidden systematic [520] or there are new physics that is beyond our knowledge [521]. The debate continues even among groups studying the same subjects but with different telescope data sets. At the meantime, more efforts have been made to improve the data processing pipelines if any test shows some unpleasant features for precision cosmology. For instance, a recent work from HSC-SSP weak lensing group finds that autocorrelation of PSF ellipticity residuals remains larger than the requirement at larger scale [522]. While the DES team also finds similar issues [523] and modifies the PSF reconstruction pipeline. Besides the PSF, there are many other systematics such as measurement method, object detection and blending, sky subtraction, and the accuracy of photometric redshift and so on. These are the systematic for all the ongoing and future surveys and need to be carefully dealt with.

Apparently, so far, all the data sets we have are not enough to answer the question of new physics or systematic. This task can be further carried out with more data from the near future, facilitated either by space-based telescope, e.g. CSST, EUCLID [524] or ground-based telescopes, e.g. LSST [525]. The latter will cover half of the sky coverage and deeper imaging down to r band of 28 mag. As one of the future optical telescope, the WFST multi-band *ugriz* imaging survey will be the largest survey in the northern sky overlapping with multiple spectroscopic surveys such as PFS, DESI, LAMOST2 and MUST. The combination of multi- band imaging and spectroscopic information will strengthen the study for precision cosmology together with LSST from the southern sky.

6.1 WFST Imaging Data Product

The WFST main survey is able to image the 2π sky every 3 nights in one filter, and reach *r* band depth of 22.93 as shown in Table 4. The final 6 years data will reach the limit up to 25.1 mag (5σ), which is comparable to the Dark Energy Survey (DES) [509] but 4 times larger in terms of survey region. In general, WFST will be the deepest *u* band imaging in the northern sky and complementary to LSST [525] in the southern sky. The imaging data production rate is about 1.4 Terabyte per night. The massive imaging data needs to be carefully processed for scientific researches. Fig. 19 shows an example of PhoSim simulated WFST field of view. The RGB color scheme is based on the *gri* band simulated images. We then will test and modify the image processing pipeline based on LSST data management stack [526], which is publicly available under the Creative Commons Attribution 4.0 International License [3)]. This suit of simulations will be used to test the image processing pipeline before real time data processing.

3) https://developer.lsst.io/stack/

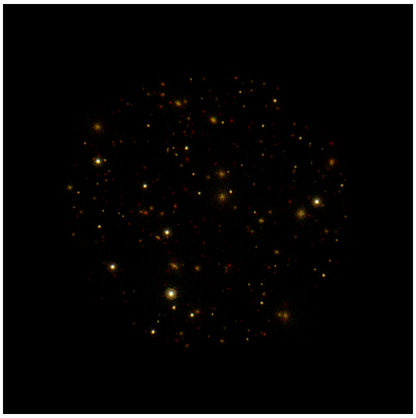

Figure 19 One pointing of WFST field image with about 6.55 deg^2. It is synthesized using *gri* band image to generate the colored image.

6.1.1 Weak Lensing Shape Catalog

With the median 0.7" seeing condition, and the wide survey area, a large sample of various catalogs will be produced from the imaging data. For the galaxy catalogs, the shape of galaxies contains valuable information of of the dark universe based on weak lensing analysis. Galaxy number density is one of the most important criteria for weak lensing studies. Among the existing shape catalogs, WFST will produce similar number density to DES, which is about 7 galaxies per arcminute square. However, the coverage is more than three times than DES final data release, resulting a $> \sqrt{3}$ higher SNR in galaxy-galaxy lensing measurements. The final estimated catalog will contain 540 million galaxies with shape, position and photometric redshift measurements. We will apply METACALIBRATION [527] as well as FPFS [528] to measure the shape catalog to cross test the potential bias due to different measurement method. For the PSF reconstruction we will apply PIFF [523] to analyse the star images and PSFEx [529] to cross test the PSF reconstruction performance.

Proper simulations are necessary to calibrate the multiplicative bias and the additive bias by mimicking the observing conditions. Mandelbaum et al 2018[530] uses $Hubble\ Space\ Telescipe$ (HST) high resolution F814w images to evaluate the impact of galaxy morphologies and nearby galaxies. This basically inherit the framework of $GREAT3$ [531]. A more advanced simulation suit CosmoDC2 [532], based on a trillion-particle cosmological N-body simulation, is able to provide galaxy properties by Semi-Analytical Models (SAM [533, 534]). For instance, galaxy size, sersic index and stellar mass can be generated to maximally mimic the LSST observations. We also develop our own simulation suit to test and modify the LSST_dm_stack pipeline, which will be described in another independent work. Fig. 20 shows the simulated image from our pipeline by combining ILLUSTRISTNG50-1 [535] and radiative transfer calculation using BC03 spectrum evolution [536], Chabrier IMF [537] and Calzetti attenuation law [538].

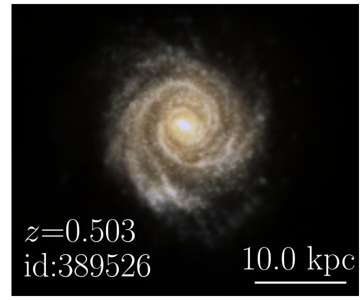

Figure 20 The simulated image based on ILLUSTRIS TNG 50-1 and radiative transfer considering gas and dust extinction.

6.1.2 Photometric Redshift Measurements

Spectroscopic surveys is far more demanding than photometric ones. Photometric redshift is then a necessary substitute for redshift estimation. SED template fitting and machine learning are the two major classes of codes to compute the photometric redshifts. In each class, ANNz2 [539] (Artificial Neuron Network) and LePAHRE [540] (SED fitting) are tested to be more reliable according to a series photometric redshift tests [541]. We also generate a mock catalog with 5 band magnitudes and errors to test the performance of the two code. Fig. 21 demonstrates the preparation testing scheme of the photoZ codes. The left panel in this figure shows the response curves of *ugriz* filters, including the atmospheric, CCD quantum efficiency effect and the filter intrinsic responsivity. A typical early type galaxy SED is scaled and over plotted on the filter response curve. The black, red and blue curves are representing the original redshift SED, red/blue shifted SED with ±200km/s. The middle panel shows the error as a function of magnitude and the right one is the testing results for Le PHARE with about 100 mocked sources.

6.2 Galaxy Formation

The WFST shear catalog is one of the products of galaxy formation study with position, galaxy shape, photometric redshift and calibrated biases as a function of resolution and SNR. Combining with the existing spectroscopic data set in the northern sky, e.g. SDSS [513] and future ones such as MUST [] and LAMOST2 [], it will significantly benefit the study of weak gravitational lensing. Especially the constraint on galaxy formation and cosmology will be improved. We will address the science in three aspects related to weak lensing analysis, i.e. galaxy-halo connection, halo assembly and cluster detection. There are two other important scientific

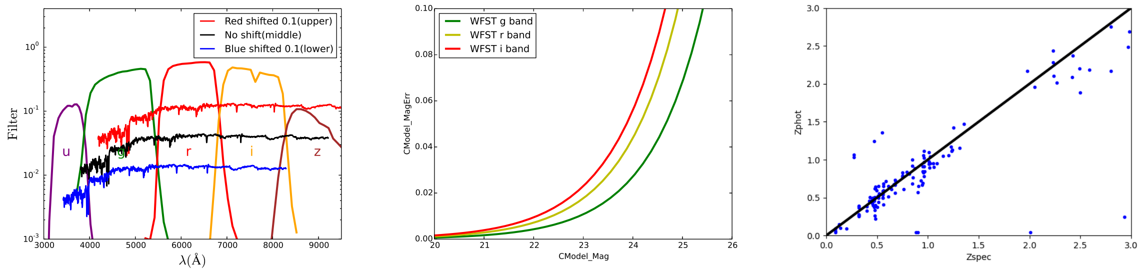

Figure 21 *Left:* The shifted SED of a typical early type galaxy.*middle:* The modeled photometry error of WFST *gri* bands. *right:*The photometric redshift measurement compared with spectroscopic redshift to mimic WFST *ugriz* photometry performance.

subjects also can be done using WFST imaging data. With the deep u band imaging, it is possible to also detect a large sample of *u* band drop out galaxy and low surface brightness galaxies.

6.2.1 Galaxy-halo Connection

Galaxies are believed to form and evolve within dark matter halos and affected by the large scale environment. Therefore exploring the connection of galaxies with their host dark matter halos and large scale environment becomes an essential step towards the understanding of the full picture of galaxy formation. There has already been many studies in literature on the galaxy-halo connections, based on various observational measurements, such as galaxy clustering [542-545], or galaxy-galaxy lensing [546-549], or combining both observations [550, 551]. However, many questions still remain[552] unclear. One of the questions is whether the host halo mass depends on the galaxy properties. If so, which galaxy properties are dominant, and how are these correlations produced? How do different environmental processes, indicated by various environmental factors, affect the galaxy properties? A recent study of Zhang et al 2022 [553] find a massive star-forming galaxy sample that about 67% of the gas has been converted to stars, which is abnormally high compared the average of 20-30% converting rate. What mechanism causes this specific mass bin bearing such high gas consumption rate?

It is also particularly interesting to investigate whether the host halos of AGNs, which identified with strong central super massive black hole activities. AGNs are different from other galaxies based on the SED features, further among the AGNs there are different types of them indicating different physical process of some emission lines. Whether different types of AGNs reside in different large-scale environments still remain an open question. Zhang et al 2021 [551] find that the halo mass of AGNs are similar to the star-forming galaxies, but lower than the quenched control sample. However, the satellite number around AGNs are more than star-forming galaxies, indicating the AGN trigger mechanism may associate with satellite galaxies.

WFST shape catalog, with deeper imaging than SDSS and multi-band photometry information. The SNR of Weak lensing analysis around galaxies will improve by a factor of 3. This leads to an improvement of factor of 2 accuracy on halo mass estimation. Fig. 22 shows the error improvement from SDSS galaxy-galaxy lensing measurement (green dots) and WFST measurement (red dots), while the lower panel is the ratio of errors between the two given the same lens sample. WFST shape catalog alone shrinks the error bar by a factor of 2.5 at all scales. It also allows us to explore a larger parameter space.

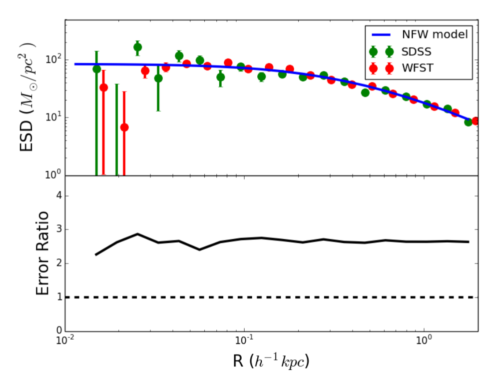

Figure 22 The comparison of the galaxy-galaxy lensing signals between SDSS shape catalog and WFST shape catalog. The lower panel is the ration between the two errors. The error shrinks by a factor of 2.5 given the same lens sample but different catalog.

6.2.2 Halo Assembly effects

It is well known that the clustering of dark matter halos strongly depends on halo mass [554]. Numerical simulations revealed that, at given halo mass, the halo clustering also depends on other halo properties, such as halo formation histories, internal substructures and spin [555, 556]. This higher order effect is usually referred to halo assembly bias.

From observations, there are many efforts as well to detect the assembly bias. For instance, Miyatake et al 2016[557] claim the detection of assembly bias based on RedMaPPer [558] clusters applying weak gravitational lensing and projected clustering analysis. However, Zu et al 2017 [559] counter-claim that the previous detection is due to the projection effect for RedMaPPer cluster members and therefor the higher order bias is even higher than the LCDM prediction. They also further predict that a 10-fold more number of clusters with deeper imaging can improve the detection. WFST will roughly increase the number up to about 40, 200 which is 4.6 times larger than the sample in Miyatake et al 2016, with the same richness range but larger redshift range ($0.1 < z < 0.8$). Combining LSST cluster sample, it can pin down the error below 10% which is about the level of predicted LCDM assembly bias. A recent interesting effort split 630 massive clusters into early- and late- formed clusters using ELUCID simulation [560], they claim that a 4σ difference on the clustering have been detected, implying a detection of assembly bias

Clusters are not the only subject to analyse the assembly bias. Lin et al 2016 [561] selects low mass samples divided into early and late formed galaxies to detect this effect. They attribute the null detection to the noisy measurements. McCarhty et al 2022 [562] extends the previous work by adding more galaxy sample and changing the clustering estimator to redshift space distortion (RSD), which is basically the Legendre expansion of the clustering, but containing velocity information. They find a large amplitude of velocity bias for early-forming central galaxies which may be originated from assembly bias. Yet the SNR of the measurement is again too noisy to confirm this claim. More lens sample and deeper imaging are needed for a significant detection.

With such a shape catalog sample, e.g. [548], we can measure the halo mass of spectroscopic selected groups of galaxies [549] and compare with other halo mass estimation methods. Galaxies with different properties, sSFR or SFR that experience different assembly history may have same halo mass, but different large scale clustering, a.k.a, assembly bias [563]. Zhang et al 2021 [551] studies the halo mass of galaxies classified as AGNs, star forming galaxies and quenched galaxies and find that the halo mass of AGN and star-forming galaxies are significantly smaller than their quenched counterpart with identical redshift and halo mass distribution. WFST data can greatly boost the understanding of assembly bias together and therefor offer another test of LCDM cosmology with LSST from the south.

*** add sblash back radius later.

6.2.3 *U-band Drop-out Galaxies at $z \sim 2$–3*

The Lyman Break Galaxies (LBGs) are star-burst galaxies at high redshift (see. a review of Giavalisco et al 2002 [564]), which can be selected using this technique combining u, g and r bands as in a recent work combining CLAUDS and HSC-SSP deep data Sawicki et al 2019 and Thibaud et al 2020[565, 566]. There are many studies in literature on the UV luminosity function (UV-LF) of LBGs that can be used to estimate the energy budget at high redshift and galaxy evolution. Since Steidel et al 1995 [567], there are Reddy et al 2009 [568] and Cai et al 2014 [569] e.t.c that studies the UV-LF of LBGs.

The selection criteria is shown in EQ. 4 of Sawicki et al 2019 their, i.e. $u - g > 0.88$, $g - r < 1.2$ and $u - g > 1.88(g - r) + 0.68$. The WFST broad band can provide all those information with deep and wide survey regions as mentioned in Sec. 2. Here, we roughly estimates the number of LBGs from both deep (1200 Sq. deg. with g band 26.4 in magnitude, -20.6 in absolute magnitude and r band 25.9) and wide (6800 Sq. deg. g band depth 25.1 in magnitude, -21.9 in absolute magnitude assuming z=3 and r band 24.7) survey region by applying the LF at z=3 in Cai et al 2014 using M_{1350} monochromatic mag as an indicator. We can obtain 10^7 galaxies (with g absolute magnitude to -20.6 considering %90 completeness with $r < 25.5$) for deep region only, two orders lower than 10^9 from LSST survey. This catalog can be a legacy catalog for future spectroscopic surveys.

LBGs at higher redshift, i.e. $z > 4.0$ using *gri* color criteria can be also selected as has been done in Steidel et al 1999 [570]. All those selections are valuable legacy catalog of WFST imaging data.

6.2.4 *Low Surface Brightness Science*

The low surface brightness (LSB) regime holds the promise to revolutionize our understanding of galaxy formation and evolution in the coming decade. In particular, demographics of satellites around galaxies of different morphological types and masses in the local universe will offer crucial tests of the lambda cold dark matter paradigm on small scales [571,572]; systematic characterization of stellar halos and tidal features in the outskirts of galaxies can provide important clues to the hierarchical assembly histories of galaxies [573, 574].

The prime focus architecture of WFST minimizes the scatter light contamination, which is particularly desirable for LSB science. The WFST six-year co-added imaging data ($\sim$ 50 min) will reach a r-band 3σ surface brightness limit of ~ 28.7 mag arcsec^{-2} by averaging a $10{\times}10$ arcsec^2 area, slightly deeper than the 275 deg^2 Strip 82 field of SDSS [575]. By scaling the results from extensive completeness simulations of [575], we expect to achieve a detection of ordinary satellite dwarf galaxies down to an average surface brightness of ~ 25.7 mag arcsec^{-2} within the effective radius at 50% complete limit. This corresponds to a stellar mass limit of ~ $10^{6.1\pm0.5}$ $M_\odot$ out to ~ 60 Mpc [576]. In addition, a surface brightness limit of 28.7 mag arcsec^{-2} allows a detection of tidal features from galaxy merger events that happened at least ~ 3-4 Gyr ago [577]. Lastly, the wide-field and homogeneous datasets from WFST will enable a robust stacking analysis of surface brightness profiles well beyond 30 mag arcsec^{-2} for galaxies of different morphological types, masses and environments, providing stringent constraints on the buildup of galaxy stellar halos in general.

Besides its combination of sky areal coverage and survey depth, one important advantage of WFST over existing optical imaging surveys, such as the Dark Energy Survey and Hyper Suprime-Cam Subaru Strategic Program, lies in its inclusion of deep *u*-band data that are indispensable in probing stellar population properties of galaxies with broadband photometry.

6.3 Cosmology

As tensions among cosmological parameters emerge, e.g. H_0 and $S_8 = \sigma_8(\frac{\Omega_m}{0.3})^{0.5}$ recently between CMB probe and SNIa [578], time-delay [579], weak lensing analysis [580]. Debates arises if this is due to some hidden systematics [520, 581, 582] or some new physics that we need more data to confirm.

WFST data will produce a large sample of SNIa (see Sec. 3.1.5), strong lensing AGN/SNIa (see Sec. 3.1.5, 3.4) systems as well as cluster catalog and shape catalog, which will boost the cosmology study in the northern sky. We will focusing on the Standard cosmology constraints and cosmologies that deviates from LCDM.

On the standard cosmology study, we proceed with the analysis of cluster mass function, cosmic shear and the combination with other measurements, e.g. clustering, cluster mass functions, time-delay and so on. For non standard cosmology, we focus on the constraints of modified gravity models, dark matter particle models e.t.c

6.3.1 Cluster detection and cosmology

Clusters of galaxies, also provides information of cosmology and galaxy formation. The famous Bullet cluster alone [583] is a smoking gun evidence of the dark matter, where the X-ray hot gas significantly deviates from the distribution of the weak lensing inferred dark matter. Beside, the X-ray shock feature is a challenge to the standard cosmology in the sense that the collision speed of the two merging giants is too low to be found in the simulations. Abell 520, another intensively studied cluster using weak lensing technique, provoke another challenge to classic galaxy formation paradigm that way fewer galaxies than theoretical prediction in the "dark core" of the cluster [584]. A recent finding of a massive rotating cluster [585], which is actually coma cluster, with rotation velocity of 197 km/s. There have already been many mysteries for clusters to probe in the future WFST survey region.

The selection of a reliable cluster is not an easy task, especially the data without spectroscopic information. However, there are still endeavors to select cluster using photometric information only, e.g. RedMaPPer[558], CAMIRA[586] which applies the red ridge galaxies. Yang et al 2021 method [587] is a novel halo-based cluster selection method modified based on Yang et al 2007 [588] to adjust the pipeline for the photometric data. However, those methods suffers from the projection effect due to the accuracy of photometric redshift and therefore the membership estimation is biased as described in Zu et al 2017 [559], and Sunayama et al 2020 [589]. Along with extended X-ray sources, Sunyaev-Zel'dovich effect [518] can also be used to detect clusters. More recently, people use shear map to select clusters, e.g. HSC-SSP shear map clusters [590].

Combining cluster catalog with different selection methods, and the galaxy-galaxy lensing, tight constraints on observable halo mass scaling relations can be achieved. Fig. 24 shows the κ (colored map) and shear map (white ticks) of a cluster selected from ILLUSTRIS TNG simulation [535].

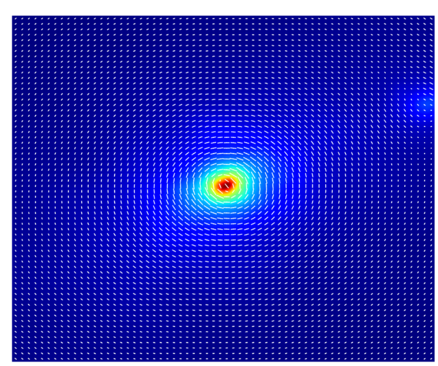

Figure 23 The shear map and kappa map of a cluster-sized dark matter halo chosen from ILLUSTRIS simulation with halo mass of $10^{14}\mathrm{h}^{-1}M_\odot$.

As mentioned in the previous section of assembly bias detection, WFST will generate a photometric selected cluster sample based on the RedMaPPer algorithm. The sample will contain more than 40,000 clusters with richness beyond 20 between $0.1 < z < 0.8$. The scientific goals are including cluster mass estimation and further mass function to constrain cosmology, cross-match the cluster with other observation e.g. SZ cluster [591], X-ray cluster [592] and weak lensing mass map. The cluster catalog together with the weak lensing shape catalog are valuable data for cosmology study and reference data for future surveys.

Once we have cluster catalogs from various observations as described in Sec **??**, we can constrain cosmology using cluster abundance and its evolution to constrain the fluctuation amplitude σ_8, the Ω_m parameter. The baryon fraction in clusters can be used to estimate the ratio of cosmic baryonic fraction $\frac{\Omega_b}{\Omega_m}$. The core structure of clusters can be a test of the nature of dark matter.

Apart from all the virtues of these cluster statistics, each of them has its own limitations, i.e. the systematics in converting cluster observables (X-ray luminosity, S-Z Compton parameter, richness and weak lensing) to mass can bias the scaling relation in mass estimation. The baryonic effect degenerate with dark matter property in the core structure analysis. Therefore, how to build a reliable cluster catalog become the first step for cluster cosmology.

6.3.2 3×2-point correlation functions

The 3 in the tile of this section denotes three types of 2-point correlations that are used in the statistics, i.e. galaxy clustering, cosmic shear, galaxy-galaxy lensing measurements. Cosmic shear alone is sensitive to the dark matter density perturbation σ_8 and the fraction dark matter in out universe Ω_m, e.g. [593]. However, the intrinsic alignments can bias the results [594]. The alignment of galaxies itself is an interesting subject [595] which studies the misalignment between the galaxies and their dark matter halos assuming a triaxial halo shape [596].

Recent weak lensing surveys, e.g. KiDS[517], HSC-SSP[522], DESc[515] and joint analysis combined with all three surveys [597] have roughly about 2σ tension with CMB experiments [518]. WFST data set, will shrink the error by a factor of 1.26 assuming an effective weak lensing area of deep square degree from the northern sky with similar depth of DES.

Apart from the constraints of simply halo mass of galaxies, cosmological constraints can be also obtained by combining clustering analysis. Leauthaud et al 2017 [598] find the weak lensing predicted σ_8 is lower than the one fits galaxy correlation well, a.k.a lensing is low? Afterwards, the combination of galaxy-galaxy lensing and clustering analysis become a standard routine to maximize the utility of different estimators, e.g. a very recent work combining galaxy-galaxy lensing and clustering using HSC-SSP data [599, 600]. It shows that galaxy-galaxy lensing at small scale can constrain halo mass of galaxies, and at larger scale beyond 2 to 3 Mpc/h can be used to infer cosmology parameters.

What worth mentioning is that a recent work by Shi et al 2018 [601] combine the redshift space distortion (RSD) from SDSS DR7 spectroscopic data and galaxy-galaxy lensing provides tight constraint on growth factor at redshift 0.1.

WFST wide/deep field survey areas overlap with eBOSS [602] that contains public spectroscopic sample that can proceed with the clustering and galaxy-galaxy lensing join analysis with LowZ and 2MASS sample. This combination will be a factor of 3.3 (wide)/3.0 (deep) in SNR compared to CFHTLenS analysis [603] and HSC S16A shape catalog [600].

6.3.3 Joint Analysis with Other Observations

Besides weak gravitational lensing, there are already many existing cosmological probes, such as the cosmic microwave background (CMB) [604] radiation, baryon acoustic oscillations (BAO) [605], and type Ia supernovae (SN Ia) [578]. The joint analysis and comparison among different probes. Especially the probes that bear different degeneracy direction for the same set of parameters, the join likelihood analysis can break the degeneracy between the parameters, e.g. Di Valentino et al 2015 [606] extend the constraint of 6 LCDM parameters to 12 parameters including the sum of neutrino mass, the sum of neutrino species effective number and the dark energy equation of state e.t.c by combining BAO, CMB, Weak Lensing and SNIa.

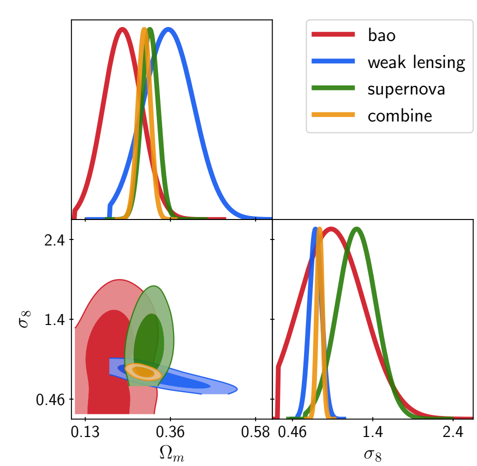

Figure 24 The joint analysis of cosmological constraints.

The joint analysis in the northern sky will be improved by WFST SNIa, Weak Lensing, clusters, time-dely and CMB. Especially, the spectroscopic catalog from eBOSS and DESI survey, will become a nature ally of WFST imaging data for the joint analysis.

6.3.4 Non-standard Cosmology

The tensions between the early probe and late probes lead people to think what if there is new physics just like the ”two dark clouds” in the early 20th century. Maybe, there are certain interactions between the dark matter and dark energy [607], which can explain the low σ_8 value from weak lensing constraint? Or can we find an substitute for dark matter [608] or dark energy [609]? What is exactly dark matter and can it be tested by cosmological probes like cosmic shear [610]? Does GR still holds at galactic scale [611]?

Weak gravitational lensing can provide strong constraints on the dark side of our universe and therefore on non-standard cosmology. For instance, a recent work from Luo et al 2021 [612] finds that the Emergent Gravity [608] can hardly explain the difference weak lensing signals between the blue/red galaxy sample with similar stellar mass. Zhang, An and Luo et al 2019 [613] ruled out one of the interacting dark matter/energy model using weak gravitational lensing analysis from SDSS DR7 shear catalog.

WFST wide/deep region will contain 7/22 times larger source galaxies per arc-minute square with similar survey area. This wide/deep shape catalog will improve the constraint by a factor 2.12/1.88 for wide/deep respectively.

7 Summary

The Wide Field Survey Telescope (WFST), located at the top of Mountain Shashiteng, will image two major surveys wide and deep, covering 8000 and 1200 square degrees separately. With the unique design of survey strategy, WFST u band depth can reach 26.0 mag for deep region, which is comparable with LSST 10 years u band depth. The high cadence enables the search for multiple time domain sources such as supernovae, tidal disruption event (TDE), the optical counterparts of gravitational wave event, the variability of AGNs and the near earth terrestrial objects. The stacked wide and deep data can also provide imaging data for cosmology study, such as weak/strong gravitational lensing, galaxy formation and constraints of cosmology.

The high cadence deep imaging survey mode of WFST can select tens of thousands of supernovae, including a few hundreds that have early-phase observations. This early-phase information provides a unique means to understand the progenitor systems. The high cadence u band data also boost the detection of UV-luminous objects, a.k.a. Fast Blue Optical Transients (FBOTs) as well as extreme supernovae which are 100 times more luminous than SNIa and CCSN. Despite of the low event rate of superluminous supernovae, WFST should be able to detect a fairly complete sample of SLSN at $z \leq 1.0$. Furthermore, the strongly-lensed supernovae at high redshift can be used to constrain Hubble parameter via the time-delay measurement among multiple-imaged systems. A rough estimation of 20 such systems will be discovered within 6 years of WFST survey, compared to 4 existing ones. This sample combining strongly-lensed AGNs from WFST legacy data alone, can pin down the H_0 constraint to $< 1.0\%$.

Kilonovae, a transient phenomenon triggered by the merging process of binary neutron stars or Black hole-neutron star are one of the sources of gravitational wave. This intriguing event has been firstly confirmed in 2017 by the follow-up observations of GW170817/GRB170817A. Kilonova can not only explain the production of heavy elements through R-process, but also can constrain H_0 with electromagnetic observations with redshift information. Kilonovae is also one of the model to explain the Gamma Ray- Burst, yet no agreement on the formation of the beamed gamma ray jet has been reached so far. The data from the early optical afterglow of GRBs will greatly help the understanding of the triggering mechanism of GRBs. There is another energetic radio fast emission, a.k.a fast radio burst (FRBs) recently come to focus as the CHIME experiment together with others discovered hundreds of repeating and non-repeating FRBs. The optical information from WFST will provide optical information for those objects and therefore the understanding of the physics of those transients.

At galaxy scale, another break through from time domain astronomy is tidal disruption events (TDEs), which is assumed to be a star destroyed by the super massive black hole in the center of a galaxy, which can be considered as a direct probe of the central SMBH associated with AGN activities. The rare event rate of TDEs makes it difficult fo be detected. However, with large field of view and high cadence survey strategy like WFST will discover TDEs at a rate of 529± 81 per year while extending the redshift of TDEs to redshift about 1.0. The TDEs by intermediate black holes (IMBH), which is one of the many models to explain FBOTs, provide a unique way to understand the gap between stellar black hole and SMBHs. Therefore support the theory of seed black holes, the baby SMBHs. The grown-up SMBHs powers the central engine of ANGs by accreting adjacent materials in the central region of galaxies. AGN itself become an important subject of astronomy. The diversity, the variability, the observations from high energy, gamma ray, x ray all the way to infrared and radio emissions. Particularly, there are a subclass of extreme variable AGNs, with more than 20% are confirmed as face-changing AGNs which bring up more questions about the physical mechanism of such variability. Together with strongly-lensed SNe, strongly-lensed AGNs will also provides the test bed of our cosmology. WFST will increase both of the samples' size and therefore better our understanding of the EV AGNs as well as cosmology. ***add high energy neutrino observation***

We also access the capability of WFST on the detection of Near Earth Objects (NEOs) and conclude that with the WFST survey ability, it will improve both the positioning and the detection of fainter NEOs. Besides NEOs, the cometary activity and the Trans-Neptunian Objects (TNOs) also known as Kuiper Belt Objects (KBOs). The dynamical anomalies of the TNOs, the distant TNOs, hints the existence of planet 9. The sample of TNOs so far only contains 14 objects with 5 chaotic ones. So more samples are needed to either confirm or exclude the planet 9 hypothesis.

The stacked imaging data are valuable legacy for the study of our Milky way, galaxy formation and cosmology as in other imaging surveys. The WFST *u* band covers the Balmer emission as the indicator of the mass accretion rate, and the other broad bands are necessary to model the extinction. Referring to dust extinction, WFST has 2-3 magnitude deeper (*r* band) photometry than Pan-STARRS1 that can improve the 3Dn dust mapping of our Galaxy. The number of dwarf galaxies near our Milky way is a direct test of "missing satellite" problem.

The study of galaxy formation and cosmology depends not only data quality but the amount of data. WFST will provide 1.4TB per night imaging data, which covers 8000 square degrees in wide region with similar depth of DES and 1200 square degree deep region with similar depth to HSC-SSP. Those date are valuable for this subject. As mentioned in Sec. 6, WFST final 6 year data will significantly improve the constraints on galaxy-halo connection, the detection of cluster and cosmology. The shape catalog will be a legacy data that can be joined with other data e.g. KiDS, DES, HSC-SSP and future space and ground telescopes. Further the join analysis with BAO, SNIa, time-delay and CMB will further tighten the constraints as well as the collaboration among the cosmology community.

In summary, WFST with the best observation condition in the northern sphere, together with future spectroscopic surveys at the same spot i.e. LAMOST II and MUST, will not only contribute to time domain astronomy but also benefits other important branches.

This work was supported by the National Natural Science Foundation of China (Grant Nos. ???) and ???.

Conflict of interest The authors declare that they have no conflict of interest.

1 I. N. Reid, C. Brewer, R. J. Brucato, W. R. McKinley, A. Maury, D. Mendenhall, J. R. Mould, J. Mueller, G. Neugebauer, J. Phinney, W. L. W. Sargent, J. Schombert, and R. Thicksten, PASP **103**, 661 (1991).

2 M. F. Skrutskie, R. M. Cutri, R. Stiening, M. D. Weinberg, S. Schneider, J. M. Carpenter, C. Beichman, R. Capps, T. Chester, J. Elias, J. Huchra, J. Liebert, C. Lonsdale, D. G. Monet, S. Price, P. Seitzer, T. Jarrett, J. D. Kirkpatrick, J. E. Gizis, E. Howard, T. Evans, J. Fowler, L. Fullmer, R. Hurt, R. Light, E. L. Kopan, K. A. Marsh, H. L. McCallon, R. Tam, S. Van Dyk, and S. Wheelock, AJ **131**, 1163 (2006).

3 J. E. Gunn, W. A. Siegmund, E. J. Mannery, R. E. Owen, C. L. Hull, R. F. Leger, L. N. Carey, G. R. Knapp, D. G. York, W. N. Boroski, S. M. Kent, R. H. Lupton, C. M. Rockosi, M. L. Evans, P. Waddell, J. E. Anderson, J. Annis, J. C. Barentine, L. M. Bartoszek, S. Bastian, S. B. Bracker, H. J. Brewington, C. I. Briegel, J. Brinkmann, Y. J. Brown, M. A. Carr, P. C. Czarapata, C. C. Drennan, T. Dombeck, G. R. Federwitz, B. A. Gillespie, C. Gonzales, S. U. Hansen, M. Harvanek, J. Hayes, W. Jordan, E. Kinney, M. Klaene, S. J. Kleinman, R. G. Kron, J. Kresinski, G. Lee, S. Limmongkol, C. W. Lindenmeyer, D. C. Long, C. L. Loomis, P. M. McGehee, P. M. Mantsch, J. Neilsen, Eric H., R. M. Neswold, P. R. Newman, A. Nitta, J. Peoples, John, J. R. Pier, P. S. Prieto, A. Prosapio, C. Rivetta, D. P. Schneider, S. Snedden, and S.-i. Wang, AJ **131**, 2332 (2006), arXiv: astro-ph/0602326.

4 DESI Collaboration, A. Aghamousa, J. Aguilar, S. Ahlen, S. Alam, L. E. Allen, C. Allende Prieto, J. Annis, S. Bailey, C. Balland, O. Ballester, C. Baltay, L. Beaufore, C. Bebek, T. C. Beers, E. F. Bell, J. L. Bernal, R. Besuner, F. Beutler, C. Blake, H. Bleuler, M. Blomqvist, R. Blum, A. S. Bolton, C. Briceno, D. Brooks, J. R. Brownstein, E. Buckley-Geer, A. Burden, E. Burtin, N. G. Busca, R. N. Cahn, Y.-C. Cai, L. Cardiel-Sas, R. G. Carlberg, P.-H. Carton, R. Casas, F. J. Castander, J. L. Cervantes-Cota, T. M. Claybaugh, M. Close, C. T. Coker, S. Cole, J. Comparat, A. P. Cooper, M. C. Cousinou, M. Crocce, J.-G. Cuby, D. P. Cunningham, T. M. Davis, K. S. Dawson, A. de la Macorra, J. De Vicente, T. Delubac, M. Derwent, A. Dey, G. Dhungana, Z. Ding, P. Doel, Y. T. Duan, A. Ealet, J. Edelstein, S. Eftekharzadeh, D. J. Eisenstein, A. Elliott, S. Escoffier, M. Evatt, P. Fagrelius, X. Fan, K. Fanning, A. Farahi, J. Farihi, G. Favole, Y. Feng, E. Fernandez, J. R. Findlay, D. P. Finkbeiner, M. J. Fitzpatrick, B. Flaugher, S. Flender, A. Font-Ribera, J. E. Forero-Romero, P. Fosalba, C. S. Frenk, M. Fumagalli, B. T. Gaensicke, G. Gallo, J. Garcia-Bellido, E. Gaztanaga, N. Pietro Gentile Fusillo, T. Gerard, I. Gershkovich, T. Giannantonio, D. Gillet, G. Gonzalez-de-Rivera, V. Gonzalez-Perez, S. Gott, O. Graur, G. Gutierrez, J. Guy, S. Habib, H. Heetderks, I. Heetderks, K. Heitmann, W. A. Hellwing, D. A. Herrera, S. Ho, S. Holland, K. Honscheid, E. Huff, T. A. Hutchinson, D. Huterer, H. S. Hwang, J. M. Illa Laguna, Y. Ishikawa, D. Jacobs, N. Jeffrey, P. Jelinsky, E. Jennings, L. Jiang, J. Jimenez, J. Johnson, R. Joyce, E. Jullo, S. Juneau, S. Kama, A. Karcher, S. Karkar, R. Kehoe, N. Kennamer, S. Kent, M. Kilbinger, A. G. Kim, D. Kirkby, T. Kisner, E. Kitanidis, J.-P. Kneib, S. Koposov, E. Kovacs, K. Koyama, A. Kremin, R. Kron, L. Kronig, A. Kueter-Young, C. G. Lacey, R. Lafever, O. Lahav, A. Lambert, M. Lampton, M. Landriau, D. Lang, T. R. Lauer, J.-M. Le Goff, L. Le Guillou, A. Le Van Suu, J. H. Lee, S.-J. Lee, D. Leitner, M. Lesser, M. E. Levi, B. L'Huillier, B. Li, M. Liang, H. Lin, E. Linder, S. R. Loebman, Z. Lukić, J. Ma, N. MacCrann, C. Magneville, L. Makarem, M. Manera, C. J. Manser, R. Marshall, P. Martini, R. Massey, T. Matheson, J. McCauley, P. McDonald, I. D. McGreer, A. Meisner, N. Metcalfe, T. N. Miller, R. Miquel, J. Moustakas, A. Myers, M. Naik, J. A. Newman, R. C. Nichol, A. Nicola, L. Nicolati da Costa, J. Nie, G. Niz, P. Norberg, B. Nord, D. Norman, P. Nugent, T. O'Brien, M. Oh, K. A. G. Olsen, C. Padilla, H. Padmanabhan, N. Padmanabhan, N. Palanque-Delabrouille, A. Palmese, D. Pappalardo, I. Pâris, C. Park, A. Patej, J. A. Peacock, H. V. Peiris, X. Peng, W. J. Percival, S. Perruchot, M. M. Pieri, R. Pogge, J. E.

Pollack, C. Poppett, F. Prada, A. Prakash, R. G. Probst, D. Rabinowitz, A. Raichoor, C. H. Ree, A. Refregier, X. Regal, B. Reid, K. Reil, M. Rezaie, C. M. Rockosi, N. Roe, S. Ronayette, A. Roodman, A. J. Ross, N. P. Ross, G. Rossi, E. Rozo, V. Ruhlmann-Kleider, E. S. Rykoff, C. Sabiu, L. Samushia, E. Sanchez, J. Sanchez, D. J. Schlegel, M. Schneider, M. Schubnell, A. Secroun, U. Seljak, H.-J. Seo, S. Serrano, A. Shafieloo, H. Shan, R. Sharples, M. J. Sholl, W. V. Shourt, J. H. Silber, D. R. Silva, M. M. Sirk, A. Slosar, A. Smith, G. F. Smoot, D. Som, Y.-S. Song, D. Sprayberry, R. Staten, A. Stefanik, G. Tarle, S. Sien Tie, J. L. Tinker, R. Tojeiro, F. Valdes, O. Valenzuela, M. Valluri, M. Vargas-Magana, L. Verde, A. R. Walker, J. Wang, Y. Wang, B. A. Weaver, C. Weaverdyck, R. H. Wechsler, D. H. Weinberg, M. White, Q. Yang, C. Yeche, T. Zhang, G.-B. Zhao, Y. Zheng, X. Zhou, Z. Zhou, Y. Zhu, H. Zou, and Y. Zu, arXiv e-prints arXiv:1611.00036 (2016), arXiv: 1611.00036.

5 A. J. Drake, S. G. Djorgovski, A. Mahabal, E. Beshore, S. Larson, M. J. Graham, R. Williams, E. Christensen, M. Catelan, A. Boattini, A. Gibbs, R. Hill, and R. Kowalski, ApJ **696**, 870 (2009), arXiv: 0809.1394.

6 N. M. Law, S. R. Kulkarni, R. G. Dekany, E. O. Ofek, R. M. Quimby, P. E. Nugent, J. Surace, C. C. Grillmair, J. S. Bloom, M. M. Kasliwal, L. Bildsten, T. Brown, S. B. Cenko, D. Ciardi, E. Croner, S. G. Djorgovski, J. van Eyken, A. V. Filippenko, D. B. Fox, A. Gal-Yam, D. Hale, N. Hamam, G. Helou, J. Henning, D. A. Howell, J. Jacobsen, R. Laher, S. Mattingly, D. McKenna, A. Pickles, D. Poznanski, G. Rahmer, A. Rau, W. Rosing, M. Shara, R. Smith, D. Starr, M. Sullivan, V. Velur, R. Walters, and J. Zolkower, PASP **121**, 1395 (2009), arXiv: 0906.5350.

7 E. C. Bellm, S. R. Kulkarni, T. Barlow, U. Feindt, M. J. Graham, A. Goobar, T. Kupfer, C.-C. Ngeow, P. Nugent, E. Ofek, T. A. Prince, R. Riddle, R. Walters, and Q.-Z. Ye, PASP **131**, 068003 (2019), arXiv: 1905.02209.

8 N. Kaiser, in *Ground-based Telescopes*, (edited by J. Oschmann, Jacobus M.), volume 5489 of *Society of Photo-Optical Instrumentation Engineers (SPIE) Conference Series*, 11–22 (2004).

9 B. J. Shappee, J. L. Prieto, D. Grupe, C. S. Kochanek, K. Z. Stanek, G. De Rosa, S. Mathur, Y. Zu, B. M. Peterson, R. W. Pogge, S. Komossa, M. Im, J. Jencson, T. W. S. Holoien, U. Basu, J. F. Beacom, D. M. Szczygieł, J. Brimacombe, S. Adams, A. Campillay, C. Choi, C. Contreras, M. Dietrich, M. Dubberley, M. Elphick, S. Foale, M. Giustini, C. Gonzalez, E. Hawkins, D. A. Howell, E. Y. Hsiao, M. Koss, K. M. Leighly, N. Morrell, D. Mudd, D. Mullins, J. M. Nugent, J. Parrent, M. M. Phillips, G. Pojmanski, W. Rosing, R. Ross, D. Sand, D. M. Terndrup, S. Valenti, Z. Walker, and Y. Yoon, ApJ **788**, 48 (2014), arXiv: 1310.2241.

10 J. L. Tonry, L. Denneau, A. N. Heinze, B. Stalder, K. W. Smith, S. J. Smartt, C. W. Stubbs, H. J. Weiland, and A. Rest, PASP **130**, 064505 (2018), arXiv: 1802.00879.

11 L. Deng, F. Yang, X. Chen, F. He, Q. Liu, B. Zhang, C. Zhang, K. Wang, N. Liu, A. Ren, Z. Luo, Z. Yan, J. Tian, and J. Pan, Nature **596**, 353 (2021).

12 W. Yuan, C. Zhang, Z. Ling, D. Zhao, W. Wang, Y. Chen, F. Lu, S.-N. Zhang, and W. Cui, in *Space Telescopes and Instrumentation 2018: Ultraviolet to Gamma Ray*, (edited by J.-W. A. den Herder, S. Nikzad, and K. Nakazawa), volume 10699 of *Society of Photo-Optical Instrumentation Engineers (SPIE) Conference Series*, 1069925 (2018).

13 H. Zhan, Chin. Sci. Bull **66**, 1290 (2021).

14 F. Zwicky, PASP **50**, 215 (1938).

15 W. L. W. Sargent, L. Searle, and C. T. Kowal, in *Supernovae and Supernova Remnants*, (edited by C. B. Cosmovici), volume 45 of *Astrophysics and Space Science Library*, 33 (1974).

16 A. V. Filippenko, W. D. Li, R. R. Treffers, and M. Modjaz, in *IAU Colloq. 183: Small Telescope Astronomy on Global Scales*, (edited by B. Paczynski, W.-P. Chen, and C. Lemme), volume 246 of *Astronomical Society of the Pacific Conference Series*, 121 (2001).

17 P. Astier, J. Guy, N. Regnault, R. Pain, E. Aubourg, D. Balam, S. Basa, R. G. Carlberg, S. Fabbro, D. Fouchez, I. M. Hook, D. A. Howell, H. Lafoux, J. D. Neill, N. Palanque-Delabrouille, K. Perrett, C. J. Pritchet, J. Rich, M. Sullivan, R. Taillet, G. Aldering, P. Antilogus, V. Arsenijevic, C. Balland, S. Baumont, J. Bronder, H. Courtois, R. S. Ellis, M. Filiol, A. C. Gonçalves, A. Goobar, D. Guide, D. Hardin, V. Lusset, C. Lidman, R. McMahon, M. Mouchet, A. Mourao, S. Perlmutter, P. Ripoche, C. Tao, and N. Walton, A&A **447**, 31 (2006), arXiv: astro-ph/0510447.

18 A. Rau, S. R. Kulkarni, N. M. Law, J. S. Bloom, D. Ciardi, G. S. Djorgovski, D. B. Fox, A. Gal-Yam, C. C. Grillmair, M. M. Kasliwal, P. E. Nugent, E. O. Ofek, R. M. Quimby, W. T. Reach, M. Shara, L. Bildsten, S. B. Cenko, A. J. Drake, A. V. Filippenko, D. J. Helfand, G. Helou, D. A. Howell, D. Poznanski, and M. Sullivan, PASP **121**, 1334 (2009), arXiv: 0906.5355.

19 LSST Science Collaboration, P. A. Abell, J. Allison, S. F. Anderson, J. R. Andrew, J. R. P. Angel, L. Armus, D. Arnett, S. J. Asztalos, T. S. Axelrod, S. Bailey, D. R. Ballantyne, J. R. Bankert, W. A. Barkhouse, J. D. Barr, L. F. Barrientos, A. J. Barth, J. G. Bartlett, A. C. Becker, J. Becla, T. C. Beers, J. P. Bernstein, R. Biswas, M. R. Blanton, J. S. Bloom, J. J. Bochanski, P. Boeshaar, K. D. Borne, M. Bradac, W. N. Brandt, C. R. Bridge, M. E. Brown, R. J. Brunner, J. S. Bullock, A. J. Burgasser, J. H. Burge, D. L. Burke, P. A. Cargile, S. Chandrasekharan, G. Chartas, S. R. Chesley, Y.-H. Chu, D. Cinabro, M. W. Claire, C. F. Claver, D. Clowe, A. J. Connolly, K. H. Cook, J. Cooke, A. Cooray, K. R. Covey, C. S. Culliton, R. de Jong, W. H. de Vries, V. P. Debattista, F. Delgado, I. P. Dell'Antonio, S. Dhital, R. Di Stefano, M. Dickinson, B. Dilday, S. G. Djorgovski, G. Dobler, C. Donalek, G. Dubois-Felsmann, J. Durech, A. Eliasdottir, M. Eracleous, L. Eyer, E. E. Falco, X. Fan, C. D. Fassnacht, H. C. Ferguson, Y. R. Fernandez, B. D. Fields, D. Finkbeiner, E. E. Figueroa, D. B. Fox, H. Francke, J. S. Frank, J. Frieman, S. Fromenteau, M. Furqan, G. Galaz, A. Gal-Yam, P. Garnavich, E. Gawiser, J. Geary, P. Gee, R. R. Gibson, K. Gilmore, E. A. Grace, R. F. Green, W. J. Gressler, C. J. Grillmair, S. Habib, J. S. Haggerty, M. Hamuy, A. W. Harris, S. L. Hawley, A. F. Heavens, L. Hebb, T. J. Henry, E. Hileman, E. J. Hilton, K. Hoadley, J. B. Holberg, M. J. Holman, S. B. Howell, L. Infante, Z. Ivezic, S. H. Jacoby, B. Jain, R, Jedicke, M. J. Jee, J. Garrett Jernigan, S. W. Jha, K. V. Johnston, R. L. Jones, M. Juric, M. Kaasalainen, Styliani, Kafka, S. M. Kahn, N. A. Kaib, J. Kalirai, J. Kantor, M. M. Kasliwal, C. R. Keeton, R. Kessler, Z. Knezevic, A. Kowalski, V. L. Krabbendam, K. S. Krughoff, S. Kulkarni, S. Kuhlman, M. Lacy, S. Lepine, M. Liang, A. Lien, P. Lira, K. S. Long, S. Lorenz, J. M. Lotz, R. H. Lupton, J. Lutz, L. M. Macri, A. A. Mahabal, R. Mandelbaum, P. Marshall, M. May, P. M. McGehee, B. T. Meadows, A. Meert, A. Milani, C. J. Miller, M. Miller, D. Mills, D. Minniti, D. Monet, A. S. Mukadam, E. Nakar, D. R. Neill, J. A. Newman, S. Nikolaev, M. Nordby, P. O'Connor, M. Oguri, J. Oliver, S. S. Olivier, J. K. Olsen, K. Olsen, E. W. Olszewski, H. Oluseyi, N. D. Padilla, A. Parker, J. Pepper, J. R. Peterson, C. Petry, P. A. Pinto, J. L. Pizagno, B. Popescu, A. Prsa, V. Radcka, M. J. Raddick, A. Rasmussen, A. Rau, J. Rho, J. E. Rhoads, G. T. Richards, S. T. Ridgway, B. E. Robertson, R. Roskar, A. Saha, A. Sarajedini, E. Scannapieco, T. Schalk, R. Schindler, S. Schmidt, S. Schmidt, D. P. Schneider, G. Schumacher, R. Scranton, J. Sebag, L. G. Seppala, O. Shemmer, J. D. Simon, M. Sivertz, H. A. Smith, J. Allyn Smith, N. Smith, A. H. Spitz, A. Stanford, K. G. Stassun, J. Strader, M. A. Strauss, C. W. Stubbs, D. W. Sweeney, A. Szalay, P. Szkody, M. Takada, P. Thorman, D. E. Trilling, V. Trimble, A. Tyson, R. Van Berg, D. Vanden Berk, J. VanderPlas, L. Verde, B. Vrsnak, L. M. Walkowicz, B. D. Wandelt, S. Wang, Y. Wang, M. Warner, R. H. Wechsler, A. A. West, O. Wiecha, B. F. Williams, B. Willman, D. Wittman, S. C. Wolff, W. M. Wood-Vasey, P. Wozniak, P. Young, A. Zentner, and H. Zhan, arXiv e-prints arXiv:0912.0201 (2009), arXiv: 0912.0201.

20 M. Postman, D. Coe, N. Benítez, L. Bradley, T. Broadhurst, M. Donahue, H. Ford, O. Graur, G. Graves, S. Jouvel, A. Koekemoer, D. Lemze, E. Medezinski, A. Molino, L. Moustakas, S. Ogaz, A. Riess, S. Rodney, P. Rosati, K. Umetsu, W. Zheng, A. Zitrin, M. Bartelmann, R. Bouwens, N. Czakon, S. Golwala, O. Host, L. Infante, S. Jha, Y. Jimenez-Teja, D. Kelson, O. Lahav, R. Lazkoz, D. Maoz, C. McCully, P. Melchior, M. Meneghetti, J. Merten, J. Moustakas, M. Nonino, B. Patel, E. Regös, J. Sayers, S. Seitz, and A. Van der Wel, ApJS **199**, 25 (2012), arXiv: 1106.3328.

21 T. Morokuma, N. Tominaga, M. Tanaka, K. Mori, E. Matsumoto, Y. Kikuchi, T. Shibata, S. Sako, T. Aoki, M. Doi, N. Kobayashi, H. Maehara, N. Matsunaga, H. Mito, T. Miyata, Y. Nakada, T. Soyano, K. Tarusawa, S. Miyazaki, F. Nakata, N. Okada, Y. Sarugaku, M. W. Richmond, H. Akitaya, G. Aldering, K. Arimatsu, C. Contreras, T. Horiuchi, E. Y. Hsiao, R. Itoh, I. Iwata, K. S. Kawabata, N. Kawai, Y. Kitagawa, M. Kokubo, D. Kuroda, P. Mazzali, T. Misawa, Y. Moritani, N. Morrell, R. Okamoto, N. Pavlyuk, M. M. Phillips, E. Pian, D. Sahu, Y. Saito, K. Sano, M. D. Stritzinger, Y. Tachibana, F. Taddia, K. Takaki, K. Tateuchi, A. Tomita, D. Tsvetkov, T. Ui, N. Ukita, Y. Urata, E. S. Walker, and T. Yoshii, PASJ **66**, 114 (2014), arXiv: 1409.1308.

22 J. L. Tonry, L. Denneau, A. N. Heinze, B. Stalder, K. W. Smith, S. J. Smartt, C. W. Stubbs, H. J. Weiland, and A. Rest, PASP **130**, 064505 (2018), arXiv: 1802.00879.

23 E. C. Bellm, S. R. Kulkarni, M. J. Graham, R. Dekany, R. M. Smith, R. Riddle, F. J. Masci, G. Helou, T. A. Prince, S. M. Adams, C. Barbarino, T. Barlow, J. Bauer, R. Beck, J. Belicki, R. Biswas, N. Blagorodnova, D. Bodewits, B. Bolin, V. Brinnel, T. Brooke, B. Bue, M. Bulla, R. Burruss, S. B. Cenko, C.-K. Chang, A. Connolly, M. Coughlin, J. Cromer, V. Cunningham, K. De, A. Delacroix, V. Desai, D. A. Duev, G. Eadie, T. L. Farnham, M. Feeney, U. Feindt, D. Flynn, A. Franckowiak, S. Frederick, C. Fremling, A. Gal-Yam, S. Gezari, M. Giomi, D. A. Goldstein, V. Z. Golkhou, A. Goobar, S. Groom, E. Hacopians, D. Hale, J. Henning, A. Y. Q. Ho, D. Hover, J. Howell, T. Hung, D. Huppenkothen, D. Imel, W.-H. Ip, Ž. Ivezić, E. Jackson, L. Jones, M. Juric, M. M. Kasliwal, S. Kaspi, S. Kaye, M. S. P. Kelley, M. Kowalski, E. Kramer, T. Kupfer, W. Landry, R. R. Laher, C.-D. Lee, H. W. Lin, Z.-Y. Lin, R. Lunnan, M. Giomi, A. Mahabal, P. Mao, A. A. Miller, S. Monkewitz, P. Murphy, C.-C. Ngeow, J. Nordin, P. Nugent, E. Ofek, M. T. Patterson, B. Penprase, M. Porter, L. Rauch, U. Rebbapragada, D. Reiley, M. Rigault, H. Rodriguez, J. van Roestel, B. Rusholme, J. van Santen, S. Schulze, D. L. Shupe, L. P. Singer, M. T. Soumagnac, R. Stein, J. Surace, J. Sollerman, P. Szkody, F. Taddia, S. Terek, A. Van Sistine, S. van Velzen, W. T. Vestrand, R. Walters, C. Ward, Q.-Z. Ye, P.-C. Yu, L. Yan, and J. Zolkower, PASP **131**, 018002 (2019), arXiv: 1902.01932.

24 S. Campana, V. Mangano, A. J. Blustin, P. Brown, D. N. Burrows, G. Chincarini, J. R. Cummings, G. Cusumano, M. Della Valle, D. Malesani, P. Mészáros, J. A. Nousek, M. Page, T. Sakamoto, E. Waxman, B. Zhang, Z. G. Dai, N. Gehrels, S. Immler, F. E. Marshall, K. O. Mason, A. Moretti, P. T. O'Brien, J. P. Osborne, K. L. Page, P. Romano, P. W. A. Roming, G. Tagliaferri, L. R. Cominsky, P. Giommi, O. Godet, J. A. Kennea, H. Krimm, L. Angelini, S. D. Barthelmy, P. T. Boyd, D. M. Palmer, A. A. Wells, and N. E. White, Nature **442**, 1008 (2006), arXiv: astro-ph/0603279.

25 N. Smith, W. Li, R. J. Foley, J. C. Wheeler, D. Pooley, R. Chornock, A. V. Filippenko, J. M. Silverman, R. Quimby, J. S. Bloom, and C. Hansen, ApJ **666**, 1116 (2007), arXiv: astro-ph/0612617.

26 S. J. Smartt, J. J. Eldridge, R. M. Crockett, and J. R. Maund, MNRAS **395**, 1409 (2009), arXiv: 0809.0403.

27 K. Nomoto, C. Kobayashi, and N. Tominaga, ARA&A **51**, 457 (2013).

28 J.-a. Jiang, M. Doi, K. Maeda, T. Shigeyama, K. Nomoto, N. Yasuda, S. W. Jha, M. Tanaka, T. Morokuma, N. Tominaga et al., Nature **550**, 80 (2017).

29 D. M. Scolnic, D. O. Jones, A. Rest, Y. C. Pan, R. Chornock, R. J. Foley, M. E. Huber, R. Kessler, G. Narayan, A. G. Riess, S. Rodney, E. Berger, D. J. Brout, P. J. Challis, M. Drout, D. Finkbeiner, R. Lunnan, R. P. Kirshner, N. E. Sanders, E. Schlafly, S. Smartt, C. W. Stubbs, J. Tonry, W. M. Wood-Vasey, M. Foley, J. Hand, E. Johnson, W. S. Burgett, K. C. Chambers, P. W. Draper, K. W. Hodapp, N. Kaiser, R. P. Kudritzki, E. A. Magnier, N. Metcalfe, F. Bresolin, E. Gall, R. Kotak, M. McCrum, and K. W. Smith, ApJ **859**, 101 (2018), arXiv: 1710.00845.

30 Ž. Ivezić, S. M. Kahn, J. A. Tyson, B. Abel, E. Acosta, R. Allsman, D. Alonso, Y. AlSayyad, S. F. Anderson, J. Andrew, J. R. P. Angel, G. Z. Angeli, R. Ansari, P. Antilogus, C. Araujo, R. Armstrong, K. T. Arndt, P. Astier, É. Aubourg, N. Auza, T. S. Axelrod, D. J. Bard, J. D. Barr, A. Barrau, J. G. Bartlett, A. E. Bauer, B. J. Bauman, S. Baumont, E. Bechtol, K. Bechtol, A. C. Becker, J. Becla, C. Beldica, S. Bellavia, F. B. Bianco, R. Biswas, G. Blanc, J. Blazek, R. D. Bland ford, J. S. Bloom, J. Bogart, T. W. Bond, M. T. Booth, A. W. Borgland, K. Borne, J. F. Bosch, D. Boutigny, C. A. Brackett, A. Bradshaw, W. N. Brand t, M. E. Brown, J. S. Bullock, P. Burchat, D. L. Burke, G. Cagnoli, D. Calabrese, S. Callahan, A. L. Callen, J. L. Carlin, E. L. Carlson, S. Chand rasekharan, G. Charles-Emerson, S. Chesley, E. C. Cheu, H.-F. Chiang, J. Chiang, C. Chirino, D. Chow, D. R. Ciardi, C. F. Claver, J. Cohen-Tanugi, J. J. Cockrum, R. Coles, A. J. Connolly, K. H. Cook, A. Cooray, K. R. Covey, C. Cribbs, W. Cui, R. Cutri, P. N. Daly, S. F. Daniel, F. Daruich, G. Daubard, G. Daues, W. Dawson, F. Delgado, A. Dellapenna, R. de Peyster, M. de Val-Borro, S. W. Digel, P. Doherty, R. Dubois, G. P. Dubois-Felsmann, J. Durech, F. Economou, T. Eifler, M. Eracleous, B. L. Emmons, A. Fausti Neto, H. Ferguson, E. Figueroa, M. Fisher-Levine, W. Focke, M. D. Foss, J. Frank, M. D. Freemon, E. Gangler, E. Gawiser, J. C. Geary, P. Gee, M. Geha, C. J. B. Gessner, R. R. Gibson, D. K. Gilmore, T. Glanzman, W. Glick, T. Goldina, D. A. Goldstein, I. Goodenow, M. L. Graham, W. J. Gressler, P. Gris, L. P. Guy, A. Guyonnet, G. Haller, R. Harris, P. A. Hascall, J. Haupt, F. Hernand ez, S. Herrmann, E. Hileman, J. Hoblitt, J. A. Hodgson, C. Hogan, J. D. Howard, D. Huang, M. E. Huffer, P. Ingraham, W. R. Innes, S. H. Jacoby, B. Jain, F. Jammes, M. J. Jee, T. Jenness, G. Jernigan, D. Jevremović, K. Johns, A. S. Johnson, M. W. G. Johnson, R. L. Jones, C. Juramy-Gilles, M. Jurić, J. S. Kalirai, N. J. Kallivayalil, B. Kalmbach, J. P. Kantor, P. Karst, M. M. Kasliwal, H. Kelly, R. Kessler, V. Kinnison, D. Kirkby, L. Knox, I. V. Kotov, V. L. Krabbendam, K. S. Krughoff, P. Kubánek, J. Kuczewski, S. Kulkarni, J. Ku, N. R. Kurita, C. S. Lage, R. Lambert, T. Lange, J. B. Langton, L. Le Guillou, D. Levine, M. Liang, K.-T. Lim, C. J. Lintott, K. E. Long, M. Lopez, P. J. Lotz, R. H. Lupton, N. B. Lust, L. A. MacArthur, A. Mahabal, R. Mand elbaum, T. W. Markiewicz, D. S. Marsh, P. J. Marshall, S. Marshall, M. May, R. McKercher, M. McQueen, J. Meyers, M. Migliore, M. Miller, D. J. Mills, C. Miraval, J. Moeyens, F. E. Moolekamp, D. G. Monet, M. Moniez, S. Monkewitz, C. Montgomery, C. B. Morrison, F. Mueller, G. P. Muller, F. Muñoz Arancibia, D. R. Neill, S. P. Newbry, J.-Y. Nief, A. Nomerotski, M. Nordby, P. O'Connor, J. Oliver, S. S. Olivier, K. Olsen, W. O'Mullane, S. Ortiz, S. Osier, R. E. Owen, R. Pain, P. E. Palecek, J. K. Parejko, J. B. Parsons, N. M. Pease, J. M. Peterson, J. R. Peterson, D. L. Petravick, M. E. Libby Petrick, C. E. Petry, F. Pierfederici, S. Pietrowicz, R. Pike, P. A. Pinto, R. Plante, S. Plate, J. P. Plutchak, P. A. Price, M. Prouza, V. Radeka, J. Rajagopal, A. P. Rasmussen, N. Regnault, K. A. Reil, D. J. Reiss, M. A. Reuter, S. T. Ridgway, V. J. Riot, S. Ritz, S. Robinson, W. Roby, A. Roodman, W. Rosing, C. Roucelle, M. R. Rumore, S. Russo, A. Saha, B. Sassolas, T. L. Schalk, P. Schellart, R. H. Schindler, S. Schmidt, D. P. Schneider, M. D. Schneider, W. Schoening, G. Schumacher, M. E. Schwamb, J. Sebag, B. Selvy, G. H. Sembroski, L. G. Seppala, A. Serio, E. Serrano, R. A. Shaw, I. Shipsey, J. Sick, N. Silvestri, C. T. Slater, J. A. Smith, R. C. Smith, S. Sobhani, C. Soldahl, L. Storrie-Lombardi,

E. Stover, M. A. Strauss, R. A. Street, C. W. Stubbs, I. S. Sullivan, D. Sweeney, J. D. Swinbank, A. Szalay, P. Takacs, S. A. Tether, J. J. Thaler, J. G. Thayer, S. Thomas, A. J. Thornton, V. Thukral, J. Tice, D. E. Trilling, M. Turri, R. Van Berg, D. Vanden Berk, K. Vetter, F. Virieux, T. Vucina, W. Wahl, L. Walkowicz, B. Walsh, C. W. Walter, D. L. Wang, S.-Y. Wang, M. Warner, O. Wiecha, B. Willman, S. E. Winters, D. Wittman, S. C. Wolff, W. M. Wood-Vasey, X. Wu, B. Xin, P. Yoachim, and H. Zhan, ApJ **873**, 111 (2019), arXiv: 0805.2366.

31 S. Perlmutter, S. Gabi, G. Goldhaber, A. Goobar, D. Groom, I. Hook, A. Kim, M. Kim, J. Lee, R. Pain et al., ApJ **483**, 565 (1997).

32 S. Perlmutter, G. Aldering, G. Goldhaber, R. A. Knop, P. Nugent, P. G. Castro, S. Deustua, S. Fabbro, A. Goobar, D. E. Groom, I. M. Hook, A. G. Kim, M. Y. Kim, J. C. Lee, N. J. Nunes, R. Pain, C. R. Pennypacker, R. Quimby, C. Lidman, R. S. Ellis, M. Irwin, R. G. McMahon, P. Ruiz-Lapuente, N. Walton, B. Schaefer, B. J. Boyle, A. V. Filippenko, T. Matheson, A. S. Fruchter, N. Panagia, H. J. M. Newberg, W. J. Couch, and The Supernova Cosmology Project, ApJ **517**, 565 (1999).

33 A. G. Riess, A. V. Filippenko, P. Challis, A. Clocchiatti, A. Diercks, P. M. Garnavich, R. L. Gilliland, C. J. Hogan, S. Jha, R. P. Kirshner, B. Leibundgut, M. M. Phillips, D. Reiss, B. P. Schmidt, R. A. Schommer, R. C. Smith, J. Spyromilio, C. Stubbs, N. B. Suntzeff, and J. Tonry, AJ **116**, 1009 (1998).

34 W. Hillebrandt, M. Kromer, F. Röpke, and A. Ruiter, Frontiers of Physics **8**, 116 (2013).

35 D. Maoz, F. Mannucci, and G. Nelemans, ARA&A **52**, 107 (2014).

36 F. Matteucci and L. Greggio, A&A **154**, 279 (1986).

37 C. Kobayashi, T. Tsujimoto, K. Nomoto, I. Hachisu, and M. Kato, ApJL **503**, L155 (1998), arXiv: astro-ph/9806335.

38 J. Whelan and J. Iben, Icko, ApJ **186**, 1007 (1973).

39 K. Nomoto, ApJ **253**, 798 (1982).

40 R. F. Webbink, ApJ **277**, 355 (1984).

41 J. Iben, I. and A. V. Tutukov, ApJ **284**, 719 (1984).

42 W. M. Sparks and T. P. Stecher, ApJ **188**, 149 (1974).

43 N. Soker, MNRAS **450**, 1333 (2015), arXiv: 1501.07729.

44 M. M. Phillips, P. Lira, N. B. Suntzeff, R. A. Schommer, M. Hamuy, and J. Maza, AJ **118**, 1766 (1999), arXiv: astro-ph/9907052.

45 A. V. Filippenko, M. W. Richmond, T. Matheson, J. C. Shields, E. M. Burbidge, R. D. Cohen, M. Dickinson, M. A. Malkan, B. Nelson, J. Pietz, D. Schlegel, P. Schmeer, H. Spinrad, C. C. Steidel, H. D. Tran, and W. Wren, ApJL **384**, L15 (1992).

46 M. M. Phillips, L. A. Wells, N. B. Suntzeff, M. Hamuy, B. Leibundgut, R. P. Kirshner, and C. B. Foltz, AJ **103**, 1632 (1992).

47 A. V. Filippenko, M. W. Richmond, D. Branch, M. Gaskell, W. Herbst, C. H. Ford, R. R. Treffers, T. Matheson, L. C. Ho, A. Dey, W. L. W. Sargent, T. A. Small, and W. J. M. van Breugel, AJ **104**, 1543 (1992).

48 D. A. Howell, M. Sullivan, P. E. Nugent, R. S. Ellis, A. J. Conley, D. Le Borgne, R. G. Carlberg, J. Guy, D. Balam, S. Basa, D. Fouchez, I. M. Hook, E. Y. Hsiao, J. D. Neill, R. Pain, K. M. Perrett, and C. J. Pritchet, Nature **443**, 308 (2006), arXiv: astro-ph/0609616.

49 M. Hicken, P. M. Garnavich, J. L. Prieto, S. Blondin, D. L. DePoy, R. P. Kirshner, and J. Parrent, ApJL **669**, L17 (2007), arXiv: 0709.1501.

50 K. Maeda, K. Kawabata, W. Li, M. Tanaka, P. A. Mazzali, T. Hattori, K. Nomoto, and A. V. Filippenko, ApJ **690**, 1745 (2009), arXiv: 0808.0138.

51 M. Yamanaka, K. S. Kawabata, K. Kinugasa, M. Tanaka, A. Imada, K. Maeda, K. Nomoto, A. Arai, S. Chiyonobu, Y. Fukazawa, O. Hashimoto, S. Honda, Y. Ikejiri, R. Itoh, Y. Kamata, N. Kawai, T. Komatsu, K. Konishi, D. Kuroda, H. Miyamoto, S. Miyazaki, O. Nagae, H. Nakaya, T. Ohsugi, T. Omodaka, N. Sakai, M. Sasada, M. Suzuki, H. Taguchi, H. Takahashi, H. Tanaka, M. Uemura, T. Yamashita, K. Yanagisawa, and M. Yoshida, ApJL **707**, L118 (2009), arXiv: 0908.2059.

52 R. A. Scalzo, G. Aldering, P. Antilogus, C. Aragon, S. Bailey, C. Baltay, S. Bongard, C. Buton, M. Childress, N. Chotard, Y. Copin, H. K. Fakhouri, A. Gal-Yam, E. Gangler, S. Hoyer, M. Kasliwal, S. Loken, P. Nugent, R. Pain, E. Pécontal, R. Pereira, S. Perlmutter, D. Rabinowitz, A. Rau, G. Rigaudier, K. Runge, G. Smadja, C. Tao, R. C. Thomas, B. Weaver, and C. Wu, ApJ **713**, 1073 (2010), arXiv: 1003.2217.

53 J. M. Silverman, M. Ganeshalingam, W. Li, A. V. Filippenko, A. A. Miller, and D. Poznanski, MNRAS **410**, 585 (2011), arXiv: 1003.2417.

54 S. Taubenberger, S. Benetti, M. Childress, R. Pakmor, S. Hachinger, P. A. Mazzali, V. Stanishev, N. Elias-Rosa, I. Agnoletto, F. Bufano, M. Ergon, A. Harutyunyan, C. Inserra, E. Kankare, M. Kromer, H. Navasardyan, J. Nicolas, A. Pastorello, E. Prosperi, F. Salgado, J. Sollerman, M. Stritzinger, M. Turatto, S. Valenti, and W. Hillebrandt, MNRAS **412**, 2735 (2011), arXiv: 1011.5665.

55 N. Jiang, T. Wang, X. Hu, L. Sun, L. Dou, and L. Xiao, ApJ **911**, 31 (2021), arXiv: 2102.08044.

56 W. Li, A. V. Filippenko, R. Chornock, E. Berger, P. Berlind, M. L. Calkins, P. Challis, C. Fassnacht, S. Jha, R. P. Kirshner, T. Matheson, W. L. W. Sargent, R. A. Simcoe, G. H. Smith, and G. Squires, PASP **115**, 453 (2003), arXiv: astro-ph/0301428.

57 M. M. Phillips, W. Li, J. A. Frieman, S. I. Blinnikov, D. DePoy, J. L. Prieto, P. Milne, C. Contreras, G. Folatelli, N. Morrell, M. Hamuy, N. B. Suntzeff, M. Roth, S. González, W. Krzeminski, A. V. Filippenko, W. L. Freedman, R. Chornock, S. Jha, B. F. Madore, S. E. Persson, C. R. Burns, P. Wyatt, D. Murphy, R. J. Foley, M. Ganeshalingam, F. J. D. Serduke, K. Krisciunas, B. Bassett, A. Becker, B. Dilday, J. Eastman, P. M. Garnavich, J. Holtzman, R. Kessler, H. Lampeitl, J. Marriner, S. Frank, J. L. Marshall, G. Miknaitis, M. Sako, D. P. Schneider, K. van der Heyden, and N. Yasuda, PASP **119**, 360 (2007), arXiv: astro-ph/0611295.

58 R. J. Foley, R. Chornock, A. V. Filippenko, M. Ganeshalingam, R. P. Kirshner, W. Li, S. B. Cenko, P. J. Challis, A. S. Friedman, M. Modjaz, J. M. Silverman, and W. M. Wood-Vasey, AJ **138**, 376 (2009), arXiv: 0902.2794.

59 R. J. Foley, P. J. Challis, R. Chornock, M. Ganeshalingam, W. Li, G. H. Marion, N. I. Morrell, G. Pignata, M. D. Stritzinger, J. M. Silverman, X. Wang, J. P. Anderson, A. V. Filippenko, W. L. Freedman, M. Hamuy, S. W. Jha, R. P. Kirshner, C. McCully, S. E. Persson, M. M. Phillips, D. E. Reichart, and A. M. Soderberg, ApJ **767**, 57 (2013), arXiv: 1212.2209.

60 M. Hamuy, M. M. Phillips, N. B. Suntzeff, J. Maza, L. E. González, M. Roth, K. Krisciunas, N. Morrell, E. M. Green, S. E. Persson, and P. J. McCarthy, Nature **424**, 651 (2003), arXiv: astro-ph/0306270.

61 G. Aldering, P. Antilogus, S. Bailey, C. Baltay, A. Bauer, N. Blanc, S. Bongard, Y. Copin, E. Gangler, S. Gilles, R. Kessler, D. Kocevski, B. C. Lee, S. Loken, P. Nugent, R. Pain, E. Pécontal, R. Pereira, S. Perlmutter, D. Rabinowitz, G. Rigaudier, R. Scalzo, G. Smadja, R. C. Thomas, L. Wang, B. A. Weaver, and Nearby Supernova Factory, ApJ **650**, 510 (2006), arXiv: astro-ph/0606499.

62 J. M. Silverman, P. E. Nugent, A. Gal-Yam, M. Sullivan, D. A. Howell, A. V. Filippenko, I. Arcavi, S. Ben-Ami, J. S. Bloom, S. B. Cenko, Y. Cao, R. Chornock, K. I. Clubb, A. L. Coil, R. J. Foley, M. L. Graham, C. V. Griffith, A. Horesh, M. M. Kasliwal, S. R. Kulkarni, D. C. Leonard, W. Li, T. Matheson, A. A. Miller, M. Modjaz, E. O. Ofek, Y.-C. Pan, D. A. Perley, D. Poznanski, R. M. Quimby, T. N. Steele, A. Sternberg, D. Xu, and O. Yaron, ApJS **207**, 3 (2013), arXiv: 1304.0763.

63 G. Leloudas, E. Y. Hsiao, J. Johansson, K. Maeda, T. J. Moriya, J. Nordin, T. Petrushevska, J. M. Silverman, J. Sollerman, M. D. Stritzinger, F. Taddia, and D. Xu, A&A **574**, A61 (2015), arXiv: 1306.1549.

64 A. V. Filippenko, A. J. Barth, T. Matheson, L. Armus, M. Brown, B. R. Espey, X.-M. Fan, R. W. Goodrich, L. C. Ho, V. T. Junkkarinen,

D. C. Koo, M. D. Lehnert, A. R. Martel, J. M. Mazzarella, J. S. Miller, G. H. Smith, D. Tytler, and G. D. Wirth, ApJL **450**, L11 (1995).
65 T. Matheson, A. V. Filippenko, W. Li, D. C. Leonard, and J. C. Shields, AJ **121**, 1648 (2001), arXiv: astro-ph/0101119.
66 R. Barbon, F. Ciatti, and L. Rosino, A&A **72**, 287 (1979).
67 E. M. Schlegel, MNRAS **244**, 269 (1990).
68 P. E. Nugent, M. Sullivan, S. B. Cenko, R. C. Thomas, D. Kasen, D. A. Howell, D. Bersier, J. S. Bloom, S. Kulkarni, M. T. Kandrashoff et al., Nature **480**, 344 (2011).
69 R. J. Foley, P. J. Challis, A. V. Filippenko, M. Ganeshalingam, W. Landsman, W. Li, G. Marion, J. M. Silverman, R. Beaton, V. Bennert et al., ApJ **744**, 38 (2011).
70 Y. Cao, S. Kulkarni, D. A. Howell, A. Gal-Yam, M. M. Kasliwal, S. Valenti, J. Johansson, R. Amanullah, A. Goobar, J. Sollerman et al., Nature **521**, 328 (2015).
71 D. Kasen, ApJ **708**, 1025 (2010).
72 K. Maeda, M. Kutsuna, and T. Shigeyama, ApJ **794**, 37 (2014).
73 M. Kutsuna and T. Shigeyama, PASJ **67**, 54 (2015), arXiv: /oup/backfile/content_public/journal/pasj/67/3/10.1093_pasj_psv028/1/psv028.pdf.
74 M. T. Smitka, P. J. Brown, N. B. Suntzeff, J. Zhang, Q. Zhai, X. Wang, J. Mo, and T. Zhang, ApJ **813**, 30 (2015).
75 G. Marion, P. J. Brown, J. Vinkó, J. M. Silverman, D. J. Sand, P. Challis, R. P. Kirshner, J. C. Wheeler, P. Berlind, W. R. Brown et al., ApJ **820**, 92 (2016).
76 G. Hosseinzadeh, D. J. Sand, S. Valenti, P. Brown, D. A. Howell, C. McCully, D. Kasen, I. Arcavi, K. A. Bostroem, L. Tartaglia et al., ApJL **845**, L11 (2017).
77 A. Miller, Y. Cao, A. Piro, N. Blagorodnova, B. Bue, S. Cenko, S. Dhawan, R. Ferretti, O. Fox, C. Fremling et al., ApJ **852**, 100 (2018).
78 J.-a. Jiang, N. Yasuda, K. Maeda, M. Doi, T. Shigeyama, N. Tominaga, M. Tanaka, T. J. Moriya, I. Takahashi, N. Suzuki, T. Morokuma, and K. Nomoto, ApJ **892**, 25 (2020), arXiv: 2002.10737.
79 N. Levanon, N. Soker, and E. García-Berro, MNRAS **447**, 2803 (2015).
80 N. Levanon and N. Soker, MNRAS **470**, 2510 (2017).
81 A. L. Piro and V. S. Morozova, ApJ **826**, 96 (2016).
82 M. R. Magee, K. Maguire, R. Kotak, S. A. Sim, J. H. Gillanders, S. J. Prentice, and K. Skillen, A&A **634**, A37 (2020), arXiv: 1912.07603.
83 K. Maeda, J.-a. Jiang, T. Shigeyama, and M. Doi, ApJ **861**, 78 (2018), arXiv: 1805.12325.
84 J.-a. Jiang, M. Doi, K. Maeda, and T. Shigeyama, ApJ **865**, 149 (2018).
85 B. T. Hayden, P. M. Garnavich, R. Kessler, J. A. Frieman, S. W. Jha, B. Bassett, D. Cinabro, B. Dilday, D. Kasen, J. Marriner et al., ApJ **712**, 350 (2010).
86 F. Bianco, D. Howell, M. Sullivan, A. Conley, D. Kasen, S. González-Gaitán, J. Guy, P. Astier, C. Balland, R. Carlberg et al., ApJ **741**, 20 (2011).
87 M. Ganeshalingam, W. Li, and A. V. Filippenko, MNRAS **416**, 2607 (2011).
88 S. González-Gaitán, A. Conley, F. Bianco, D. Howell, M. Sullivan, K. Perrett, R. Carlberg, P. Astier, D. Balam, C. Balland et al., ApJ **745**, 44 (2012).
89 W. Zheng, J. M. Silverman, A. V. Filippenko, D. Kasen, P. E. Nugent, M. Graham, X. Wang, S. Valenti, F. Ciabattari, P. L. Kelly, O. D. Fox, I. Shivvers, K. I. Clubb, S. B. Cenko, D. Balam, D. A. Howell, E. Hsiao, W. Li, G. H. Marion, D. Sand, J. Vinko, J. C. Wheeler, and J. Zhang, ApJL **778**, L15 (2013), arXiv: 1310.5188.
90 A. A. Miller, Y. Yao, M. Bulla, C. Pankow, E. C. Bellm, S. B. Cenko, R. Dekany, C. Fremling, M. J. Graham, T. Kupfer, R. R. Laher, A. A. Mahabal, F. J. Masci, P. E. Nugent, R. Riddle, B. Rusholme, R. M. Smith, D. L. Shupe, J. van Roestel, and S. R. Kulkarni, arXiv e-prints arXiv:2001.00598 (2020), arXiv: 2001.00598.
91 A. L. Piro and E. Nakar, ApJ **769**, 67 (2013).
92 P. A. Mazzali, M. Sullivan, S. Hachinger, R. S. Ellis, P. E. Nugent, D. A. Howell, A. Gal-Yam, K. Maguire, J. Cooke, and R. Thomas, MNRAS **439**, 1959 (2014).
93 L. Ensman and A. Burrows, ApJ **393**, 742 (1992).
94 C. D. Matzner and C. F. McKee, ApJ **510**, 379 (1999), arXiv: astro-ph/9807046.
95 N. Tominaga, T. Morokuma, S. I. Blinnikov, P. Baklanov, E. I. Sorokina, and K. Nomoto, ApJS **193**, 20 (2011), arXiv: 1102.2360.
96 M. C. Bersten, G. Folatelli, F. García, S. D. van Dyk, O. G. Benvenuto, M. Orellana, V. Buso, J. L. Sánchez, M. Tanaka, K. Maeda, A. V. Filippenko, W. Zheng, T. G. Brink, S. B. Cenko, T. de Jaeger, S. Kumar, T. J. Moriya, K. Nomoto, D. A. Perley, I. Shivvers, and N. Smith, Nature **554**, 497 (2018), arXiv: 1802.09360.
97 A. Y. Q. Ho, D. A. Perley, A. Gal-Yam, R. Lunnan, J. Sollerman, S. Schulze, K. K. Das, D. Dobie, Y. Yao, C. Fremling, S. Adams, S. Anand, I. Andreoni, E. C. Bellm, R. J. Bruch, K. B. Burdge, A. J. Castro-Tirado, A. Dahiwale, K. De, R. Dekany, A. J. Drake, D. A. Duev, M. J. Graham, G. Helou, D. L. Kaplan, V. Karambelkar, M. M. Kasliwal, E. C. Kool, S. R. Kulkarni, A. A. Mahabal, M. S. Medford, A. A. Miller, J. Nordin, E. Ofek, G. Petitpas, R. Riddle, Y. Sharma, R. Smith, A. J. Stewart, K. Taggart, L. Tartaglia, A. Tzanidakis, and J. M. Winters, arXiv e-prints arXiv:2105.08811 (2021), arXiv: 2105.08811.
98 M. R. Drout, R. Chornock, A. M. Soderberg, N. E. Sanders, R. McKinnon, A. Rest, R. J. Foley, D. Milisavljevic, R. Margutti, E. Berger, M. Calkins, W. Fong, S. Gezari, M. E. Huber, E. Kankare, R. P. Kirshner, C. Leibler, R. Lunnan, S. Mattila, G. H. Marion, G. Narayan, A. G. Riess, K. C. Roth, D. Scolnic, S. J. Smartt, J. L. Tonry, W. S. Burgett, K. C. Chambers, K. W. Hodapp, R. Jedicke, N. Kaiser, E. A. Magnier, N. Metcalfe, J. S. Morgan, P. A. Price, and C. Waters, ApJ **794**, 23 (2014), arXiv: 1405.3668.
99 D. A. Perley, P. A. Mazzali, L. Yan, S. B. Cenko, S. Gezari, K. Taggart, N. Blagorodnova, C. Fremling, B. Mockler, A. Singh, N. Tominaga, M. Tanaka, A. M. Watson, T. Ahumada, G. C. Anupama, C. Ashall, R. L. Becerra, D. Bersier, V. Bhalerao, J. S. Bloom, N. R. Butler, C. Copperwheat, M. W. Coughlin, K. De, A. J. Drake, D. A. Duev, S. Frederick, J. J. González, A. Goobar, M. Heida, A. Y. Q. Ho, J. Horst, T. Hung, R. Itoh, J. E. Jencson, M. M. Kasliwal, N. Kawai, T. Khanam, S. R. Kulkarni, B. Kumar, H. Kumar, A. S. Kutyrev, W. H. Lee, K. Maeda, A. Mahabal, K. L. Murata, J. D. Neill, C.-C. Ngeow, B. Penprase, E. Pian, R. Quimby, E. Ramirez-Ruiz, M. G. Richer, C. G. Román-Zúñiga, D. K. Sahu, S. Srivastav, Q. Socia, J. Sollerman, Y. Tachibana, F. Taddia, S. Tinyanont, E. Troja, C. Ward, J. Wee, and P.-C. Yu, MNRAS **484**, 1031 (2019), arXiv: 1808.00969.
100 M. Tanaka, N. Tominaga, T. Morokuma, N. Yasuda, H. Furusawa, P. V. Baklanov, S. I. Blinnikov, T. J. Moriya, M. Doi, J.-a. Jiang, T. Kato, Y. Kikuchi, H. Kuncarayakti, T. Nagao, K. Nomoto, and Y. Taniguchi, ApJ **819**, 5 (2016), arXiv: 1601.03261.
101 D. L. Coppejans, R. Margutti, G. Terreran, A. J. Nayana, E. R. Coughlin, T. Laskar, K. D. Alexander, M. Bietenholz, D. Caprioli, P. Chandra, M. R. Drout, D. Frederiks, C. Frohmaier, K. H. Hurley, C. S. Kochanek, M. MacLeod, A. Meisner, P. E. Nugent, A. Ridnaia, D. J. Sand, D. Svinkin, C. Ward, S. Yang, A. Baldeschi, I. V. Chilingarian, Y. Dong, C. Esquivia, W. Fong, C. Guidorzi, P. Lundqvist, D. Milisavljevic, K. Paterson, D. E. Reichart, B. Shappee, M. C. Stroh, S. Valenti, B. A. Zauderer, and B. Zhang, ApJL **895**, L23 (2020), arXiv: 2003.10503.
102 A. Y. Q. Ho, D. A. Perley, S. R. Kulkarni, D. Z. J. Dong, K. De, P. Chandra, I. Andreoni, E. C. Bellm, K. B. Burdge, M. Coughlin, R. Dekany, M. Feeney, D. D. Frederiks, C. Fremling, V. Z. Golkhou, M. J. Graham, D. Hale, G. Helou, A. Horesh, M. M. Kasliwal, R. R. Laher, F. J. Masci, A. A. Miller, M. Porter, A. Ridnaia, B. Rusholme, D. L. Shupe, M. T. Soumagnac, and D. S. Svinkin, ApJ **895**, 49 (2020), arXiv: 2003.01222.

103 D. A. Perley, A. Y. Q. Ho, Y. Yao, C. Fremling, J. P. Anderson, S. Schulze, H. Kumar, G. C. Anupama, S. Barway, E. C. Bellm, V. Bhalerao, T.-W. Chen, D. A. Duev, L. Galbany, M. J. Graham, M. Gromadzki, C. P. Gutiérrez, N. Ihanec, C. Inserram, M. M. Kasliwal, E. C. Kool, S. R. Kulkarni, R. R. Laher, F. J. Masci, J. D. Neill, M. Nicholl, M. Pursiainen, J. van Roestel, Y. Sharma, J. Sollerman, R. Walters, and P. Wiseman, arXiv e-prints arXiv:2103.01968 (2021), arXiv: 2103.01968.

104 R. Margutti, B. D. Metzger, R. Chornock, I. Vurm, N. Roth, B. W. Grefenstette, V. Savchenko, R. Cartier, J. F. Steiner, G. Terreran, B. Margalit, G. Migliori, D. Milisavljevic, K. D. Alexander, M. Bietenholz, P. K. Blanchard, E. Bozzo, D. Brethauer, I. V. Chilingarian, D. L. Coppejans, L. Ducci, C. Ferrigno, W. Fong, D. Götz, C. Guidorzi, A. Hajela, K. Hurley, E. Kuulkers, P. Laurent, S. Mereghetti, M. Nicholl, D. Patnaude, P. Ubertini, J. Banovetz, N. Bartel, E. Berger, E. R. Coughlin, T. Eftekhari, D. D. Frederiks, A. V. Kozlova, T. Laskar, D. S. Svinkin, M. R. Drout, A. MacFadyen, and K. Paterson, ApJ **872**, 18 (2019), arXiv: 1810.10720.

105 O. D. Fox and N. Smith, MNRAS **488**, 3772 (2019), arXiv: 1903.01535.

106 S.-C. Leung, S. Blinnikov, K. Nomoto, P. Baklanov, E. Sorokina, and A. Tolstov, ApJ **903**, 66 (2020), arXiv: 2008.11404.

107 D. Kasen and L. Bildsten, ApJ **717**, 245 (2010), arXiv: 0911.0680.

108 B. D. Metzger and A. L. Piro, MNRAS **439**, 3916 (2014), arXiv: 1311.1519.

109 M. Lyutikov and S. Toonen, MNRAS **487**, 5618 (2019), arXiv: 1812.07569.

110 D. R. Pasham, W. C. G. Ho, W. Alston, R. Remillard, M. Ng, K. Gendreau, B. D. Metzger, D. Altamirano, D. Chakrabarty, A. Fabian, J. Miller, P. Bult, Z. Arzoumanian, J. F. Steiner, T. Strohmayer, F. Tombesi, J. Homan, E. M. Cackett, and A. Harding, Nature Astronomy (2021), arXiv: 2112.04531.

111 A. Gal-Yam, Science **337**, 927 (2012), arXiv: 1208.3217.

112 R. Knop, G. Aldering, S. Deustua, G. Goldhaber, M. Kim, P. Nugent, E. Helin, S. Pravdo, D. Rabinowitz, and K. Lawrence, IAUC **7128**, 1 (1999).

113 A. Gal-Yam, ARA&A **57**, 305 (2019), arXiv: 1812.01428.

114 M. Nicholl, Astronomy and Geophysics **62**, 5.34 (2021), arXiv: 2109.08697.

115 R. M. Quimby, G. Aldering, J. C. Wheeler, P. Höflich, C. W. Akerlof, and E. S. Rykoff, ApJL **668**, L99 (2007), arXiv: 0709.0302.

116 A. Gal-Yam, P. Mazzali, E. O. Ofek, P. E. Nugent, S. R. Kulkarni, M. M. Kasliwal, R. M. Quimby, A. V. Filippenko, S. B. Cenko, R. Chornock, R. Waldman, D. Kasen, M. Sullivan, E. C. Beshore, A. J. Drake, R. C. Thomas, J. S. Bloom, D. Poznanski, A. A. Miller, R. J. Foley, J. M. Silverman, I. Arcavi, R. S. Ellis, and J. Deng, Nature **462**, 624 (2009), arXiv: 1001.1156.

117 T. J. Moriya, E. I. Sorokina, and R. A. Chevalier, SSRv **214**, 59 (2018), arXiv: 1803.01875.

118 R. M. Quimby, F. Yuan, C. Akerlof, and J. C. Wheeler, MNRAS **431**, 912 (2013), arXiv: 1302.0911.

119 C. Inserra and S. J. Smartt, ApJ **796**, 87 (2014), arXiv: 1409.4429.

120 C. Inserra, R. C. Nichol, D. Scovacricchi, J. Amiaux, M. Brescia, C. Burigana, E. Cappellaro, C. S. Carvalho, S. Cavuoti, V. Conforti, J. C. Cuillandre, A. da Silva, A. De Rosa, M. Della Valle, J. Dinis, E. Franceschi, I. Hook, P. Hudelot, K. Jahnke, T. Kitching, H. Kurki-Suonio, I. Lloro, G. Longo, E. Maiorano, M. Maris, J. D. Rhodes, R. Scaramella, S. J. Smartt, M. Sullivan, C. Tao, R. Toledo-Moreo, I. Tereno, M. Trifoglio, and L. Valenziano, A&A **609**, A83 (2018), arXiv: 1710.09585.

121 Z. Barkat, G. Rakavy, and N. Sack, PRL **18**, 379 (1967).

122 G. Rakavy and G. Shaviv, ApJ **148**, 803 (1967).

123 G. S. Fraley, Ap&SS **2**, 96 (1968).

124 S. E. Woosley, S. Blinnikov, and A. Heger, Nature **450**, 390 (2007), arXiv: 0710.3314.

125 S. Gomez, E. Berger, M. Nicholl, P. K. Blanchard, V. A. Villar, L. Patton, R. Chornock, J. Leja, G. Hosseinzadeh, and P. S. Cowperthwaite, ApJ **881**, 87 (2019), arXiv: 1904.07259.

126 M. Nicholl, P. K. Blanchard, E. Berger, R. Chornock, R. Margutti, S. Gomez, R. Lunnan, A. A. Miller, W.-f. Fong, G. Terreran, A. Vigna-Gómez, K. Bhirombhakdi, A. Bieryla, P. Challis, R. R. Laher, F. J. Masci, and K. Paterson, Nature Astronomy **4**, 893 (2020), arXiv: 2004.05840.

127 S. Miyazaki, Y. Komiyama, S. Kawanomoto, Y. Doi, H. Furusawa, T. Hamana, Y. Hayashi, H. Ikeda, Y. Kamata, H. Karoji, M. Koike, T. Kurakami, S. Miyama, T. Morokuma, F. Nakata, K. Namikawa, H. Nakaya, K. Nariai, Y. Obuchi, Y. Oishi, N. Okada, Y. Okura, P. Tait, T. Takata, Y. Tanaka, M. Tanaka, T. Terai, D. Tomono, F. Uraguchi, T. Usuda, Y. Utsumi, Y. Yamada, H. Yamanoi, H. Aihara, H. Fujimori, S. Mineo, H. Miyatake, M. Oguri, T. Uchida, M. M. Tanaka, N. Yasuda, M. Takada, H. Murayama, A. J. Nishizawa, N. Sugiyama, M. Chiba, T. Futamase, S.-Y. Wang, H.-Y. Chen, P. T. P. Ho, E. J. Y. Liaw, C.-F. Chiu, C.-L. Ho, T.-C. Lai, Y.-C. Lee, D.-Z. Jeng, S. Iwamura, R. Armstrong, S. Bickerton, J. Bosch, J. E. Gunn, R. H. Lupton, C. Loomis, P. Price, S. Smith, M. A. Strauss, E. L. Turner, H. Suzuki, Y. Miyazaki, M. Muramatsu, K. Yamamoto, M. Endo, Y. Ezaki, N. Ito, N. Kawaguchi, S. Sofuku, T. Taniike, K. Akutsu, N. Dojo, K. Kasumi, T. Matsuda, K. Imoto, Y. Miwa, M. Suzuki, K. Takeshi, and H. Yokota, PASJ **70**, S1 (2018).

128 H. Aihara, N. Arimoto, R. Armstrong, S. Arnouts, N. A. Bahcall, S. Bickerton, J. Bosch, K. Bundy, P. L. Capak, and J. H. H. Chan, PASJ **70**, S4 (2018).

129 J. Guy, P. Astier, S. Baumont, D. Hardin, R. Pain, N. Regnault, S. Basa, R. G. Carlberg, A. Conley, and S. Fabbro, A&A **466**, 11 (2007).

130 C. Saunders, G. Aldering, P. Antilogus, S. Bailey, C. Baltay, K. Barbary, D. Baugh, K. Boone, S. Bongard, C. Buton, J. Chen, N. Chotard, Y. Copin, S. Dixon, P. Fagrelius, H. K. Fakhouri, U. Feindt, D. Fouchez, E. Gangler, B. Hayden, W. Hillebrandt, A. G. Kim, M. Kowalski, D. Küsters, P. F. Leget, S. Lombardo, J. Nordin, R. Pain, E. Pecontal, R. Pereira, S. Perlmutter, D. Rabinowitz, M. Rigault, D. Rubin, K. Runge, G. Smadja, C. Sofiatti, N. Suzuki, C. Tao, S. Taubenberger, R. C. Thomas, M. Vincenzi, and T. Nearby Supernova Factory, ApJ **869**, 167 (2018), arXiv: 1810.09476.

131 P. F. Léget, E. Gangler, F. Mondon, G. Aldering, P. Antilogus, C. Aragon, S. Bailey, C. Baltay, K. Barbary, S. Bongard, K. Boone, C. Buton, N. Chotard, Y. Copin, S. Dixon, P. Fagrelius, U. Feindt, D. Fouchez, B. Hayden, W. Hillebrandt, A. Kim, M. Kowalski, D. Kuesters, S. Lombardo, Q. Lin, J. Nordin, R. Pain, E. Pecontal, R. Pereira, S. Perlmutter, K. A. Ponder, M. V. Pruzhinskaya, D. Rabinowitz, M. Rigault, K. Runge, D. Rubin, C. Saunders, L. P. Says, G. Smadja, C. Sofiatti, N. Suzuki, S. Taubenberger, C. Tao, and R. C. Thomas, A&A **636**, A46 (2020), arXiv: 1909.11239.

132 D. O. Jones, A. G. Riess, D. M. Scolnic, Y. C. Pan, E. Johnson, D. A. Coulter, K. G. Dettman, M. M. Foley, R. J. Foley, M. E. Huber, S. W. Jha, C. D. Kilpatrick, R. P. Kirshner, A. Rest, A. S. B. Schultz, and M. R. Siebert, ApJ **867**, 108 (2018), arXiv: 1805.05911.

133 M. Roman, D. Hardin, M. Betoule, P. Astier, C. Balland, R. S. Ellis, S. Fabbro, J. Guy, I. Hook, D. A. Howell, C. Lidman, A. Mitra, A. Möller, A. M. Mourão, J. Neveu, N. Palanque-Delabrouille, C. J. Pritchet, N. Regnault, V. Ruhlmann-Kleider, C. Saunders, and M. Sullivan, A&A **615**, A68 (2018), arXiv: 1706.07697.

134 R. P. Kirshner and J. Kwan, ApJ **193**, 27 (1974).

135 M. Hamuy and P. A. Pinto, ApJL **566**, L63 (2002), arXiv: astro-ph/0201279.

136 Ó. Rodríguez, A. Clocchiatti, and M. Hamuy, AJ **148**, 107 (2014), arXiv: 1409.3198.

137 T. de Jaeger, S. González-Gaitán, J. P. Anderson, L. Galbany, M. Hamuy, M. M. Phillips, M. D. Stritzinger, C. P. Gutiérrez, L. Bolt, C. R. Burns, A. Campillay, S. Castellón, C. Contreras, G. Folatelli,

W. L. Freedman, E. Y. Hsiao, K. Krisciunas, W. Krzeminski, H. Kuncarayakti, N. Morrell, F. Olivares E., S. E. Persson, and N. Suntzeff, ApJ **815**, 121 (2015), arXiv: 1511.05145.
138 S. Refsdal, MNRAS **128**, 307 (1964).
139 R. M. Quimby, M. Oguri, A. More, S. More, T. J. Moriya, M. C. Werner, M. Tanaka, G. Folatelli, M. C. Bersten, K. Maeda, and K. Nomoto, Science **344**, 396 (2014), arXiv: 1404.6014.
140 K. C. Wong, S. H. Suyu, G. C. F. Chen, C. E. Rusu, M. Millon, D. Sluse, V. Bonvin, C. D. Fassnacht, S. Taubenberger, M. W. Auger, S. Birrer, J. H. H. Chan, F. Courbin, S. Hilbert, O. Tihhonova, T. Treu, A. Agnello, X. Ding, I. Jee, E. Komatsu, A. J. Shajib, A. Sonnenfeld, R. D. Blandford, L. V. E. Koopmans, P. J. Marshall, and G. Meylan, MNRAS **498**, 1420 (2020), arXiv: 1907.04869.
141 M. Oguri and Y. Kawano, MNRAS **338**, L25 (2003), arXiv: astro-ph/0211499.
142 X. Ding, T. Treu, S. Birrer, A. Agnello, D. Sluse, C. Fassnacht, M. W. Auger, K. C. Wong, S. H. Suyu, T. Morishita, C. E. Rusu, and A. Galan, MNRAS **501**, 269 (2021), arXiv: 2005.13550.
143 P. L. Kelly, S. A. Rodney, T. Treu, R. J. Foley, G. Brammer, K. B. Schmidt, A. Zitrin, A. Sonnenfeld, L.-G. Strolger, O. Graur, A. V. Filippenko, S. W. Jha, A. G. Riess, M. Bradac, B. J. Weiner, D. Scolnic, M. A. Malkan, A. von der Linden, M. Trenti, J. Hjorth, R. Gavazzi, A. Fontana, J. C. Merten, C. McCully, T. Jones, M. Postman, A. Dressler, B. Patel, S. B. Cenko, M. L. Graham, and B. E. Tucker, Science **347**, 1123 (2015), arXiv: 1411.6009.
144 A. Goobar, R. Amanullah, S. R. Kulkarni, P. E. Nugent, J. Johansson, C. Steidel, D. Law, E. Mörtsell, R. Quimby, N. Blagorodnova, A. Brandeker, Y. Cao, A. Cooray, R. Ferretti, C. Fremling, L. Hangard, M. Kasliwal, T. Kupfer, R. Lunnan, F. Masci, A. A. Miller, H. Nayyeri, J. D. Neill, E. O. Ofek, S. Papadogiannakis, T. Petrushevska, V. Ravi, J. Sollerman, M. Sullivan, F. Taddia, R. Walters, D. Wilson, L. Yan, and O. Yaron, Science **356**, 291 (2017), arXiv: 1611.00014.
145 S. A. Rodney, G. B. Brammer, J. D. R. Pierel, J. Richard, S. Toft, K. F. O'Connor, M. Akhshik, and K. E. Whitaker, Nature Astronomy **5**, 1118 (2021), arXiv: 2106.08935.
146 M. Oguri and P. J. Marshall, MNRAS **405**, 2579 (2010), arXiv: 1001.2037.
147 W. Li, R. Chornock, J. Leaman, A. V. Filippenko, D. Poznanski, X. Wang, M. Ganeshalingam, and F. Mannucci, MNRAS **412**, 1473 (2011), arXiv: 1006.4613.
148 E. Y. Hsiao, A. Conley, D. A. Howell, M. Sullivan, C. J. Pritchet, R. G. Carlberg, P. E. Nugent, and M. M. Phillips, ApJ **663**, 1187 (2007), arXiv: astro-ph/0703529.
149 M. J. Rees, Nature **333**, 523 (1988).
150 C. R. Evans and C. S. Kochanek, ApJL **346**, L13 (1989).
151 E. S. Phinney, in *The Center of the Galaxy*, (edited by M. Morris), volume 136, 543 (1989).
152 N. Bade, S. Komossa, and M. Dahlem, A&A **309**, L35 (1996).
153 R. Saxton, S. Komossa, K. Auchettl, and P. G. Jonker, SSRv **216**, 85 (2020).
154 S. Sazonov, M. Gilfanov, P. Medvedev, Y. Yao, G. Khorunzhev, A. Semena, R. Sunyaev, R. Burenin, A. Lyapin, A. Meshcheryakov, G. Uskov, I. Zaznobin, K. A. Postnov, A. V. Dodin, A. A. Belinski, A. M. Cherepashchuk, M. Eselevich, S. N. Dodonov, A. A. Grokhovskaya, S. S. Kotov, I. F. Bikmaev, R. Y. Zhuchkov, R. I. Gumerov, S. van Velzen, and S. Kulkarni, MNRAS **508**, 3820 (2021), arXiv: 2108.02449.
155 S. van Velzen, T. W. S. Holoien, F. Onori, T. Hung, and I. Arcavi, SSRv **216**, 124 (2020), arXiv: 2008.05461.
156 S. Gezari, ARA&A **59** (2021), arXiv: 2104.14580.
157 S. van Velzen, S. Gezari, E. Hammerstein, N. Roth, S. Frederick, C. Ward, T. Hung, S. B. Cenko, R. Stein, D. A. Perley, K. Taggart, R. J. Foley, J. Sollerman, N. Blagorodnova, I. Andreoni, E. C. Bellm, V. Brinnel, K. De, R. Dekany, M. Feeney, C. Fremling, M. Giomi, V. Z. Golkhou, M. J. Graham, A. Y. Q. Ho, M. M. Kasliwal, C. D. Kilpatrick, S. R. Kulkarni, T. Kupfer, R. R. Laher, A. Mahabal, F. J. Masci, A. A. Miller, J. Nordin, R. Riddle, B. Rusholme, J. van Santen, Y. Sharma, D. L. Shupe, and M. T. Soumagnac, ApJ **908**, 4 (2021), arXiv: 2001.01409.
158 D. Lin, J. Strader, E. R. Carrasco, D. Page, A. J. Romanowsky, J. Homan, J. A. Irwin, R. A. Remillard, O. Godet, N. A. Webb, H. Baumgardt, R. Wijnands, D. Barret, P.-A. Duc, J. P. Brodie, and S. D. J. Gwyn, Nature Astronomy **2**, 656 (2018), arXiv: 1806.05692.
159 F. K. Liu, S. Li, and S. Komossa, ApJ **786**, 103 (2014), arXiv: 1404.4933.
160 X. Shu, W. Zhang, S. Li, N. Jiang, L. Dou, Z. Yan, F.-G. Xie, R. Shen, L. Sun, F. Liu, and T. Wang, Nature Communications **11**, 5876 (2020), arXiv: 2012.11818.
161 J. S. Bloom, D. Giannios, B. D. Metzger, S. B. Cenko, D. A. Perley, N. R. Butler, N. R. Tanvir, A. J. Levan, P. T. O'Brien, L. E. Strubbe, F. De Colle, E. Ramirez-Ruiz, W. H. Lee, S. Nayakshin, E. Quataert, A. R. King, A. Cucchiara, J. Guillochon, G. C. Bower, A. S. Fruchter, A. N. Morgan, and A. J. van der Horst, Science **333**, 203 (2011), arXiv: 1104.3257.
162 S. Mattila, M. Pérez-Torres, A. Efstathiou, P. Mimica, M. Fraser, E. Kankare, A. Alberdi, M. Á. Aloy, T. Heikkilä, P. G. Jonker, P. Lundqvist, I. Martí-Vidal, W. P. S. Meikle, C. Romero-Cañizales, S. J. Smartt, S. Tsygankov, E. Varenius, A. Alonso-Herrero, M. Bondi, C. Fransson, R. Herrero-Illana, T. Kangas, R. Kotak, N. Ramírez-Olivencia, P. Väisänen, R. J. Beswick, D. L. Clements, R. Greimel, J. Harmanen, J. Kotilainen, K. Nandra, T. Reynolds, S. Ryder, N. A. Walton, K. Wiik, and G. Östlin, Science **361**, 482 (2018), arXiv: 1806.05717.
163 N. Jiang, L. Dou, T. Wang, C. Yang, J. Lyu, and H. Zhou, ApJL **828**, L14 (2016), arXiv: 1605.04640.
164 S. van Velzen, A. J. Mendez, J. H. Krolik, and V. Gorjian, ApJ **829**, 19 (2016), arXiv: 1605.04304.
165 R. Stein, S. v. Velzen, M. Kowalski, A. Franckowiak, S. Gezari, J. C. A. Miller-Jones, S. Frederick, I. Sfaradi, M. F. Bietenholz, A. Horesh, R. Fender, S. Garrappa, T. Ahumada, I. Andreoni, J. Belicki, E. C. Bellm, M. Böttcher, V. Brinnel, R. Burruss, S. B. Cenko, M. W. Coughlin, V. Cunningham, A. Drake, G. R. Farrar, M. Feeney, R. J. Foley, A. Gal-Yam, V. Z. Golkhou, A. Goobar, M. J. Graham, E. Hammerstein, G. Helou, T. Hung, M. M. Kasliwal, C. D. Kilpatrick, A. K. H. Kong, T. Kupfer, R. R. Laher, A. A. Mahabal, F. J. Masci, J. Necker, J. Nordin, D. A. Perley, M. Rigault, S. Reusch, H. Rodriguez, C. Rojas-Bravo, B. Rusholme, D. L. Shupe, L. P. Singer, J. Sollerman, M. T. Soumagnac, D. Stern, K. Taggart, J. van Santen, C. Ward, P. Woudt, and Y. Yao, Nature Astronomy **5**, 510 (2021), arXiv: 2005.05340.
166 K. D. French, I. Arcavi, and A. Zabludoff, ApJL **818**, L21 (2016), arXiv: 1601.04705.
167 W. Lu and P. Kumar, ApJ **865**, 128 (2018), arXiv: 1802.02151.
168 L. Dai, J. C. McKinney, N. Roth, E. Ramirez-Ruiz, and M. C. Miller, ApJL **859**, L20 (2018), arXiv: 1803.03265.
169 F. K. Liu, C. Y. Cao, M. A. Abramowicz, M. Wielgus, R. Cao, and Z. Q. Zhou, ApJ **908**, 179 (2021), arXiv: 2012.05552.
170 A. Zabludoff, I. Arcavi, S. La Massa, H. B. Perets, B. Trakhtenbrot, B. A. Zauderer, K. Auchettl, J. L. Dai, K. D. French, T. Hung, E. Kara, G. Lodato, W. P. Maksym, Y. Qin, E. Ramirez-Ruiz, N. Roth, J. C. Runnoe, and T. Wevers, SSRv **217**, 54 (2021), arXiv: 2103.12150.
171 T. Wevers, S. van Velzen, P. G. Jonker, N. C. Stone, T. Hung, F. Onori, S. Gezari, and N. Blagorodnova, MNRAS **471**, 1694 (2017), arXiv: 1706.08965.
172 D. R. Pasham, R. A. Remillard, P. C. Fragile, A. Franchini, N. C. Stone, G. Lodato, J. Homan, D. Chakrabarty, F. K. Baganoff, J. F. Steiner, E. R. Coughlin, and N. R. Pasham, Science **363**, 531 (2019), arXiv: 1810.10713.
173 D. Korytov, A. Hearin, E. Kovacs, P. Larsen, E. Rangel, J. Hol-

lowed, A. J. Benson, K. Heitmann, Y.-Y. Mao, A. Bahmanyar, C. Chang, D. Campbell, J. DeRose, H. Finkel, N. Frontiere, E. Gawiser, S. Habib, B. Joachimi, F. Lanusse, N. Li, R. Mandelbaum, C. Morrison, J. A. Newman, A. Pope, E. Rykoff, M. Simet, C.-H. To, V. Vikraman, R. H. Wechsler, M. White, and (The LSST Dark Energy Science Collaboration, ApJS **245**, 26 (2019), arXiv: 1907.06530.

174 N. C. Stone and B. D. Metzger, MNRAS **455**, 859 (2016), arXiv: 1410.7772.

175 J. Guillochon, M. Nicholl, V. A. Villar, B. Mockler, G. Narayan, K. S. Mandel, E. Berger, and P. K. G. Williams, ApJS **236**, 6 (2018), arXiv: 1710.02145.

176 J. E. Greene, J. Strader, and L. C. Ho, ARA&A **58**, 257 (2020), arXiv: 1911.09678.

177 M. MacLeod, J. Guillochon, E. Ramirez-Ruiz, D. Kasen, and S. Rosswog, ApJ **819**, 3 (2016), arXiv: 1508.02399.

178 A. Tanikawa, M. Giersz, and M. Arca Sedda, arXiv e-prints arXiv:2103.14185 (2021), arXiv: 2103.14185.

179 L.-D. Liu, B. Zhang, L.-J. Wang, and Z.-G. Dai, ApJL **868**, L24 (2018), arXiv: 1809.05048.

180 D. A. Perley, P. A. Mazzali, L. Yan, S. B. Cenko, S. Gezari, K. Taggart, N. Blagorodnova, C. Fremling, B. Mockler, A. Singh, N. Tominaga, M. Tanaka, A. M. Watson, T. Ahumada, G. C. Anupama, C. Ashall, R. L. Becerra, D. Bersier, V. Bhalerao, J. S. Bloom, N. R. Butler, C. Copperwheat, M. W. Coughlin, K. De, A. J. Drake, D. A. Duev, S. Frederick, J. J. González, A. Goobar, M. Heida, A. Y. Q. Ho, J. Horst, T. Hung, R. Itoh, J. E. Jencson, M. M. Kasliwal, N. Kawai, T. Khanam, S. R. Kulkarni, B. Kumar, H. Kumar, A. S. Kutyrev, W. H. Lee, K. Maeda, A. Mahabal, K. L. Murata, J. D. Neill, C.-C. Ngeow, B. Penprase, E. Pian, R. Quimby, E. Ramirez-Ruiz, M. G. Richer, C. G. Román-Zúñiga, D. K. Sahu, S. Srivastav, Q. Socia, J. Sollerman, Y. Tachibana, F. Taddia, S. Tinyanont, E. Troja, C. Ward, J. Wee, and P.-C. Yu, MNRAS **484**, 1031 (2019), arXiv: 1808.00969.

181 S. J. Prentice, K. Maguire, S. J. Smartt, M. R. Magee, P. Schady, S. Sim, T. W. Chen, P. Clark, C. Colin, M. Fulton, O. McBrien, D. O'Neill, K. W. Smith, C. Ashall, K. C. Chambers, L. Denneau, H. A. Flewelling, A. Heinze, T. W. S. Holoien, M. E. Huber, C. S. Kochanek, P. A. Mazzali, J. L. Prieto, A. Rest, B. J. Shappee, B. Stalder, K. Z. Stanek, M. D. Stritzinger, T. A. Thompson, and J. L. Tonry, ApJL **865**, L3 (2018), arXiv: 1807.05965.

182 A. Y. Q. Ho, D. A. Perley, S. R. Kulkarni, D. Z. J. Dong, K. De, P. Chandra, I. Andreoni, E. C. Bellm, K. B. Burdge, M. Coughlin, R. Dekany, M. Feeney, D. D. Frederiks, C. Fremling, V. Z. Golkhou, M. J. Graham, D. Hale, G. Helou, A. Horesh, M. M. Kasliwal, R. R. Laher, F. J. Masci, A. A. Miller, M. Porter, A. Ridnaia, B. Rusholme, D. L. Shupe, M. T. Soumagnac, and D. S. Svinkin, ApJ **895**, 49 (2020), arXiv: 2003.01222.

183 D. L. Coppejans, R. Margutti, G. Terreran, A. J. Nayana, E. R. Coughlin, T. Laskar, K. D. Alexander, M. Bietenholz, D. Caprioli, P. Chandra, M. R. Drout, D. Frederiks, C. Frohmaier, K. H. Hurley, C. S. Kochanek, M. MacLeod, A. Meisner, P. E. Nugent, A. Ridnaia, D. J. Sand, D. Svinkin, C. Ward, S. Yang, A. Baldeschi, I. V. Chilingarian, Y. Dong, C. Esquivia, W. Fong, C. Guidorzi, P. Lundqvist, D. Milisavljevic, K. Paterson, D. E. Reichart, B. Shappee, M. C. Stroh, S. Valenti, B. A. Zauderer, and B. Zhang, ApJL **895**, L23 (2020), arXiv: 2003.10503.

184 D. A. Perley, A. Y. Q. Ho, Y. Yao, C. Fremling, J. P. Anderson, S. Schulze, H. Kumar, G. C. Anupama, S. Barway, E. C. Bellm, V. Bhalerao, T.-W. Chen, D. A. Duev, L. Galbany, M. J. Graham, M. Gromadzki, C. P. Gutiérrez, N. Ihanec, C. Inserra, M. M. Kasliwal, E. C. Kool, S. R. Kulkarni, R. R. Laher, F. J. Masci, J. D. Neill, M. Nicholl, M. Pursiainen, J. van Roestel, Y. Sharma, J. Sollerman, R. Walters, and P. Wiseman, MNRAS **508**, 5138 (2021), arXiv: 2103.01968.

185 Y. Yao, A. Y. Q. Ho, P. Medvedev, J. Nayana A., D. A. Perley, S. R. Kulkarni, P. Chandra, S. Sazonov, M. Gilfanov, G. Khorunzhev, D. K. Khatami, and R. Sunyaev, arXiv e-prints arXiv:2112.00751 (2021), arXiv: 2112.00751.

186 A. Y. Q. Ho, D. A. Perley, A. Gal-Yam, R. Lunnan, J. Sollerman, S. Schulze, K. K. Das, D. Dobie, Y. Yao, C. Fremling, S. Adams, S. Anand, I. Andreoni, E. C. Bellm, R. J. Bruch, K. B. Burdge, A. J. Castro-Tirado, A. Dahiwale, K. De, R. Dekany, A. J. Drake, D. A. Duev, M. J. Graham, G. Helou, D. L. Kaplan, V. Karambelkar, M. M. Kasliwal, E. C. Kool, S. R. Kulkarni, A. A. Mahabal, M. S. Medford, A. A. Miller, J. Nordin, E. Ofek, G. Petitpas, R. Riddle, Y. Sharma, R. Smith, A. J. Stewart, K. Taggart, L. Tartaglia, A. Tzanidakis, and J. M. Winters, arXiv e-prints arXiv:2105.08811 (2021), arXiv: 2105.08811.

187 J. Law-Smith, M. MacLeod, J. Guillochon, P. Macias, and E. Ramirez-Ruiz, ApJ **841**, 132 (2017), arXiv: 1701.08162.

188 T. W. S. Holoien, P. J. Vallely, K. Auchettl, K. Z. Stanek, C. S. Kochanek, K. D. French, J. L. Prieto, B. J. Shappee, J. S. Brown, M. M. Fausnaugh, S. Dong, T. A. Thompson, S. Bose, J. M. M. Neustadt, P. Cacella, J. Brimacombe, M. R. Kendurkar, R. L. Beaton, K. Boutsia, L. Chomiuk, T. Connor, N. Morrell, A. B. Newman, G. C. Rudie, L. Shishkovksy, and J. Strader, ApJ **883**, 111 (2019), arXiv: 1904.09293.

189 W. Yuan, C. Zhang, Z. Ling, D. Zhao, W. Wang, Y. Chen, F. Lu, S.-N. Zhang, and W. Cui, in *Space Telescopes and Instrumentation 2018: Ultraviolet to Gamma Ray*, (edited by J.-W. A. den Herder, S. Nikzad, and K. Nakazawa), volume 10699 of *Society of Photo-Optical Instrumentation Engineers (SPIE) Conference Series*, 1069925 (2018).

190 S. Gezari, S. B. Cenko, and I. Arcavi, ApJL **851**, L47 (2017), arXiv: 1712.03968.

191 J.-H. Chen and R.-F. Shen, ApJ **914**, 69 (2021), arXiv: 2104.08827.

192 A. V. Payne, B. J. Shappee, J. T. Hinkle, P. J. Vallely, C. S. Kochanek, T. W. S. Holoien, K. Auchettl, K. Z. Stanek, T. A. Thompson, J. M. M. Neustadt, M. A. Tucker, J. D. Armstrong, J. Brimacombe, P. Cacella, R. Cornect, L. Denneau, M. M. Fausnaugh, H. Flewelling, D. Grupe, A. N. Heinze, L. A. Lopez, B. Monard, J. L. Prieto, A. C. Schneider, S. S. Sheppard, J. L. Tonry, and H. Weiland, ApJ **910**, 125 (2021), arXiv: 2009.03321.

193 B. P. Abbott, R. Abbott, T. D. Abbott, F. Acernese, K. Ackley, C. Adams, T. Adams, P. Addesso, R. X. Adhikari, V. B. Adya, C. Affeldt, M. Afrough, B. Agarwal, M. Agathos, K. Agatsuma, N. Aggarwal, O. D. Aguiar, L. Aiello, A. Ain, P. Ajith, B. Allen, G. Allen, A. Allocca, P. A. Altin, A. Amato, A. Ananyeva, S. B. Anderson, W. G. Anderson, S. V. Angelova, S. Antier, S. Appert, K. Arai, M. C. Araya, J. S. Areeda, N. Arnaud, K. G. Arun, S. Ascenzi, G. Ashton, M. Ast, S. M. Aston, P. Astone, D. V. Atallah, P. Aufmuth, C. Aulbert, K. AultONeal, C. Austin, A. Avila-Alvarez, S. Babak, P. Bacon, M. K. M. Bader, S. Bae, M. Bailes, P. T. Baker, F. Baldaccini, G. Ballardin, S. W. Ballmer, S. Banagiri, J. C. Barayoga, S. E. Barclay, B. C. Barish, D. Barker, K. Barkett, F. Barone, B. Barr, L. Barsotti, M. Barsuglia, D. Barta, S. D. Barthelmy, J. Bartlett, I. Bartos, R. Bassiri, A. Basti, J. C. Batch, M. Bawaj, J. C. Bayley, M. Bazzan, B. Bécsy, C. Beer, M. Bejger, I. Belahcene, A. S. Bell, B. K. Berger, G. Bergmann, S. Bernuzzi, J. J. Bero, C. P. L. Berry, D. Bersanetti, A. Bertolini, J. Betzwieser, S. Bhagwat, R. Bhandare, I. A. Bilenko, G. Billingsley, C. R. Billman, J. Birch, R. Birney, O. Birnholtz, S. Biscans, S. Biscoveanu, A. Bisht, M. Bitossi, C. Biwer, M. A. Bizouard, J. K. Blackburn, J. Blackman, C. D. Blair, D. G. Blair, R. M. Blair, S. Bloemen, O. Bock, N. Bode, M. Boer, G. Bogaert, A. Bohe, F. Bondu, E. Bonilla, R. Bonnand, B. A. Boom, R. Bork, V. Boschi, S. Bose, K. Bossie, Y. Bouffanais, A. Bozzi, C. Bradaschia, P. R. Brady, M. Branchesi, J. E. Brau, T. Briant, A. Brillet, M. Brinkmann, V. Brisson, P. Brockill, J. E. Broida, A. F. Brooks, D. A. Brown, D. D. Brown, S. Brunett, C. C. Buchanan, A. Buikema, T. Bulik, H. J. Bulten, A. Buonanno, D. Buskulic, C. Buy, R. L. Byer, M. Cabero, L. Cadonati, G. Cagnoli, C. Cahillane, J. Calderón Bustillo, T. A. Callister, E. Calloni, J. B. Camp, M. Canepa, P. Canizares, K. C.

Cannon, H. Cao, J. Cao, C. D. Capano, E. Capocasa, F. Carbognani, S. Caride, M. F. Carney, G. Carullo, J. Casanueva Diaz, C. Casentini, S. Caudill, M. Cavaglià, F. Cavalier, R. Cavalieri, G. Cella, C. B. Cepeda, P. Cerdá-Durán, G. Cerretani, E. Cesarini, S. J. Chamberlin, M. Chan, S. Chao, P. Charlton, E. Chase, E. Chassande-Mottin, D. Chatterjee, K. Chatziioannou, B. D. Cheeseboro, H. Y. Chen, X. Chen, Y. Chen, H. P. Cheng, H. Chia, A. Chincarini, A. Chiummo, T. Chmiel, H. S. Cho, M. Cho, J. H. Chow, N. Christensen, Q. Chu, A. J. K. Chua, S. Chua, A. K. W. Chung, S. Chung, G. Ciani, R. Ciolfi, C. E. Cirelli, A. Cirone, F. Clara, J. A. Clark, P. Clearwater, F. Cleva, C. Cocchieri, E. Coccia, P. F. Cohadon, D. Cohen, A. Colla, C. G. Collette, L. R. Cominsky, M. Constancio, L. Conti, S. J. Cooper, P. Corban, T. R. Corbitt, I. Cordero-Carrión, K. R. Corley, N. Cornish, A. Corsi, S. Cortese, C. A. Costa, M. W. Coughlin, S. B. Coughlin, J. P. Coulon, S. T. Countryman, P. Couvares, P. B. Covas, E. E. Cowan, D. M. Coward, M. J. Cowart, D. C. Coyne, R. Coyne, J. D. E. Creighton, T. D. Creighton, J. Cripe, S. G. Crowder, T. J. Cullen, A. Cumming, L. Cunningham, E. Cuoco, T. Dal Canton, G. Dálya, S. L. Danilishin, S. D'Antonio, K. Danzmann, A. Dasgupta, C. F. Da Silva Costa, V. Dattilo, I. Dave, M. Davier, D. Davis, E. J. Daw, B. Day, S. De, D. DeBra, J. Degallaix, M. De Laurentis, S. Deléglise, W. Del Pozzo, N. Demos, T. Denker, T. Dent, R. De Pietri, V. Dergachev, R. De Rosa, R. T. DeRosa, C. De Rossi, R. DeSalvo, O. de Varona, J. Devenson, S. Dhurandhar, M. C. Díaz, T. Dietrich, L. Di Fiore, M. Di Giovanni, T. Di Girolamo, A. Di Lieto, S. Di Pace, I. Di Palma, F. Di Renzo, Z. Doctor, V. Dolique, F. Donovan, K. L. Dooley, S. Doravari, I. Dorrington, R. Douglas, M. Dovale Álvarez, T. P. Downes, M. Drago, C. Dreissigacker, J. C. Driggers, Z. Du, M. Ducrot, R. Dudi, P. Dupej, S. E. Dwyer, T. B. Edo, M. C. Edwards, A. Effler, H. B. Eggenstein, P. Ehrens, J. Eichholz, S. S. Eikenberry, R. A. Eisenstein, R. C. Essick, D. Estevez, Z. B. Etienne, T. Etzel, M. Evans, T. M. Evans, M. Factourovich, V. Fafone, H. Fair, S. Fairhurst, X. Fan, S. Farinon, B. Farr, W. M. Farr, E. J. Fauchon-Jones, M. Favata, M. Fays, C. Fee, H. Fehrmann, J. Feicht, M. M. Fejer, A. Fernandez-Galiana, I. Ferrante, E. C. Ferreira, F. Ferrini, F. Fidecaro, D. Finstad, I. Fiori, D. Fiorucci, M. Fishbach, R. P. Fisher, M. Fitz-Axen, R. Flaminio, M. Fletcher, H. Fong, J. A. Font, P. W. F. Forsyth, S. S. Forsyth, J. D. Fournier, S. Frasca, F. Frasconi, Z. Frei, A. Freise, R. Frey, V. Frey, E. M. Fries, P. Fritschel, V. V. Frolov, P. Fulda, M. Fyffe, H. Gabbard, B. U. Gadre, S. M. Gaebel, J. R. Gair, L. Gammaitoni, M. R. Ganija, S. G. Gaonkar, C. Garcia-Quiros, F. Garufi, B. Gateley, S. Gaudio, G. Gaur, V. Gayathri, N. Gehrels, G. Gemme, E. Genin, A. Gennai, D. George, J. George, L. Gergely, V. Germain, S. Ghonge, A. Ghosh, A. Ghosh, S. Ghosh, J. A. Giaime, K. D. Giardina, A. Giazotto, K. Gill, L. Glover, E. Goetz, R. Goetz, S. Gomes, B. Goncharov, G. González, J. M. Gonzalez Castro, A. Gopakumar, M. L. Gorodetsky, S. E. Gossan, M. Gosselin, R. Gouaty, A. Grado, C. Graef, M. Granata, A. Grant, S. Gras, C. Gray, G. Greco, A. C. Green, E. M. Gretarsson, P. Groot, H. Grote, S. Grunewald, P. Gruning, G. M. Guidi, X. Guo, A. Gupta, M. K. Gupta, K. E. Gushwa, E. K. Gustafson, R. Gustafson, O. Halim, B. R. Hall, E. D. Hall, E. Z. Hamilton, G. Hammond, M. Haney, M. M. Hanke, J. Hanks, C. Hanna, M. D. Hannam, O. A. Hannuksela, J. Hanson, T. Hardwick, J. Harms, G. M. Harry, I. W. Harry, M. J. Hart, C. J. Haster, K. Haughian, J. Healy, A. Heidmann, M. C. Heintze, H. Heitmann, P. Hello, G. Hemming, M. Hendry, I. S. Heng, J. Hennig, A. W. Heptonstall, M. Heurs, S. Hild, T. Hinderer, W. C. G. Ho, D. Hoak, D. Hofman, K. Holt, D. E. Holz, P. Hopkins, C. Horst, J. Hough, E. A. Houston, E. J. Howell, A. Hreibi, Y. M. Hu, E. A. Huerta, D. Huet, B. Hughey, S. Husa, S. H. Huttner, T. Huynh-Dinh, N. Indik, R. Inta, G. Intini, H. N. Isa, J. M. Isac, M. Isi, B. R. Iyer, K. Izumi, T. Jacqmin, K. Jani, P. Jaranowski, S. Jawahar, F. Jiménez-Forteza, W. W. Johnson, N. K. Johnson-McDaniel, D. I. Jones, R. Jones, R. J. G. Jonker, L. Ju, J. Junker, C. V. Kalaghatgi, V. Kalogera, B. Kamai, S. Kandhasamy, G. Kang, J. B. Kanner, S. J. Kapadia, S. Karki, K. S. Karvinen, M. Kasprzack, W. Kastaun, M. Katolik, E. Katsavounidis, W. Katzman, S. Kaufer, K. Kawabe, F. Kéfélian, D. Keitel, A. J. Kemball, R. Kennedy, C. Kent, J. S. Key, F. Y. Khalili, I. Khan, S. Khan, Z. Khan, E. A. Khazanov, N. Kijbunchoo, C. Kim, J. C. Kim, K. Kim, W. Kim, W. S. Kim, Y. M. Kim, S. J. Kimbrell, E. J. King, P. J. King, M. Kinley-Hanlon, R. Kirchhoff, J. S. Kissel, L. Kleybolte, S. Klimenko, T. D. Knowles, P. Koch, S. M. Koehlenbeck, S. Koley, V. Kondrashov, A. Kontos, M. Korobko, W. Z. Korth, I. Kowalska, D. B. Kozak, C. Krämer, V. Kringel, B. Krishnan, A. Królak, G. Kuehn, P. Kumar, R. Kumar, S. Kumar, L. Kuo, A. Kutynia, S. Kwang, B. D. Lackey, K. H. Lai, M. Landry, R. N. Lang, J. Lange, B. Lantz, R. K. Lanza, S. L. Larson, A. Lartaux-Vollard, P. D. Lasky, M. Laxen, A. Lazzarini, C. Lazzaro, P. Leaci, S. Leavey, C. H. Lee, H. K. Lee, H. M. Lee, H. W. Lee, K. Lee, J. Lehmann, A. Lenon, E. Leon, M. Leonardi, N. Leroy, N. Letendre, Y. Levin, T. G. F. Li, S. D. Linker, T. B. Littenberg, J. Liu, X. Liu, R. K. L. Lo, N. A. Lockerbie, L. T. London, J. E. Lord, M. Lorenzini, V. Loriette, M. Lormand, G. Losurdo, J. D. Lough, C. O. Lousto, G. Lovelace, H. Lück, D. Lumaca, A. P. Lundgren, R. Lynch, Y. Ma, R. Macas, S. Macfoy, B. Machenschalk, M. MacInnis, D. M. Macleod, I. Magaña Hernandez, F. Magaña-Sandoval, L. Magaña Zertuche, R. M. Magee, E. Majorana, I. Maksimovic, N. Man, V. Mandic, V. Mangano, G. L. Mansell, M. Manske, M. Mantovani, F. Marchesoni, F. Marion, S. Márka, Z. Márka, C. Markakis, A. S. Markosyan, A. Markowitz, E. Maros, A. Marquina, P. Marsh, F. Martelli, L. Martellini, I. W. Martin, R. M. Martin, D. V. Martynov, J. N. Marx, K. Mason, E. Massera, A. Masserot, T. J. Massinger, M. Masso-Reid, S. Mastrogiovanni, A. Matas, F. Matichard, L. Matone, N. Mavalvala, N. Mazumder, R. McCarthy, D. E. McClelland, S. McCormick, L. McCuller, S. C. McGuire, G. McIntyre, J. McIver, D. J. McManus, L. McNeill, T. McRae, S. T. McWilliams, D. Meacher, G. D. Meadors, M. Mehmet, J. Meidam, E. Mejuto-Villa, A. Melatos, G. Mendell, R. A. Mercer, E. L. Merilh, M. Merzougui, S. Meshkov, C. Messenger, C. Messick, R. Metzdorff, P. M. Meyers, H. Miao, C. Michel, H. Middleton, E. E. Mikhailov, L. Milano, A. L. Miller, B. B. Miller, J. Miller, M. Millhouse, M. C. Milovich-Goff, O. Minazzoli, Y. Minenkov, J. Ming, C. Mishra, S. Mitra, V. P. Mitrofanov, G. Mitselmakher, R. Mittleman, D. Moffa, A. Moggi, K. Mogushi, M. Mohan, S. R. P. Mohapatra, I. Molina, M. Montani, C. J. Moore, D. Moraru, G. Moreno, S. Morisaki, S. R. Morriss, B. Mours, C. M. Mow-Lowry, G. Mueller, A. W. Muir, A. Mukherjee, D. Mukherjee, S. Mukherjee, N. Mukund, A. Mullavey, J. Munch, E. A. Muñiz, M. Muratore, P. G. Murray, A. Nagar, K. Napier, I. Nardecchia, L. Naticchioni, R. K. Nayak, J. Neilson, G. Nelemans, T. J. N. Nelson, M. Nery, A. Neunzert, L. Nevin, J. M. Newport, G. Newton, K. K. Y. Ng, P. Nguyen, T. T. Nguyen, D. Nichols, A. B. Nielsen, S. Nissanke, A. Nitz, A. Noack, F. Nocera, D. Nolting, C. North, L. K. Nuttall, J. Oberling, G. D. O'Dea, G. H. Ogin, J. J. Oh, S. H. Oh, F. Ohme, M. A. Okada, M. Oliver, P. Oppermann, R. J. Oram, B. O'Reilly, R. Ormiston, L. F. Ortega, R. O'Shaughnessy, S. Ossokine, D. J. Ottaway, H. Overmier, B. J. Owen, A. E. Pace, J. Page, M. A. Page, A. Pai, S. A. Pai, J. R. Palamos, O. Palashov, C. Palomba, A. Pal-Singh, H. Pan, H.-W. Pan, B. Pang, P. T. H. Pang, C. Pankow, F. Pannarale, B. C. Pant, F. Paoletti, A. Paoli, M. A. Papa, A. Parida, W. Parker, D. Pascucci, A. Pasqualetti, R. Passaquieti, D. Passuello, M. Patil, B. Patricelli, B. L. Pearlstone, M. Pedraza, R. Pedurand, L. Pekowsky, A. Pele, S. Penn, C. J. Perez, A. Perreca, L. M. Perri, H. P. Pfeiffer, M. Phelps, O. J. Piccinni, M. Pichot, F. Piergiovanni, V. Pierro, G. Pillant, L. Pinard, I. M. Pinto, M. Pirello, M. Pitkin, M. Poe, R. Poggiani, P. Popolizio, E. K. Porter, A. Post, J. Powell, J. Prasad, J. W. W. Pratt, G. Pratten, V. Predoi, T. Prestegard, M. Prijatelj, M. Principe, S. Privitera, R. Prix, G. A. Prodi, L. G. Prokhorov, O. Puncken, M. Punturo, P. Puppo, M. Pürrer, H. Qi, V. Quetschke, E. A. Quintero, R. Quitzow-James, F. J. Raab, D. S. Rabeling, H. Radkins, P. Raffai, S. Raja, C. Rajan, B. Rajbhandari,

M. Rakhmanov, K. E. Ramirez, A. Ramos-Buades, P. Rapagnani, V. Raymond, M. Razzano, J. Read, T. Regimbau, L. Rei, S. Reid, D. H. Reitze, W. Ren, S. D. Reyes, F. Ricci, P. M. Ricker, S. Rieger, K. Riles, M. Rizzo, N. A. Robertson, R. Robie, F. Robinet, A. Rocchi, L. Rolland, J. G. Rollins, V. J. Roma, J. D. Romano, R. Romano, C. L. Romel, J. H. Romie, D. Rosińska, M. P. Ross, S. Rowan, A. Rüdiger, P. Ruggi, G. Rutins, K. Ryan, S. Sachdev, T. Sadecki, L. Sadeghian, M. Sakellariadou, L. Salconi, M. Saleem, F. Salemi, A. Samajdar, L. Sammut, L. M. Sampson, E. J. Sanchez, L. E. Sanchez, N. Sanchis-Gual, V. Sandberg, J. R. Sanders, B. Sassolas, B. S. Sathyaprakash, P. R. Saulson, O. Sauter, R. L. Savage, A. Sawadsky, P. Schale, M. Scheel, J. Scheuer, J. Schmidt, P. Schmidt, R. Schnabel, R. M. S. Schofield, A. Schönbeck, E. Schreiber, D. Schuette, B. W. Schulte, B. F. Schutz, S. G. Schwalbe, J. Scott, S. M. Scott, E. Seidel, D. Sellers, A. S. Sengupta, D. Sentenac, V. Sequino, A. Sergeev, D. A. Shaddock, T. J. Shaffer, A. A. Shah, M. S. Shahriar, M. B. Shaner, L. Shao, B. Shapiro, P. Shawhan, A. Sheperd, D. H. Shoemaker, D. M. Shoemaker, K. Siellez, X. Siemens, M. Sieniawska, D. Sigg, A. D. Silva, L. P. Singer, A. Singh, A. Singhal, A. M. Sintes, B. J. J. Slagmolen, B. Smith, J. R. Smith, R. J. E. Smith, S. Somala, E. J. Son, J. A. Sonnenberg, B. Sorazu, F. Sorrentino, T. Souradeep, A. P. Spencer, A. K. Srivastava, K. Staats, A. Staley, M. Steinke, J. Steinlechner, S. Steinlechner, D. Steinmeyer, S. P. Stevenson, R. Stone, D. J. Stops, K. A. Strain, G. Stratta, S. E. Strigin, A. Strunk, R. Sturani, A. L. Stuver, T. Z. Summerscales, L. Sun, S. Sunil, J. Suresh, P. J. Sutton, B. L. Swinkels, M. J. Szczepańczyk, M. Tacca, S. C. Tait, C. Talbot, D. Talukder, D. B. Tanner, M. Tápai, A. Taracchini, J. D. Tasson, J. A. Taylor, R. Taylor, S. V. Tewari, T. Theeg, F. Thies, E. G. Thomas, M. Thomas, P. Thomas, K. A. Thorne, K. S. Thorne, E. Thrane, S. Tiwari, V. Tiwari, K. V. Tokmakov, K. Toland, M. Tonelli, Z. Tornasi, A. Torres-Forné, C. I. Torrie, D. Töyrä, F. Travasso, G. Traylor, J. Trinastic, M. C. Tringali, L. Trozzo, K. W. Tsang, M. Tse, R. Tso, L. Tsukada, D. Tsuna, D. Tuyenbayev, K. Ueno, D. Ugolini, C. S. Unnikrishnan, A. L. Urban, S. A. Usman, H. Vahlbruch, G. Vajente, G. Valdes, M. Vallisneri, N. van Bakel, M. van Beuzekom, J. F. J. van den Brand, C. Van Den Broeck, D. C. Vander-Hyde, L. van der Schaaf, J. V. van Heijningen, A. A. van Veggel, M. Vardaro, V. Varma, S. Vass, M. Vasúth, A. Vecchio, G. Vedovato, J. Veitch, P. J. Veitch, K. Venkateswara, G. Venugopalan, D. Verkindt, F. Vetrano, A. Viceré, A. D. Viets, S. Vinciguerra, D. J. Vine, J. Y. Vinet, S. Vitale, T. Vo, H. Vocca, C. Vorvick, S. P. Vyatchanin, A. R. Wade, L. E. Wade, M. Wade, R. Walet, M. Walker, L. Wallace, S. Walsh, G. Wang, H. Wang, J. Z. Wang, W. H. Wang, Y. F. Wang, R. L. Ward, J. Warner, M. Was, J. Watchi, B. Weaver, L. W. Wei, M. Weinert, A. J. Weinstein, R. Weiss, L. Wen, E. K. Wessel, P. Weßels, J. Westerweck, T. Westphal, K. Wette, J. T. Whelan, S. E. Whitcomb, B. F. Whiting, C. Whittle, D. Wilken, D. Williams, R. D. Williams, A. R. Williamson, J. L. Willis, B. Willke, M. H. Wimmer, W. Winkler, C. C. Wipf, H. Wittel, G. Woan, J. Woehler, J. Wofford, K. W. K. Wong, J. Worden, J. L. Wright, D. S. Wu, D. M. Wysocki, S. Xiao, H. Yamamoto, C. C. Yancey, L. Yang, M. J. Yap, M. Yazback, H. Yu, H. Yu, M. Yvert, A. ZadroŻny, M. Zanolin, T. Zelenova, J. P. Zendri, M. Zevin, L. Zhang, M. Zhang, T. Zhang, Y. H. Zhang, C. Zhao, M. Zhou, Z. Zhou, S. J. Zhu, X. J. Zhu, A. B. Zimmerman, M. E. Zucker, J. Zweizig, LIGO Scientific Collaboration, and Virgo Collaboration, PRL **119**, 161101 (2017), arXiv: 1710.05832.

194 A. Goldstein, P. Veres, E. Burns, M. S. Briggs, R. Hamburg, D. Kocevski, C. A. Wilson-Hodge, R. D. Preece, S. Poolakkil, O. J. Roberts, C. M. Hui, V. Connaughton, J. Racusin, A. von Kienlin, T. Dal Canton, N. Christensen, T. Littenberg, K. Siellez, L. Blackburn, J. Broida, E. Bissaldi, W. H. Cleveland, M. H. Gibby, M. M. Giles, R. M. Kippen, S. McBreen, J. McEnery, C. A. Meegan, W. S. Paciesas, and M. Stanbro, ApJL **848**, L14 (2017), arXiv: 1710.05446.

195 V. Savchenko, C. Ferrigno, E. Kuulkers, A. Bazzano, E. Bozzo, S. Brandt, J. Chenevez, T. J. L. Courvoisier, R. Diehl, A. Domingo, L. Hanlon, E. Jourdain, A. von Kienlin, P. Laurent, F. Lebrun, A. Lutovinov, A. Martin-Carrillo, S. Mereghetti, L. Natalucci, J. Rodi, J. P. Roques, R. Sunyaev, and P. Ubertini, ApJL **848**, L15 (2017), arXiv: 1710.05449.

196 I. Andreoni, K. Ackley, J. Cooke, A. Acharyya, J. R. Allison, G. E. Anderson, M. C. B. Ashley, D. Baade, M. Bailes, K. Bannister, A. Beardsley, M. S. Bessell, F. Bian, P. A. Bland, M. Boer, T. Booler, A. Brandeker, I. S. Brown, D. A. H. Buckley, S. W. Chang, D. M. Coward, S. Crawford, H. Crisp, B. Crosse, A. Cucchiara, M. Cupák, J. S. de Gois, A. Deller, H. A. R. Devillepoix, D. Dobie, E. Elmer, D. Emrich, W. Farah, T. J. Farrell, T. Franzen, B. M. Gaensler, D. K. Galloway, B. Gendre, T. Giblin, A. Goobar, J. Green, P. J. Hancock, B. A. D. Hartig, E. J. Howell, L. Horsley, A. Hotan, R. M. Howie, L. Hu, Y. Hu, C. W. James, S. Johnston, M. Johnston-Hollitt, D. L. Kaplan, M. Kasliwal, E. F. Keane, D. Kenney, A. Klotz, R. Lau, R. Laugier, E. Lenc, X. Li, E. Liang, C. Lidman, L. C. Luvaul, C. Lynch, B. Ma, D. Macpherson, J. Mao, D. E. McClelland, C. McCully, A. Möller, M. F. Morales, D. Morris, T. Murphy, K. Noysena, C. A. Onken, N. B. Orange, S. Osłowski, D. Pallot, J. Paxman, S. B. Potter, T. Pritchard, W. Raja, R. Ridden-Harper, E. Romero-Colmenero, E. M. Sadler, E. K. Sansom, R. A. Scalzo, B. P. Schmidt, S. M. Scott, N. Seghouani, Z. Shang, R. M. Shannon, L. Shao, M. M. Shara, R. Sharp, M. Sokolowski, J. Sollerman, J. Staff, K. Steele, T. Sun, N. B. Suntzeff, C. Tao, S. Tingay, M. C. Towner, P. Thierry, C. Trott, B. E. Tucker, P. Väisänen, V. V. Krishnan, M. Walker, L. Wang, X. Wang, R. Wayth, M. Whiting, A. Williams, T. Williams, C. Wolf, C. Wu, X. Wu, J. Yang, X. Yuan, H. Zhang, J. Zhou, and H. Zovaro, PASA **34**, e069 (2017), arXiv: 1710.05846.

197 I. Arcavi, C. McCully, G. Hosseinzadeh, D. A. Howell, S. Vasylyev, D. Poznanski, M. Zaltzman, D. Maoz, L. Singer, S. Valenti, D. Kasen, J. Barnes, T. Piran, and W.-f. Fong, ApJL **848**, L33 (2017), arXiv: 1710.05842.

198 R. Chornock, E. Berger, D. Kasen, P. S. Cowperthwaite, M. Nicholl, V. A. Villar, K. D. Alexander, P. K. Blanchard, T. Eftekhari, W. Fong, R. Margutti, P. K. G. Williams, J. Annis, D. Brout, D. A. Brown, H. Y. Chen, M. R. Drout, B. Farr, R. J. Foley, J. A. Frieman, C. L. Fryer, K. Herner, D. E. Holz, R. Kessler, T. Matheson, B. D. Metzger, E. Quataert, A. Rest, M. Sako, D. M. Scolnic, N. Smith, and M. Soares-Santos, ApJL **848**, L19 (2017), arXiv: 1710.05454.

199 D. A. Coulter, R. J. Foley, C. D. Kilpatrick, M. R. Drout, A. L. Piro, B. J. Shappee, M. R. Siebert, J. D. Simon, N. Ulloa, D. Kasen, B. F. Madore, A. Murguia-Berthier, Y. C. Pan, J. X. Prochaska, E. Ramirez-Ruiz, A. Rest, and C. Rojas-Bravo, Science **358**, 1556 (2017), arXiv: 1710.05452.

200 P. S. Cowperthwaite, E. Berger, V. A. Villar, B. D. Metzger, M. Nicholl, R. Chornock, P. K. Blanchard, W. Fong, R. Margutti, M. Soares-Santos, K. D. Alexander, S. Allam, J. Annis, D. Brout, D. A. Brown, R. E. Butler, H. Y. Chen, H. T. Diehl, Z. Doctor, M. R. Drout, T. Eftekhari, B. Farr, D. A. Finley, R. J. Foley, J. A. Frieman, C. L. Fryer, J. García-Bellido, M. S. S. Gill, J. Guillochon, K. Herner, D. E. Holz, D. Kasen, R. Kessler, J. Marriner, T. Matheson, J. Neilsen, E. H., E. Quataert, A. Palmese, A. Rest, M. Sako, D. M. Scolnic, N. Smith, D. L. Tucker, P. K. G. Williams, E. Balbinot, J. L. Carlin, E. R. Cook, F. Durret, T. S. Li, P. A. A. Lopes, A. C. C. Lourenço, J. L. Marshall, G. E. Medina, J. Muir, R. R. Muñoz, M. Sauseda, D. J. Schlegel, L. F. Secco, A. K. Vivas, W. Wester, A. Zenteno, Y. Zhang, T. M. C. Abbott, M. Banerji, K. Bechtol, A. Benoit-Lévy, E. Bertin, E. Buckley-Geer, D. L. Burke, D. Capozzi, A. Carnero Rosell, M. Carrasco Kind, F. J. Castander, M. Crocce, C. E. Cunha, C. B. D'Andrea, L. N. da Costa, C. Davis, D. L. DePoy, S. Desai, J. P. Dietrich, A. Drlica-Wagner, T. F. Eifler, A. E. Evrard, E. Fernandez, B. Flaugher, P. Fosalba, E. Gaztanaga, D. W. Gerdes, T. Giannantonio, D. A. Goldstein, D. Gruen, R. A. Gruendl, G. Gutierrez, K. Honscheid, B. Jain, D. J. James, T. Jeltema, M. W. G. Johnson, M. D. Johnson, S. Kent, E. Krause, R. Kron, K. Kuehn, N. Nuropatkin,

O. Lahav, M. Lima, H. Lin, M. A. G. Maia, M. March, P. Martini, R. G. McMahon, F. Menanteau, C. J. Miller, R. Miquel, J. J. Mohr, E. Neilsen, R. C. Nichol, R. L. C. Ogando, A. A. Plazas, N. Roe, A. K. Romer, A. Roodman, E. S. Rykoff, E. Sanchez, V. Scarpine, R. Schindler, M. Schubnell, I. Sevilla-Noarbe, M. Smith, R. C. Smith, F. Sobreira, E. Suchyta, M. E. C. Swanson, G. Tarle, D. Thomas, R. C. Thomas, M. A. Troxel, V. Vikram, A. R. Walker, R. H. Wechsler, J. Weller, B. Yanny, and J. Zuntz, ApJL **848**, L17 (2017), arXiv: 1710.05840.

201 M. C. Díaz, L. M. Macri, D. Garcia Lambas, C. Mendes de Oliveira, J. L. Nilo Castellón, T. Ribeiro, B. Sánchez, W. Schoenell, L. R. Abramo, S. Akras, J. S. Alcaniz, R. Artola, M. Beroiz, S. Bonoli, J. Cabral, R. Camuccio, M. Castillo, V. Chavushyan, P. Coelho, C. Colazo, M. V. Costa-Duarte, H. Cuevas Larenas, D. L. DePoy, M. Domínguez Romero, D. Dultzin, D. Fernández, J. García, C. Girardini, D. R. Gonçalves, T. S. Gonçalves, S. Gurovich, Y. Jiménez-Teja, A. Kanaan, M. Lares, R. Lopes de Oliveira, O. López-Cruz, J. L. Marshall, R. Melia, A. Molino, N. Padilla, T. Peñuela, V. M. Placco, C. Quiñones, A. Ramírez Rivera, V. Renzi, L. Riguccini, E. Ríos-López, H. Rodriguez, L. Sampedro, M. Schneiter, L. Sodré, M. Starck, S. Torres-Flores, M. Tornatore, and A. Zadrożny, ApJL **848**, L29 (2017), arXiv: 1710.05844.

202 M. R. Drout, A. L. Piro, B. J. Shappee, C. D. Kilpatrick, J. D. Simon, C. Contreras, D. A. Coulter, R. J. Foley, M. R. Siebert, N. Morrell, K. Boutsia, F. Di Mille, T. W. S. Holoien, D. Kasen, J. A. Kollmeier, B. F. Madore, A. J. Monson, A. Murguia-Berthier, Y. C. Pan, J. X. Prochaska, E. Ramirez-Ruiz, A. Rest, C. Adams, K. Alatalo, E. Bañados, J. Baughman, T. C. Beers, R. A. Bernstein, T. Bitsakis, A. Campillay, T. T. Hansen, C. R. Higgs, A. P. Ji, G. Maravelias, J. L. Marshall, C. Moni Bidin, J. L. Prieto, K. C. Rasmussen, C. Rojas-Bravo, A. L. Strom, N. Ulloa, J. Vargas-González, Z. Wan, and D. D. Whitten, Science **358**, 1570 (2017), arXiv: 1710.05443.

203 P. A. Evans, S. B. Cenko, J. A. Kennea, S. W. K. Emery, N. P. M. Kuin, O. Korobkin, R. T. Wollaeger, C. L. Fryer, K. K. Madsen, F. A. Harrison, Y. Xu, E. Nakar, K. Hotokezaka, A. Lien, S. Campana, S. R. Oates, E. Troja, A. A. Breeveld, F. E. Marshall, S. D. Barthelmy, A. P. Beardmore, D. N. Burrows, G. Cusumano, A. D'Aì, P. D'Avanzo, V. D'Elia, M. de Pasquale, W. P. Even, C. J. Fontes, K. Forster, J. Garcia, P. Giommi, B. Grefenstette, C. Gronwall, D. H. Hartmann, M. Heida, A. L. Hungerford, M. M. Kasliwal, H. A. Krimm, A. J. Levan, D. Malesani, A. Melandri, H. Miyasaka, J. A. Nousek, P. T. O'Brien, J. P. Osborne, C. Pagani, K. L. Page, D. M. Palmer, M. Perri, S. Pike, J. L. Racusin, S. Rosswog, M. H. Siegel, T. Sakamoto, B. Sbarufatti, G. Tagliaferri, N. R. Tanvir, and A. Tohuvavohu, Science **358**, 1565 (2017), arXiv: 1710.05437.

204 L. Hu, X. Wu, I. Andreoni, M. C. B. Ashley, J. Cooke, X. Cui, F. Du, Z. Dai, B. Gu, Y. Hu, H. Lu, X. Li, Z. Li, E. Liang, L. Liu, B. Ma, Z. Shang, T. Sun, N. B. Suntzeff, C. Tao, S. A. Udden, L. Wang, X. Wang, H. Wen, D. Xiao, J. Su, J. Yang, S. Yang, X. Yuan, H. Zhou, H. Zhang, J. Zhou, and Z. Zhu, Science Bulletin **62**, 1433 (2017), arXiv: 1710.05462.

205 M. M. Kasliwal, E. Nakar, L. P. Singer, D. L. Kaplan, D. O. Cook, A. Van Sistine, R. M. Lau, C. Fremling, O. Gottlieb, J. E. Jencson, S. M. Adams, U. Feindt, K. Hotokezaka, S. Ghosh, D. A. Perley, P. C. Yu, T. Piran, J. R. Allison, G. C. Anupama, A. Balasubramanian, K. W. Bannister, J. Bally, J. Barnes, S. Barway, E. Bellm, V. Bhalerao, D. Bhattacharya, N. Blagorodnova, J. S. Bloom, P. R. Brady, C. Cannella, D. Chatterjee, S. B. Cenko, B. E. Cobb, C. Copperwheat, A. Corsi, K. De, D. Dobie, S. W. K. Emery, P. A. Evans, O. D. Fox, D. A. Frail, C. Frohmaier, A. Goobar, G. Hallinan, F. Harrison, G. Helou, T. Hinderer, A. Y. Q. Ho, A. Horesh, W. H. Ip, R. Itoh, D. Kasen, H. Kim, N. P. M. Kuin, T. Kupfer, C. Lynch, K. Madsen, P. A. Mazzali, A. A. Miller, K. Mooley, T. Murphy, C. C. Ngeow, D. Nichols, S. Nissanke, P. Nugent, E. O. Ofek, H. Qi, R. M. Quimby, S. Rosswog, F. Rusu, E. M. Sadler, P. Schmidt, J. Sollerman, I. Steele, A. R. Williamson, Y. Xu, L. Yan, Y. Yatsu, C. Zhang, and W. Zhao, Science **358**, 1559 (2017), arXiv: 1710.05436.

206 V. M. Lipunov, E. Gorbovskoy, V. G. Kornilov, N. . Tyurina, P. Balanutsa, A. Kuznetsov, D. Vlasenko, D. Kuvshinov, I. Gorbunov, D. A. H. Buckley, A. V. Krylov, R. Podesta, C. Lopez, F. Podesta, H. Levato, C. Saffe, C. Mallamachi, S. Potter, N. M. Budnev, O. Gress, Y. Ishmuhametova, V. Vladimirov, D. Zimnukhov, V. Yurkov, Y. Sergienko, A. Gabovich, R. Rebolo, M. Serra-Ricart, G. Israelyan, V. Chazov, X. Wang, A. Tlatov, and M. I. Panchenko, ApJL **850**, L1 (2017), arXiv: 1710.05461.

207 C. McCully, D. Hiramatsu, D. A. Howell, G. Hosseinzadeh, I. Arcavi, D. Kasen, J. Barnes, M. M. Shara, T. B. Williams, P. Väisänen, S. B. Potter, E. Romero-Colmenero, S. M. Crawford, D. A. H. Buckley, J. Cooke, I. Andreoni, T. A. Pritchard, J. Mao, M. Gromadzki, and J. Burke, ApJL **848**, L32 (2017), arXiv: 1710.05853.

208 M. Nicholl, E. Berger, D. Kasen, B. D. Metzger, J. Elias, C. Briceño, K. D. Alexander, P. K. Blanchard, R. Chornock, P. S. Cowperthwaite, T. Eftekhari, W. Fong, R. Margutti, V. A. Villar, P. K. G. Williams, W. Brown, J. Annis, A. Bahramian, D. Brout, D. A. Brown, H. Y. Chen, J. C. Clemens, E. Dennihy, B. Dunlap, D. E. Holz, E. Marchesini, F. Massaro, N. Moskowitz, I. Pelisoli, A. Rest, F. Ricci, M. Sako, M. Soares-Santos, and J. Strader, ApJL **848**, L18 (2017), arXiv: 1710.05456.

209 E. Pian, P. D'Avanzo, S. Benetti, M. Branchesi, E. Brocato, S. Campana, E. Cappellaro, S. Covino, V. D'Elia, J. P. U. Fynbo, F. Getman, G. Ghirlanda, G. Ghisellini, A. Grado, G. Greco, J. Hjorth, C. Kouveliotou, A. Levan, L. Limatola, D. Malesani, P. A. Mazzali, A. Melandri, P. Møller, L. Nicastro, E. Palazzi, S. Piranomonte, A. Rossi, O. S. Salafia, J. Selsing, G. Stratta, M. Tanaka, N. R. Tanvir, L. Tomasella, D. Watson, S. Yang, L. Amati, L. A. Antonelli, S. Ascenzi, M. G. Bernardini, M. Boër, F. Bufano, A. Bulgarelli, M. Capaccioli, P. Casella, A. J. Castro-Tirado, E. Chassande-Mottin, R. Ciolfi, C. M. Copperwheat, M. Dadina, G. De Cesare, A. di Paola, Y. Z. Fan, B. Gendre, G. Giuffrida, A. Giunta, L. K. Hunt, G. L. Israel, Z. P. Jin, M. M. Kasliwal, S. Klose, M. Lisi, F. Longo, E. Maiorano, M. Mapelli, N. Masetti, L. Nava, B. Patricelli, D. Perley, A. Pescalli, T. Piran, A. Possenti, L. Pulone, M. Razzano, R. Salvaterra, P. Schipani, M. Spera, A. Stamerra, L. Stella, G. Tagliaferri, V. Testa, E. Troja, M. Turatto, S. D. Vergani, and D. Vergani, Nature **551**, 67 (2017), arXiv: 1710.05858.

210 B. J. Shappee, J. D. Simon, M. R. Drout, A. L. Piro, N. Morrell, J. L. Prieto, D. Kasen, T. W. S. Holoien, J. A. Kollmeier, D. D. Kelson, D. A. Coulter, R. J. Foley, C. D. Kilpatrick, M. R. Siebert, B. F. Madore, A. Murguia-Berthier, Y. C. Pan, J. X. Prochaska, E. Ramirez-Ruiz, A. Rest, C. Adams, K. Alatalo, E. Bañados, J. Baughman, R. A. Bernstein, T. Bitsakis, K. Boutsia, J. R. Bravo, F. Di Mille, C. R. Higgs, A. P. Ji, G. Maravelias, J. L. Marshall, V. M. Placco, G. Prieto, and Z. Wan, Science **358**, 1574 (2017), arXiv: 1710.05432.

211 S. J. Smartt, T. W. Chen, A. Jerkstrand, M. Coughlin, E. Kankare, S. A. Sim, M. Fraser, C. Inserra, K. Maguire, K. C. Chambers, M. E. Huber, T. Krühler, G. Leloudas, M. Magee, L. J. Shingles, K. W. Smith, D. R. Young, J. Tonry, R. Kotak, A. Gal-Yam, J. D. Lyman, D. S. Homan, C. Agliozzo, J. P. Anderson, C. R. Angus, C. Ashall, C. Barbarino, F. E. Bauer, M. Berton, M. T. Botticella, M. Bulla, J. Bulger, G. Cannizzaro, Z. Cano, R. Cartier, A. Cikota, P. Clark, A. De Cia, M. Della Valle, L. Denneau, M. Dennefeld, L. Dessart, G. Dimitriadis, N. Elias-Rosa, R. E. Firth, H. Flewelling, A. Flörs, A. Franckowiak, C. Frohmaier, L. Galbany, S. González-Gaitán, J. Greiner, M. Gromadzki, A. N. Guelbenzu, C. P. Gutiérrez, A. Hamanowicz, L. Hanlon, J. Harmanen, K. E. Heintz, A. Heinze, M. S. Hernandez, S. T. Hodgkin, I. M. Hook, L. Izzo, P. A. James, P. G. Jonker, W. E. Kerzendorf, S. Klose, Z. Kostrzewa-Rutkowska, M. Kowalski, M. Kromer, H. Kuncarayakti, A. Lawrence, T. B. Lowe, E. A. Magnier, I. Manulis, A. Martin-Carrillo, S. Mattila,

O. McBrien, A. Müller, J. Nordin, D. O'Neill, F. Onori, J. T. Palmerio, A. Pastorello, F. Patat, G. Pignata, P. Podsiadlowski, M. L. Pumo, S. J. Prentice, A. Rau, A. Razza, A. Rest, T. Reynolds, R. Roy, A. J. Ruiter, K. A. Rybicki, L. Salmon, P. Schady, A. S. B. Schultz, T. Schweyer, I. R. Seitenzahl, M. Smith, J. Sollerman, B. Stalder, C. W. Stubbs, M. Sullivan, H. Szegedi, F. Taddia, S. Taubenberger, G. Terreran, B. van Soelen, J. Vos, R. J. Wainscoat, N. A. Walton, C. Waters, H. Weiland, M. Willman, P. Wiseman, D. E. Wright, Ł. Wyrzykowski, and O. Yaron, Nature **551**, 75 (2017), arXiv: 1710.05841.

212 M. Soares-Santos, D. E. Holz, J. Annis, R. Chornock, K. Herner, E. Berger, D. Brout, H. Y. Chen, R. Kessler, M. Sako, S. Allam, D. L. Tucker, R. E. Butler, A. Palmese, Z. Doctor, H. T. Diehl, J. Frieman, B. Yanny, H. Lin, D. Scolnic, P. Cowperthwaite, E. Neilsen, J. Marriner, N. Kuropatkin, W. G. Hartley, F. Paz-Chinchón, K. D. Alexander, E. Balbinot, P. Blanchard, D. A. Brown, J. L. Carlin, C. Conselice, E. R. Cook, A. Drlica-Wagner, M. R. Drout, F. Durret, T. Eftekhari, B. Farr, D. A. Finley, R. J. Foley, W. Fong, C. L. Fryer, J. García-Bellido, M. S. S. Gill, R. A. Gruendl, C. Hanna, D. Kasen, T. S. Li, P. A. A. Lopes, A. C. C. Lourenço, R. Margutti, J. L. Marshall, T. Matheson, G. E. Medina, B. D. Metzger, R. R. Muñoz, J. Muir, M. Nicholl, E. Quataert, A. Rest, M. Sauseda, D. J. Schlegel, L. F. Secco, F. Sobreira, A. Stebbins, V. A. Villar, K. Vivas, A. R. Walker, W. Wester, P. K. G. Williams, A. Zenteno, Y. Zhang, T. M. C. Abbott, F. B. Abdalla, M. Banerji, K. Bechtol, A. Benoit-Lévy, E. Bertin, D. Brooks, E. Buckley-Geer, D. L. Burke, A. Carnero Rosell, M. Carrasco Kind, J. Carretero, F. J. Castander, M. Crocce, C. E. Cunha, C. B. D'Andrea, L. N. da Costa, C. Davis, S. Desai, J. P. Dietrich, P. Doel, T. F. Eifler, E. Fernandez, B. Flaugher, P. Fosalba, E. Gaztanaga, D. W. Gerdes, T. Giannantonio, D. A. Goldstein, D. Gruen, J. Gschwend, G. Gutierrez, K. Honscheid, B. Jain, D. J. James, T. Jeltema, M. W. G. Johnson, M. D. Johnson, S. Kent, E. Krause, R. Kron, K. Kuehn, S. Kuhlmann, O. Lahav, M. Lima, M. A. G. Maia, M. March, R. G. McMahon, F. Menanteau, R. Miquel, J. J. Mohr, R. C. Nichol, B. Nord, R. L. C. Ogando, D. Petravick, A. A. Plazas, A. K. Romer, A. Roodman, E. S. Rykoff, E. Sanchez, V. Scarpine, M. Schubnell, I. Sevilla-Noarbe, M. Smith, R. C. Smith, E. Suchyta, M. E. C. Swanson, G. Tarle, D. Thomas, R. C. Thomas, M. A. Troxel, V. Vikram, R. H. Wechsler, J. Weller, Dark Energy Survey, and Dark Energy Camera GW-EM Collaboration, ApJL **848**, L16 (2017), arXiv: 1710.05459.

213 Y. Utsumi, M. Tanaka, N. Tominaga, M. Yoshida, S. Barway, T. Nagayama, T. Zenko, K. Aoki, T. Fujiyoshi, H. Furusawa, K. S. Kawabata, S. Koshida, C.-H. Lee, T. Morokuma, K. Motohara, F. Nakata, R. Ohsawa, K. Ohta, H. Okita, A. Tajitsu, I. Tanaka, T. Terai, N. Yasuda, F. Abe, Y. Asakura, I. A. Bond, S. Miyazaki, T. Sumi, P. J. Tristram, S. Honda, R. Itoh, Y. Itoh, M. Kawabata, K. Morihana, H. Nagashima, T. Nakaoka, T. Ohshima, J. Takahashi, M. Takayama, W. Aoki, S. Baar, M. Doi, F. Finet, N. Kanda, N. Kawai, J. H. Kim, D. Kuroda, W. Liu, K. Matsubayashi, K. L. Murata, H. Nagai, T. Saito, Y. Saito, S. Sako, Y. Sekiguchi, Y. Tamura, M. Tanaka, M. Uemura, and M. S. Yamaguchi, PASJ **69**, 101 (2017), arXiv: 1710.05848.

214 S. Valenti, D. J. Sand, S. Yang, E. Cappellaro, L. Tartaglia, A. Corsi, S. W. Jha, D. E. Reichart, J. Haislip, and V. Kouprianov, ApJL **848**, L24 (2017), arXiv: 1710.05854.

215 N. R. Tanvir, A. J. Levan, C. González-Fernández, O. Korobkin, I. Mandel, S. Rosswog, J. Hjorth, P. D'Avanzo, A. S. Fruchter, C. L. Fryer, T. Kangas, B. Milvang-Jensen, S. Rosetti, D. Steeghs, R. T. Wollaeger, Z. Cano, C. M. Copperwheat, S. Covino, V. D'Elia, A. de Ugarte Postigo, P. A. Evans, W. P. Even, S. Fairhurst, R. Figuera Jaimes, C. J. Fontes, Y. I. Fujii, J. P. U. Fynbo, B. P. Gompertz, J. Greiner, G. Hodosan, M. J. Irwin, P. Jakobsson, U. G. Jørgensen, D. A. Kann, J. D. Lyman, D. Malesani, R. G. McMahon, A. Melandri, P. T. O'Brien, J. P. Osborne, E. Palazzi, D. A. Perley, E. Pian, S. Piranomonte, M. Rabus, E. Rol, A. Rowlinson, S. Schulze, P. Sutton, C. C. Thöne, K. Ulaczyk, D. Watson, K. Wiersema, and R. A. M. J. Wijers, ApJL **848**, L27 (2017), arXiv: 1710.05455.

216 R. Oechslin, H. T. Janka, and A. Marek, A&A **467**, 395 (2007), arXiv: astro-ph/0611047.

217 A. Bauswein, S. Goriely, and H. T. Janka, ApJ **773**, 78 (2013), arXiv: 1302.6530.

218 K. Hotokezaka, K. Kiuchi, K. Kyutoku, H. Okawa, Y.-i. Sekiguchi, M. Shibata, and K. Taniguchi, PRD **87**, 024001 (2013), arXiv: 1212.0905.

219 S. Rosswog, M. Liebendörfer, F. K. Thielemann, M. B. Davies, W. Benz, and T. Piran, A&A **341**, 499 (1999), arXiv: astro-ph/9811367.

220 Y. Sekiguchi, K. Kiuchi, K. Kyutoku, and M. Shibata, PRD **91**, 064059 (2015), arXiv: 1502.06660.

221 R. Surman, G. C. McLaughlin, M. Ruffert, H. T. Janka, and W. R. Hix, ApJL **679**, L117 (2008), arXiv: 0803.1785.

222 B. D. Metzger, T. A. Thompson, and E. Quataert, ApJ **676**, 1130 (2008), arXiv: 0708.3395.

223 V. Nedora, S. Bernuzzi, D. Radice, A. Perego, A. Endrizzi, and N. Ortiz, ApJL **886**, L30 (2019), arXiv: 1907.04872.

224 E. Symbalisty and D. N. Schramm, ApL **22**, 143 (1982).

225 B. D. Metzger, G. Martínez-Pinedo, S. Darbha, E. Quataert, A. Arcones, D. Kasen, R. Thomas, P. Nugent, I. V. Panov, and N. T. Zinner, MNRAS **406**, 2650 (2010), arXiv: 1001.5029.

226 N. R. Tanvir, A. J. Levan, A. S. Fruchter, J. Hjorth, R. A. Hounsell, K. Wiersema, and R. L. Tunnicliffe, Nature **500**, 547 (2013), arXiv: 1306.4971.

227 E. Berger, W. Fong, and R. Chornock, ApJL **774**, L23 (2013), arXiv: 1306.3960.

228 Z.-P. Jin, K. Hotokezaka, X. Li, M. Tanaka, P. D'Avanzo, Y.-Z. Fan, S. Covino, D.-M. Wei, and T. Piran, Nature Communications **7**, 12898 (2016), arXiv: 1603.07869.

229 E. Troja, G. Ryan, L. Piro, H. van Eerten, S. B. Cenko, Y. Yoon, S. K. Lee, M. Im, T. Sakamoto, P. Gatkine, A. Kutyrev, and S. Veilleux, Nature Communications **9**, 4089 (2018), arXiv: 1806.10624.

230 Z.-P. Jin, S. Covino, N.-H. Liao, X. Li, P. D'Avanzo, Y.-Z. Fan, and D.-M. Wei, Nature Astronomy **4**, 77 (2020), arXiv: 1901.06269.

231 Z.-P. Jin, H. Zhou, S. Covino, N.-H. Liao, X. Li, L. Lei, P. D'Avanzo, Y.-Z. Fan, and D.-M. Wei, arXiv e-prints arXiv:2109.07694 (2021), arXiv: 2109.07694.

232 Y.-W. Yu, L.-D. Liu, and Z.-G. Dai, ApJ **861**, 114 (2018), arXiv: 1711.01898.

233 J.-J. Geng, Z.-G. Dai, Y.-F. Huang, X.-F. Wu, L.-B. Li, B. Li, and Y.-Z. Meng, ApJL **856**, L33 (2018), arXiv: 1803.07219.

234 L. Li and Z.-G. Dai, ApJ **918**, 52 (2021), arXiv: 2106.04788.

235 T. Dietrich, M. W. Coughlin, P. T. H. Pang, M. Bulla, J. Heinzel, L. Issa, I. Tews, and S. Antier, Science **370**, 1450 (2020), arXiv: 2002.11355.

236 S. Goriely, A. Bauswein, and H.-T. Janka, ApJL **738**, L32 (2011), arXiv: 1107.0899.

237 O. Korobkin, S. Rosswog, A. Arcones, and C. Winteler, MNRAS **426**, 1940 (2012), arXiv: 1206.2379.

238 J. d. J. Mendoza-Temis, M.-R. Wu, K. Langanke, G. Martínez-Pinedo, A. Bauswein, and H.-T. Janka, PRC **92**, 055805 (2015), arXiv: 1409.6135.

239 J. Barnes and D. Kasen, ApJ **775**, 18 (2013), arXiv: 1303.5787.

240 D. Radice, F. Galeazzi, J. Lippuner, L. F. Roberts, C. D. Ott, and L. Rezzolla, MNRAS **460**, 3255 (2016), arXiv: 1601.02426.

241 B. D. Metzger, Living Reviews in Relativity **23**, 1 (2019), arXiv: 1910.01617.

242 B. D. Metzger and R. Fernández, MNRAS **441**, 3444 (2014), arXiv: 1402.4803.

243 C. Barbieri, O. S. Salafia, M. Colpi, G. Ghirlanda, A. Perego, and A. Colombo, ApJL **887**, L35 (2019), arXiv: 1912.03894.

244 B. Margalit and B. D. Metzger, ApJL **850**, L19 (2017), arXiv: 1710.05938.
245 N. Farrow, X.-J. Zhu, and E. Thrane, ApJ **876**, 18 (2019), arXiv: 1902.03300.
246 M. Nicholl, B. Margalit, P. Schmidt, G. P. Smith, E. J. Ridley, and J. Nuttall, MNRAS **505**, 3016 (2021), arXiv: 2102.02229.
247 T. Dietrich and M. Ujevic, Classical and Quantum Gravity **34**, 105014 (2017), arXiv: 1612.03665.
248 D. Radice, A. Perego, K. Hotokezaka, S. A. Fromm, S. Bernuzzi, and L. F. Roberts, ApJ **869**, 130 (2018), arXiv: 1809.11161.
249 V. A. Villar, J. Guillochon, E. Berger, B. D. Metzger, P. S. Cowperthwaite, M. Nicholl, K. D. Alexander, P. K. Blanchard, R. Chornock, T. Eftekhari, W. Fong, R. Margutti, and P. K. G. Williams, ApJL **851**, L21 (2017), arXiv: 1710.11576.
250 Ž. Ivezić, S. M. Kahn, J. A. Tyson, B. Abel, E. Acosta, R. Allsman, D. Alonso, Y. AlSayyad, S. F. Anderson, J. Andrew, J. R. P. Angel, G. Z. Angeli, R. Ansari, P. Antilogus, C. Araujo, R. Armstrong, K. T. Arndt, P. Astier, É. Aubourg, N. Auza, T. S. Axelrod, D. J. Bard, J. D. Barr, A. Barrau, J. G. Bartlett, A. E. Bauer, B. J. Bauman, S. Baumont, E. Bechtol, K. Bechtol, A. C. Becker, J. Becla, C. Beldica, S. Bellavia, F. B. Bianco, R. Biswas, G. Blanc, J. Blazek, R. D. Blandford, J. S. Bloom, J. Bogart, T. W. Bond, M. T. Booth, A. W. Borgland, K. Borne, J. F. Bosch, D. Boutigny, C. A. Brackett, A. Bradshaw, W. N. Brandt, M. E. Brown, J. S. Bullock, P. Burchat, D. L. Burke, G. Cagnoli, D. Calabrese, S. Callahan, A. L. Callen, J. L. Carlin, E. L. Carlson, S. Chandrasekharan, G. Charles-Emerson, S. Chesley, E. C. Cheu, H.-F. Chiang, J. Chiang, C. Chirino, D. Chow, D. R. Ciardi, C. F. Claver, J. Cohen-Tanugi, J. J. Cockrum, R. Coles, A. J. Connolly, K. H. Cook, A. Cooray, K. R. Covey, C. Cribbs, W. Cui, R. Cutri, P. N. Daly, S. F. Daniel, F. Daruich, G. Daubard, G. Daues, W. Dawson, F. Delgado, A. Dellapenna, R. de Peyster, M. de Val-Borro, S. W. Digel, P. Doherty, R. Dubois, G. P. Dubois-Felsmann, J. Durech, F. Economou, T. Eifler, M. Eracleous, B. L. Emmons, A. Fausti Neto, H. Ferguson, E. Figueroa, M. Fisher-Levine, W. Focke, M. D. Foss, J. Frank, M. D. Freemon, E. Gangler, E. Gawiser, J. C. Geary, P. Gee, M. Geha, C. J. B. Gessner, R. R. Gibson, D. K. Gilmore, T. Glanzman, W. Glick, T. Goldina, D. A. Goldstein, I. Goodenow, M. L. Graham, W. J. Gressler, P. Gris, L. P. Guy, A. Guyonnet, G. Haller, R. Harris, P. A. Hascall, J. Haupt, F. Hernandez, S. Herrmann, E. Hileman, J. Hoblitt, J. A. Hodgson, C. Hogan, J. D. Howard, D. Huang, M. E. Huffer, P. Ingraham, W. R. Innes, S. H. Jacoby, B. Jain, F. Jammes, M. J. Jee, T. Jenness, G. Jernigan, D. Jevremović, K. Johns, A. S. Johnson, M. W. G. Johnson, R. L. Jones, C. Juramy-Gilles, M. Jurić, J. S. Kalirai, N. J. Kallivayalil, B. Kalmbach, J. P. Kantor, P. Karst, M. M. Kasliwal, H. Kelly, R. Kessler, V. Kinnison, D. Kirkby, L. Knox, I. V. Kotov, V. L. Krabbendam, K. S. Krughoff, P. Kubánek, J. Kuczewski, S. Kulkarni, J. Ku, N. R. Kurita, C. S. Lage, R. Lambert, T. Lange, J. B. Langton, L. Le Guillou, D. Levine, M. Liang, K.-T. Lim, C. J. Lintott, K. E. Long, M. Lopez, P. J. Lotz, R. H. Lupton, N. B. Lust, L. A. MacArthur, A. Mahabal, R. Mandelbaum, T. W. Markiewicz, D. S. Marsh, P. J. Marshall, S. Marshall, M. May, R. McKercher, M. McQueen, J. Meyers, M. Migliore, M. Miller, D. J. Mills, C. Miraval, J. Moeyens, F. E. Moolekamp, D. G. Monet, M. Moniez, S. Monkewitz, C. Montgomery, C. B. Morrison, F. Mueller, G. P. Muller, F. Muñoz Arancibia, D. R. Neill, S. P. Newbry, J.-Y. Nief, A. Nomerotski, M. Nordby, P. O'Connor, J. Oliver, S. S. Olivier, K. Olsen, W. O'Mullane, S. Ortiz, S. Osier, R. E. Owen, R. Pain, P. E. Palecek, J. K. Parejko, J. B. Parsons, N. M. Pease, J. M. Peterson, J. R. Peterson, D. L. Petravick, M. E. Libby Petrick, C. E. Petry, F. Pierfederici, S. Pietrowicz, R. Pike, P. A. Pinto, R. Plante, S. Plate, J. P. Plutchak, P. A. Price, M. Prouza, V. Radeka, J. Rajagopal, A. P. Rasmussen, N. Regnault, K. A. Reil, D. J. Reiss, M. A. Reuter, S. T. Ridgway, V. J. Riot, S. Ritz, S. Robinson, W. Roby, A. Roodman, W. Rosing, C. Roucelle, M. R. Rumore, S. Russo, A. Saha, B. Sassolas, T. L. Schalk, P. Schellart, R. H. Schindler, S. Schmidt, D. P. Schneider, M. D. Schneider, W. Schoening, G. Schumacher, M. E. Schwamb, J. Sebag, B. Selvy, G. H. Sembroski, L. G. Seppala, A. Serio, E. Serrano, R. A. Shaw, I. Shipsey, J. Sick, N. Silvestri, C. T. Slater, J. A. Smith, R. C. Smith, S. Sobhani, C. Soldahl, L. Storrie-Lombardi, E. Stover, M. A. Strauss, R. A. Street, C. W. Stubbs, I. S. Sullivan, D. Sweeney, J. D. Swinbank, A. Szalay, P. Takacs, S. A. Tether, J. J. Thaler, J. G. Thayer, S. Thomas, A. J. Thornton, V. Thukral, J. Tice, D. E. Trilling, M. Turri, R. Van Berg, D. Vanden Berk, K. Vetter, F. Virieux, T. Vucina, W. Wahl, L. Walkowicz, B. Walsh, C. W. Walter, D. L. Wang, S.-Y. Wang, M. Warner, O. Wiecha, B. Willman, S. E. Winters, D. Wittman, S. C. Wolff, W. M. Wood-Vasey, X. Wu, B. Xin, P. Yoachim, and H. Zhan, ApJ **873**, 111 (2019), arXiv: 0805.2366.
251 R. Abbott, T. D. Abbott, S. Abraham, F. Acernese, K. Ackley, A. Adams, C. Adams, R. X. Adhikari, V. B. Adya, C. Affeldt, M. Agathos, K. Agatsuma, N. Aggarwal, O. D. Aguiar, L. Aiello, A. Ain, P. Ajith, G. Allen, A. Allocca, P. A. Altin, A. Amato, S. Anand, A. Ananyeva, S. B. Anderson, W. G. Anderson, S. V. Angelova, S. Ansoldi, J. M. Antelis, S. Antier, S. Appert, K. Arai, M. C. Araya, J. S. Areeda, M. Arène, N. Arnaud, S. M. Aronson, K. G. Arun, Y. Asali, S. Ascenzi, G. Ashton, S. M. Aston, P. Astone, F. Aubin, P. Aufmuth, K. AultONeal, C. Austin, V. Avendano, S. Babak, F. Badaracco, M. K. M. Bader, S. Bae, A. M. Baer, S. Bagnasco, J. Baird, M. Ball, G. Ballardin, S. W. Ballmer, A. Bals, A. Balsamo, G. Baltus, S. Banagiri, D. Bankar, R. S. Bankar, J. C. Barayoga, C. Barbieri, B. C. Barish, D. Barker, P. Barneo, S. Barnum, F. Barone, B. Barr, L. Barsotti, M. Barsuglia, D. Barta, J. Bartlett, I. Bartos, R. Bassiri, A. Basti, M. Bawaj, J. C. Bayley, M. Bazzan, B. R. Becher, B. Bécsy, V. M. Bedakihale, M. Bejger, I. Belahcene, D. Beniwal, M. G. Benjamin, T. F. Bennett, J. D. Bentley, F. Bergamin, B. K. Berger, G. Bergmann, S. Bernuzzi, C. P. L. Berry, D. Bersanetti, A. Bertolini, J. Betzwieser, R. Bhandare, A. V. Bhandari, D. Bhattacharjee, J. Bidler, I. A. Bilenko, G. Billingsley, R. Birney, O. Birnholtz, S. Biscans, M. Bischi, S. Biscoveanu, A. Bisht, M. Bitossi, M. A. Bizouard, J. K. Blackburn, J. Blackman, C. D. Blair, D. G. Blair, R. M. Blair, O. Blanch, F. Bobba, N. Bode, M. Boer, Y. Boetzel, G. Bogaert, M. Boldrini, F. Bondu, E. Bonilla, R. Bonnand, P. Booker, B. A. Boom, R. Bork, V. Boschi, S. Bose, V. Bossilkov, V. Boudart, Y. Bouffanais, A. Bozzi, C. Bradaschia, P. R. Brady, A. Bramley, M. Branchesi, J. E. Brau, M. Breschi, T. Briant, J. H. Briggs, F. Brighenti, A. Brillet, M. Brinkmann, P. Brockill, A. F. Brooks, J. Brooks, D. D. Brown, S. Brunett, G. Bruno, R. Bruntz, A. Buikema, T. Bulik, H. J. Bulten, A. Buonanno, R. Buscicchio, D. Buskulic, R. L. Byer, M. Cabero, L. Cadonati, M. Caesar, G. Cagnoli, C. Cahillane, J. Calderón Bustillo, J. D. Callaghan, T. A. Callister, E. Calloni, J. B. Camp, M. Canepa, K. C. Cannon, H. Cao, J. Cao, G. Carapella, F. Carbognani, M. F. Carney, M. Carpinelli, G. Carullo, T. L. Carver, J. Casanueva Diaz, C. Casentini, S. Caudill, M. Cavaglià, F. Cavalier, R. Cavalieri, G. Cella, P. Cerdá-Durán, E. Cesarini, W. Chaibi, K. Chakravarti, C. L. Chan, C. Chan, K. Chandra, P. Chanial, S. Chao, P. Charlton, E. A. Chase, E. Chassande-Mottin, D. Chatterjee, D. Chattopadhyay, M. Chaturvedi, K. Chatziioannou, A. Chen, H. Y. Chen, X. Chen, Y. Chen, H. P. Cheng, C. K. Cheong, H. Y. Chia, F. Chiadini, R. Chierici, A. Chincarini, A. Chiummo, G. Cho, H. S. Cho, M. Cho, S. Choate, N. Christensen, Q. Chu, S. Chua, K. W. Chung, S. Chung, G. Ciani, P. Ciecielag, M. Cieślar, M. Cifaldi, A. A. Ciobanu, R. Ciolfi, F. Cipriano, A. Cirone, F. Clara, E. N. Clark, J. A. Clark, L. Clarke, P. Clearwater, S. Clesse, F. Cleva, E. Coccia, P. F. Cohadon, D. E. Cohen, M. Colleoni, C. G. Collette, C. Collins, M. Colpi, J. Constancio, M., L. Conti, S. J. Cooper, P. Corban, T. R. Corbitt, I. Cordero-Carrión, S. Corezzi, K. R. Corley, N. Cornish, D. Corre, A. Corsi, S. Cortese, C. A. Costa, R. Cotesta, M. W. Coughlin, S. B. Coughlin, J. P. Coulon, S. T. Countryman, P. Couvares, P. B. Covas, D. M. Coward, M. J. Cowart, D. C. Coyne, R. Coyne, J. D. E. Creighton, T. D. Creighton,

M. Croquette, S. G. Crowder, J. R. Cudell, T. J. Cullen, A. Cumming, R. Cummings, L. Cunningham, E. Cuoco, M. Curylo, T. Dal Canton, G. Dálya, A. Dana, L. M. DaneshgaranBajastani, B. D'Angelo, S. L. Danilishin, S. D'Antonio, K. Danzmann, C. Darsow-Fromm, A. Dasgupta, L. E. H. Datrier, V. Dattilo, I. Dave, M. Davier, G. S. Davies, D. Davis, E. J. Daw, R. Dean, D. DeBra, M. Deenadayalan, J. Degallaix, M. De Laurentis, S. Deléglise, V. Del Favero, F. De Lillo, N. De Lillo, W. Del Pozzo, L. M. DeMarchi, F. De Matteis, V. D'Emilio, N. Demos, T. Denker, T. Dent, A. Depasse, R. De Pietri, R. De Rosa, C. De Rossi, R. DeSalvo, O. de Varona, S. Dhurandhar, M. C. Díaz, J. Diaz-Ortiz, M., N. A. Didio, T. Dietrich, L. Di Fiore, C. DiFronzo, C. Di Giorgio, F. Di Giovanni, M. Di Giovanni, T. Di Girolamo, A. Di Lieto, B. Ding, S. Di Pace, I. Di Palma, F. Di Renzo, A. K. Divakarla, A. Dmitriev, Z. Doctor, L. D'Onofrio, F. Donovan, K. L. Dooley, S. Doravari, I. Dorrington, T. P. Downes, M. Drago, J. C. Driggers, Z. Du, J. G. Ducoin, P. Dupej, O. Durante, D. D'Urso, P. A. Duverne, S. E. Dwyer, P. J. Easter, G. Eddolls, B. Edelman, T. B. Edo, O. Edy, A. Effler, J. Eichholz, S. S. Eikenberry, M. Eisenmann, R. A. Eisenstein, A. Ejlli, L. Errico, R. C. Essick, H. Estellés, D. Estevez, Z. B. Etienne, T. Etzel, M. Evans, T. M. Evans, B. E. Ewing, V. Fafone, H. Fair, S. Fairhurst, X. Fan, A. M. Farah, S. Farinon, B. Farr, W. M. Farr, E. J. Fauchon-Jones, M. Favata, M. Fays, M. Fazio, J. Feicht, M. M. Fejer, F. Feng, E. Fenyvesi, D. L. Ferguson, A. Fernandez-Galiana, I. Ferrante, T. A. Ferreira, F. Fidecaro, P. Figura, I. Fiori, D. Fiorucci, M. Fishbach, R. P. Fisher, J. M. Fishner, R. Fittipaldi, M. Fitz-Axen, V. Fiumara, R. Flaminio, E. Floden, E. Flynn, H. Fong, J. A. Font, P. W. F. Forsyth, J. D. Fournier, S. Frasca, F. Frasconi, Z. Frei, A. Freise, R. Frey, V. Frey, P. Fritschel, V. V. Frolov, G. G. Fronzé, P. Fulda, M. Fyffe, H. A. Gabbard, B. U. Gadre, S. M. Gaebel, J. R. Gair, J. Gais, S. Galaudage, R. Gamba, D. Ganapathy, A. Ganguly, S. G. Gaonkar, B. Garaventa, C. García-Quirós, F. Garufi, B. Gateley, S. Gaudio, V. Gayathri, G. Gemme, A. Gennai, D. George, J. George, L. Gergely, S. Ghonge, A. Ghosh, A. Ghosh, S. Ghosh, B. Giacomazzo, L. Giacoppo, J. A. Giaime, K. D. Giardina, D. R. Gibson, C. Gier, K. Gill, P. Giri, J. Glanzer, A. E. Gleckl, P. Godwin, E. Goetz, R. Goetz, N. Gohlke, B. Goncharov, G. González, A. Gopakumar, S. E. Gossan, M. Gosselin, R. Gouaty, B. Grace, A. Grado, M. Granata, V. Granata, A. Grant, S. Gras, P. Grassia, C. Gray, R. Gray, G. Greco, A. C. Green, R. Green, E. M. Gretarsson, H. L. Griggs, G. Grignani, A. Grimaldi, E. Grimes, S. J. Grimm, H. Grote, S. Grunewald, P. Gruning, J. G. Guerrero, G. M. Guidi, A. R. Guimaraes, G. Guixé, H. K. Gulati, Y. Guo, A. Gupta, A. Gupta, P. Gupta, E. K. Gustafson, R. Gustafson, F. Guzman, L. Haegel, O. Halim, E. D. Hall, E. Z. Hamilton, G. Hammond, M. Haney, M. M. Hanke, J. Hanks, C. Hanna, O. A. Hannuksela, O. Hannuksela, H. Hansen, T. J. Hansen, J. Hanson, T. Harder, T. Hardwick, K. Haris, J. Harms, G. M. Harry, I. W. Harry, D. Hartwig, R. K. Hasskew, C. J. Haster, K. Haughian, F. J. Hayes, J. Healy, A. Heidmann, M. C. Heintze, J. Heinze, J. Heinzel, H. Heitmann, F. Hellman, P. Hello, A. F. Helmling-Cornell, G. Hemming, M. Hendry, I. S. Heng, E. Hennes, J. Hennig, M. H. Hennig, F. Hernandez Vivanco, M. Heurs, S. Hild, P. Hill, A. S. Hines, S. Hochheim, E. Hofgard, D. Hofman, J. N. Hohmann, A. M. Holgado, N. A. Holland, I. J. Hollows, Z. J. Holmes, K. Holt, D. E. Holz, P. Hopkins, C. Horst, J. Hough, E. J. Howell, C. G. Hoy, D. Hoyland, Y. Huang, M. T. Hübner, A. D. Huddart, E. A. Huerta, B. Hughey, V. Hui, S. Husa, S. H. Huttner, B. M. Hutzler, R. Huxford, T. Huynh-Dinh, B. Idzkowski, A. Iess, S. Imperato, H. Inchauspe, C. Ingram, G. Intini, M. Isi, B. R. Iyer, V. Jaberian-Hamedan, T. Jacqmin, S. J. Jadhav, S. P. Jadhav, A. L. James, K. Jani, K. Janssens, N. N. Janthalur, P. Jaranowski, D. Jariwala, R. Jaume, A. C. Jenkins, M. Jeunon, J. Jiang, G. R. Johns, A. W. Jones, D. I. Jones, J. D. Jones, P. Jones, R. Jones, R. J. G. Jonker, L. Ju, J. Junker, C. V. Kalaghatgi, V. Kalogera, B. Kamai, S. Kandhasamy, G. Kang, J. B. Kanner, S. J. Kapadia, D. P. Kapasi, C. Karathanasis, S. Karki, R. Kashyap, M. Kasprzack, W. Kastaun, S. Katsanevas, E. Katsavounidis, W. Katzman, K. Kawabe, F. Kéfélian, D. Keitel, J. S. Key, S. Khadka, F. Y. Khalili, I. Khan, S. Khan, E. A. Khazanov, N. Khetan, M. Khursheed, N. Kijbunchoo, C. Kim, G. J. Kim, J. C. Kim, K. Kim, W. S. Kim, Y. M. Kim, C. Kimball, P. J. King, M. Kinley-Hanlon, R. Kirchhoff, J. S. Kissel, L. Kleybolte, S. Klimenko, T. D. Knowles, E. Knyazev, P. Koch, S. M. Koehlenbeck, G. Koekoek, S. Koley, M. Kolstein, K. Komori, V. Kondrashov, A. Kontos, N. Koper, M. Korobko, W. Z. Korth, M. Kovalam, D. B. Kozak, C. Krämer, V. Kringel, N. V. Krishnendu, A. Królak, G. Kuehn, A. Kumar, P. Kumar, R. Kumar, R. Kumar, K. Kuns, S. Kwang, B. D. Lackey, D. Laghi, E. Lalande, T. L. Lam, A. Lamberts, M. Landry, B. B. Lane, R. N. Lang, J. Lange, B. Lantz, R. K. Lanza, I. La Rosa, A. Lartaux-Vollard, P. D. Lasky, M. Laxen, A. Lazzarini, C. Lazzaro, P. Leaci, S. Leavey, Y. K. Lecoeuche, H. M. Lee, H. W. Lee, J. Lee, K. Lee, J. Lehmann, E. Leon, N. Leroy, N. Letendre, Y. Levin, A. Li, J. Li, K. J. L. Li, T. G. F. Li, X. Li, F. Linde, S. D. Linker, J. N. Linley, T. B. Littenberg, J. Liu, X. Liu, M. Llorens-Monteagudo, R. K. L. Lo, A. Lockwood, L. T. London, A. Longo, M. Lorenzini, V. Loriette, M. Lormand, G. Losurdo, J. D. Lough, C. O. Lousto, G. Lovelace, H. Lück, D. Lumaca, A. P. Lundgren, Y. Ma, R. Macas, M. MacInnis, D. M. Macleod, I. A. O. MacMillan, A. Macquet, I. Magaña Hernandez, F. Magaña-Sandoval, C. Magazzù, R. M. Magee, E. Majorana, I. Maksimovic, S. Maliakal, A. Malik, N. Man, V. Mandic, V. Mangano, G. L. Mansell, M. Manske, M. Mantovani, M. Mapelli, F. Marchesoni, F. Marion, S. Márka, Z. Márka, C. Markakis, A. S. Markosyan, A. Markowitz, E. Maros, A. Marquina, S. Marsat, F. Martelli, I. W. Martin, R. M. Martin, M. Martinez, V. Martinez, D. V. Martynov, H. Masalehdan, K. Mason, E. Massera, A. Masserot, T. J. Massinger, M. Masso-Reid, S. Mastrogiovanni, A. Matas, M. Mateu-Lucena, F. Matichard, M. Matiushechkina, N. Mavalvala, E. Maynard, J. J. McCann, R. McCarthy, D. E. McClelland, S. McCormick, L. McCuller, S. C. McGuire, C. McIsaac, J. McIver, D. J. McManus, T. McRae, S. T. McWilliams, D. Meacher, G. D. Meadors, M. Mehmet, A. K. Mehta, A. Melatos, D. A. Melchor, G. Mendell, A. Menendez-Vazquez, R. A. Mercer, L. Mereni, K. Merfeld, E. L. Merilh, J. D. Merritt, M. Merzougui, S. Meshkov, C. Messenger, C. Messick, R. Metzdorff, P. M. Meyers, F. Meylahn, A. Mhaske, A. Miani, H. Miao, I. Michaloliakos, C. Michel, H. Middleton, L. Milano, A. L. Miller, S. Miller, M. Millhouse, J. C. Mills, E. Milotti, M. C. Milovich-Goff, O. Minazzoli, Y. Minenkov, L. M. Mir, A. Mishkin, C. Mishra, T. Mistry, S. Mitra, V. P. Mitrofanov, G. Mitselmakher, R. Mittleman, G. Mo, K. Mogushi, S. R. P. Mohapatra, S. R. Mohite, I. Molina, M. Molina-Ruiz, M. Mondin, M. Montani, C. J. Moore, D. Moraru, F. Morawski, G. Moreno, S. Morisaki, B. Mours, C. M. Mow-Lowry, S. Mozzon, F. Muciaccia, A. Mukherjee, D. Mukherjee, S. Mukherjee, S. Mukherjee, N. Mukund, A. Mullavey, J. Munch, E. A. Muñiz, P. G. Murray, S. L. Nadji, A. Nagar, I. Nardecchia, L. Naticchioni, R. K. Nayak, B. F. Neil, J. Neilson, G. Nelemans, T. J. N. Nelson, M. Nery, A. Neunzert, K. Y. Ng, S. Ng, C. Nguyen, P. Nguyen, T. Nguyen, S. A. Nichols, S. Nissanke, F. Nocera, M. Noh, C. North, D. Nothard, L. K. Nuttall, J. Oberling, B. D. O'Brien, J. O'Dell, G. Oganesyan, G. H. Ogin, J. J. Oh, S. H. Oh, F. Ohme, H. Ohta, M. A. Okada, C. Olivetto, P. Oppermann, R. J. Oram, B. O'Reilly, R. G. Ormiston, N. Ormsby, L. F. Ortega, R. O'Shaughnessy, S. Ossokine, C. Osthelder, D. J. Ottaway, H. Overmier, B. J. Owen, A. E. Pace, G. Pagano, M. A. Page, G. Pagliaroli, A. Pai, S. A. Pai, J. R. Palamos, O. Palashov, C. Palomba, H. Pan, P. K. Panda, T. H. Pang, C. Pankow, F. Pannarale, B. C. Pant, F. Paoletti, A. Paoli, A. Paolone, W. Parker, D. Pascucci, A. Pasqualetti, R. Passaquieti, D. Passuello, M. Patel, B. Patricelli, E. Payne, T. C. Pechsiri, M. Pedraza, M. Pegoraro, A. Pele, S. Penn, A. Perego, C. J. Perez, C. Périgois, A. Perreca, S. Perriès, J. Petermann, D. Petterson, H. P. Pfeiffer, K. A. Pham, K. S. Phukon, O. J. Piccinni, M. Pichot, M. Piendibene, F. Piergiovanni,

L. Pierini, V. Pierro, G. Pillant, F. Pilo, L. Pinard, I. M. Pinto, K. Piotrzkowski, M. Pirello, M. Pitkin, E. Placidi, W. Plastino, C. Pluchar, R. Poggiani, E. Polini, D. Y. T. Pong, S. Ponrathnam, P. Popolizio, E. K. Porter, A. Poverman, J. Powell, M. Pracchia, A. K. Prajapati, K. Prasai, R. Prasanna, G. Pratten, T. Prestegard, M. Principe, G. A. Prodi, L. Prokhorov, P. Prosposito, A. Puecher, M. Punturo, F. Puosi, P. Puppo, M. Pürrer, H. Qi, V. Quetschke, P. J. Quinonez, R. Quitzow-James, F. J. Raab, G. Raaijmakers, H. Radkins, N. Radulesco, P. Raffai, H. Rafferty, S. X. Rail, S. Raja, C. Rajan, B. Rajbhandari, M. Rakhmanov, K. E. Ramirez, T. D. Ramirez, A. Ramos-Buades, J. Rana, K. Rao, P. Rapagnani, U. D. Rapol, B. Ratto, V. Raymond, M. Razzano, J. Read, T. Regimbau, L. Rei, S. Reid, D. H. Reitze, P. Rettegno, F. Ricci, C. J. Richardson, J. W. Richardson, L. Richardson, P. M. Ricker, G. Riemenschneider, K. Riles, M. Rizzo, N. A. Robertson, F. Robinet, A. Rocchi, J. A. Rocha, S. Rodriguez, R. D. Rodriguez-Soto, L. Rolland, J. G. Rollins, V. J. Roma, M. Romanelli, R. Romano, C. L. Romel, A. Romero, I. M. Romero-Shaw, J. H. Romie, S. Ronchini, C. A. Rose, D. Rose, K. Rose, M. J. B. Rosell, D. Rosińska, S. G. Rosofsky, M. P. Ross, S. Rowan, S. J. Rowlinson, S. Roy, S. Roy, P. Ruggi, K. Ryan, S. Sachdev, T. Sadecki, M. Sakellariadou, O. S. Salafia, L. Salconi, M. Saleem, A. Samajdar, E. J. Sanchez, J. H. Sanchez, L. E. Sanchez, N. Sanchis-Gual, J. R. Sanders, K. A. Santiago, E. Santos, T. R. Saravanan, N. Sarin, B. Sassolas, B. S. Sathyaprakash, O. Sauter, R. L. Savage, V. Savant, D. Sawant, S. Sayah, D. Schaetzl, P. Schale, M. Scheel, J. Scheuer, A. Schindler-Tyka, P. Schmidt, R. Schnabel, R. M. S. Schofield, A. Schönbeck, E. Schreiber, B. W. Schulte, B. F. Schutz, O. Schwarm, E. Schwartz, J. Scott, S. M. Scott, M. Seglar-Arroyo, E. Seidel, D. Sellers, A. S. Sengupta, N. Sennett, D. Sentenac, V. Sequino, A. Sergeev, Y. Setyawati, T. Shaffer, M. S. Shahriar, S. Sharifi, A. Sharma, P. Sharma, P. Shawhan, H. Shen, M. Shikauchi, R. Shink, D. H. Shoemaker, D. M. Shoemaker, K. Shukla, S. ShyamSundar, M. Sieniawska, D. Sigg, L. P. Singer, D. Singh, N. Singh, A. Singha, A. Singhal, A. M. Sintes, V. Sipala, V. Skliris, B. J. J. Slagmolen, T. J. Slaven-Blair, J. Smetana, J. R. Smith, R. J. E. Smith, S. N. Somala, E. J. Son, S. Soni, B. Sorazu, V. Sordini, F. Sorrentino, N. Sorrentino, R. Soulard, T. Souradeep, E. Sowell, A. P. Spencer, M. Spera, A. K. Srivastava, V. Srivastava, K. Staats, C. Stachie, D. A. Steer, M. Steinke, J. Steinlechner, S. Steinlechner, D. Steinmeyer, S. P. Stevenson, G. Stolle-McAllister, D. J. Stops, M. Stover, K. A. Strain, G. Stratta, A. Strunk, R. Sturani, A. L. Stuver, J. Südbeck, S. Sudhagar, V. Sudhir, H. G. Suh, T. Z. Summerscales, H. Sun, L. Sun, S. Sunil, A. Sur, J. Suresh, P. J. Sutton, B. L. Swinkels, M. J. Szczepańczyk, M. Tacca, S. C. Tait, C. Talbot, A. J. Tanasijczuk, D. B. Tanner, D. Tao, A. Tapia, E. N. Tapia San Martin, J. D. Tasson, R. Taylor, R. Tenorio, L. Terkowski, M. P. Thirugnanasambandam, L. Thomas, M. Thomas, P. Thomas, J. E. Thompson, S. R. Thondapu, K. A. Thorne, E. Thrane, S. Tiwari, S. Tiwari, V. Tiwari, K. Toland, A. E. Tolley, M. Tonelli, Z. Tornasi, A. Torres-Forné, C. I. Torrie, I. Tosta e Melo, D. Töyrä, A. T. Tran, A. Trapananti, F. Travasso, G. Traylor, M. C. Tringali, A. Tripathee, A. Trovato, R. J. Trudeau, D. S. Tsai, K. W. Tsang, M. Tse, R. Tso, L. Tsukada, D. Tsuna, T. Tsutsui, M. Turconi, A. S. Ubhi, R. P. Udall, K. Ueno, D. Ugolini, C. S. Unnikrishnan, A. L. Urban, S. A. Usman, A. C. Utina, H. Vahlbruch, G. Vajente, A. Vajpeyi, G. Valdes, M. Valentini, V. Valsan, N. van Bakel, M. v. Beuzekom, J. F. J. van den Brand, C. Van Den Broeck, D. C. Vander-Hyde, L. van der Schaaf, J. V. van Heijningen, M. Vardaro, A. F. Vargas, V. Varma, S. Vass, M. Vasúth, A. Vecchio, G. Vedovato, J. Veitch, P. J. Veitch, K. Venkateswara, J. Venneberg, G. Venugopalan, D. Verkindt, Y. Verma, D. Veske, F. Vetrano, A. Viceré, A. D. Viets, V. Villa-Ortega, J. Y. Vinet, S. Vitale, T. Vo, H. Vocca, C. Vorvick, S. P. Vyatchanin, A. R. Wade, L. E. Wade, M. Wade, R. C. Walet, M. Walker, G. S. Wallace, L. Wallace, S. Walsh, J. Z. Wang, S. Wang, W. H. Wang, Y. F. Wang, R. L. Ward, J. Warner, M. Was, N. Y. Washington, J. Watchi, B. Weaver, L. Wei, M. Weinert, A. J. Weinstein, R. Weiss, F. Wellmann, L. Wen, P. Weßels, J. W. Westhouse, K. Wette, J. T. Whelan, D. D. White, L. V. White, B. F. Whiting, C. Whittle, D. M. Wilken, D. Williams, M. J. Williams, A. R. Williamson, J. L. Willis, B. Willke, D. J. Wilson, M. H. Wimmer, W. Winkler, C. C. Wipf, G. Woan, J. Woehler, J. K. Wofford, I. C. F. Wong, J. Wrangel, J. L. Wright, D. S. Wu, D. M. Wysocki, L. Xiao, H. Yamamoto, L. Yang, Y. Yang, Z. Yang, M. J. Yap, D. W. Yeeles, A. Yoon, H. Yu, H. Yu, S. H. R. Yuen, A. Zadrożny, M. Zanolin, T. Zelenova, J. P. Zendri, M. Zevin, J. Zhang, L. Zhang, R. Zhang, T. Zhang, C. Zhao, G. Zhao, M. Zhou, Z. Zhou, X. J. Zhu, A. B. Zimmerman, M. E. Zucker, J. Zweizig, LIGO Scientific Collaboration, and Virgo Collaboration, ApJL **913**, L7 (2021), arXiv: 2010.14533.

252 J. Yu, H. Song, S. Ai, H. Gao, F. Wang, Y. Wang, Y. Lu, W. Fang, and W. Zhao, ApJ **916**, 54 (2021), arXiv: 2104.12374.

253 D.-L. Zhang, X.-Q. Li, S.-L. Xiong, W.-x. Peng, Fan-Zhang, Yanguo-Li, Z.-H. An, Y.-B. Xu, X.-L. Sun, and Y. Zhu, arXiv e-prints arXiv:1804.04499 (2018), arXiv: 1804.04499.

254 N. Gehrels, G. Chincarini, P. Giommi, K. O. Mason, J. A. Nousek, A. A. Wells, N. E. White, S. D. Barthelmy, D. N. Burrows, L. R. Cominsky, K. C. Hurley, F. E. Marshall, P. Mészáros, P. W. A. Roming, L. Angelini, L. M. Barbier, T. Belloni, S. Campana, P. A. Caraveo, M. M. Chester, O. Citterio, T. L. Cline, M. S. Cropper, J. R. Cummings, A. J. Dean, E. D. Feigelson, E. E. Fenimore, D. A. Frail, A. S. Fruchter, G. P. Garmire, K. Gendreau, G. Ghisellini, J. Greiner, J. E. Hill, S. D. Hunsberger, H. A. Krimm, S. R. Kulkarni, P. Kumar, F. Lebrun, N. M. Lloyd-Ronning, C. B. Markwardt, B. J. Mattson, R. F. Mushotzky, J. P. Norris, J. Osborne, B. Paczynski, D. M. Palmer, H. S. Park, A. M. Parsons, J. Paul, M. J. Rees, C. S. Reynolds, J. E. Rhoads, T. P. Sasseen, B. E. Schaefer, A. T. Short, A. P. Smale, I. A. Smith, L. Stella, G. Tagliaferri, T. Takahashi, M. Tashiro, L. K. Townsley, J. Tueller, M. J. L. Turner, M. Vietri, W. Voges, M. J. Ward, R. Willingale, F. M. Zerbi, and W. W. Zhang, ApJ **611**, 1005 (2004), arXiv: astro-ph/0405233.

255 D. Götz, J. Osborne, B. Cordier, J. Paul, P. Evans, A. Beardmore, A. Martindale, R. Willingale, P. O'Brien, S. Basa, C. Rossin, O. Godet, N. Webb, J. Greiner, K. Nandra, N. Meidinger, E. Perinati, A. Santangelo, K. Mercier, and F. Gonzalez, in *Space Telescopes and Instrumentation 2014: Ultraviolet to Gamma Ray*, (edited by T. Takahashi, J.-W. A. den Herder, and M. Bautz), volume 9144 of *Society of Photo-Optical Instrumentation Engineers (SPIE) Conference Series*, 914423 (2014), arXiv: 1407.2406.

256 C. Meegan, G. Lichti, P. N. Bhat, E. Bissaldi, M. S. Briggs, V. Connaughton, R. Diehl, G. Fishman, J. Greiner, A. S. Hoover, A. J. van der Horst, A. von Kienlin, R. M. Kippen, C. Kouveliotou, S. McBreen, W. S. Paciesas, R. Preece, H. Steinle, M. S. Wallace, R. B. Wilson, and C. Wilson-Hodge, ApJ **702**, 791 (2009), arXiv: 0908.0450.

257 B. Zhang and P. Mészáros, ApJ **571**, 876 (2002), arXiv: astro-ph/0112118.

258 K. D. Alexander, R. Margutti, P. K. Blanchard, W. Fong, E. Berger, A. Hajela, T. Eftekhari, R. Chornock, P. S. Cowperthwaite, D. Giannios, C. Guidorzi, A. Kathirgamaraju, A. MacFadyen, B. D. Metzger, M. Nicholl, L. Sironi, V. A. Villar, P. K. G. Williams, X. Xie, and J. Zrake, ApJL **863**, L18 (2018), arXiv: 1805.02870.

259 D. Lazzati, R. Perna, B. J. Morsony, D. Lopez-Camara, M. Cantiello, R. Ciolfi, B. Giacomazzo, and J. C. Workman, PRL **120**, 241103 (2018), arXiv: 1712.03237.

260 K. P. Mooley, E. Nakar, K. Hotokezaka, G. Hallinan, A. Corsi, D. A. Frail, A. Horesh, T. Murphy, E. Lenc, D. L. Kaplan, K. de, D. Dobie, P. Chandra, A. Deller, O. Gottlieb, M. M. Kasliwal, S. R. Kulkarni, S. T. Myers, S. Nissanke, T. Piran, C. Lynch, V. Bhalerao, S. Bourke, K. W. Bannister, and L. P. Singer, Nature **554**, 207 (2018), arXiv: 1711.11573.

261 E. Troja, L. Piro, G. Ryan, H. van Eerten, R. Ricci, M. H. Wieringa,

S. Lotti, T. Sakamoto, and S. B. Cenko, MNRAS **478**, L18 (2018), arXiv: 1801.06516.

262 G. Ghirlanda, O. S. Salafia, Z. Paragi, M. Giroletti, J. Yang, B. Marcote, J. Blanchard, I. Agudo, T. An, M. G. Bernardini, R. Beswick, M. Branchesi, S. Campana, C. Casadio, E. Chassande-Mottin, M. Colpi, S. Covino, P. D'Avanzo, V. D'Elia, S. Frey, M. Gawronski, G. Ghisellini, L. I. Gurvits, P. G. Jonker, H. J. van Langevelde, A. Melandri, J. Moldon, L. Nava, A. Perego, M. A. Perez-Torres, C. Reynolds, R. Salvaterra, G. Tagliaferri, T. Venturi, S. D. Vergani, and M. Zhang, Science **363**, 968 (2019), arXiv: 1808.00469.

263 R. Sari, T. Piran, and R. Narayan, ApJL **497**, L17 (1998), arXiv: astro-ph/9712005.

264 P. Mészáros and M. J. Rees, MNRAS **306**, L39 (1999), arXiv: astro-ph/9902367.

265 The LIGO Scientific Collaboration, the Virgo Collaboration, and the KAGRA Collaboration, arXiv e-prints arXiv:2111.03606 (2021), arXiv: 2111.03606.

266 J.-P. Zhu, S. Wu, Y.-P. Yang, B. Zhang, H. Gao, Y.-W. Yu, Z. Li, Z. Cao, L.-D. Liu, Y. Huang, and X.-H. Zhang, ApJ **917**, 24 (2021), arXiv: 2011.02717.

267 M. J. Graham, K. E. S. Ford, B. McKernan, N. P. Ross, D. Stern, K. Burdge, M. Coughlin, S. G. Djorgovski, A. J. Drake, D. Duev, M. Kasliwal, A. A. Mahabal, S. van Velzen, J. Belecki, E. C. Bellm, R. Burruss, S. B. Cenko, V. Cunningham, G. Helou, S. R. Kulkarni, F. J. Masci, T. Prince, D. Reiley, H. Rodriguez, B. Rusholme, R. M. Smith, and M. T. Soumagnac, PRL **124**, 251102 (2020), arXiv: 2006.14122.

268 T. Piran, A. Shemi, and R. Narayan, MNRAS **263**, 861 (1993), arXiv: astro-ph/9301004.

269 P. Meszaros and M. J. Rees, ApJ **405**, 278 (1993).

270 K. D. Alexander, E. Berger, W. Fong, P. K. G. Williams, C. Guidorzi, R. Margutti, B. D. Metzger, J. Annis, P. K. Blanchard, D. Brout, D. A. Brown, H. Y. Chen, R. Chornock, P. S. Cowperthwaite, M. Drout, T. Eftekhari, J. Frieman, D. E. Holz, M. Nicholl, A. Rest, M. Sako, M. Soares-Santos, and V. A. Villar, ApJL **848**, L21 (2017), arXiv: 1710.05457.

271 D. Lazzati, R. Perna, B. J. Morsony, D. Lopez-Camara, M. Cantiello, R. Ciolfi, B. Giacomazzo, and J. C. Workman, PRL **120**, 241103 (2018), arXiv: 1712.03237.

272 T. Piran, PhR **314**, 575 (1999), arXiv: astro-ph/9810256.

273 Z. G. Dai and T. Lu, A&A **333**, L87 (1998), arXiv: astro-ph/9810402.

274 B. Zhang and H. Yan, ApJ **726**, 90 (2011), arXiv: 1011.1197.

275 P. Mészáros and M. J. Rees, ApJ **476**, 232 (1997), arXiv: astro-ph/9606043.

276 P. Mészáros and M. J. Rees, MNRAS **306**, L39 (1999), arXiv: astro-ph/9902367.

277 R. Sari and T. Piran, ApJ **520**, 641 (1999), arXiv: astro-ph/9901338.

278 B. Zhang, S. Kobayashi, and P. Mészáros, ApJ **595**, 950 (2003), arXiv: astro-ph/0302525.

279 Y. Z. Fan, D. M. Wei, and C. F. Wang, A&A **424**, 477 (2004), arXiv: astro-ph/0405392.

280 W. T. Vestrand, J. A. Wren, A. Panaitescu, P. R. Wozniak, H. Davis, D. M. Palmer, G. Vianello, N. Omodei, S. Xiong, M. S. Briggs, M. Elphick, W. Paciesas, and W. Rosing, Science **343**, 38 (2014), arXiv: 1311.5489.

281 E. Troja, V. M. Lipunov, C. G. Mundell, N. R. Butler, A. M. Watson, S. Kobayashi, S. B. Cenko, F. E. Marshall, R. Ricci, A. Fruchter, M. H. Wieringa, E. S. Gorbovskoy, V. Kornilov, A. Kutyrev, W. H. Lee, V. Toy, N. V. Tyurina, N. M. Budnev, D. A. H. Buckley, J. González, O. Gress, A. Horesh, M. I. Panasyuk, J. X. Prochaska, E. Ramirez-Ruiz, R. Rebolo Lopez, M. G. Richer, C. Roman-Zuniga, M. Serra-Ricart, V. Yurkov, and N. Gehrels, Nature **547**, 425 (2017).

282 A. M. Beloborodov and Z. L. Uhm, ApJL **651**, L1 (2006), arXiv: astro-ph/0607641.

283 Z. L. Uhm, ApJ **733**, 86 (2011), arXiv: 1003.1115.

284 J. J. Geng, X. F. Wu, L. Li, Y. F. Huang, and Z. G. Dai, ApJ **792**, 31 (2014), arXiv: 1407.0588.

285 J. J. Geng, X. F. Wu, Y. F. Huang, L. Li, and Z. G. Dai, ApJ **825**, 107 (2016), arXiv: 1605.01334.

286 S. Ai and B. Zhang, MNRAS **507**, 1788 (2021), arXiv: 2104.06450.

287 Y. Li, X. Wen, X. Sun, X. Liu, X. Liang, D. Guo, W. Peng, K. Gong, G. Li, H. Wang, S. Xiong, J. Liao, H. Lu, J. Wang, Z. An, D. Zhang, M. Gao, G. Chen, Y. Liu, S. Yang, R. Qiao, F. Zhang, X. Zhao, Y. Xu, Y. Zhu, and X. Li, Scientia Sinica Physica, Mechanica & Astronomica **50**, 129508 (2020).

288 J. Wei, B. Cordier, S. Antier, P. Antilogus, J. L. Atteia, A. Bajat, S. Basa, V. Beckmann, M. G. Bernardini, S. Boissier, L. Bouchet, V. Burwitz, A. Claret, Z. G. Dai, F. Daigne, J. Deng, D. Dornic, H. Feng, T. Foglizzo, H. Gao, N. Gehrels, O. Godet, A. Goldwurm, F. Gonzalez, L. Gosset, D. Götz, C. Gouiffes, F. Grise, A. Gros, J. Guilet, X. Han, M. Huang, Y. F. Huang, M. Jouret, A. Klotz, O. La Marle, C. Lachaud, E. Le Floch, W. Lee, N. Leroy, L. X. Li, S. C. Li, Z. Li, E. W. Liang, H. Lyu, K. Mercier, G. Migliori, R. Mochkovitch, P. O'Brien, J. Osborne, J. Paul, E. Perinati, P. Petitjean, F. Piron, Y. Qiu, A. Rau, J. Rodriguez, S. Schanne, N. Tanvir, E. Vangioni, S. Vergani, F. Y. Wang, J. Wang, X. G. Wang, X. Y. Wang, A. Watson, N. Webb, J. J. Wei, R. Willingale, C. Wu, X. F. Wu, L. P. Xin, D. Xu, S. Yu, W. F. Yu, Y. W. Yu, B. Zhang, S. N. Zhang, Y. Zhang, and X. L. Zhou, arXiv e-prints arXiv:1610.06892 (2016), arXiv: 1610.06892.

289 R. Salvaterra, M. Della Valle, S. Campana, G. Chincarini, S. Covino, P. D'Avanzo, A. Fernández-Soto, C. Guidorzi, F. Mannucci, R. Margutti, C. C. Thöne, L. A. Antonelli, S. D. Barthelmy, M. de Pasquale, V. D'Elia, F. Fiore, D. Fugazza, L. K. Hunt, E. Maiorano, S. Marinoni, F. E. Marshall, E. Molinari, J. Nousek, E. Pian, J. L. Racusin, L. Stella, L. Amati, G. Andreuzzi, G. Cusumano, E. E. Fenimore, P. Ferrero, P. Giommi, D. Guetta, S. T. Holland, K. Hurley, G. L. Israel, J. Mao, C. B. Markwardt, N. Masetti, C. Pagani, E. Palazzi, D. M. Palmer, S. Piranomonte, G. Tagliaferri, and V. Testa, Nature **461**, 1258 (2009), arXiv: 0906.1578.

290 N. R. Tanvir, D. B. Fox, A. J. Levan, E. Berger, K. Wiersema, J. P. U. Fynbo, A. Cucchiara, T. Krühler, N. Gehrels, J. S. Bloom, J. Greiner, P. A. Evans, E. Rol, F. Olivares, J. Hjorth, P. Jakobsson, J. Farihi, R. Willingale, R. L. C. Starling, S. B. Cenko, D. Perley, J. R. Maund, J. Duke, R. A. M. J. Wijers, A. J. Adamson, A. Allan, M. N. Bremer, D. N. Burrows, A. J. Castro-Tirado, B. Cavanagh, A. de Ugarte Postigo, M. A. Dopita, T. A. Fatkhullin, A. S. Fruchter, R. J. Foley, J. Gorosabel, J. Kennea, T. Kerr, S. Klose, H. A. Krimm, V. N. Komarova, S. R. Kulkarni, A. S. Moskvitin, C. G. Mundell, T. Naylor, K. Page, B. E. Penprase, M. Perri, P. Podsiadlowski, K. Roth, R. E. Rutledge, T. Sakamoto, P. Schady, B. P. Schmidt, A. M. Soderberg, J. Sollerman, A. W. Stephens, G. Stratta, T. N. Ukwatta, D. Watson, E. Westra, T. Wold, and C. Wolf, Nature **461**, 1254 (2009), arXiv: 0906.1577.

291 A. Cucchiara, A. J. Levan, D. B. Fox, N. R. Tanvir, T. N. Ukwatta, E. Berger, T. Krühler, A. Küpcü Yoldaş, X. F. Wu, K. Toma, J. Greiner, F. E. Olivares, A. Rowlinson, L. Amati, T. Sakamoto, K. Roth, A. Stephens, A. Fritz, J. P. U. Fynbo, J. Hjorth, D. Malesani, P. Jakobsson, K. Wiersema, P. T. O'Brien, A. M. Soderberg, R. J. Foley, A. S. Fruchter, J. Rhoads, R. E. Rutledge, B. P. Schmidt, M. A. Dopita, P. Podsiadlowski, R. Willingale, C. Wolf, S. R. Kulkarni, and P. D'Avanzo, Astrophys. J. **736**, 7 (2011), arXiv: 1105.4915.

292 R. Salvaterra, Journal of High Energy Astrophysics **7**, 35 (2015), arXiv: 1503.03072.

293 F. Y. Wang, Z. G. Dai, and E. W. Liang, NewAR **67**, 1 (2015), arXiv: 1504.00735.

294 R. Salvaterra, S. Campana, G. Chincarini, S. Covino, and G. Tagliaferri, MNRAS **385**, 189 (2008), arXiv: 0710.4280.

295 G. Ghirlanda, R. Salvaterra, G. Ghisellini, S. Mereghetti, G. Tagliaferri, S. Campana, J. P. Osborne, P. O'Brien, N. Tanvir, D. Willingale, L. Amati, S. Basa, M. G. Bernardini, D. Burlon, S. Covino,

P. D'Avanzo, F. Frontera, D. Götz, A. Melandri, L. Nava, L. Piro, and S. D. Vergani, MNRAS **448**, 2514 (2015), arXiv: 1502.02676.

296 J. Wei, X. Wu, F. Wang, Z. Liu, Z.-G. Dai, and B. Zhang, Scientia Sinica Physica, Mechanica & Astronomica **48**, 039505 (2018).

297 D. R. Lorimer, M. Bailes, M. A. McLaughlin, D. J. Narkevic, and F. Crawford, Science **318**, 777 (2007), arXiv: 0709.4301.

298 The CHIME/FRB Collaboration, :, M. Amiri, B. C. Andersen, K. Bandura, S. Berger, M. Bhardwaj, M. M. Boyce, P. J. Boyle, C. Brar, D. Breitman, T. Cassanelli, P. Chawla, T. Chen, J. F. Cliche, A. Cook, D. Cubranic, A. P. Curtin, M. Deng, M. Dobbs, Fengqiu, Dong, G. Eadie, M. Fandino, E. Fonseca, B. M. Gaensler, U. Giri, D. C. Good, M. Halpern, A. S. Hill, G. Hinshaw, A. Josephy, J. F. Kaczmarek, Z. Kader, J. W. Kania, V. M. Kaspi, T. L. Landecker, D. Lang, C. Leung, D. Li, H.-H. Lin, K. W. Masui, R. Mckinven, J. Mena-Parra, M. Merryfield, B. W. Meyers, D. Michilli, N. Milutinovic, A. Mirhosseini, M. Münchmeyer, A. Naidu, L. Newburgh, C. Ng, C. Patel, U.-L. Pen, E. Petroff, T. Pinsonneault-Marotte, Z. Pleunis, M. Rafiei-Ravandi, M. Rahman, S. M. Ransom, A. Renard, P. Sanghavi, P. Scholz, J. R. Shaw, K. Shin, S. R. Siegel, A. E. Sikora, S. Singh, K. M. Smith, I. Stairs, C. M. Tan, S. P. Tendulkar, K. Vanderlinde, H. Wang, D. Wulf, and A. V. Zwaniga, arXiv e-prints arXiv:2106.04352 (2021), arXiv: 2106.04352.

299 J. P. Macquart, J. X. Prochaska, M. McQuinn, K. W. Bannister, S. Bhandari, C. K. Day, A. T. Deller, R. D. Ekers, C. W. James, L. Marnoch, S. Osłowski, C. Phillips, S. D. Ryder, D. R. Scott, R. M. Shannon, and N. Tejos, Nature **581**, 391 (2020), arXiv: 2005.13161.

300 S. Bhandari, K. E. Heintz, K. Aggarwal, L. Marnoch, C. K. Day, J. Sydnor, S. Burke-Spolaor, C. J. Law, J. X. Prochaska, N. Tejos, K. W. Bannister, B. J. Butler, A. T. Deller, R. D. Ekers, C. Flynn, W.-f. Fong, C. W. James, T. J. W. Lazio, R. Luo, E. K. Mahony, S. D. Ryder, E. M. Sadler, R. M. Shannon, J. Han, K. Lee, and B. Zhang, arXiv e-prints arXiv:2108.01282 (2021), arXiv: 2108.01282.

301 S. Bhandari, E. M. Sadler, J. X. Prochaska, S. Simha, S. D. Ryder, L. Marnoch, K. W. Bannister, J.-P. Macquart, C. Flynn, R. M. Shannon, N. Tejos, F. Corro-Guerra, C. K. Day, A. T. Deller, R. Ekers, S. Lopez, E. K. Mahony, C. Nuñez, and C. Phillips, ApJL **895**, L37 (2020), arXiv: 2005.13160.

302 Y. Li and B. Zhang, ApJL **899**, L6 (2020), arXiv: 2005.02371.

303 C. D. Bochenek, V. Ravi, K. V. Belov, G. Hallinan, J. Kocz, S. R. Kulkarni, and D. L. McKenna, Nature **587**, 59 (2020), arXiv: 2005.10828.

304 CHIME/FRB Collaboration, B. C. Andersen, K. M. Bandura, M. Bhardwaj, A. Bij, M. M. Boyce, P. J. Boyle, C. Brar, T. Cassanelli, P. Chawla, T. Chen, J. F. Cliche, A. Cook, D. Cubranic, A. P. Curtin, N. T. Denman, M. Dobbs, F. Q. Dong, M. Fandino, E. Fonseca, B. M. Gaensler, U. Giri, D. C. Good, M. Halpern, A. S. Hill, G. F. Hinshaw, C. Höfer, A. Josephy, J. W. Kania, V. M. Kaspi, T. L. Landecker, C. Leung, D. Z. Li, H. H. Lin, K. W. Masui, R. McKinven, J. Mena-Parra, M. Merryfield, B. W. Meyers, D. Michilli, N. Milutinovic, A. Mirhosseini, M. Münchmeyer, A. Naidu, L. B. Newburgh, C. Ng, C. Patel, U. L. Pen, T. Pinsonneault-Marotte, Z. Pleunis, B. M. Quine, M. Rafiei-Ravandi, M. Rahman, S. M. Ransom, A. Renard, P. Sanghavi, P. Scholz, J. R. Shaw, K. Shin, S. R. Siegel, S. Singh, R. J. Smegal, K. M. Smith, I. H. Stairs, C. M. Tan, S. P. Tendulkar, I. Tretyakov, K. Vanderlinde, H. Wang, D. Wulf, and A. V. Zwaniga, Nature **587**, 54 (2020), arXiv: 2005.10324.

305 L. Lin, C. F. Zhang, P. Wang, H. Gao, X. Guan, J. L. Han, J. C. Jiang, P. Jiang, K. J. Lee, D. Li, Y. P. Men, C. C. Miao, C. H. Niu, J. R. Niu, C. Sun, B. J. Wang, Z. L. Wang, H. Xu, J. L. Xu, J. W. Xu, Y. H. Yang, Y. P. Yang, W. Yu, B. Zhang, B. B. Zhang, D. J. Zhou, W. W. Zhu, A. J. Castro-Tirado, Z. G. Dai, M. Y. Ge, Y. D. Hu, C. K. Li, Y. Li, Z. Li, E. W. Liang, S. M. Jia, R. Querel, L. Shao, F. Y. Wang, X. G. Wang, X. F. Wu, S. L. Xiong, R. X. Xu, Y. S. Yang, G. Q. Zhang, S. N. Zhang, T. C. Zheng, and J. H. Zou, Nature **587**, 63 (2020), arXiv: 2005.11479.

306 S.-X. Yi, H. Gao, and B. Zhang, ApJL **792**, L21 (2014), arXiv: 1407.0348.

307 Y.-P. Yang, B. Zhang, and J.-Y. Wei, ApJ **878**, 89 (2019), arXiv: 1905.02429.

308 C. K. Li, L. Lin, S. L. Xiong, M. Y. Ge, X. B. Li, T. P. Li, F. J. Lu, S. N. Zhang, Y. L. Tuo, Y. Nang, B. Zhang, S. Xiao, Y. Chen, L. M. Song, Y. P. Xu, C. Z. Liu, S. M. Jia, X. L. Cao, J. L. Qu, S. Zhang, Y. D. Gu, J. Y. Liao, X. F. Zhao, Y. Tan, J. Y. Nie, H. S. Zhao, S. J. Zheng, Y. G. Zheng, Q. Luo, C. Cai, B. Li, W. C. Xue, Q. C. Bu, Z. Chang, G. Chen, L. Chen, T. X. Chen, Y. B. Chen, Y. P. Chen, W. Cui, W. W. Cui, J. K. Deng, Y. W. Dong, Y. Y. Du, M. X. Fu, G. H. Gao, H. Gao, M. Gao, Y. D. Gu, J. Guan, C. C. Guo, D. W. Han, Y. Huang, J. Huo, L. H. Jiang, W. C. Jiang, J. Jin, Y. J. Jin, L. D. Kong, G. Li, M. S. Li, W. Li, X. Li, X. F. Li, Y. G. Li, Z. W. Li, X. H. Liang, B. S. Liu, G. Q. Liu, H. W. Liu, X. J. Liu, Y. N. Liu, B. Lu, X. F. Lu, T. Luo, X. Ma, B. Meng, G. Ou, N. Sai, R. C. Shang, X. Y. Song, L. Sun, L. Tao, C. Wang, G. F. Wang, J. Wang, W. S. Wang, Y. S. Wang, X. Y. Wen, B. B. Wu, B. Y. Wu, M. Wu, G. C. Xiao, H. Xu, J. W. Yang, S. Yang, Y. J. Yang, Y. J. Yang, Q. B. Yi, Q. Q. Yin, Y. You, W. C. Zhang, W. Z. Zhang, Y. Zhang, Y. Zhang, Y. F. Zhang, Y. J. Zhang, Z. Zhang, Z. Zhang, Z. L. Zhang, D. K. Zhou, J. F. Zhou, Y. Zhu, Y. X. Zhu, and R. L. Zhuang, Nature Astronomy **5**, 378 (2021), arXiv: 2005.11071.

309 A. M. Beloborodov, ApJ **896**, 142 (2020), arXiv: 1908.07743.

310 G. Chen, V. Ravi, and W. Lu, ApJ **897**, 146 (2020), arXiv: 2004.10787.

311 L. Nicastro, C. Guidorzi, E. Palazzi, L. Zampieri, M. Turatto, and A. Gardini, Universe **7**, 76 (2021), arXiv: 2103.07786.

312 Anita Collaboration, P. W. Gorham, P. Allison, S. W. Barwick, J. J. Beatty, D. Z. Besson, W. R. Binns, C. Chen, P. Chen, J. M. Clem, A. Connolly, P. F. Dowkontt, M. A. Duvernois, R. C. Field, D. Goldstein, A. Goodhue, C. Hast, C. L. Hebert, S. Hoover, M. H. Israel, J. Kowalski, J. G. Learned, K. M. Liewer, J. T. Link, E. Lusczek, S. Matsuno, B. C. Mercurio, C. Miki, P. Miočinović, J. Nam, C. J. Naudet, R. J. Nichol, K. Palladino, K. Reil, A. Romero-Wolf, M. Rosen, L. Ruckman, D. Saltzberg, D. Seckel, G. S. Varner, D. Walz, Y. Wang, C. Williams, F. Wu, and ANITA Collaboration, Astroparticle Physics **32**, 10 (2009), arXiv: 0812.1920.

313 G. Safronov, A. D. Avrorin, A. V. Avrorin, V. M. Aynutdinov, Z. Bardáčová, R. Bannasch, I. A. Belolaptikov, V. B. Brudanin, N. M. Budnev, G. V. Domogatsky, E. Eckerová, T. V. Elzhov, L. Fajt, S. V. Fialkovski, A. R. Gafarov, K. V. Golubkov, N. S. Gorshkov, T. I. Gress, R. A. Ivanov, M. S. Katulin, K. G. Kebkal, O. G. Kebkal, E. V. Khramov, M. M. Kolbin, K. V. Konischev, K. A. Kopański, A. V. Korobchenko, A. P. Koshechkin, V. A. Kozhin, M. K. Kryukov, M. V. Kruglov, V. F. Kulepov, M. B. Milenin, R. R. Mirgazov, D. V. Naumov, V. Nazari, W. Noga, D. P. Petukhov, E. N. Pliskovsky, M. I. Rozanov, V. D. Rushay, E. V. Ryabov, G. B. Safronov, B. A. Shaybonov, M. D. Shelepov, F. Šimkovic, A. V. Skurikhin, A. G. Solovjev, M. N. Sorokovikov, I. Štekl, E. O. Sushenok, O. V. Suvorova, V. A. Tabolenko, B. A. Tarashansky, Y. V. Yablokova, S. Yakovlev, and D. N. Zaborova, in *40th International Conference on High Energy Physics*, 606 (2021), arXiv: 2012.03373.

314 F. Halzen, in *26th International Cosmic Ray Conference (ICRC26), Volume 2*, volume 2 of *International Cosmic Ray Conference*, 428 (1999).

315 IceCube Collaboration, Science **342**, 1242856 (2013), arXiv: 1311.5238.

316 A. Rau, S. R. Kulkarni, N. M. Law, J. S. Bloom, D. Ciardi, G. S. Djorgovski, D. B. Fox, A. Gal-Yam, C. C. Grillmair, M. M. Kasliwal, P. E. Nugent, E. O. Ofek, R. M. Quimby, W. T. Reach, M. Shara, L. Bildsten, S. B. Cenko, A. J. Drake, A. V. Filippenko, D. J. Helfand, G. Helou, D. A. Howell, D. Poznanski, and M. Sullivan, PASP **121**, 1334 (2009), arXiv: 0906.5355.

317 E. A. Magnier, E. Schlafly, D. Finkbeiner, M. Juric, J. L. Tonry, W. S.

Burgett, K. C. Chambers, H. A. Flewelling, N. Kaiser, R. P. Kudritzki, J. S. Morgan, P. A. Price, W. E. Sweeney, and C. W. Stubbs, ApJS **205**, 20 (2013), arXiv: 1303.3634.

318 IceCube Collaboration, M. G. Aartsen, M. Ackermann, J. Adams, J. A. Aguilar, M. Ahlers, M. Ahrens, I. A. Samarai, D. Altmann, K. Andeen, T. Anderson, I. Ansseau, G. Anton, C. Argüelles, B. Arsioli, J. Auffenberg, S. Axani, H. Bagherpour, X. Bai, J. P. Barron, S. W. Barwick, V. Baum, R. Bay, J. J. Beatty, J. Becker Tjus, K. H. Becker, S. BenZvi, D. Berley, E. Bernardini, D. Z. Besson, G. Binder, D. Bindig, E. Blaufuss, S. Blot, C. Bohm, M. Börner, F. Bos, S. Böser, O. Botner, E. Bourbeau, J. Bourbeau, F. Bradascio, J. Braun, M. Brenzke, H. P. Bretz, S. Bron, J. Brostean-Kaiser, A. Burgman, R. S. Busse, T. Carver, E. Cheung, D. Chirkin, A. Christov, K. Clark, L. Classen, S. Coenders, G. H. Collin, J. M. Conrad, P. Coppin, P. Correa, D. F. Cowen, R. Cross, P. Dave, M. Day, J. P. A. M. de André, C. De Clercq, J. J. DeLaunay, H. Dembinski, S. DeRidder, P. Desiati, K. D. de Vries, G. de Wasseige, M. de With, T. DeYoung, J. C. Díaz-Vélez, V. di Lorenzo, H. Dujmovic, J. P. Dumm, M. Dunkman, E. Dvorak, B. Eberhardt, T. Ehrhardt, B. Eichmann, P. Eller, P. A. Evenson, S. Fahey, A. R. Fazely, J. Felde, K. Filimonov, C. Finley, S. Flis, A. Franckowiak, E. Friedman, A. Fritz, T. K. Gaisser, J. Gallagher, L. Gerhardt, K. Ghorbani, P. Giommi, T. Glauch, T. Glüsenkamp, A. Goldschmidt, J. G. Gonzalez, D. Grant, Z. Griffith, C. Haack, A. Hallgren, F. Halzen, K. Hanson, D. Hebecker, D. Heereman, K. Helbing, R. Hellauer, S. Hickford, J. Hignight, G. C. Hill, K. D. Hoffman, R. Hoffmann, T. Hoinka, B. Hokanson-Fasig, K. Hoshina, F. Huang, M. Huber, K. Hultqvist, M. Hünnefeld, R. Hussain, S. In, N. Iovine, A. Ishihara, E. Jacobi, G. S. Japaridze, M. Jeong, K. Jero, B. J. P. Jones, P. Kalaczynski, W. Kang, A. Kappes, D. Kappesser, T. Karg, A. Karle, U. Katz, M. Kauer, A. Keivani, J. L. Kelley, A. Kheirandish, J. Kim, M. Kim, T. Kintscher, J. Kiryluk, T. Kittler, S. R. Klein, R. Koirala, H. Kolanoski, L. Köpke, C. Kopper, S. Kopper, J. P. Koschinsky, D. J. Koskinen, M. Kowalski, B. Krammer, K. Krings, M. Kroll, G. Krückl, S. Kunwar, N. Kurahashi, T. Kuwabara, A. Kyriacou, M. Labare, J. L. Lanfranchi, M. J. Larson, F. Lauber, K. Leonard, M. Lesiak-Bzdak, M. Leuermann, Q. R. Liu, C. J. Lozano Mariscal, L. Lu, J. Lünemann, W. Luszczak, J. Madsen, G. Maggi, K. B. M. Mahn, S. Mancina, R. Maruyama, K. Mase, R. Maunu, K. Meagher, M. Medici, M. Meier, T. Menne, G. Merino, T. Meures, S. Miarecki, J. Micallef, G. Momenté, T. Montaruli, R. W. Moore, R. Morse, M. Moulai, R. Nahnhauer, P. Nakarmi, U. Naumann, G. Neer, H. Niederhausen, S. C. Nowicki, D. R. Nygren, A. Obertacke Pollmann, A. Olivas, A. O'Murchadha, E. O'Sullivan, P. Padovani, T. Palczewski, H. Pandya, D. V. Pankova, P. Peiffer, J. A. Pepper, C. Pérez de los Heros, D. Pieloth, E. Pinat, M. Plum, P. B. Price, G. T. Przybylski, C. Raab, L. Rädel, M. Rameez, K. Rawlins, I. C. Rea, R. Reimann, B. Relethford, M. Relich, E. Resconi, W. Rhode, M. Richman, S. Robertson, M. Rongen, C. Rott, T. Ruhe, D. Ryckbosch, D. Rysewyk, I. Safa, N. Sahakyan, T. Sälzer, S. E. Sanchez Herrera, A. Sandrock, J. Sandroos, M. Santander, S. Sarkar, S. Sarkar, K. Satalecka, P. Schlunder, T. Schmidt, A. Schneider, S. Schoenen, S. Schöneberg, L. Schumacher, S. Sclafani, D. Seckel, S. Seunarine, J. Soedingrekso, D. Soldin, M. Song, G. M. Spiczak, C. Spiering, J. Stachurska, M. Stamatikos, T. Stanev, A. Stasik, J. Stettner, A. Steuer, T. Stezelberger, R. G. Stokstad, A. Stößl, N. L. Strotjohann, T. Stuttard, G. W. Sullivan, M. Sutherland, I. Taboada, J. Tatar, F. Tenholt, S. Ter-Antonyan, A. Terliuk, S. Tilav, P. A. Toale, M. N. Tobin, C. Toennis, S. Toscano, D. Tosi, M. Tselengidou, C. F. Tung, A. Turcati, C. F. Turley, B. Ty, E. Unger, M. Usner, J. Vandenbroucke, W. Van Driessche, D. van Eijk, N. van Eijndhoven, S. Vanheule, J. van Santen, E. Vogel, M. Vraeghe, C. Walck, A. Wallace, M. Wallraff, F. D. Wandler, N. Wandkowsky, A. Waza, C. Weaver, M. J. Weiss, C. Wendt, J. Werthebach, S. Westerhoff, B. J. Whelan, N. Whitehorn, K. Wiebe, C. H. Wiebusch, L. Wille, D. R. Williams, L. Wills, M. Wolf, J. Wood, T. R. Wood, K. Woschnagg, D. L. Xu, X. W. Xu, Y. Xu, J. P. Yanez, G. Yodh, S. Yoshida, and T. Yuan, Science **361**, 147 (2018), arXiv: 1807.08794.

319 A. Franckowiak, S. Garrappa, V. Paliya, B. Shappee, R. Stein, N. L. Strotjohann, M. Kowalski, S. Buson, S. Kiehlmann, W. Max-Moerbeck, and R. Angioni, ApJ **893**, 162 (2020), arXiv: 2001.10232.

320 F. W. Stecker, C. Done, M. H. Salamon, and P. Sommers, Physical Review Letters **66**, 2697 (1991).

321 IceCube Collaboration, M. G. Aartsen, M. Ackermann, J. Adams, J. A. Aguilar, M. Ahlers, M. Ahrens, I. Al Samarai, D. Altmann, K. Andeen, T. Anderson, I. Ansseau, G. Anton, C. Argüelles, J. Auffenberg, S. Axani, H. Bagherpour, X. Bai, J. P. Barron, S. W. Barwick, V. Baum, R. Bay, J. J. Beatty, J. Becker Tjus, K. H. Becker, S. BenZvi, D. Berley, E. Bernardini, D. Z. Besson, G. Binder, D. Bindig, E. Blaufuss, S. Blot, C. Bohm, M. Börner, F. Bos, S. Böser, O. Botner, E. Bourbeau, J. Bourbeau, F. Bradascio, J. Braun, M. Brenzke, H. P. Bretz, S. Bron, J. Brostean-Kaiser, A. Burgman, R. S. Busse, T. Carver, E. Cheung, D. Chirkin, A. Christov, K. Clark, L. Classen, S. Coenders, G. H. Collin, J. M. Conrad, P. Coppin, P. Correa, D. F. Cowen, R. Cross, P. Dave, M. Day, J. P. A. M. de André, C. De Clercq, J. J. DeLaunay, H. Dembinski, S. De Ridder, P. Desiati, K. D. de Vries, G. de Wasseige, M. de With, T. DeYoung, J. C. Díaz-Vélez, V. di Lorenzo, H. Dujmovic, J. P. Dumm, M. Dunkman, E. Dvorak, B. Eberhardt, T. Ehrhardt, B. Eichmann, P. Eller, P. A. Evenson, S. Fahey, A. R. Fazely, J. Felde, K. Filimonov, C. Finley, S. Flis, A. Franckowiak, E. Friedman, A. Fritz, T. K. Gaisser, J. Gallagher, L. Gerhardt, K. Ghorbani, T. Glauch, T. Glüsenkamp, A. Goldschmidt, J. G. Gonzalez, D. Grant, Z. Griffith, C. Haack, A. Hallgren, F. Halzen, K. Hanson, D. Hebecker, D. Heereman, K. Helbing, R. Hellauer, S. Hickford, J. Hignight, G. C. Hill, K. D. Hoffman, R. Hoffmann, T. Hoinka, B. Hokanson-Fasig, K. Hoshina, F. Huang, M. Huber, K. Hultqvist, M. Hünnefeld, R. Hussain, S. In, N. Iovine, A. Ishihara, E. Jacobi, G. S. Japaridze, M. Jeong, K. Jero, B. J. P. Jones, P. Kalaczynski, W. Kang, A. Kappes, D. Kappesser, T. Karg, A. Karle, U. Katz, M. Kauer, A. Keivani, J. L. Kelley, A. Kheirandish, J. Kim, M. Kim, T. Kintscher, J. Kiryluk, T. Kittler, S. R. Klein, R. Koirala, H. Kolanoski, L. Köpke, C. Kopper, S. Kopper, J. P. Koschinsky, D. J. Koskinen, M. Kowalski, K. Krings, M. Kroll, G. Krückl, S. Kunwar, N. Kurahashi, T. Kuwabara, A. Kyriacou, M. Labare, J. L. Lanfranchi, M. J. Larson, F. Lauber, K. Leonard, M. Lesiak-Bzdak, M. Leuermann, Q. R. Liu, C. J. Lozano Mariscal, L. Lu, J. Lünemann, W. Luszczak, J. Madsen, G. Maggi, K. B. M. Mahn, S. Mancina, R. Maruyama, K. Mase, R. Maunu, K. Meagher, M. Medici, M. Meier, T. Menne, G. Merino, T. Meures, S. Miarecki, J. Micallef, G. Momenté, T. Montaruli, R. W. Moore, R. Morse, M. Moulai, R. Nahnhauer, P. Nakarmi, U. Naumann, G. Neer, H. Niederhausen, S. C. Nowicki, D. R. Nygren, A. Obertacke Pollmann, A. Olivas, A. O'Murchadha, E. O'Sullivan, T. Palczewski, H. Pandya, D. V. Pankova, P. Peiffer, J. A. Pepper, C. Pérez de los Heros, D. Pieloth, E. Pinat, M. Plum, P. B. Price, G. T. Przybylski, C. Raab, L. Rädel, M. Rameez, L. Rauch, K. Rawlins, I. C. Rea, R. Reimann, B. Relethford, M. Relich, E. Resconi, W. Rhode, M. Richman, S. Robertson, M. Rongen, C. Rott, T. Ruhe, D. Ryckbosch, D. Rysewyk, I. Safa, T. Sälzer, S. E. Sanchez Herrera, A. Sandrock, J. Sandroos, M. Santander, S. Sarkar, S. Sarkar, K. Satalecka, P. Schlunder, T. Schmidt, A. Schneider, S. Schoenen, S. Schöneberg, L. Schumacher, S. Sclafani, D. Seckel, S. Seunarine, J. Soedingrekso, D. Soldin, M. Song, G. M. Spiczak, C. Spiering, J. Stachurska, M. Stamatikos, T. Stanev, A. Stasik, R. Stein, J. Stettner, A. Steuer, T. Stezelberger, R. G. Stokstad, A. Stößl, N. L. Strotjohann, T. Stuttard, G. W. Sullivan, M. Sutherland, I. Taboada, J. Tatar, F. Tenholt, S. Ter-Antonyan, A. Terliuk, S. Tilav, P. A. Toale, M. N. Tobin, C. Toennis, S. Toscano, D. Tosi, M. Tselengidou, C. F. Tung, A. Turcati, C. F. Turley, B. Ty, E. Unger, M. Usner, J. Vandenbroucke, W. Van Driessche, D. van Eijk, N. van Eijnd-

hoven, S. Vanheule, J. van Santen, E. Vogel, M. Vraeghe, C. Walck, A. Wallace, M. Wallraff, F. D. Wandler, N. Wandkowsky, A. Waza, C. Weaver, M. J. Weiss, C. Wendt, J. Werthebach, S. Westerhoff, B. J. Whelan, N. Whitehorn, K. Wiebe, C. H. Wiebusch, L. Wille, D. R. Williams, L. Wills, M. Wolf, J. Wood, T. R. Wood, K. Woschnagg, D. L. Xu, X. W. Xu, Y. Xu, J. P. Yanez, G. Yodh, S. Yoshida, T. Yuan, Fermi-LAT Collaboration, S. Abdollahi, M. Ajello, R. Angioni, L. Baldini, J. Ballet, G. Barbiellini, D. Bastieri, K. Bechtol, R. Bellazzini, B. Berenji, E. Bissaldi, R. D. Blandford, R. Bonino, E. Bottacini, J. Bregeon, P. Bruel, R. Buehler, T. H. Burnett, E. Burns, S. Buson, R. A. Cameron, R. Caputo, P. A. Caraveo, E. Cavazzuti, E. Charles, S. Chen, C. C. Cheung, J. Chiang, G. Chiaro, S. Ciprini, J. Cohen-Tanugi, J. Conrad, D. Costantin, S. Cutini, F. D'Ammando, F. de Palma, S. W. Digel, N. Di Lalla, M. Di Mauro, L. Di Venere, A. Domínguez, C. Favuzzi, A. Franckowiak, Y. Fukazawa, S. Funk, P. Fusco, F. Gargano, D. Gasparrini, N. Giglietto, M. Giomi, P. Giommi, F. Giordano, M. Giroletti, T. Glanzman, D. Green, I. A. Grenier, M. H. Grondin, S. Guiriec, A. K. Harding, M. Hayashida, E. Hays, J. W. Hewitt, D. Horan, G. Jóhannesson, M. Kadler, S. Kensei, D. Kocevski, F. Krauss, M. Kreter, M. Kuss, G. La Mura, S. Larsson, L. Latronico, M. Lemoine-Goumard, J. Li, F. Longo, F. Loparco, M. N. Lovellette, P. Lubrano, J. D. Magill, S. Maldera, D. Malyshev, A. Manfreda, M. N. Mazziotta, J. E. McEnery, M. Meyer, P. F. Michelson, T. Mizuno, M. E. Monzani, A. Morselli, I. V. Moskalenko, M. Negro, E. Nuss, R. Ojha, N. Omodei, M. Orienti, E. Orlando, M. Palatiello, V. S. Paliya, J. S. Perkins, M. Persic, M. Pesce-Rollins, F. Piron, T. A. Porter, G. Principe, S. Rainò, R. Rando, B. Rani, M. Razzano, S. Razzaque, A. Reimer, O. Reimer, N. Renault-Tinacci, S. Ritz, L. S. Rochester, P. M. Saz Parkinson, C. Sgrò, E. J. Siskind, G. Spandre, P. Spinelli, D. J. Suson, H. Tajima, M. Takahashi, Y. Tanaka, J. B. Thayer, D. J. Thompson, L. Tibaldo, D. F. Torres, E. Torresi, G. Tosti, E. Troja, J. Valverde, G. Vianello, M. Vogel, K. Wood, M. Wood, G. Zaharijas, MAGIC Collaboration, M. L. Ahnen, S. Ansoldi, L. A. Antonelli, C. Arcaro, D. Baack, A. Babić, B. Banerjee, P. Bangale, U. Barres de Almeida, J. A. Barrio, J. Becerra González, W. Bednarek, E. Bernardini, A. Berti, W. Bhattacharyya, A. Biland, O. Blanch, G. Bonnoli, A. Carosi, R. Carosi, G. Ceribella, A. Chatterjee, S. M. Colak, P. Colin, E. Colombo, J. L. Contreras, J. Cortina, S. Covino, P. Cumani, P. Da Vela, F. Dazzi, A. De Angelis, B. De Lotto, M. Delfino, J. Delgado, F. Di Pierro, A. Domínguez, D. Dominis Prester, D. Dorner, M. Doro, S. Einecke, D. Elsaesser, V. Fallah Ramazani, A. Fernández-Barral, D. Fidalgo, L. Foffano, K. Pfrang, M. V. Fonseca, L. Font, A. Franceschini, C. Fruck, D. Galindo, S. Gallozzi, R. J. García López, M. Garczarczyk, M. Gaug, P. Giammaria, N. Godinović, D. Gora, D. Guberman, D. Hadasch, A. Hahn, T. Hassan, M. Hayashida, J. Herrera, J. Hose, D. Hrupec, S. Inoue, K. Ishio, Y. Konno, H. Kubo, J. Kushida, D. Lelas, E. Lindfors, S. Lombardi, F. Longo, M. López, C. Maggio, P. Majumdar, M. Makariev, G. Maneva, M. Manganaro, K. Mannheim, L. Maraschi, M. Mariotti, M. Martínez, S. Masuda, D. Mazin, M. Minev, J. M. M, R. Mirzoyan, A. Moralejo, V. Moreno, E. Moretti, T. Nagayoshi, V. Neustroev, A. Niedzwiecki, M. Nievas Rosillo, C. Nigro, K. Nilsson, D. Ninci, K. Nishijima, K. Noda, L. Nogués, S. Paiano, J. Palacio, D. Paneque, R. Paoletti, J. M. Paredes, G. Pedaletti, M. Peresano, M. Persic, P. G. Prada Moroni, E. Prandini, I. Puljak, J. Rodriguez Garcia, I. Reichardt, W. Rhode, M. Ribó, J. Rico, C. Righi, A. Rugliancich, T. Saito, K. Satalecka, T. Schweizer, J. Sitarek, I. Šnidaric ´, D. Sobczynska, A. Stamerra, M. Strzys, T. Surić, M. Takahashi, F. Tavecchio, P. Temnikov, T. Terzić, M. Teshima, N. Torres-Albà, A. Treves, S. Tsujimoto, G. Vanzo, M. Vazquez Acosta, I. Vovk, J. E. Ward, M. Will, S, D. Zaric ´, AGILE Team, F. Lucarelli, M. Tavani, G. Piano, I. Donnarumma, C. Pittori, F. Verrecchia, G. Barbiellini, A. Bulgarelli, P. Caraveo, P. W. Cattaneo, S. Colafrancesco, E. Costa, G. Di Cocco, A. Ferrari, F. Gianotti, A. Giuliani, P. Lipari, S. Mereghetti, A. Morselli, L. Pacciani, F. Paoletti, N. Parmiggiani, A. Pellizzoni, P. Picozza, M. Pilia, A. Rappoldi, A. Trois, S. Vercellone, V. Vittorini, ASAS-SN Team, K. Z. Stanek, A. Franckowiak, C. S. Kochanek, J. F. Beacom, T. A. Thompson, T. W. S. Holoien, S. Dong, J. L. Prieto, B. J. Shappee, S. Holmbo, HAWC Collaboration, A. U. Abeysekara, A. Albert, R. Alfaro, C. Alvarez, R. Arceo, J. C. Arteaga-Velázquez, D. Avila Rojas, H. A. Ayala Solares, A. Becerril, E. Belmont-Moreno, A. Bernal, K. S. Caballero-Mora, T. Capistrán, A. Carramiñana, S. Casanova, M. Castillo, U. Cotti, J. Cotzomi, S. Coutiño de León, C. De León, E. De la Fuente, R. Diaz Hernandez, S. Dichiara, B. L. Dingus, M. A. DuVernois, J. C. Díaz-Vélez, R. W. Ellsworth, K. Engel, D. W. Fiorino, H. Fleischhack, N. Fraija, J. A. García-González, F. Garfias, A. González Muñoz, M. M. González, J. A. Goodman, Z. Hampel-Arias, J. P. Harding, S. Hernandez, B. Hona, F. Hueyotl-Zahuantitla, C. M. Hui, P. Hüntemeyer, A. Iriarte, A. Jardin-Blicq, V. Joshi, S. Kaufmann, G. J. Kunde, A. Lara, R. J. Lauer, W. H. Lee, D. Lennarz, H. León Vargas, J. T. Linnemann, A. L. Longinotti, G. Luis-Raya, R. Luna-García, K. Malone, S. S. Marinelli, O. Martinez, I. Martinez-Castellanos, J. Martínez-Castro, H. Martínez-Huerta, J. A. Matthews, P. Miranda-Romagnoli, E. Moreno, M. Mostafá, A. Nayerhoda, L. Nellen, M. Newbold, M. U. Nisa, R. Noriega-Papaqui, R. Pelayo, J. Pretz, E. G. Pérez-Pérez, Z. Ren, C. D. Rho, C. Rivière, D. Rosa-González, M. Rosenberg, E. Ruiz-Velasco, E. Ruiz-Velasco, F. Salesa Greus, A. Sandoval, M. Schneider, H. Schoorlemmer, G. Sinnis, A. J. Smith, R. W. Springer, P. Surajbali, O. Tibolla, K. Tollefson, I. Torres, L. Villaseñor, T. Weisgarber, F. Werner, T. Yapici, Y. Gaurang, A. Zepeda, H. Zhou, J. D. Álvarez, H. E. S. S. Collaboration, H. Abdalla, E. O. Angüner, C. Armand, M. Backes, Y. Becherini, D. Berge, M. Böttcher, C. Boisson, J. Bolmont, S. Bonnefoy, P. Bordas, F. Brun, M. Büchele, T. Bulik, S. Caroff, A. Carosi, S. Casanova, M. Cerruti, N. Chakraborty, S. Chandra, A. Chen, S. Colafrancesco, I. D. Davids, C. Deil, J. Devin, A. Djannati-Ataï, K. Egberts, G. Emery, S. Eschbach, A. Fiasson, G. Fontaine, S. Funk, M. Füßling, Y. A. Gallant, F. Gaté, G. Giavitto, D. Glawion, J. F. Glicenstein, D. Gottschall, M. H. Grondin, M. Haupt, G. Henri, J. A. Hinton, C. Hoischen, T. L. Holch, D. Huber, M. Jamrozy, D. Jankowsky, F. Jankowsky, L. Jouvin, I. Jung-Richardt, D. Kerszberg, B. Khélifi, J. King, S. Klepser, W. Kluz ´niak, N. Komin, M. Kraus, J. Lefaucheur, A. Lemière, M. Lemoine-Goumard, J. P. Lenain, E. Leser, T. Lohse, R. López-Coto, M. Lorentz, I. Lypova, V. Marandon, G. Guillem Martí-Devesa, G. Maurin, A. M. W. Mitchell, R. Moderski, M. Mohamed, L. Mohrmann, E. Moulin, T. Murach, M. de Naurois, F. Niederwanger, J. Niemiec, L. Oakes, P. O'Brien, S. Ohm, M. Ostrowski, I. Oya, M. Panter, R. D. Parsons, C. Perennes, Q. Piel, S. Pita, V. Poireau, A. Priyana Noel, H. Prokoph, G. Pühlhofer, A. Quirrenbach, S. Raab, R. Rauth, M. Renaud, F. Rieger, L. Rinchiuso, C. Romoli, G. Rowell, B. Rudak, D. A. Sasaki, M. Sanchez, R. Schlickeiser, F. Schüssler, A. Schulz, U. Schwanke, M. Seglar-Arroyo, N. Shafi, R. Simoni, H. Sol, C. Stegmann, C. Steppa, T. Tavernier, A. M. Taylor, D. Tiziani, C. Trichard, M. Tsirou, C. van Eldik, C. van Rensburg, B. van Soelen, J. Veh, P. Vincent, F. Voisin, S. J. Wagner, R. M. Wagner, A. Wierzcholska, R. Zanin, A. A. Zdziarski, A. Zech, A. Ziegler, J. Zorn, N. Żywucka, INTEGRAL Team, V. Savchenko, C. Ferrigno, A. Bazzano, R. Diehl, E. Kuulkers, P. Laurent, S. Mereghetti, L. Natalucci, F. Panessa, J. Rodi, P. Ubertini, K. Kanata, S. O. Teams, T. Morokuma, K. Ohta, Y. T. Tanaka, H. Mori, M. Yamanaka, K. S. Kawabata, Y. Utsumi, T. Nakaoka, M. Kawabata, H. Nagashima, M. Yoshida, Y. Matsuoka, R. Itoh, Kapteyn Team, W. Keel, Liverpool Telescope Team, C. Copperwheat, I. Steele, Swift/NuSTAR Team, S. B. Cenko, D. F. Cowen, J. J. DeLaunay, P. A. Evans, D. B. Fox, A. Keivani, J. A. Kennea, F. E. Marshall, J. P. Osborne, M. Santander, A. Tohuvavohu, C. F. Turley, VERITAS Collaboration, A. U. Abeysekara, A. Archer, W. Benbow, R. Bird, A. Brill, R. Brose, M. Buchovecky, J. H. Buckley,

V. Bugaev, J. L. Christiansen, M. P. Connolly, W. Cui, M. K. Daniel, M. Errando, A. Falcone, Q. Feng, J. P. Finley, L. Fortson, A. Furniss, O. Gueta, M. Hütten, O. Hervet, G. Hughes, T. B. Humensky, C. A. Johnson, P. Kaaret, P. Kar, N. Kelley-Hoskins, M. Kertzman, D. Kieda, M. Krause, F. Krennrich, S. Kumar, M. J. Lang, T. T. Y. Lin, G. Maier, S. McArthur, P. Moriarty, R. Mukherjee, D. Nieto, S. O'Brien, R. A. Ong, A. N. Otte, N. Park, A. Petrashyk, M. Pohl, A. Popkow, S. E. Pueschel, J. Quinn, K. Ragan, P. T. Reynolds, G. T. Richards, E. Roache, C. Rulten, I. Sadeh, M. Santander, S. S. Scott, G. H. Sembroski, K. Shahinyan, I. Sushch, S. Trépanier, J. Tyler, V. V. Vassiliev, S. P. Wakely, A. Weinstein, R. M. Wells, P. Wilcox, A. Wilhelm, D. A. Williams, B. Zitzer, VLA/B Team, A. J. Tetarenko, A. E. Kimball, J. C. A. Miller-Jones, and G. R. Sivakoff, Science **361**, eaat1378 (2018), arXiv: 1807.08816.

322 E. O'Sullivan and C. Finley, in *36th International Cosmic Ray Conference (ICRC2019)*, volume 36 of *International Cosmic Ray Conference*, 973 (2019), arXiv: 1908.05526.

323 E. Waxman and J. Bahcall, Physical Review Letters **78**, 2292 (1997), arXiv: astro-ph/9701231.

324 D. Xiao and Z. G. Dai, ApJ **790**, 59 (2014), arXiv: 1406.2792.

325 H.-N. He, A. Kusenko, S. Nagataki, Y.-Z. Fan, and D.-M. Wei, ApJ **856**, 119 (2018), arXiv: 1803.07478.

326 E. E. Salpeter, ApJ **140**, 796 (1964).

327 D. Lynden-Bell, Nature **223**, 690 (1969).

328 R. Antonucci, Nature **495**, 165 (2013).

329 R. Antonucci, arXiv e-prints arXiv:1501.02001 (2015), arXiv: 1501.02001.

330 A. Lawrence, Nature Astronomy **2**, 102 (2018), arXiv: 1802.00408.

331 R. Antonucci, Nature Astronomy **2**, 504 (2018).

332 C. L. MacLeod, Ž. Ivezić, C. S. Kochanek, S. Kozłowski, B. Kelly, E. Bullock, A. Kimball, B. Sesar, D. Westman, K. Brooks, R. Gibson, A. C. Becker, and W. H. de Vries, ApJ **721**, 1014 (2010), arXiv: 1004.0276.

333 B. W. Lyke, A. N. Higley, J. N. McLane, D. P. Schurhammer, A. D. Myers, A. J. Ross, K. Dawson, S. Chabanier, P. Martini, N. G. Busca, H. d. Mas des Bourboux, M. Salvato, A. Streblyanska, P. Zarrouk, E. Burtin, S. F. Anderson, J. Bautista, D. Bizyaev, W. N. Brandt, J. Brinkmann, J. R. Brownstein, J. Comparat, P. Green, A. de la Macorra, A. Muñoz Gutiérrez, J. Hou, J. A. Newman, N. Palanque-Delabrouille, I. Pâris, W. J. Percival, P. Petitjean, J. Rich, G. Rossi, D. P. Schneider, A. Smith, M. Vivek, and B. A. Weaver, ApJS **250**, 8 (2020), arXiv: 2007.09001.

334 C. L. MacLeod, Ž. Ivezić, B. Sesar, W. de Vries, C. S. Kochanek, B. C. Kelly, A. C. Becker, R. H. Lupton, P. B. Hall, G. T. Richards, S. F. Anderson, and D. P. Schneider, ApJ **753**, 106 (2012), arXiv: 1112.0679.

335 A. Rau, S. R. Kulkarni, N. M. Law, J. S. Bloom, D. Ciardi, G. S. Djorgovski, D. B. Fox, A. Gal-Yam, C. C. Grillmair, M. M. Kasliwal, P. E. Nugent, E. O. Ofek, R. M. Quimby, W. T. Reach, M. Shara, L. Bildsten, S. B. Cenko, A. J. Drake, A. V. Filippenko, D. J. Helfand, G. Helou, D. A. Howell, D. Poznanski, and M. Sullivan, PASP **121**, 1334 (2009), arXiv: 0906.5355.

336 F. J. Masci, R. R. Laher, B. Rusholme, D. L. Shupe, S. Groom, J. Surace, E. Jackson, S. Monkewitz, R. Beck, D. Flynn, S. Terek, W. Landry, E. Hacopians, V. Desai, J. Howell, T. Brooke, D. Imel, S. Wachter, Q.-Z. Ye, H.-W. Lin, S. B. Cenko, V. Cunningham, U. Rebbapragada, B. Bue, A. A. Miller, A. Mahabal, E. C. Bellm, M. T. Patterson, M. Jurić, V. Z. Golkhou, E. O. Ofek, R. Walters, M. Graham, M. M. Kasliwal, R. G. Dekany, T. Kupfer, K. Burdge, C. B. Cannella, T. Barlow, A. Van Sistine, M. Giomi, C. Fremling, N. Blagorodnova, D. Levitan, R. Riddle, R. M. Smith, G. Helou, T. A. Prince, and S. R. Kulkarni, PASP **131**, 018003 (2019), arXiv: 1902.01872.

337 K. C. Chambers, E. A. Magnier, N. Metcalfe, H. A. Flewelling, M. E. Huber, C. Z. Waters, L. Denneau, P. W. Draper, D. Farrow, D. P. Finkbeiner, C. Holmberg, J. Koppenhoefer, P. A. Price, A. Rest, R. P. Saglia, E. F. Schlafly, S. J. Smartt, W. Sweeney, R. J. Wainscoat, W. S. Burgett, S. Chastel, T. Grav, J. N. Heasley, K. W. Hodapp, R. Jedicke, N. Kaiser, R. P. Kudritzki, G. A. Luppino, R. H. Lupton, D. G. Monet, J. S. Morgan, P. M. Onaka, B. Shiao, C. W. Stubbs, J. L. Tonry, R. White, E. Bañados, E. F. Bell, R. Bender, E. J. Bernard, M. Boegner, F. Boffi, M. T. Botticella, A. Calamida, S. Casertano, W. P. Chen, X. Chen, S. Cole, N. Deacon, C. Frenk, A. Fitzsimmons, S. Gezari, V. Gibbs, C. Goessl, T. Goggia, R. Gourgue, B. Goldman, P. Grant, E. K. Grebel, N. C. Hambly, G. Hasinger, A. F. Heavens, T. M. Heckman, R. Henderson, T. Henning, M. Holman, U. Hopp, W. H. Ip, S. Isani, M. Jackson, C. D. Keyes, A. M. Koekemoer, R. Kotak, D. Le, D. Liska, K. S. Long, J. R. Lucey, M. Liu, N. F. Martin, G. Masci, B. McLean, E. Mindel, P. Misra, E. Morganson, D. N. A. Murphy, A. Obaika, G. Narayan, M. A. Nieto-Santisteban, P. Norberg, J. A. Peacock, E. A. Pier, M. Postman, N. Primak, C. Rae, A. Rai, A. Riess, A. Riffeser, H. W. Rix, S. Röser, R. Russel, L. Rutz, E. Schilbach, A. S. B. Schultz, D. Scolnic, L. Strolger, A. Szalay, S. Seitz, E. Small, K. W. Smith, D. R. Soderblom, P. Taylor, R. Thomson, A. N. Taylor, A. R. Thakar, J. Thiel, D. Thilker, D. Unger, Y. Urata, J. Valenti, J. Wagner, T. Walder, F. Walter, S. P. Watters, S. Werner, W. M. Wood-Vasey, and R. Wyse, arXiv e-prints arXiv:1612.05560 (2016), arXiv: 1612.05560.

338 J. H. Krolik, K. Horne, T. R. Kallman, M. A. Malkan, R. A. Edelson, and G. A. Kriss, ApJ **371**, 541 (1991).

339 M. Sun, Y. Xue, W. N. Brandt, W.-M. Gu, J. R. Trump, Z. Cai, Z. He, D.-b. Lin, T. Liu, and J. Wang, ApJ **891**, 178 (2020), arXiv: 2002.08564.

340 M. Sun, Y. Xue, H. Guo, J. Wang, W. N. Brandt, J. R. Trump, Z. He, T. Liu, J. Wu, and H. Li, ApJ **902**, 7 (2020), arXiv: 2008.09967.

341 Z.-Y. Cai, J.-X. Wang, F.-F. Zhu, M.-Y. Sun, W.-M. Gu, X.-W. Cao, and F. Yuan, ApJ **855**, 117 (2018), arXiv: 1711.06266.

342 Z.-Y. Cai, J.-X. Wang, and M. Sun, ApJ **892**, 63 (2020), arXiv: 2002.11116.

343 M.-H. Ulrich, L. Maraschi, and C. M. Urry, ARA&A **35**, 445 (1997).

344 B. C. Kelly, J. Bechtold, and A. Siemiginowska, ApJ **698**, 895 (2009), arXiv: 0903.5315.

345 H. Guo, J. Wang, Z. Cai, and M. Sun, ApJ **847**, 132 (2017), arXiv: 1709.05271.

346 W.-y. Kang, J.-X. Wang, Z.-Y. Cai, H.-X. Guo, F.-F. Zhu, X.-W. Cao, W.-M. Gu, and F. Yuan, ApJ **868**, 58 (2018), arXiv: 1810.03776.

347 Z. Cai, Y. Sun, J. Wang, F. Zhu, W. Gu, and F. Yuan, Science China Physics, Mechanics, and Astronomy **62**, 69511 (2019), arXiv: 1811.06984.

348 W.-Y. Kang, J.-X. Wang, Z.-Y. Cai, and W.-K. Ren, ApJ **911**, 148 (2021), arXiv: 2103.01424.

349 Z. He, T. Wang, G. Liu, H. Wang, W. Bian, K. Tchernyshyov, G. Mou, Y. Xu, H. Zhou, R. Green, and J. Xu, Nature Astronomy **3**, 265 (2019), arXiv: 1812.08982.

350 Z. He, G. Liu, T. Wang, and G. Mou, Science Advances **8**, eabk3291 (2022).

351 S. Kozłowski, A&A **597**, A128 (2017), arXiv: 1611.08248.

352 K. L. Suberlak, Ž. Ivezić, and C. MacLeod, ApJ **907**, 96 (2021), arXiv: 2012.12907.

353 C. Xin, M. Charisi, Z. Haiman, and D. Schiminovich, MNRAS **495**, 1403 (2020), arXiv: 2001.03154.

354 Z. Yu, P. Martini, T. M. Davis, R. A. Gruendl, J. K. Hoormann, C. S. Kochanek, C. Lidman, D. Mudd, B. M. Peterson, W. Wester, S. Allam, J. Annis, J. Asorey, S. Avila, M. Banerji, E. Bertin, D. Brooks, E. Buckley-Geer, J. Calcino, A. C. Rosell, D. Carollo, M. C. Kind, J. Carretero, C. E. Cunha, C. B. D'Andrea, L. N. d. Costa, J. De Vicente, S. Desai, H. T. Diehl, P. Doel, T. F. Eifler, B. Flaugher, P. Fosalba, J. Frieman, J. García-Bellido, E. Gaztanaga, K. Glazebrook, D. Gruen, J. Gschwend, G. Gutierrez, W. G. Hartley, S. R. Hinton, D. L. Hollowood, K. Honscheid, B. Hoyle, D. J. James, A. G.

Kim, E. Krause, K. Kuehn, N. Kuropatkin, G. F. Lewis, M. Lima, E. Macaulay, M. A. G. Maia, J. L. Marshall, F. Menanteau, R. Miquel, A. Möller, A. A. Plazas, A. K. Romer, E. Sanchez, V. Scarpine, M. Schubnell, S. Serrano, M. Smith, R. C. Smith, M. Soares-Santos, F. Sobreira, E. Suchyta, E. Swann, M. E. C. Swanson, G. Tarle, B. E. Tucker, D. L. Tucker, and V. Vikram, ApJS **246**, 16 (2020), arXiv: 1811.03638.

355 Y. Homayouni, J. R. Trump, C. J. Grier, Y. Shen, D. A. Starkey, W. N. Brandt, G. Fonseca Alvarez, P. B. Hall, K. Horne, K. Kinemuchi, J. I-Hsiu Li, I. D. McGreer, M. Sun, L. C. Ho, and D. P. Schneider, ApJ **880**, 126 (2019), arXiv: 1806.08360.

356 J. H. H. Chan, M. Millon, V. Bonvin, and F. Courbin, A&A **636**, A52 (2020).

357 K. L. Smith, R. F. Mushotzky, P. T. Boyd, M. Malkan, S. B. Howell, and D. M. Gelino, ApJ **857**, 141 (2018), arXiv: 1803.06436.

358 F.-F. Zhu, J.-X. Wang, Z.-Y. Cai, Y.-H. Sun, M.-Y. Sun, and J.-X. Zhang, ApJ **860**, 29 (2018), arXiv: 1711.00870.

359 R. Edelson, J. Gelbord, E. Cackett, S. Connolly, C. Done, M. Fausnaugh, E. Gardner, N. Gehrels, M. Goad, K. Horne, I. McHardy, B. M. Peterson, S. Vaughan, M. Vestergaard, A. Breeveld, A. J. Barth, M. Bentz, M. Bottorff, W. N. Brandt, S. M. Crawford, E. Dalla Bontà, D. Emmanoulopoulos, P. Evans, R. Figuera Jaimes, A. V. Filippenko, G. Ferland, D. Grupe, M. Joner, J. Kennea, K. T. Korista, H. A. Krimm, G. Kriss, D. C. Leonard, S. Mathur, H. Netzer, J. Nousek, K. Page, E. Romero-Colmenero, M. Siegel, D. A. Starkey, T. Treu, H. A. Vogler, H. Winkler, and W. Zheng, ApJ **840**, 41 (2017), arXiv: 1703.06901.

360 R. Edelson, J. Gelbord, E. Cackett, B. M. Peterson, K. Horne, A. J. Barth, D. A. Starkey, M. Bentz, W. N. Brandt, M. Goad, M. Joner, K. Korista, H. Netzer, K. Page, P. Uttley, S. Vaughan, A. Breeveld, S. B. Cenko, C. Done, P. Evans, M. Fausnaugh, G. Ferland, D. Gonzalez-Buitrago, J. Gropp, D. Grupe, J. Kaastra, J. Kennea, G. Kriss, S. Mathur, M. Mehdipour, D. Mudd, J. Nousek, T. Schmidt, M. Vestergaard, and C. Villforth, ApJ **870**, 123 (2019), arXiv: 1811.07956.

361 T. Li, M. Sun, X. Xu, W. N. Brandt, J. R. Trump, Z. Yu, J. Wang, Y. Xue, Z. Cai, W.-M. Gu, Y. Homayouni, T. Liu, J.-F. Wang, Z. Zhang, and H.-K. Li, ApJL **912**, L29 (2021), arXiv: 2104.12327.

362 Y.-H. Sun, J.-X. Wang, X.-Y. Chen, and Z.-Y. Zheng, ApJ **792**, 54 (2014), arXiv: 1407.4230.

363 Z.-Y. Cai, J.-X. Wang, W.-M. Gu, Y.-H. Sun, M.-C. Wu, X.-X. Huang, and X.-Y. Chen, ApJ **826**, 7 (2016), arXiv: 1605.03185.

364 N. Rumbaugh, Y. Shen, E. Morganson, X. Liu, M. Banerji, R. G. McMahon, F. B. Abdalla, A. Benoit-Lévy, E. Bertin, D. Brooks, E. Buckley-Geer, D. Capozzi, A. Carnero Rosell, M. Carrasco Kind, J. Carretero, C. E. Cunha, C. B. D'Andrea, L. N. da Costa, D. L. DePoy, S. Desai, P. Doel, J. Frieman, J. García-Bellido, D. Gruen, R. A. Gruendl, J. Gschwend, G. Gutierrez, K. Honscheid, D. J. James, K. Kuehn, S. Kuhlmann, N. Kuropatkin, M. Lima, M. A. G. Maia, J. L. Marshall, P. Martini, F. Menanteau, A. A. Plazas, K. Reil, A. Roodman, E. Sanchez, V. Scarpine, R. Schindler, M. Schubnell, E. Sheldon, M. Smith, M. Soares-Santos, F. Sobreira, E. Suchyta, M. E. C. Swanson, A. R. Walker, W. Wester, and DES Collaboration, ApJ **854**, 160 (2018), arXiv: 1706.07875.

365 D. E. Vanden Berk, B. C. Wilhite, R. G. Kron, S. F. Anderson, R. J. Brunner, P. B. Hall, Ž. Ivezić, G. T. Richards, D. P. Schneider, D. G. York, J. V. Brinkmann, D. Q. Lamb, R. C. Nichol, and D. J. Schlegel, ApJ **601**, 692 (2004), arXiv: astro-ph/0310336.

366 B. Sesar, Ž. Ivezić, R. H. Lupton, M. Jurić, J. E. Gunn, G. R. Knapp, N. DeLee, J. A. Smith, G. Miknaitis, H. Lin, D. Tucker, M. Doi, M. Tanaka, M. Fukugita, J. Holtzman, S. Kent, B. Yanny, D. Schlegel, D. Finkbeiner, N. Padmanabhan, C. M. Rockosi, N. Bond, B. Lee, C. Stoughton, S. Jester, H. Harris, P. Harding, J. Brinkmann, D. P. Schneider, D. York, M. W. Richmond, and D. Vanden Berk, AJ **134**, 2236 (2007), arXiv: 0704.0655.

367 W. Ren, J. Wang, Z. Cai, and H. Guo, arXiv e-prints arXiv:2111.07057 (2021), arXiv: 2111.07057.

368 C. L. MacLeod, P. J. Green, S. F. Anderson, A. Bruce, M. Eracleous, M. Graham, D. Homan, A. Lawrence, A. LeBleu, N. P. Ross, J. J. Ruan, J. Runnoe, D. Stern, W. Burgett, K. C. Chambers, N. Kaiser, E. Magnier, and N. Metcalfe, ApJ **874**, 8 (2019), arXiv: 1810.00087.

369 Z. Sheng, T. Wang, N. Jiang, C. Yang, L. Yan, L. Dou, and B. Peng, ApJL **846**, L7 (2017), arXiv: 1707.02686.

370 Z. Sheng, T. Wang, N. Jiang, J. Ding, Z. Cai, H. Guo, L. Sun, L. Dou, and C. Yang, ApJ **889**, 46 (2020), arXiv: 1905.02904.

371 N. P. Ross, K. E. S. Ford, M. Graham, B. McKernan, D. Stern, A. M. Meisner, R. J. Assef, A. Dey, A. J. Drake, H. D. Jun, and D. Lang, MNRAS **480**, 4468 (2018), arXiv: 1805.06921.

372 D. Stern, B. McKernan, M. J. Graham, K. E. S. Ford, N. P. Ross, A. M. Meisner, R. J. Assef, M. Baloković, M. Brightman, A. Dey, A. Drake, S. G. Djorgovski, P. Eisenhardt, and H. D. Jun, ApJ **864**, 27 (2018), arXiv: 1805.06920.

373 H. Noda and C. Done, MNRAS **480**, 3898 (2018), arXiv: 1805.07873.

374 J. Dexter and M. C. Begelman, MNRAS **483**, L17 (2019), arXiv: 1807.03314.

375 M. Sniegowska, B. Czerny, E. Bon, and N. Bon, A&A **641**, A167 (2020), arXiv: 2007.06441.

376 J.-M. Wang and E. Bon, A&A **643**, L9 (2020), arXiv: 2010.04417.

377 P. Martini and D. P. Schneider, ApJL **597**, L109 (2003), arXiv: astro-ph/0309650.

378 M. J. Graham, S. G. Djorgovski, A. J. Drake, D. Stern, A. A. Mahabal, E. Glikman, S. Larson, and E. Christensen, MNRAS **470**, 4112 (2017), arXiv: 1706.03079.

379 A. Lawrence, A. G. Bruce, C. MacLeod, S. Gezari, M. Elvis, M. Ward, S. J. Smartt, K. W. Smith, D. Wright, M. Fraser, P. Marshall, N. Kaiser, W. Burgett, E. Magnier, J. Tonry, K. Chambers, R. Wainscoat, C. Waters, P. Price, N. Metcalfe, S. Valenti, R. Kotak, A. Mead, C. Inserra, T. W. Chen, and A. Soderberg, MNRAS **463**, 296 (2016), arXiv: 1605.07842.

380 M. J. Graham, K. E. S. Ford, B. McKernan, N. P. Ross, D. Stern, K. Burdge, M. Coughlin, S. G. Djorgovski, A. J. Drake, D. Duev, M. Kasliwal, A. A. Mahabal, S. van Velzen, J. Belecki, E. C. Bellm, R. Burruss, S. B. Cenko, V. Cunningham, G. Helou, S. R. Kulkarni, F. J. Masci, T. Prince, D. Reiley, H. Rodriguez, B. Rusholme, R. M. Smith, and M. T. Soumagnac, PRL **124**, 251102 (2020), arXiv: 2006.14122.

381 A. I. MacFadyen and M. Milosavljević, ApJ **672**, 83 (2008), arXiv: astro-ph/0607467.

382 B. D. Farris, P. Duffell, A. I. MacFadyen, and Z. Haiman, ApJ **783**, 134 (2014), arXiv: 1310.0492.

383 M. J. Graham, S. G. Djorgovski, D. Stern, A. J. Drake, A. A. Mahabal, C. Donalek, E. Glikman, S. Larson, and E. Christensen, MNRAS **453**, 1562 (2015), arXiv: 1507.07603.

384 T. Liu, S. Gezari, S. Heinis, E. A. Magnier, W. S. Burgett, K. Chambers, H. Flewelling, M. Huber, K. W. Hodapp, N. Kaiser, R.-P. Kudritzki, J. L. Tonry, R. J. Wainscoat, and C. Waters, ApJL **803**, L16 (2015), arXiv: 1503.02083.

385 Z.-Y. Zheng, N. R. Butler, Y. Shen, L. Jiang, J.-X. Wang, X. Chen, and J. Cuadra, ApJ **827**, 56 (2016), arXiv: 1512.08730.

386 T. Liu, S. Gezari, W. Burgett, K. Chambers, P. Draper, K. Hodapp, M. Huber, R. P. Kudritzki, E. Magnier, N. Metcalfe, J. Tonry, R. Wainscoat, and C. Waters, ApJ **833**, 6 (2016), arXiv: 1609.09503.

387 T. Liu, S. Gezari, M. Ayers, W. Burgett, K. Chambers, K. Hodapp, M. E. Huber, R. P. Kudritzki, N. Metcalfe, J. Tonry, R. Wainscoat, and C. Waters, ApJ **884**, 36 (2019), arXiv: 1906.08315.

388 J. E. Greene and L. C. Ho, ApJ **610**, 722 (2004), arXiv: astro-ph/0404110.

389 X.-B. Dong, L. C. Ho, W. Yuan, T.-G. Wang, X. Fan, H. Zhou, and N. Jiang, ApJ **755**, 167 (2012), arXiv: 1206.3843.

390 M. Mezcua, F. Civano, S. Marchesi, H. Suh, G. Fabbiano, and M. Volonteri, MNRAS **478**, 2576 (2018), arXiv: 1802.01567.
391 A. E. Reines, J. J. Condon, J. Darling, and J. E. Greene, ApJ **888**, 36 (2020), arXiv: 1909.04670.
392 M. Volonteri, G. Lodato, and P. Natarajan, MNRAS **383**, 1079 (2008), arXiv: 0709.0529.
393 T. Morokuma, N. Tominaga, M. Tanaka, N. Yasuda, H. Furusawa, Y. Taniguchi, T. Kato, J.-a. Jiang, T. Nagao, H. Kuncarayakti, K. Morokuma-Matsui, H. Ikeda, S. Blinnikov, K. Nomoto, M. Kokubo, and M. Doi, PASJ **68**, 40 (2016), arXiv: 1603.02302.
394 V. F. Baldassare, M. Geha, and J. Greene, ApJ **868**, 152 (2018), arXiv: 1808.09578.
395 V. F. Baldassare, M. Geha, and J. Greene, ApJ **896**, 10 (2020), arXiv: 1910.06342.
396 J. Martínez-Palomera, P. Lira, I. Bhalla-Ladd, F. Förster, and R. M. Plotkin, ApJ **889**, 113 (2020), arXiv: 1912.02860.
397 C. J. Burke, Y. Shen, O. Blaes, C. F. Gammie, K. Horne, Y.-F. Jiang, X. Liu, I. M. McHardy, C. W. Morgan, S. Scaringi, and Q. Yang, Science **373**, 789 (2021), arXiv: 2108.05389.
398 M. C. Begelman, R. D. Blandford, and M. J. Rees, Nature **287**, 307 (1980).
399 A. Escala, R. B. Larson, P. S. Coppi, and D. Mardones, ApJ **630**, 152 (2005), arXiv: astro-ph/0406304.
400 M. Volonteri and P. Madau, ApJL **687**, L57 (2008), arXiv: 0809.4007.
401 F. Pretorius, PRL **95**, 121101 (2005), arXiv: gr-qc/0507014.
402 M. Campanelli, C. O. Lousto, P. Marronetti, and Y. Zlochower, PRL **96**, 111101 (2006), arXiv: gr-qc/0511048.
403 J. G. Baker, J. Centrella, D.-I. Choi, M. Koppitz, J. R. van Meter, and M. C. Miller, ApJL **653**, L93 (2006), arXiv: astro-ph/0603204.
404 G. Canalizo and A. Stockton, ApJ **555**, 719 (2001), arXiv: astro-ph/0103332.
405 S. Van Wassenhove, M. Volonteri, L. Mayer, M. Dotti, J. Bellovary, and S. Callegari, ApJL **748**, L7 (2012), arXiv: 1111.0223.
406 E. Treister, K. Schawinski, C. M. Urry, and B. D. Simmons, ApJL **758**, L39 (2012), arXiv: 1209.5393.
407 A. Loeb, PRL **99**, 041103 (2007), arXiv: astro-ph/0703722.
408 L. Blecha and A. Loeb, MNRAS **390**, 1311 (2008), arXiv: 0805.1420.
409 J. J. Condon, J. Darling, Y. Y. Kovalev, and L. Petrov, ApJ **834**, 184 (2017), arXiv: 1606.04067.
410 R. S. Barrows, J. M. Comerford, and J. E. Greene, ApJ **869**, 154 (2018), arXiv: 1811.01973.
411 C. J. Skipper and I. W. A. Browne, MNRAS **475**, 5179 (2018), arXiv: 1801.03456.
412 A. E. Reines, J. J. Condon, J. Darling, and J. E. Greene, ApJ **888**, 36 (2020), arXiv: 1909.04670.
413 D. Lena, A. Robinson, A. Marconi, D. J. Axon, A. Capetti, D. Merritt, and D. Batcheldor, ApJ **795**, 146 (2014), arXiv: 1409.3976.
414 D. C. Kim, I. Yoon, G. C. Privon, A. S. Evans, D. Harvey, S. Stierwalt, and J. H. Kim, ApJ **840**, 71 (2017), arXiv: 1704.05549.
415 M. Chiaberge, J. C. Ely, E. T. Meyer, M. Georganopoulos, A. Marinucci, S. Bianchi, G. R. Tremblay, B. Hilbert, J. P. Kotyla, A. Capetti, S. A. Baum, F. D. Macchetto, G. Miley, C. P. O'Dea, E. S. Perlman, W. B. Sparks, and C. Norman, A&A **600**, A57 (2017), arXiv: 1611.05501.
416 C. Ward, S. Gezari, S. Frederick, E. Hammerstein, P. Nugent, S. van Velzen, A. Drake, A. García-Pérez, I. Oyoo, E. C. Bellm, D. A. Duev, M. J. Graham, M. M. Kasliwal, S. Kaye, A. A. Mahabal, F. J. Masci, B. Rusholme, M. T. Soumagnac, and L. Yan, ApJ **913**, 102 (2021), arXiv: 2011.11656.
417 S. Mao and P. Schneider, MNRAS **295**, 587 (1998), arXiv: astro-ph/9707187.
418 R. B. Metcalf and P. Madau, ApJ **563**, 9 (2001), arXiv: astro-ph/0108224.
419 A. M. Nierenberg, T. Treu, S. A. Wright, C. D. Fassnacht, and M. W. Auger, MNRAS **442**, 2434 (2014), arXiv: 1402.1496.
420 C. Y. Peng, C. D. Impey, H.-W. Rix, C. S. Kochanek, C. R. Keeton, E. E. Falco, J. Lehár, and B. A. McLeod, ApJ **649**, 616 (2006), arXiv: astro-ph/0603248.
421 C. S. Kochanek, ApJ **605**, 58 (2004), arXiv: astro-ph/0307422.
422 P. L. Schechter, D. Pooley, J. A. Blackburne, and J. Wambsganss, ApJ **793**, 96 (2014), arXiv: 1405.0038.
423 J. Jiménez-Vicente and E. Mediavilla, ApJ **885**, 75 (2019), arXiv: 1910.10509.
424 N. F. Bate, G. Vernardos, M. J. O'Dowd, D. M. Neri-Larios, R. L. Webster, D. J. E. Floyd, R. L. Barone-Nugent, K. Labrie, A. L. King, and S. Y. Yong, MNRAS **479**, 4796 (2018), arXiv: 1807.03553.
425 M. A. Cornachione, C. W. Morgan, H. R. Burger, V. N. Shalyapin, L. J. Goicoechea, F. J. Vrba, S. E. Dahm, and T. M. Tilleman, ApJ **905**, 7 (2020), arXiv: 2012.05856.
426 Planck Collaboration, N. Aghanim, Y. Akrami, M. Ashdown, J. Aumont, C. Baccigalupi, M. Ballardini, A. J. Banday, R. B. Barreiro, N. Bartolo, S. Basak, R. Battye, K. Benabed, J. P. Bernard, M. Bersanelli, P. Bielewicz, J. J. Bock, J. R. Bond, J. Borrill, F. R. Bouchet, F. Boulanger, M. Bucher, C. Burigana, R. C. Butler, E. Calabrese, J. F. Cardoso, J. Carron, A. Challinor, H. C. Chiang, J. Chluba, L. P. L. Colombo, C. Combet, D. Contreras, B. P. Crill, F. Cuttaia, P. de Bernardis, G. de Zotti, J. Delabrouille, J. M. Delouis, E. Di Valentino, J. M. Diego, O. Doré, M. Douspis, A. Ducout, X. Dupac, S. Dusini, G. Efstathiou, F. Elsner, T. A. Enßlin, H. K. Eriksen, Y. Fantaye, M. Farhang, J. Fergusson, R. Fernandez-Cobos, F. Finelli, F. Forastieri, M. Frailis, A. A. Fraisse, E. Franceschi, A. Frolov, S. Galeotta, S. Galli, K. Ganga, R. T. Génova-Santos, M. Gerbino, T. Ghosh, J. González-Nuevo, K. M. Górski, S. Gratton, A. Gruppuso, J. E. Gudmundsson, J. Hamann, W. Handley, F. K. Hansen, D. Herranz, S. R. Hildebrandt, E. Hivon, Z. Huang, A. H. Jaffe, W. C. Jones, A. Karakci, E. Keihänen, R. Keskitalo, K. Kiiveri, J. Kim, T. S. Kisner, L. Knox, N. Krachmalnicoff, M. Kunz, H. Kurki-Suonio, G. Lagache, J. M. Lamarre, A. Lasenby, M. Lattanzi, C. R. Lawrence, M. Le Jeune, P. Lemos, J. Lesgourgues, F. Levrier, A. Lewis, M. Liguori, P. B. Lilje, M. Lilley, V. Lindholm, M. López-Caniego, P. M. Lubin, Y. Z. Ma, J. F. Macías-Pérez, G. Maggio, D. Maino, N. Mandolesi, A. Mangilli, A. Marcos-Caballero, M. Maris, P. G. Martin, M. Martinelli, E. Martínez-González, S. Matarrese, N. Mauri, J. D. McEwen, P. R. Meinhold, A. Melchiorri, A. Mennella, M. Migliaccio, M. Millea, S. Mitra, M. A. Miville-Deschênes, D. Molinari, L. Montier, G. Morgante, A. Moss, P. Natoli, H. U. Nørgaard-Nielsen, L. Pagano, D. Paoletti, B. Partridge, G. Patanchon, H. V. Peiris, F. Perrotta, V. Pettorino, F. Piacentini, L. Polastri, G. Polenta, J. L. Puget, J. P. Rachen, M. Reinecke, M. Remazeilles, A. Renzi, G. Rocha, C. Rosset, G. Roudier, J. A. Rubiño-Martín, B. Ruiz-Granados, L. Salvati, M. Sandri, M. Savelainen, D. Scott, E. P. S. Shellard, C. Sirignano, G. Sirri, L. D. Spencer, R. Sunyaev, A. S. Suur-Uski, J. A. Tauber, D. Tavagnacco, M. Tenti, L. Toffolatti, M. Tomasi, T. Trombetti, L. Valenziano, J. Valiviita, B. Van Tent, L. Vibert, P. Vielva, F. Villa, N. Vittorio, B. D. Wandelt, I. K. Wehus, M. White, S. D. M. White, A. Zacchei, and A. Zonca, A&A **641**, A6 (2020), arXiv: 1807.06209.
427 A. G. Riess, S. Casertano, W. Yuan, J. B. Bowers, L. Macri, J. C. Zinn, and D. Scolnic, ApJL **908**, L6 (2021), arXiv: 2012.08534.
428 A. G. Riess, W. Yuan, L. M. Macri, D. Scolnic, D. Brout, S. Casertano, D. O. Jones, Y. Murakami, L. Breuval, T. G. Brink, A. V. Filippenko, S. Hoffmann, S. W. Jha, W. D. Kenworthy, J. Mackenty, B. E. Stahl, and W. Zheng, arXiv e-prints arXiv:2112.04510 (2021), arXiv: 2112.04510.
429 D. Walsh, R. F. Carswell, and R. J. Weymann, Nature **279**, 381 (1979).
430 N. Jackson, H. Rampadarath, E. O. Ofek, M. Oguri, and M.-S. Shin, MNRAS **419**, 2014 (2012), arXiv: 1109.4325.
431 N. Inada, M. Oguri, M.-S. Shin, I. Kayo, M. A. Strauss, T. Mo-

rokuma, C. E. Rusu, M. Fukugita, C. S. Kochanek, G. T. Richards, D. P. Schneider, D. G. York, N. A. Bahcall, J. A. Frieman, P. B. Hall, and R. L. White, AJ **143**, 119 (2012), arXiv: 1203.1087.
432 Y. Shu, R. Marques-Chaves, N. W. Evans, and I. Pérez-Fournon, MNRAS **481**, L136 (2018), arXiv: 1809.07337.
433 Y. Shu, S. E. Koposov, N. W. Evans, V. Belokurov, R. G. McMahon, M. W. Auger, and C. A. Lemon, MNRAS **489**, 4741 (2019), arXiv: 1909.02010.
434 C. A. Lemon, M. W. Auger, and R. G. McMahon, MNRAS **483**, 4242 (2019), arXiv: 1810.04480.
435 J. H. H. Chan, S. H. Suyu, A. Sonnenfeld, A. T. Jaelani, A. More, A. Yonehara, Y. Kubota, J. Coupon, C.-H. Lee, M. Oguri, C. E. Rusu, and K. C. Wong, A&A **636**, A87 (2020), arXiv: 1911.02587.
436 C. Desira, Y. Shu, M. W. Auger, R. G. McMahon, C. A. Lemon, T. Anguita, and F. Neira, MNRAS **509**, 738 (2022).
437 Z. Kostrzewa-Rutkowska, S. Kozłowski, C. Lemon, T. Anguita, J. Greiner, M. W. Auger, Ł. Wyrzykowski, Y. Apostolovski, J. Bolmer, A. Udalski, M. K. Szymański, I. Soszyński, R. Poleski, P. Pietrukowicz, J. Skowron, P. Mróz, K. Ulaczyk, and M. Pawlak, MNRAS **476**, 663 (2018), arXiv: 1801.08481.
438 D. C. Y. Chao, J. H. H. Chan, S. H. Suyu, N. Yasuda, T. Morokuma, A. T. Jaelani, T. Nagao, and C. E. Rusu, arXiv e-prints arXiv:2009.07854 (2020), arXiv: 2009.07854.
439 Y. Shu, V. Belokurov, and N. W. Evans, MNRAS **502**, 2912 (2021), arXiv: 2011.04667.
440 M. Millon, F. Courbin, V. Bonvin, E. Paic, G. Meylan, M. Tewes, D. Sluse, P. Magain, J. H. H. Chan, A. Galan, R. Joseph, C. Lemon, O. Tihhonova, R. I. Anderson, M. Marmier, B. Chazelas, M. Lendl, A. H. M. J. Triaud, and A. Wyttenbach, A&A **640**, A105 (2020), arXiv: 2002.05736.
441 M. Millon, F. Courbin, V. Bonvin, E. Buckley-Geer, C. D. Fassnacht, J. Frieman, P. J. Marshall, S. H. Suyu, T. Treu, T. Anguita, V. Motta, A. Agnello, J. H. H. Chan, D. C. Y. Chao, M. Chijani, D. Gilman, K. Gilmore, C. Lemon, J. R. Lucey, A. Melo, E. Paic, K. Rojas, D. Sluse, P. R. Williams, A. Hempel, S. Kim, R. Lachaume, and M. Rabus, A&A **642**, A193 (2020), arXiv: 2006.10066.
442 L. W. Alvarez, W. Alvarez, F. Asaro, and H. V. Michel, Science **208**, 1095 (1980).
443 L. Denneau, R. Jedicke, T. Grav, M. Granvik, J. Kubica, A. Milani, P. Vereš, R. Wainscoat, D. Chang, F. Pierfederici, N. Kaiser, K. C. Chambers, J. N. Heasley, E. A. Magnier, P. A. Price, J. Myers, J. Kleyna, H. Hsieh, D. Farnocchia, C. Waters, W. H. Sweeney, D. Green, B. Bolin, W. S. Burgett, J. S. Morgan, J. L. Tonry, K. W. Hodapp, S. Chastel, S. Chesley, A. Fitzsimmons, M. Holman, T. Spahr, D. Tholen, G. V. Williams, S. Abe, J. D. Armstrong, T. H. Bressi, R. Holmes, T. Lister, R. S. McMillan, M. Micheli, E. V. Ryan, W. H. Ryan, and J. V. Scotti, PASP **125**, 357 (2013), arXiv: 1302.7281.
444 E. A. Magnier, K. C. Chambers, H. A. Flewelling, J. C. Hoblitt, M. E. Huber, P. A. Price, W. E. Sweeney, C. Z. Waters, L. Denneau, P. W. Draper, K. W. Hodapp, R. Jedicke, N. Kaiser, R. P. Kudritzki, N. Metcalfe, C. W. Stubbs, and R. J. Wainscoat, ApJS **251**, 3 (2020), arXiv: 1612.05240.
445 Q. Ye, F. J. Masci, W.-H. Ip, T. A. Prince, G. Helou, D. Farnocchia, E. C. Bellm, R. Dekany, M. J. Graham, S. R. Kulkarni, T. Kupfer, A. Mahabal, C.-C. Ngeow, D. J. Reiley, and M. T. Soumagnac, AJ **159**, 70 (2020), arXiv: 1912.06109.
446 P. Wiegert, K. Innanen, and S. Mikkola, Icarus **145**, 33 (2000), arXiv: astro-ph/9912254.
447 H. H. Hsieh and D. Jewitt, Science **312**, 561 (2006).
448 A. Morbidelli, J. I. Lunine, D. P. O'Brien, S. N. Raymond, and K. J. Walsh, Annual Review of Earth and Planetary Sciences **40**, 251 (2012), arXiv: 1208.4694.
449 N. Haghighipour, T. I. Maindl, C. Schäfer, R. Speith, and R. Dvorak, ApJ **830**, 22 (2016), arXiv: 1606.06226.
450 H. H. Hsieh, C. O. Chandler, L. Denneau, A. Fitzsimmons, N. Erasmus, M. S. P. Kelley, M. M. Knight, T. A. Lister, J. Pittichová, S. S. Sheppard, A. Thirouin, C. A. Trujillo, H. Usher, E. Gomez, J. Chatelain, S. Greenstreet, T. Angel, R. Miles, P. Roche, and B. Wooding, ApJL **922**, L9 (2021), arXiv: 2109.14822.
451 F. L. Whipple, ApJ **111**, 375 (1950).
452 J. X. Luu, PASP **105**, 946 (1993).
453 A. Morbidelli and D. Nesvorný, in *The Trans-Neptunian Solar System*, (edited by D. Prialnik, M. A. Barucci, and L. Young), 25–59 (2020).
454 J. M. Petit, J. J. Kavelaars, B. J. Gladman, R. L. Jones, J. W. Parker, C. Van Laerhoven, P. Nicholson, G. Mars, P. Rousselot, O. Mousis, B. Marsden, A. Bieryla, M. Taylor, M. L. N. Ashby, P. Benavidez, A. Campo Bagatin, and G. Bernabeu, AJ **142**, 131 (2011), arXiv: 1108.4836.
455 D. Nesvorný, ARA&A **56**, 137 (2018), arXiv: 1807.06647.
456 M. Marsset, W. C. Fraser, R. E. Pike, M. T. Bannister, M. E. Schwamb, K. Volk, J. J. Kavelaars, M. Alexandersen, Y.-T. Chen, B. J. Gladman, S. D. J. Gwyn, M. J. Lehner, N. Peixinho, J.-M. Petit, and S.-Y. Wang, AJ **157**, 94 (2019), arXiv: 1812.02190.
457 D. Nesvorný, D. Vokrouhlický, W. F. Bottke, and H. F. Levison, Nature Astronomy **2**, 878 (2018), arXiv: 1809.04007.
458 K. Batygin and M. E. Brown, AJ **151**, 22 (2016), arXiv: 1601.05438.
459 K. Batygin, F. C. Adams, M. E. Brown, and J. C. Becker, PhR **805**, 1 (2019), arXiv: 1902.10103.
460 E. Gullbring, P. P. Petrov, I. Ilyin, I. Tuominen, G. F. Gahm, and K. Loden, A&A **314**, 835 (1996).
461 J. Bouvier, K. N. Grankin, S. H. P. Alencar, C. Dougados, M. Fernández, G. Basri, C. Batalha, E. Guenther, M. A. Ibrahimov, T. Y. Magakian, S. Y. Melnikov, P. P. Petrov, M. V. Rud, and M. R. Zapatero Osorio, A&A **409**, 169 (2003), arXiv: astro-ph/0306551.
462 L. I. Biddle, C. M. Johns-Krull, J. Llama, L. Prato, and B. A. Skiff, ApJL **853**, L34 (2018), arXiv: 1801.06234.
463 L. Hartmann, G. Herczeg, and N. Calvet, ARA&A **54**, 135 (2016).
464 E. Gullbring, L. Hartmann, C. Briceño, and N. Calvet, ApJ **492**, 323 (1998).
465 J. M. Alcalá, A. Natta, C. F. Manara, L. Spezzi, B. Stelzer, A. Frasca, K. Biazzo, E. Covino, S. Randich, E. Rigliaco, L. Testi, F. Comerón, G. Cupani, and V. D'Elia, A&A **561**, A2 (2014), arXiv: 1310.2069.
466 F. H. Shu, F. C. Adams, and S. Lizano, ARA&A **25**, 23 (1987).
467 S. J. Kenyon, L. W. Hartmann, K. M. Strom, and S. E. Strom, AJ **99**, 869 (1990).
468 S. J. Kenyon and L. Hartmann, ApJS **101**, 117 (1995).
469 L. Hartmann and S. J. Kenyon, ARA&A **34**, 207 (1996).
470 Z. Chen, W. Sun, R. Chini, M. Haas, Z. Jiang, and X. Chen, ApJ **922**, 90 (2021), arXiv: 2108.12554.
471 M. Audard, P. Ábrahám, M. M. Dunham, J. D. Green, N. Grosso, K. Hamaguchi, J. H. Kastner, Á. Kóspál, G. Lodato, M. M. Romanova, S. L. Skinner, E. I. Vorobyov, and Z. Zhu, in *Protostars and Planets VI*, (edited by H. Beuther, R. S. Klessen, C. P. Dullemond, and T. Henning), 387 (2014), arXiv: 1401.3368.
472 L. A. Hillenbrand and K. P. Findeisen, ApJ **808**, 68 (2015), arXiv: 1506.01126.
473 S. E. Sale, J. E. Drew, G. Barentsen, H. J. Farnhill, R. Raddi, M. J. Barlow, J. Eislöffel, J. S. Vink, P. Rodríguez-Gil, and N. J. Wright, MNRAS **443**, 2907 (2014), arXiv: 1406.0009.
474 B. Q. Chen, Y. Huang, H. B. Yuan, C. Wang, D. W. Fan, M. S. Xiang, H. W. Zhang, Z. J. Tian, and X. W. Liu, MNRAS **483**, 4277 (2019), arXiv: 1807.02241.
475 G. M. Green, E. Schlafly, C. Zucker, J. S. Speagle, and D. Finkbeiner, ApJ **887**, 93 (2019), arXiv: 1905.02734.
476 H. L. Guo, B. Q. Chen, H. B. Yuan, Y. Huang, D. Z. Liu, Y. Yang, X. Y. Li, W. X. Sun, and X. W. Liu, ApJ **906**, 47 (2021), arXiv: 2010.14092.
477 T. Röhser, J. Kerp, D. Lenz, and B. Winkel, A&A **596**, A94 (2016),

arXiv: 1609.06540.

478 S. Ramírez Alegría, J. Borissova, A. N. Chené, C. Bonatto, R. Kurtev, P. Amigo, M. Kuhn, M. Gromadzki, and J. A. Carballo-Bello, A&A **588**, A40 (2016), arXiv: 1602.04898.

479 G. A. Gontcharov, M. Y. Khovritchev, A. V. Mosenkov, V. B. Il'in, A. A. Marchuk, S. S. Savchenko, A. A. Smirnov, P. A. Usachev, and D. M. Poliakov, MNRAS **508**, 2688 (2021), arXiv: 2109.13115.

480 E. J. Lee, M.-A. Miville-Deschênes, and N. W. Murray, ApJ **833**, 229 (2016), arXiv: 1608.05415.

481 Y. Su, J. Yang, S. Zhang, Y. Gong, H. Wang, X. Zhou, M. Wang, Z. Chen, Y. Sun, X. Chen, Y. Xu, and Z. Jiang, ApJS **240**, 9 (2019), arXiv: 1901.00285.

482 T. Cantat-Gaudin, C. Jordi, A. Vallenari, A. Bragaglia, L. Balaguer-Núñez, C. Soubiran, D. Bossini, A. Moitinho, A. Castro-Ginard, A. Krone-Martins, L. Casamiquela, R. Sordo, and R. Carrera, A&A **618**, A93 (2018), arXiv: 1805.08726.

483 D. Bossini, A. Vallenari, A. Bragaglia, T. Cantat-Gaudin, R. Sordo, L. Balaguer-Núñez, C. Jordi, A. Moitinho, C. Soubiran, L. Casamiquela, R. Carrera, and U. Heiter, A&A **623**, A108 (2019), arXiv: 1901.04733.

484 Ž. Ivezić, B. Sesar, M. Jurić, N. Bond, J. Dalcanton, C. M. Rockosi, B. Yanny, H. J. Newberg, T. C. Beers, C. Allende Prieto, R. Wilhelm, Y. S. Lee, T. Sivarani, J. E. Norris, C. A. L. Bailer-Jones, P. Re Fiorentin, D. Schlegel, A. Uomoto, R. H. Lupton, G. R. Knapp, J. E. Gunn, K. R. Covey, J. Allyn Smith, G. Miknaitis, M. Doi, M. Tanaka, M. Fukugita, S. Kent, D. Finkbeiner, J. A. Munn, J. R. Pier, T. Quinn, S. Hawley, S. Anderson, F. Kiuchi, A. Chen, J. Bushong, H. Sohi, D. Haggard, A. Kimball, J. Barentine, H. Brewington, M. Harvanek, S. Kleinman, J. Krzesinski, D. Long, A. Nitta, S. Snedden, B. Lee, H. Harris, J. Brinkmann, D. P. Schneider, and D. G. York, ApJ **684**, 287 (2008), arXiv: 0804.3850.

485 I. Baraffe, D. Homeier, F. Allard, and G. Chabrier, A&A **577**, A42 (2015), arXiv: 1503.04107.

486 Y.-B. Li, A. L. Luo, Y.-J. Lu, X.-S. Zhang, J. Li, R. Wang, F. Zuo, M. Xiang, Y.-S. Ting, T. Marchetti, S. Li, Y.-F. Wang, S. Zhang, K. Hattori, Y.-H. Zhao, H.-W. Zhang, and G. Zhao, ApJS **252**, 3 (2021), arXiv: 2011.10206.

487 F. Giovannelli and L. Sabau-Graziati, Chinese Journal of Astronomy and Astrophysics **3**, 202 (2003).

488 C. Mateu, B. Holl, J. De Ridder, and L. Rimoldini, MNRAS **496**, 3291 (2020), arXiv: 2006.09416.

489 L. L. Watkins, R. P. van der Marel, S. T. Sohn, and N. W. Evans, ApJ **873**, 118 (2019), arXiv: 1804.11348.

490 C. Mateu and A. K. Vivas, MNRAS **479**, 211 (2018), arXiv: 1802.07798.

491 X. Chen, S. Wang, L. Deng, R. de Grijs, C. Liu, and H. Tian, Nature Astronomy **3**, 320 (2019), arXiv: 1902.00998.

492 D. M. Skowron, J. Skowron, P. Mróz, A. Udalski, P. Pietrukowicz, I. Soszyński, M. K. Szymański, R. Poleski, S. Kozłowski, K. Ulaczyk, K. Rybicki, and P. Iwanek, Science **365**, 478 (2019), arXiv: 1806.10653.

493 X. Chen, S. Wang, L. Deng, R. de Grijs, M. Yang, and H. Tian, ApJS **249**, 18 (2020), arXiv: 2005.08662.

494 S.-B. Qian, L.-Y. Zhu, L. Liu, X.-D. Zhang, X.-D. Shi, J.-J. He, and J. Zhang, Research in Astronomy and Astrophysics **20**, 163 (2020).

495 O. J. Eggen, Memoirs of the Royal Astronomical Society **70**, 111 (1967).

496 S.-B. Qian, J.-J. He, J. Zhang, L.-Y. Zhu, X.-D. Shi, E.-G. Zhao, and X. Zhou, Research in Astronomy and Astrophysics **17**, 087 (2017), arXiv: 1705.03996.

497 W. H. G. Lewin and M. van der Klis, *Compact Stellar X-ray Sources*, volume 39 (2006).

498 Q. Z. Liu, J. van Paradijs, and E. P. J. van den Heuvel, A&A **455**, 1165 (2006), arXiv: 0707.0549.

499 Q. Z. Liu, J. van Paradijs, and E. P. J. van den Heuvel, A&A **469**, 807 (2007), arXiv: 0707.0544.

500 P. Reig, Astrophysics and Space Science **332**, 1 (2011).

501 J. Casares, I. Negueruela, M. Ribó, I. Ribas, J. M. Paredes, A. Herrero, and S. Simón-Díaz, Nature **505**, 378 (2014).

502 I. Negueruela, Arxiv preprint astro-ph/9807158 (1998).

503 J. Yan, H. Li, and Q. Liu, ApJ **744**, 37 (2012), arXiv: 1111.0715.

504 L. M. van Haaften, G. Nelemans, R. Voss, M. V. van der Sluys, and S. Toonen, A&A **579**, A33 (2015), arXiv: 1505.03629.

505 D. R. Weisz, A. E. Dolphin, E. D. Skillman, J. Holtzman, K. M. Gilbert, J. J. Dalcanton, and B. F. Williams, ApJ **789**, 147 (2014), arXiv: 1404.7144.

506 M. Geha, T. M. Brown, J. Tumlinson, J. S. Kalirai, J. D. Simon, E. N. Kirby, D. A. VandenBerg, R. R. Muñoz, R. J. Avila, P. Guhathakurta, and H. C. Ferguson, ApJ **771**, 29 (2013), arXiv: 1304.7769.

507 J. S. Bullock and M. Boylan-Kolchin, ARA&A **55**, 343 (2017), arXiv: 1707.04256.

508 K. Spekkens, B. S. Mason, J. E. Aguirre, and B. Nhan, ApJ **773**, 61 (2013), arXiv: 1301.5306.

509 The Dark Energy Survey Collaboration, arXiv e-prints astro-ph/0510346 (2005), arXiv: astro-ph/0510346.

510 S. Sharma, J. Bland-Hawthorn, K. V. Johnston, and J. Binney, ApJ **730**, 3 (2011), arXiv: 1101.3561.

511 P. Kroupa, MNRAS **322**, 231 (2001), arXiv: astro-ph/0009005.

512 S. Koposov, V. Belokurov, N. W. Evans, P. C. Hewett, M. J. Irwin, G. Gilmore, D. B. Zucker, H. W. Rix, M. Fellhauer, E. F. Bell, and E. V. Glushkova, ApJ **686**, 279 (2008), arXiv: 0706.2687.

513 K. N. Abazajian, J. K. Adelman-McCarthy, M. A. Agüeros, S. S. Allam, C. Allende Prieto, D. An, K. S. J. Anderson, S. F. Anderson, J. Annis, N. A. Bahcall, and et al., ApJS **182**, 543 (2009), arXiv: 0812.0649.

514 C. Heymans, L. Van Waerbeke, L. Miller, T. Erben, H. Hildebrandt, H. Hoekstra, T. D. Kitching, Y. Mellier, P. Simon, C. Bonnett, J. Coupon, L. Fu, J. Harnois Déraps, M. J. Hudson, M. Kilbinger, K. Kuijken, B. Rowe, T. Schrabback, E. Semboloni, E. van Uitert, S. Vafaei, and M. Velander, MNRAS **427**, 146 (2012), arXiv: 1210.0032.

515 T. M. C. Abbott, F. B. Abdalla, S. Allam, A. Amara, J. Annis, J. Asorey, S. Avila, O. Ballester, M. Banerji, W. Barkhouse, L. Baruah, M. Baumer, K. Bechtol, M. R. Becker, A. Benoit-Lévy, G. M. Bernstein, E. Bertin, J. Blazek, S. Bocquet, D. Brooks, D. Brout, E. Buckley-Geer, D. L. Burke, V. Busti, R. Campisano, L. Cardiel-Sas, A. Carnero Rosell, M. Carrasco Kind, J. Carretero, F. J. Castander, R. Cawthon, C. Chang, X. Chen, C. Conselice, G. Costa, M. Crocce, C. E. Cunha, C. B. D'Andrea, L. N. da Costa, R. Das, G. Daues, T. M. Davis, C. Davis, J. De Vicente, D. L. DePoy, J. DeRose, S. Desai, H. T. Diehl, J. P. Dietrich, S. Dodelson, P. Doel, A. Drlica-Wagner, T. F. Eifler, A. E. Elliott, A. E. Evrard, A. Farahi, A. Fausti Neto, E. Fernandez, D. A. Finley, B. Flaugher, R. J. Foley, P. Fosalba, D. N. Friedel, J. Frieman, J. García-Bellido, E. Gaztanaga, D. W. Gerdes, T. Giannantonio, M. S. S. Gill, K. Glazebrook, D. A. Goldstein, M. Gower, D. Gruen, R. A. Gruendl, J. Gschwend, R. R. Gupta, G. Gutierrez, S. Hamilton, W. G. Hartley, S. R. Hinton, J. M. Hislop, D. Hollowood, K. Honscheid, B. Hoyle, D. Huterer, B. Jain, D. J. James, T. Jeltema, M. W. G. Johnson, M. D. Johnson, T. Kacprzak, S. Kent, G. Khullar, M. Klein, A. Kovacs, A. M. G. Koziol, E. Krause, A. Kremin, R. Kron, K. Kuehn, S. Kuhlmann, N. Kuropatkin, O. Lahav, J. Lasker, T. S. Li, R. T. Li, A. R. Liddle, M. Lima, H. Lin, P. López-Reyes, N. MacCrann, M. A. G. Maia, J. D. Maloney, M. Manera, M. March, J. Marriner, J. L. Marshall, P. Martini, T. McClintock, T. McKay, R. G. McMahon, P. Melchior, F. Menanteau, C. J. Miller, R. Miquel, J. J. Mohr, E. Morganson, J. Mould, E. Neilsen, R. C. Nichol, F. Nogueira, B. Nord, P. Nugent, L. Nunes, R. L. C. Ogando, L. Old, A. B. Pace, A. Palmese, F. Paz-Chinchón, H. V. Peiris, W. J. Percival, D. Petravick, A. A. Plazas, J. Poh, C. Pond, A. Porredon, A. Pujol, A. Refregier, K. Reil,

P. M. Ricker, R. P. Rollins, A. K. Romer, A. Roodman, P. Rooney, A. J. Ross, E. S. Rykoff, M. Sako, M. L. Sanchez, E. Sanchez, B. Santiago, A. Saro, V. Scarpine, D. Scolnic, S. Serrano, I. Sevilla-Noarbe, E. Sheldon, N. Shipp, M. L. Silveira, M. Smith, R. C. Smith, J. A. Smith, M. Soares-Santos, F. Sobreira, J. Song, A. Stebbins, E. Suchyta, M. Sullivan, M. E. C. Swanson, G. Tarle, J. Thaler, D. Thomas, R. C. Thomas, M. A. Troxel, D. L. Tucker, V. Vikram, A. K. Vivas, A. R. Walker, R. H. Wechsler, J. Weller, W. Wester, R. C. Wolf, H. Wu, B. Yanny, A. Zenteno, Y. Zhang, J. Zuntz, DES Collaboration, S. Juneau, M. Fitzpatrick, R. Nikutta, D. Nidever, K. Olsen, A. Scott, and NOAO Data Lab, ApJS **239**, 18 (2018), arXiv: 1801.03181.

516 H. Aihara, R. Armstrong, S. Bickerton, J. Bosch, J. Coupon, H. Furusawa, Y. Hayashi, H. Ikeda, Y. Kamata, and H. Karoji, PASJ **70**, S8 (2018), arXiv: 1702.08449.

517 K. Kuijken, C. Heymans, H. Hildebrandt, R. Nakajima, T. Erben, J. T. A. de Jong, M. Viola, A. Choi, H. Hoekstra, L. Miller, E. van Uitert, A. Amon, C. Blake, M. Brouwer, A. Buddendiek, I. F. Conti, M. Eriksen, A. Grado, J. Harnois-Déraps, E. Helmich, R. Herbonnet, N. Irisarri, T. Kitching, D. Klaes, F. La Barbera, N. Napolitano, M. Radovich, P. Schneider, C. Sifón, G. Sikkema, P. Simon, A. Tudorica, E. Valentijn, G. Verdoes Kleijn, and L. van Waerbeke, MNRAS **454**, 3500 (2015), arXiv: 1507.00738.

518 Planck Collaboration, N. Aghanim, Y. Akrami, M. Ashdown, J. Aumont, C. Baccigalupi, M. Ballardini, A. J. Banday, R. B. Barreiro, and N. Bartolo, arXiv e-prints arXiv:1807.06209 (2018), arXiv: 1807.06209.

519 K. C. Wong, S. H. Suyu, G. C. F. Chen, C. E. Rusu, M. Millon, D. Sluse, V. Bonvin, C. D. Fassnacht, S. Taubenberger, M. W. Auger, S. Birrer, J. H. H. Chan, F. Courbin, S. Hilbert, O. Tihhonova, T. Treu, A. Agnello, X. Ding, I. Jee, E. Komatsu, A. J. Shajib, A. Sonnenfeld, R. D. Bland ford, L. V. E. Koopmans, P. J. Marshall, and G. Meylan, arXiv e-prints arXiv:1907.04869 (2019), arXiv: 1907.04869.

520 G. Efstathiou, MNRAS **505**, 3866 (2021), arXiv: 2103.08723.

521 S. Vagnozzi, Physical Review D **102**, 023518 (2020).

522 X. Li, H. Miyatake, W. Luo, S. More, M. Oguri, T. Hamana, R. Mandelbaum, M. Shirasaki, M. Takada, R. Armstrong, A. Kannawadi, S. Takita, S. Miyazaki, A. J. Nishizawa, A. A. Plazas Malagón, M. A. Strauss, M. Tanaka, and N. Yoshida, arXiv e-prints arXiv:2107.00136 (2021), arXiv: 2107.00136.

523 M. Jarvis, G. M. Bernstein, A. Amon, C. Davis, P. F. Léget, K. Bechtol, I. Harrison, M. Gatti, A. Roodman, C. Chang, R. Chen, A. Choi, S. Desai, A. Drlica-Wagner, D. Gruen, R. A. Gruendl, A. Hernandez, N. MacCrann, J. Meyers, A. Navarro-Alsina, S. Pandey, A. A. Plazas, L. F. Secco, E. Sheldon, M. A. Troxel, S. Vorperian, K. Wei, J. Zuntz, T. M. C. Abbott, M. Aguena, S. Allam, S. Avila, S. Bhargava, S. L. Bridle, D. Brooks, A. Carnero Rosell, M. Carrasco Kind, J. Carretero, M. Costanzi, L. N. da Costa, J. De Vicente, H. T. Diehl, P. Doel, S. Everett, B. Flaugher, P. Fosalba, J. Frieman, J. García-Bellido, E. Gaztanaga, D. W. Gerdes, G. Gutierrez, S. R. Hinton, D. L. Hollowood, K. Honscheid, D. J. James, S. Kent, K. Kuehn, N. Kuropatkin, O. Lahav, M. A. G. Maia, M. March, J. L. Marshall, P. Melchior, F. Menanteau, R. Miquel, R. L. C. Ogando, F. Paz-Chinchón, E. S. Rykoff, E. Sanchez, V. Scarpine, M. Schubnell, S. Serrano, I. Sevilla-Noarbe, M. Smith, E. Suchyta, M. E. C. Swanson, G. Tarle, T. N. Varga, A. R. Walker, W. Wester, R. D. Wilkinson, R. D. Wilkinson, and DES Collaboration, MNRAS **501**, 1282 (2021), arXiv: 2011.03409.

524 O. Pirnay, G. P. Lousberg, V. Monamy, P. Gloesener, K. Rieth, F. Lemagne, G. Réaud, and C. Flebus, in *Space Telescopes and Instrumentation 2018: Optical, Infrared, and Millimeter Wave*, volume 10698 of *Society of Photo-Optical Instrumentation Engineers (SPIE) Conference Series*, 1069835 (2018).

525 K. Bechtol, A. Drlica-Wagner, K. N. Abazajian, M. Abidi, S. Adhikari, Y. Ali-Haïmoud, J. Annis, B. Ansarinejad, R. Armstrong, and J. Asorey, in *BAAS* , volume 51, 207 (2019), arXiv: 1903.04425.

526 T. Jenness, arXiv e-prints arXiv:1611.00751 (2016), arXiv: 1611.00751.

527 E. S. Sheldon and E. M. Huff, ApJ **841**, 24 (2017), arXiv: 1702.02601.

528 X. Li, M. Oguri, N. Katayama, W. Luo, W. Wang, J. Han, H. Miyatake, K. Nakamura, and S. More, ApJS **251**, 19 (2020), arXiv: 1911.02195.

529 E. Bertin, PSFEx: Point Spread Function Extractor (2013), arXiv: 1301.001.

530 R. Mandelbaum, ARA&A **56**, 393 (2018), arXiv: 1710.03235.

531 R. Mandelbaum, B. Rowe, R. Armstrong, D. Bard, E. Bertin, J. Bosch, D. Boutigny, F. Courbin, W. A. Dawson, A. Donnarumma, I. Fenech Conti, R. Gavazzi, M. Gentile, M. S. S. Gill, D. W. Hogg, E. M. Huff, M. J. Jee, T. Kacprzak, M. Kilbinger, T. Kuntzer, D. Lang, W. Luo, M. C. March, P. J. Marshall, J. E. Meyers, L. Miller, H. Miyatake, R. Nakajima, F. M. Ngolé Mboula, G. Nurbaeva, Y. Okura, S. Paulin-Henriksson, J. Rhodes, M. D. Schneider, H. Shan, E. S. Sheldon, M. Simet, J.-L. Starck, F. Sureau, M. Tewes, K. Zarb Adami, J. Zhang, and J. Zuntz, MNRAS **450**, 2963 (2015), arXiv: 1412.1825.

532 D. Korytov, A. Hearin, E. Kovacs, P. Larsen, E. Rangel, J. Hollowed, A. J. Benson, K. Heitmann, Y.-Y. Mao, A. Bahmanyar, C. Chang, D. Campbell, J. DeRose, H. Finkel, N. Frontiere, E. Gawiser, S. Habib, B. Joachimi, F. Lanusse, N. Li, R. Mandelbaum, C. Morrison, J. A. Newman, A. Pope, E. Rykoff, M. Simet, C.-H. To, V. Vikraman, R. H. Wechsler, and M. White, The Astrophysical Journal. Supplement Series (Online) **245** (2019).

533 L. Wang, V. Gonzalez-Perez, L. Xie, A. P. Cooper, C. S. Frenk, L. Gao, W. A. Hellwing, J. Helly, M. R. Lovell, and L. Jiang, MNRAS **468**, 4579 (2017), arXiv: 1612.04540.

534 X. Yang, Y. Zhang, H. Wang, C. Liu, T. Lu, S. Li, F. Shi, Y. P. Jing, H. J. Mo, F. C. van den Bosch, X. Kang, W. Cui, H. Guo, G. Li, S. H. Lim, Y. Lu, W. Luo, C. Wei, and L. Yang, ApJ **860**, 30 (2018), arXiv: 1712.00883.

535 D. Nelson, A. Pillepich, V. Springel, R. Weinberger, L. Hernquist, R. Pakmor, S. Genel, P. Torrey, M. Vogelsberger, G. Kauffmann, F. Marinacci, and J. Naiman, MNRAS **475**, 624 (2018), arXiv: 1707.03395.

536 G. Bruzual and S. Charlot, MNRAS **344**, 1000 (2003), arXiv: astro-ph/0309134.

537 G. Chabrier, PASP **115**, 763 (2003), arXiv: astro-ph/0304382.

538 D. Calzetti, L. Armus, R. C. Bohlin, A. L. Kinney, J. Koornneef, and T. Storchi-Bergmann, ApJ **533**, 682 (2000), arXiv: astro-ph/9911459.

539 I. Sadeh, F. B. Abdalla, and O. Lahav, PASP **128**, 104502 (2016), arXiv: 1507.00490.

540 S. Arnouts and O. Ilbert, LePHARE: Photometric Analysis for Redshift Estimate (2011), arXiv: 1108.009.

541 S. J. Schmidt, A. I. Malz, J. Y. H. Soo, I. A. Almosallam, M. Brescia, S. Cavuoti, J. Cohen-Tanugi, A. J. Connolly, J. DeRose, P. E. Freeman, M. L. Graham, K. G. Iyer, M. J. Jarvis, J. B. Kalmbach, E. Kovacs, A. B. Lee, G. Longo, C. B. Morrison, J. A. Newman, E. Nourbakhsh, E. Nuss, T. Pospisil, H. Tranin, R. H. Wechsler, R. Zhou, R. Izbicki, and LSST Dark Energy Science Collaboration, MNRAS **499**, 1587 (2020), arXiv: 2001.03621.

542 Y. P. Jing, H. J. Mo, and G. Börner, ApJ **494**, 1 (1998), arXiv: astro-ph/9707106.

543 J. A. Peacock and R. E. Smith, MNRAS **318**, 1144 (2000), arXiv: astro-ph/0005010.

544 M. Krumpe, T. Miyaji, and A. L. Coil, ApJ **713**, 558 (2010), arXiv: 1002.3598.

545 Y. Shirasaki, M. Akiyama, T. Nagao, Y. Toba, W. He, M. Ohishi, Y. Mizumoto, S. Miyazaki, A. J. Nishizawa, and T. Usuda, PASJ **70**, S30 (2018), arXiv: 1704.05971.

546 R. Mandelbaum, U. Seljak, G. Kauffmann, C. M. Hirata, and J. Brinkmann, MNRAS **368**, 715 (2006), arXiv: astro-ph/0511164.

547 A. Leauthaud, A. Finoguenov, J.-P. Kneib, J. E. Taylor, R. Massey,

J. Rhodes, O. Ilbert, K. Bundy, J. Tinker, M. R. George, P. Capak, A. M. Koekemoer, D. E. Johnston, Y.-Y. Zhang, N. Cappelluti, R. S. Ellis, M. Elvis, S. Giodini, C. Heymans, O. Le Fèvre, S. Lilly, H. J. McCracken, Y. Mellier, A. Réfrégier, M. Salvato, N. Scoville, G. Smoot, M. Tanaka, L. Van Waerbeke, and M. Wolk, ApJ **709**, 97 (2010), arXiv: 0910.5219.

548 W. Luo, X. Yang, J. Zhang, D. Tweed, L. Fu, H. J. Mo, F. C. van den Bosch, C. Shu, R. Li, N. Li, X. Liu, C. Pan, Y. Wang, and M. Radovich, ApJ **836**, 38 (2017), arXiv: 1607.05406.

549 W. Luo, X. Yang, T. Lu, F. Shi, J. Zhang, H. J. Mo, C. Shu, L. Fu, M. Radovich, J. Zhang, N. Li, T. Sunayama, and L. Wang, ArXiv e-prints (2017), arXiv: 1712.09030.

550 Y. Zu and R. Mandelbaum, MNRAS **454**, 1161 (2015), arXiv: 1505.02781.

551 Z. Zhang, H. Wang, W. Luo, H. J. Mo, Z. Liang, R. Li, X. Yang, T. Wang, H. Zhang, H. Hong, X. Wang, E. Wang, P. Li, and J. Shi, A&A **650**, A155 (2021), arXiv: 2012.10640.

552 R. H. Wechsler and J. L. Tinker, ARA&A **56**, 435 (2018), arXiv: 1804.03097.

553 Z. Zhang, H. Wang, W. Luo, J. Zhang, H. J. Mo, Y. Jing, X. Yang, and H. Li, arXiv e-prints arXiv:2112.04777 (2021), arXiv: 2112.04777.

554 H. J. Mo, Y. P. Jing, and S. D. M. White, MNRAS **282**, 1096 (1996), arXiv: astro-ph/9602052.

555 Y. P. Jing, Y. Suto, and H. J. Mo, ApJ **657**, 664 (2007), arXiv: astro-ph/0610099.

556 L. Gao and S. D. M. White, MNRAS **377**, L5 (2007), arXiv: astro-ph/0611921.

557 H. Miyatake, S. More, M. Takada, D. N. Spergel, R. Mandelbaum, E. S. Rykoff, and E. Rozo, PRL **116**, 041301 (2016), arXiv: 1506.06135.

558 E. S. Rykoff, E. Rozo, D. Hollowood, A. Bermeo-Hernandez, T. Jeltema, J. Mayers, A. K. Romer, P. Rooney, A. Saro, C. Vergara Cervantes, R. H. Wechsler, H. Wilcox, T. M. C. Abbott, F. B. Abdalla, S. Allam, J. Annis, A. Benoit-Lévy, G. M. Bernstein, E. Bertin, D. Brooks, D. L. Burke, D. Capozzi, A. Carnero Rosell, M. Carrasco Kind, F. J. Castander, M. Childress, C. A. Collins, C. E. Cunha, C. B. D'Andrea, L. N. da Costa, T. M. Davis, S. Desai, H. T. Diehl, J. P. Dietrich, P. Doel, A. E. Evrard, D. A. Finley, B. Flaugher, P. Fosalba, J. Frieman, K. Glazebrook, D. A. Goldstein, D. Gruen, R. A. Gruendl, G. Gutierrez, M. Hilton, K. Honscheid, B. Hoyle, D. J. James, S. T. Kay, K. Kuehn, N. Kuropatkin, O. Lahav, G. F. Lewis, C. Lidman, M. Lima, M. A. G. Maia, R. G. Mann, J. L. Marshall, P. Martini, P. Melchior, C. J. Miller, R. Miquel, J. J. Mohr, R. C. Nichol, B. Nord, R. Ogando, A. A. Plazas, K. Reil, M. Sahlén, E. Sanchez, B. Santiago, V. Scarpine, M. Schubnell, I. Sevilla-Noarbe, R. C. Smith, M. Soares-Santos, F. Sobreira, J. P. Stott, E. Suchyta, M. E. C. Swanson, G. Tarle, D. Thomas, D. Tucker, S. Uddin, P. T. P. Viana, V. Vikram, A. R. Walker, Y. Zhang, and DES Collaboration, ApJS **224**, 1 (2016), arXiv: 1601.00621.

559 Y. Zu, R. Mandelbaum, M. Simet, E. Rozo, and E. S. Rykoff, MNRAS **470**, 551 (2017), arXiv: 1611.00366.

560 H. Wang, H. J. Mo, X. Yang, Y. P. Jing, and W. P. Lin, ApJ **794**, 94 (2014), arXiv: 1407.3451.

561 Y.-T. Lin, R. Mandelbaum, Y.-H. Huang, H.-J. Huang, N. Dalal, B. Diemer, H.-Y. Jian, and A. Kravtsov, ApJ **819**, 119 (2016), arXiv: 1504.07632.

562 K. S. McCarthy, Z. Zheng, H. Guo, W. Luo, and Y.-T. Lin, MNRAS **509**, 380 (2022), arXiv: 2104.13379.

563 K. S. McCarthy, Z. Zheng, H. Guo, W. Luo, and Y.-T. Lin, MNRAS **509**, 380 (2022), arXiv: 2104.13379.

564 M. Giavalisco, ARA&A **40**, 579 (2002).

565 M. Sawicki, S. Arnouts, J. Huang, J. Coupon, A. Golob, S. Gwyn, S. Foucaud, T. Moutard, I. Iwata, C. Liu, L. Chen, G. Desprez, Y. Harikane, Y. Ono, M. A. Strauss, M. Tanaka, N. Thibert, M. Balogh, K. Bundy, S. Chapman, J. E. Gunn, B.-C. Hsieh, O. Ilbert, Y. Jing, O. LeFèvre, C. Li, Y. Matsuda, S. Miyazaki, T. Nagao, A. J. Nishizawa, M. Ouchi, K. Shimasaku, J. Silverman, S. de la Torre, L. Tresse, W.-H. Wang, C. J. Willott, T. Yamada, X. Yang, and H. K. C. Yee, MNRAS **489**, 5202 (2019), arXiv: 1909.05898.

566 T. Moutard, M. Sawicki, S. Arnouts, A. Golob, J. Coupon, O. Ilbert, X. Yang, and S. Gwyn, MNRAS **494**, 1894 (2020), arXiv: 2001.06904.

567 C. C. Steidel, M. Pettini, and D. Hamilton, AJ **110**, 2519 (1995), arXiv: astro-ph/9509089.

568 N. A. Reddy and C. C. Steidel, ApJ **692**, 778 (2009), arXiv: 0810.2788.

569 Z.-Y. Cai, A. Lapi, A. Bressan, G. De Zotti, M. Negrello, and L. Danese, ApJ **785**, 65 (2014), arXiv: 1403.0055.

570 C. C. Steidel, K. L. Adelberger, M. Giavalisco, M. Dickinson, and M. Pettini, ApJ **519**, 1 (1999), arXiv: astro-ph/9811399.

571 S. G. Carlsten, J. E. Greene, A. H. G. Peter, J. P. Greco, and R. L. Beaton, ApJ **902**, 124 (2020), arXiv: 2006.02444.

572 W. Wang, M. Takada, X. Li, S. G. Carlsten, T.-W. Lan, J. Shi, H. Miyatake, S. More, R. L. Beaton, R. Lupton, Y.-T. Lin, T. Qiu, and W. Luo, MNRAS **500**, 3776 (2021), arXiv: 2009.06882.

573 A. Merritt, A. Pillepich, P. van Dokkum, D. Nelson, L. Hernquist, F. Marinacci, and M. Vogelsberger, MNRAS **495**, 4570 (2020), arXiv: 2004.11402.

574 I. Trujillo, M. D'Onofrio, D. Zaritsky, A. Madrigal-Aguado, N. Chamba, G. Golini, M. Akhlaghi, Z. Sharbaf, R. Infante-Sainz, J. Román, C. Morales-Socorro, D. J. Sand, and G. Martin, A&A **654**, A40 (2021), arXiv: 2109.07478.

575 J. Fliri and I. Trujillo, MNRAS **456**, 1359 (2016), arXiv: 1603.04474.

576 S. Danieli, P. van Dokkum, and C. Conroy, ApJ **856**, 69 (2018), arXiv: 1711.00860.

577 K. V. Johnston, J. S. Bullock, S. Sharma, A. Font, B. E. Robertson, and S. N. Leitner, ApJ **689**, 936 (2008), arXiv: 0807.3911.

578 A. G. Riess, W. Yuan, L. M. Macri, D. Scolnic, D. Brout, S. Casertano, D. O. Jones, Y. Murakami, L. Breuval, T. G. Brink, A. V. Filippenko, S. Hoffmann, S. W. Jha, W. D. Kenworthy, J. Mackenty, B. E. Stahl, and W. Zheng, arXiv e-prints arXiv:2112.04510 (2021), arXiv: 2112.04510.

579 K. C. Wong, S. H. Suyu, G. C. F. Chen, C. E. Rusu, M. Millon, D. Sluse, V. Bonvin, C. D. Fassnacht, S. Taubenberger, M. W. Auger, S. Birrer, J. H. H. Chan, F. Courbin, S. Hilbert, O. Tihhonova, T. Treu, A. Agnello, X. Ding, I. Jee, E. Komatsu, A. J. Shajib, A. Sonnenfeld, R. D. Blandford, L. V. E. Koopmans, P. J. Marshall, and G. Meylan, MNRAS **498**, 1420 (2020), arXiv: 1907.04869.

580 M. A. Troxel, N. MacCrann, J. Zuntz, T. F. Eifler, E. Krause, S. Dodelson, D. Gruen, J. Blazek, O. Friedrich, S. Samuroff, J. Prat, L. F. Secco, C. Davis, A. Ferté, J. DeRose, A. Alarcon, A. Amara, E. Baxter, M. R. Becker, G. M. Bernstein, S. L. Bridle, R. Cawthon, C. Chang, A. Choi, J. De Vicente, A. Drlica-Wagner, J. Elvin-Poole, J. Frieman, M. Gatti, W. G. Hartley, K. Honscheid, B. Hoyle, E. M. Huff, D. Huterer, B. Jain, M. Jarvis, T. Kacprzak, D. Kirk, N. Kokron, C. Krawiec, O. Lahav, A. R. Liddle, J. Peacock, M. M. Rau, A. Refregier, R. P. Rollins, E. Rozo, E. S. Rykoff, C. Sánchez, I. Sevilla-Noarbe, E. Sheldon, A. Stebbins, T. N. Varga, P. Vielzeuf, M. Wang, R. H. Wechsler, B. Yanny, T. M. C. Abbott, F. B. Abdalla, S. Allam, J. Annis, K. Bechtol, A. Benoit-Lévy, E. Bertin, D. Brooks, E. Buckley-Geer, D. L. Burke, A. Carnero Rosell, M. Carrasco Kind, J. Carretero, F. J. Castander, M. Crocce, C. E. Cunha, C. B. D'Andrea, L. N. da Costa, D. L. DePoy, S. Desai, H. T. Diehl, J. P. Dietrich, P. Doel, E. Fernandez, B. Flaugher, P. Fosalba, J. García-Bellido, E. Gaztanaga, D. W. Gerdes, T. Giannantonio, D. A. Goldstein, R. A. Gruendl, J. Gschwend, G. Gutierrez, D. J. James, T. Jeltema, M. W. G. Johnson, M. D. Johnson, S. Kent, K. Kuehn, S. Kuhlmann, N. Kuropatkin, T. S. Li, M. Lima, H. Lin, M. A. G. Maia, M. March, J. L. Marshall, P. Martini, P. Melchior, F. Menanteau, R. Miquel, J. J. Mohr, E. Neilsen, R. C. Nichol, B. Nord,

D. Petravick, A. A. Plazas, A. K. Romer, A. Roodman, M. Sako, E. Sanchez, V. Scarpine, R. Schindler, M. Schubnell, M. Smith, R. C. Smith, M. Soares-Santos, F. Sobreira, E. Suchyta, M. E. C. Swanson, G. Tarle, D. Thomas, D. L. Tucker, V. Vikram, A. R. Walker, J. Weller, Y. Zhang, and DES Collaboration, PRD **98**, 043528 (2018), arXiv: 1708.01538.

581 M. A. Troxel, E. Krause, C. Chang, T. F. Eifler, O. Friedrich, D. Gruen, N. MacCrann, A. Chen, C. Davis, J. DeRose, S. Dodelson, M. Gatti, B. Hoyle, D. Huterer, M. Jarvis, F. Lacasa, P. Lemos, H. V. Peiris, J. Prat, S. Samuroff, C. Sánchez, E. Sheldon, P. Vielzeuf, M. Wang, J. Zuntz, O. Lahav, F. B. Abdalla, S. Allam, J. Annis, S. Avila, E. Bertin, D. Brooks, D. L. Burke, A. Carnero Rosell, M. Carrasco Kind, J. Carretero, M. Crocce, C. E. Cunha, C. B. D'Andrea, L. N. da Costa, J. De Vicente, H. T. Diehl, P. Doel, A. E. Evrard, B. Flaugher, P. Fosalba, J. Frieman, J. García-Bellido, E. Gaztanaga, D. W. Gerdes, R. A. Gruendl, J. Gschwend, G. Gutierrez, W. G. Hartley, D. L. Hollowood, K. Honscheid, D. J. James, D. Kirk, K. Kuehn, N. Kuropatkin, T. S. Li, M. Lima, M. March, F. Menanteau, R. Miquel, J. J. Mohr, R. L. C. Ogando, A. A. Plazas, A. Roodman, E. Sanchez, V. Scarpine, R. Schindler, I. Sevilla-Noarbe, M. Smith, M. Soares-Santos, F. Sobreira, E. Suchyta, M. E. C. Swanson, D. Thomas, A. R. Walker, and R. H. Wechsler, MNRAS **479**, 4998 (2018), arXiv: 1804.10663.

582 S. Birrer, A. J. Shajib, A. Galan, M. Millon, T. Treu, A. Agnello, M. Auger, G. C. F. Chen, L. Christensen, T. Collett, F. Courbin, C. D. Fassnacht, L. V. E. Koopmans, P. J. Marshall, J. W. Park, C. E. Rusu, D. Sluse, C. Spiniello, S. H. Suyu, S. Wagner-Carena, K. C. Wong, M. Barnabè, A. S. Bolton, O. Czoske, X. Ding, J. A. Frieman, and L. Van de Vyvere, A&A **643**, A165 (2020), arXiv: 2007.02941.

583 D. Clowe, A. Gonzalez, and M. Markevitch, ApJ **604**, 596 (2004), arXiv: astro-ph/0312273.

584 A. Mahdavi, H. Hoekstra, A. Babul, D. D. Balam, and P. L. Capak, ApJ **668**, 806 (2007), arXiv: 0706.3048.

585 C. Tang, P. Zhang, W. Luo, N. Li, Y.-F. Cai, and S. Pi, ApJ **911**, 44 (2021), arXiv: 2009.12011.

586 M. Oguri, Y.-T. Lin, S.-C. Lin, A. J. Nishizawa, A. More, S. More, B.-C. Hsieh, E. Medezinski, H. Miyatake, H.-Y. Jian, L. Lin, M. Takada, N. Okabe, J. S. Speagle, J. Coupon, A. Leauthaud, R. H. Lupton, S. Miyazaki, P. A. Price, M. Tanaka, I. N. Chiu, Y. Komiyama, Y. Okura, M. M. Tanaka, and T. Usuda, PASJ **70**, S20 (2018), arXiv: 1701.00818.

587 X. Yang, H. Xu, M. He, Y. Gu, A. Katsianis, J. Meng, F. Shi, H. Zou, Y. Zhang, C. Liu, Z. Wang, F. Dong, Y. Lu, Q. Li, Y. Chen, H. Wang, H. Mo, J. Fu, H. Guo, A. Leauthaud, Y. Luo, J. Zhang, and Y. Zu, ApJ **909**, 143 (2021), arXiv: 2012.14998.

588 X. Yang, H. J. Mo, F. C. van den Bosch, A. Pasquali, C. Li, and M. Barden, ApJ **671**, 153 (2007), arXiv: 0707.4640.

589 T. Sunayama, Y. Park, M. Takada, Y. Kobayashi, T. Nishimichi, T. Kurita, S. More, M. Oguri, and K. Osato, MNRAS **496**, 4468 (2020), arXiv: 2002.03867.

590 M. Oguri, S. Miyazaki, X. Li, W. Luo, I. Mitsuishi, H. Miyatake, S. More, A. J. Nishizawa, N. Okabe, N. Ota, A. A. Plazas Malagón, and Y. Utsumi, PASJ **73**, 817 (2021), arXiv: 2103.15016.

591 Planck Collaboration, P. A. R. Ade, N. Aghanim, M. Arnaud, M. Ashdown, J. Aumont, C. Baccigalupi, A. J. Banday, R. B. Barreiro, R. Barrena, J. G. Bartlett, N. Bartolo, E. Battaner, R. Battye, K. Benabed, A. Benoît, A. Benoit-Lévy, J. P. Bernard, M. Bersanelli, P. Bielewicz, I. Bikmaev, H. Böhringer, A. Bonaldi, L. Bonavera, J. R. Bond, J. Borrill, F. R. Bouchet, M. Bucher, R. Burenin, C. Burigana, R. C. Butler, E. Calabrese, J. F. Cardoso, P. Carvalho, A. Catalano, A. Challinor, A. Chamballu, R. R. Chary, H. C. Chiang, G. Chon, P. R. Christensen, D. L. Clements, S. Colombi, L. P. L. Colombo, C. Combet, B. Comis, F. Couchot, A. Coulais, B. P. Crill, A. Curto, F. Cuttaia, H. Dahle, L. Danese, R. D. Davies, R. J. Davis, P. de Bernardis, A. de Rosa, G. de Zotti, J. Delabrouille, F. X. Désert, C. Dickinson, J. M. Diego, K. Dolag, H. Dole, S. Donzelli, O. Doré, M. Douspis, A. Ducout, X. Dupac, G. Efstathiou, P. R. M. Eisenhardt, F. Elsner, T. A. Enßlin, H. K. Eriksen, E. Falgarone, J. Fergusson, F. Feroz, A. Ferragamo, F. Finelli, O. Forni, M. Frailis, A. A. Fraisse, E. Franceschi, A. Frejsel, S. Galeotta, S. Galli, K. Ganga, R. T. Génova-Santos, M. Giard, Y. Giraud-Héraud, E. Gjerløw, J. González-Nuevo, K. M. Górski, K. J. B. Grainge, S. Gratton, A. Gregorio, A. Gruppuso, J. E. Gudmundsson, F. K. Hansen, D. Hanson, D. L. Harrison, A. Hempel, S. Henrot-Versillé, C. Hernández-Monteagudo, D. Herranz, S. R. Hildebrandt, E. Hivon, M. Hobson, W. A. Holmes, A. Hornstrup, W. Hovest, K. M. Huffenberger, G. Hurier, A. H. Jaffe, T. R. Jaffe, T. Jin, W. C. Jones, M. Juvela, E. Keihänen, R. Keskitalo, I. Khamitov, T. S. Kisner, R. Kneissl, J. Knoche, M. Kunz, H. Kurki-Suonio, G. Lagache, J. M. Lamarre, A. Lasenby, M. Lattanzi, C. R. Lawrence, R. Leonardi, J. Lesgourgues, F. Levrier, M. Liguori, P. B. Lilje, M. Linden-Vørnle, M. López-Caniego, P. M. Lubin, J. F. Macías-Pérez, G. Maggio, D. Maino, D. S. Y. Mak, N. Mandolesi, A. Mangilli, P. G. Martin, E. Martínez-González, S. Masi, S. Matarrese, P. Mazzotta, P. McGehee, S. Mei, A. Melchiorri, J. B. Melin, L. Mendes, A. Mennella, M. Migliaccio, S. Mitra, M. A. Miville-Deschênes, A. Moneti, L. Montier, G. Morgante, D. Mortlock, A. Moss, D. Munshi, J. A. Murphy, P. Naselsky, A. Nastasi, F. Nati, P. Natoli, C. B. Netterfield, H. U. Nørgaard-Nielsen, F. Noviello, D. Novikov, I. Novikov, M. Olamaie, C. A. Oxborrow, F. Paci, L. Pagano, F. Pajot, D. Paoletti, F. Pasian, G. Patanchon, T. J. Pearson, O. Perdereau, L. Perotto, Y. C. Perrott, F. Perrotta, V. Pettorino, F. Piacentini, M. Piat, E. Pierpaoli, D. Pietrobon, S. Plaszczynski, E. Pointecouteau, G. Polenta, G. W. Pratt, G. Prézeau, S. Prunet, J. L. Puget, J. P. Rachen, W. T. Reach, R. Rebolo, M. Reinecke, M. Remazeilles, C. Renault, A. Renzi, I. Ristorcelli, G. Rocha, C. Rosset, M. Rossetti, G. Roudier, E. Rozo, J. A. Rubiño-Martín, C. Rumsey, B. Rusholme, E. S. Rykoff, M. Sandri, D. Santos, R. D. E. Saunders, M. Savelainen, G. Savini, M. P. Schammel, D. Scott, M. D. Seiffert, E. P. S. Shellard, T. W. Shimwell, L. D. Spencer, S. A. Stanford, D. Stern, V. Stolyarov, R. Stompor, A. Streblyanska, R. Sudiwala, R. Sunyaev, D. Sutton, A. S. Suur-Uski, J. F. Sygnet, J. A. Tauber, L. Terenzi, L. Toffolatti, M. Tomasi, D. Tramonte, M. Tristram, M. Tucci, J. Tuovinen, G. Umana, L. Valenziano, J. Valiviita, B. Van Tent, P. Vielva, F. Villa, L. A. Wade, B. D. Wandelt, I. K. Wehus, S. D. M. White, E. L. Wright, D. Yvon, A. Zacchei, and A. Zonca, A&A **594**, A27 (2016), arXiv: 1502.01598.

592 E. Bulbul, A. Liu, T. Pasini, J. Comparat, D. Hoang, M. Klein, V. Ghirardini, M. Salvato, A. Merloni, R. Seppi, J. Wolf, S. F. Anderson, Y. E. Bahar, M. Brusa, M. Brueggen, J. Buchner, T. Dwelly, H. Ibarra-Medel, J. Ider Chitham, T. Liu, K. Nandra, M. E. Ramos-Ceja, J. S. Sanders, and Y. Shen, arXiv e-prints arXiv:2110.09544 (2021), arXiv: 2110.09544.

593 C. Hikage, M. Oguri, T. Hamana, S. More, R. Mandelbaum, M. Takada, F. Köhlinger, H. Miyatake, A. J. Nishizawa, H. Aihara, R. Armstrong, J. Bosch, J. Coupon, A. Ducout, P. Ho, B.-C. Hsieh, Y. Komiyama, F. Lanusse, A. Leauthaud, R. H. Lupton, E. Medezinski, S. Mineo, S. Miyama, S. Miyazaki, R. Murata, H. Murayama, M. Shirasaki, C. Sifón, M. Simet, J. Speagle, D. N. Spergel, M. A. Strauss, N. Sugiyama, M. Tanaka, Y. Utsumi, S.-Y. Wang, and Y. Yamada, PASJ **71**, 43 (2019), arXiv: 1809.09148.

594 T. Okumura and Y. P. Jing, ApJL **694**, L83 (2009), arXiv: 0812.2935.

595 T. Okumura, Y. P. Jing, and C. Li, ApJ **694**, 214 (2009), arXiv: 0809.3790.

596 Y. P. Jing and Y. Suto, ApJL **529**, L69 (2000), arXiv: astro-ph/9909478.

597 A. Amon, N. C. Robertson, H. Miyatake, C. Heymans, M. White, J. DeRose, S. Yuan, R. H. Wechsler, T. N. Varga, S. Bocquet, A. Dvornik, S. More, A. J. Ross, H. Hoekstra, A. Alarcon, M. Asgari, J. Blazek, A. Campos, R. Chen, A. Choi, M. Crocce, H. T. Diehl,

C. Doux, K. Eckert, J. Elvin-Poole, S. Everett, A. Ferté, M. Gatti, G. Giannini, D. Gruen, R. A. Gruendl, W. G. Hartley, K. Herner, H. Hildebrandt, S. Huang, E. M. Huff, B. Joachimi, S. Lee, N. MacCrann, J. Myles, A. Navarro- Alsina, T. Nishimichi, J. Prat, L. F. Secco, I. Sevilla-Noarbe, E. Sheldon, T. Shin, T. Trster, M. A. Troxel, I. Tutusaus, A. H. Wright, B. Yin, M. Aguena, S. Allam, J. Annis, D. Bacon, M. Bilicki, D. Brooks, D. L. Burke, A. Carnero Rosell, J. Carretero, F. J. Castander, R. Cawthon, M. Costanzi, L. N. da Costa, M. E. S. Pereira, J. de Jong, J. De Vicente, S. Desai, J. P. Dietrich, P. Doel, I. Ferrero, J. Frieman, J. García-Bellido, D. W. Gerdes, J. Gschwend, G. Gutierrez, S. R. Hinton, D. L. Hollowood, K. Honscheid, D. Huterer, A. Kannawadi, K. Kuehn, N. Kuropatkin, O. Lahav, M. Lima, M. A. G. Maia, J. L. Marshall, F. Menanteau, R. Miquel, J. J. Mohr, R. Morgan, J. Muir, F. Paz-Chinchon, A. Pieres, A. A. Plazas Malagón, A. Porredon, M. Rodriguez-Monroy, A. Roodman, E. Sanchez, S. Serrano, H. Shan, E. Suchyta, M. E. C. Swanson, G. Tarle, D. Thomas, C. To, and Y. Zhang, arXiv e-prints arXiv:2202.07440 (2022), arXiv: 2202.07440.

598 A. Leauthaud, S. Saito, S. Hilbert, A. Barreira, S. More, M. White, S. Alam, P. Behroozi, K. Bundy, J. Coupon, T. Erben, C. Heymans, H. Hildebrandt, R. Mandelbaum, L. Miller, B. Moraes, M. E. S. Pereira, S. A. Rodríguez-Torres, F. Schmidt, H.-Y. Shan, M. Viel, and F. Villaescusa-Navarro, MNRAS **467**, 3024 (2017), arXiv: 1611.08606.

599 S. Sugiyama, M. Takada, H. Miyatake, T. Nishimichi, M. Shirasaki, Y. Kobayashi, S. More, R. Takahashi, K. Osato, M. Oguri, J. Coupon, C. Hikage, B.-C. Hsieh, Y. Komiyama, A. Leauthaud, X. Li, W. Luo, R. H. Lupton, H. Murayama, A. J. Nishizawa, Y. Park, P. A. Price, M. Simet, J. S. Speagle, M. A. Strauss, and M. Tanaka, arXiv e-prints arXiv:2111.10966 (2021), arXiv: 2111.10966.

600 H. Miyatake, S. Sugiyama, M. Takada, T. Nishimichi, M. Shirasaki, Y. Kobayashi, R. Mandelbaum, S. More, M. Oguri, K. Osato, Y. Park, R. Takahashi, J. Coupon, C. Hikage, B.-C. Hsieh, A. Leauthaud, X. Li, W. Luo, R. H. Lupton, S. Miyazaki, H. Murayama, A. J. Nishizawa, P. A. Price, M. Simet, J. S. Speagle, M. A. Strauss, M. Tanaka, and N. Yoshida, arXiv e-prints arXiv:2111.02419 (2021), arXiv: 2111.02419.

601 F. Shi, X. Yang, H. Wang, Y. Zhang, H. J. Mo, F. C. van den Bosch, W. Luo, D. Tweed, S. Li, C. Liu, Y. Lu, and L. Yang, ApJ **861**, 137 (2018), arXiv: 1712.04163.

602 R. Ahumada, C. A. Prieto, A. Almeida, F. Anders, S. F. Anderson, B. H. Andrews, B. Anguiano, R. Arcodia, E. Armengaud, M. Aubert, S. Avila, V. Avila-Reese, C. Badenes, C. Balland, K. Barger, J. K. Barrera-Ballesteros, S. Basu, J. Bautista, R. L. Beaton, T. C. Beers, B. I. T. Benavides, C. F. Bender, M. Bernardi, M. Bershady, F. Beutler, C. M. Bidin, J. Bird, D. Bizyaev, G. A. Blanc, M. R. Blanton, M. Boquien, J. Borissova, J. Bovy, W. N. Brandt, J. Brinkmann, J. R. Brownstein, K. Bundy, M. Bureau, A. Burgasser, E. Burtin, M. Cano-Díaz, R. Capasso, M. Cappellari, R. Carrera, S. Chabanier, W. Chaplin, M. Chapman, B. Cherinka, C. Chiappini, P. Doohyun Choi, S. D. Chojnowski, H. Chung, N. Clerc, D. Coffey, J. M. Comerford, J. Comparat, L. da Costa, M.-C. Cousinou, K. Covey, J. D. Crane, K. Cunha, G. d. S. Ilha, Y. S. Dai, S. B. Damsted, J. Darling, J. Davidson, James W., R. Davies, K. Dawson, N. De, A. de la Macorra, N. De Lee, A. B. d. A. Queiroz, A. Deconto Machado, S. de la Torre, F. Dell'Agli, H. du Mas des Bourboux, A. M. Diamond-Stanic, S. Dillon, J. Donor, N. Drory, C. Duckworth, T. Dwelly, G. Ebelke, S. Eftekharzadeh, A. Davis Eigenbrot, Y. P. Elsworth, M. Eracleous, G. Erfanianfar, S. Escoffier, X. Fan, E. Farr, J. G. Fernández-Trincado, D. Feuillet, A. Finoguenov, P. Fofie, A. Fraser-McKelvie, P. M. Frinchaboy, S. Fromenteau, H. Fu, L. Galbany, R. A. Garcia, D. A. García-Hernández, L. A. G. Oehmichen, J. Ge, M. A. G. Maia, D. Geisler, J. Gelfand, J. Goddy, V. Gonzalez-Perez, K. Grabowski, P. Green, C. J. Grier, H. Guo, J. Guy, P. Harding, S. Hasselquist, A. J. Hawken, C. R. Hayes, F. Hearty, S. Hekker, D. W. Hogg, J. A. Holtzman, D. Horta, J. Hou, B.-C. Hsieh, D. Huber, J. A. S. Hunt, J. I. Chitham, J. Imig, M. Jaber, C. E. J. Angel, J. A. Johnson, A. M. Jones, H. Jönsson, E. Jullo, Y. Kim, K. Kinemuchi, I. Kirkpatrick, Charles C., G. W. Kite, M. Klaene, J.-P. Kneib, J. A. Kollmeier, H. Kong, M. Kounkel, D. Krishnarao, I. Lacerna, T.-W. Lan, R. R. Lane, D. R. Law, J.-M. Le Goff, H. W. Leung, H. Lewis, C. Li, J. Lian, L. Lin, D. Long, P. Longa-Peña, B. Lundgren, B. W. Lyke, J. Ted Mackereth, C. L. MacLeod, S. R. Majewski, A. Manchado, C. Maraston, P. Martini, T. Masseron, K. L. Masters, S. Mathur, R. M. McDermid, A. Merloni, M. Merrifield, S. Mészáros, A. Miglio, D. Minniti, R. Minsley, T. Miyaji, F. G. Mohammad, B. Mosser, E.-M. Mueller, D. Muna, A. Muñoz-Gutiérrez, A. D. Myers, S. Nadathur, P. Nair, K. Nandra, J. C. do Nascimento, R. J. Nevin, J. A. Newman, D. L. Nidever, C. Nitschelm, P. Noterdaeme, J. E. O'Connell, M. D. Olmstead, D. Oravetz, A. Oravetz, Y. Osorio, Z. J. Pace, N. Padilla, N. Palanque-Delabrouille, P. A. Palicio, H.-A. Pan, K. Pan, J. Parker, R. Paviot, S. Peirani, K. P. Ramŕez, S. Penny, W. J. Percival, I. Perez-Fournon, I. Pérez-Ràfols, P. Petitjean, M. M. Pieri, M. Pinsonneault, V. J. Poovelil, J. T. Povick, A. Prakash, A. M. Price-Whelan, M. J. Raddick, A. Raichoor, A. Ray, S. B. Rembold, M. Rezaie, R. A. Riffel, R. Riffel, H.-W. Rix, A. C. Robin, A. Roman-Lopes, C. Román-Zúñiga, B. Rose, A. J. Ross, G. Rossi, K. Rowlands, K. H. R. Rubin, M. Salvato, A. G. Sánchez, L. Sánchez-Menguiano, J. R. Sánchez-Gallego, C. Sayres, A. Schaefer, R. P. Schiavon, J. S. Schimoia, E. Schlafly, D. Schlegel, D. P. Schneider, M. Schultheis, A. Schwope, H.-J. Seo, A. Serenelli, A. Shafieloo, S. J. Shamsi, Z. Shao, S. Shen, M. Shetrone, R. Shirley, V. S. Aguirre, J. D. Simon, M. F. Skrutskie, A. Slosar, R. Smethurst, J. Sobeck, B. C. Sodi, D. Souto, D. V. Stark, K. G. Stassun, M. Steinmetz, D. Stello, J. Stermer, T. Storchi-Bergmann, A. Streblyanska, G. S. Stringfellow, A. Stutz, G. Suárez, J. Sun, M. Taghizadeh-Popp, M. S. Talbot, J. Tayar, A. R. Thakar, R. Theriault, D. Thomas, Z. C. Thomas, J. Tinker, R. Tojeiro, H. H. Toledo, C. A. Tremonti, N. W. Troup, S. Tuttle, E. Unda-Sanzana, M. Valentini, J. Vargas-González, M. Vargas-Magaña, J. A. Vázquez-Mata, M. Vivek, D. Wake, Y. Wang, B. A. Weaver, A.-M. Weijmans, V. Wild, J. C. Wilson, R. F. Wilson, N. Wolthuis, W. M. Wood-Vasey, R. Yan, M. Yang, C. Yèche, O. Zamora, P. Zarrouk, G. Zasowski, K. Zhang, C. Zhao, G. Zhao, Z. Zheng, Z. Zheng, G. Zhu, and H. Zou, ApJS **249**, 3 (2020), arXiv: 1912.02905.

603 A. Leauthaud, S. Saito, S. Hilbert, A. Barreira, S. More, M. White, S. Alam, P. Behroozi, K. Bundy, J. Coupon, T. Erben, C. Heymans, H. Hildebrandt, R. Mandelbaum, L. Miller, B. Moraes, M. E. S. Pereira, S. A. Rodríguez-Torres, F. Schmidt, H.-Y. Shan, M. Viel, and F. Villaescusa-Navarro, MNRAS **467**, 3024 (2017), arXiv: 1611.08606.

604 Planck Collaboration, P. A. R. Ade, N. Aghanim, M. Arnaud, M. Ashdown, J. Aumont, C. Baccigalupi, A. J. Banday, R. B. Barreiro, J. G. Bartlett, and et al., A&A **594**, A13 (2016), arXiv: 1502.01589.

605 D. J. Eisenstein, I. Zehavi, D. W. Hogg, R. Scoccimarro, M. R. Blanton, R. C. Nichol, R. Scranton, H.-J. Seo, M. Tegmark, Z. Zheng, S. F. Anderson, J. Annis, N. Bahcall, J. Brinkmann, S. Burles, F. J. Castander, A. Connolly, I. Csabai, M. Doi, M. Fukugita, J. A. Frieman, K. Glazebrook, J. E. Gunn, J. S. Hendry, G. Hennessy, Z. Ivezić, S. Kent, G. R. Knapp, H. Lin, Y.-S. Loh, R. H. Lupton, B. Margon, T. A. McKay, A. Meiksin, J. A. Munn, A. Pope, M. W. Richmond, D. Schlegel, D. P. Schneider, K. Shimasaku, C. Stoughton, M. A. Strauss, M. SubbaRao, A. S. Szalay, I. Szapudi, D. L. Tucker, B. Yanny, and D. G. York, ApJ **633**, 560 (2005), arXiv: astro-ph/0501171.

606 E. Di Valentino, A. Melchiorri, and J. Silk, PRD **92**, 121302 (2015), arXiv: 1507.06646.

607 J. Zhang, R. An, S. Liao, W. Luo, Z. Li, and B. Wang, PRD **98**, 103530 (2018), arXiv: 1811.01519.

608 E. P. Verlinde, ArXiv e-prints (2016), arXiv: 1611.02269.

609 T. Kobayashi, Reports on Progress in Physics **82**, 086901 (2019), arXiv: 1901.07183.
610 M. Dentler, D. J. E. Marsh, R. Hložek, A. Laguë, K. K. Rogers, and D. Grin, arXiv e-prints arXiv:2111.01199 (2021), arXiv: 2111.01199.
611 Z. Chen, W. Luo, Y.-F. Cai, and E. N. Saridakis, PRD **102**, 104044 (2020), arXiv: 1907.12225.
612 W. Luo, J. Zhang, V. Halenka, X. Yang, S. More, C. J. Miller, L. Liu, and F. Shi, ApJ **914**, 96 (2021), arXiv: 2003.09818.
613 J. Zhang, R. An, W. Luo, Z. Li, S. Liao, and B. Wang, ApJL **875**, L11 (2019), arXiv: 1807.05522.